Assessment of the Idaho National Laboratory Remote-Handled Low-Level Waste Disposal Facility Hydraulic Performance

Annette L. Schafer

September 2017

Idaho National Laboratory

Assessment of the Idaho National Laboratory Remote-Handled Low-Level Waste Disposal Facility Hydraulic Performance

Annette L. Schafer

September 2017

Idaho National Laboratory
Idaho Falls, Idaho 83415

http://www.inl.gov

Prepared for the
U.S. Department of Energy
Office of Nuclear Energy
Under DOE Idaho Operations Office
Contract DE-AC07-05ID14517

EXECUTIVE SUMMARY

This document provides a summary of the expected hydraulic performance of the vault drainage system installed at Idaho National Laboratory's Remote-Handled Low-Level Waste disposal facility. Hydraulic performance was assessed through analysis of the mechanical properties of the drainage system and backfill materials, including material gradation and proctor data; laboratory data, including bulk density, porosity, unsaturated hydraulic conductivity, moisture-retention data, and van Genuchten parameters; and field-data collected using in-situ instrumentation with data collected during focused vault-scale infiltration characterization tests.

Hydraulic performance of the vault drainage system was designed to promote a greater than 500-year vault concrete longevity. The predicted hydraulic performance is, in part, a function of the materials used in construction, sequencing of the hydraulic drainage materials, and the as-built condition of the materials following compaction necessary to ensure vault stability. Specifying specific as-built hydraulic properties is exceedingly difficult at the facility specification/design phase. Instead, material mechanical properties were specified and confirmed early during the construction process. As the drainage materials were installed, samples were sent to a laboratory for hydraulic property testing and, after drainage system installation was complete around the performance assessment vaults, field-scale infiltration tests were conducted with data collection to verify the as-built hydraulic performance.

This report provides summary data for the measured mechanical properties, laboratory data, and field infiltration characterization test data. Mechanical data have relatively little variability because of the sieve system used when the materials were crushed onsite. Laboratory data were obtained for a relatively small number of material samples, but the data obtained for each sample are extensive. However, laboratory data provide the moisture retention relationships and relative hydraulic conductivity-moisture content relationships for uninstalled materials. Conducting field-scale infiltration tests with collection of moisture retention data and wetting front propagation data allows extension of laboratory data to the as-installed conditions of the vault drainage system. These combined data types are integrated using a numerical simulation of the infiltration characterization test to refine model parameters. The infiltration characterization model will be used to support the hydraulic and concrete performance of the vault system provided in the facility performance assessment.

CONTENTS

FIGURES

TABLES

ACRONYMS

ASTM   American Society of Testing and Materials

AT   advanced tensiometer

ATR   Advanced Test Reactor

DOE   U.S. Department of Energy

DOE-ID   U.S. Department of Energy Idaho Operations Office

HFEF   Hot Fuel Examination Facility

HPP   hydraulic properties package

INL   Idaho National Laboratory

LCC   large concept cask

LLW   low-level waste

NRF   Naval Reactors Facility

PA   performance assessment

PVC   polyvinyl chloride

RH   remote-handled

VDC   volt direct current

WCR   water content reflectometer

Assessment of the Idaho National Laboratory Remote-Handled Low-Level Waste Disposal Facility Hydraulic Performance

1. BACKGROUND

A performance assessment (PA) for the Idaho National Laboratory (INL) Remote-Handled Low-Level Waste (RH-LLW) disposal facility is required to demonstrate that the facility design will meet the performance objectives established for long-term protection of the public and the environment following closure of the facility as outlined in U.S. Department of Energy (DOE) Order 435.1, "Radioactive Waste Management." Protectiveness of the facility in terms of the groundwater pathway is a function of the design features that control the hydrologic and geochemical conditions within and below the vault system. The facility design includes features to promote drainage of infiltrating water to limit accumulation of moisture next to the reinforced concrete disposal vaults and containerized waste. The PA groundwater pathway model accounts for a cement-impacted geochemical environment within and below the vault system to inhibit corrosion of stainless steel waste containers (i.e., waste liners), steel reinforcement in the concrete vault, and the effects on release and migration of non-anionic radionuclides. Upon closure of the facility, an engineered barrier (i.e., cover) will be placed over the facility to reduce infiltration through the waste zone, retarding the release and migration rate of radionuclides beneath the facility. The final facility design is summarized in Section 2.

1.1 Purpose and Scope

This analysis supplements evaluation of engineered features designed to enhance performance of the facility discussed in the PA. The entire engineered features evaluation considers the impact of the combination of barriers (e.g., waste forms, stainless steel waste containers, precast concrete vaults, hydraulic drainage system, and an engineered cover) and their effectiveness as a unit. These features have been selected to enhance performance of the vault system.

As part of the engineered features evaluation, the expected performance of the hydraulic drainage system is required. The hydraulic drainage system influences the concrete vault system's longevity by determining the water-cement contact time and amount of water expected to be in contact with the vault system. The hydraulic drainage system has been designed to minimize the volume of water in contact with the cement and water-cement contact time.

This report summarizes the combination of mechanical and laboratory hydraulic test data for hydraulic drainage materials and results from infiltration tests conducted after vault installation. Laboratory test data include bulk density, porosity, water content, and hydraulic conductivity of samples taken during installation of the reinforced concrete vaults at the INL RH-LLW Disposal Facility. Field infiltration tests were conducted in order to quantify the as-built or as-installed hydraulic properties and wetting front propagation behavior of the drainage materials.

2. FACILITY LAYOUT

The RH-LLW Disposal Facility will receive waste from the Advanced Test Reactor (ATR) Complex, Naval Reactors Facility (NRF), and the Materials and Fuels Complex (MFC) (see Table 1). The RH-LLW Disposal Facility is located approximately 0.3 miles south of the ATR Complex. Waste containers will be placed in precast concrete vaults constructed with hexagonal precast concrete bases with integral risers, upper riser sections, and precast concrete vault plugs (Figure 1). Dimensions of the vault components for each waste container type are given in Table 2 with the total vault height, including plugs, risers, and bases. The vaults are arranged by cask type and oriented in parallel rows (Figure 2).

1

Table 1. Dimensions of waste containers.

Waste Generation Facility	Container Type	Waste Type	Waste Container Size		Total Number of Containers	Number of Container Layers	Stacked Container Height (cm)
			OD (cm)	Height (cm)			
ATR	Nu Pac 14-210L	Resins	191	203	120	2	406
NRF	Large Concept	Resins/Activated Metals	152	432	192	1	432
NRF	55-Ton Scrap	Resins/Activated Metals	122	267	164	2	534
MFC	Modified FTC	Activated Metals/Debris	74	445	272	1	444
ATR	HFEF-5	Activated Metals	33	191	56	2	381
MFC	HFEF-5	Activated Metals/Debris	33	191	115	2	381

Table 2. Dimensions of vaults.

Waste Generation Facility	Container Type	Waste Type	Number of Index Positions (Number Containers/Layer)	Vault Dimensions				
				ID (cm)	Inner Vault Height (cm)	Base Thickness (cm)	Plug Height (cm)	Total Vault Height (cm)
ATR	Nu Pac 14-20L	Resins	1	213	442	46	152	640
NRF	Large Concept	Resins/Activated Metals	1	168	442	46	152	640
NRF	55-Ton	Resins/Activated Metals	1	137	564	46	152	762
MFC	Modified FTC	Activated Metals/Debris	3	76	442	46	152	640
ATR	HFEF-5	Activated Metals	6	38	442	46	152	640
MFC	HFEF-5	Activated Metals/Debris	6	38	442	46	152	640
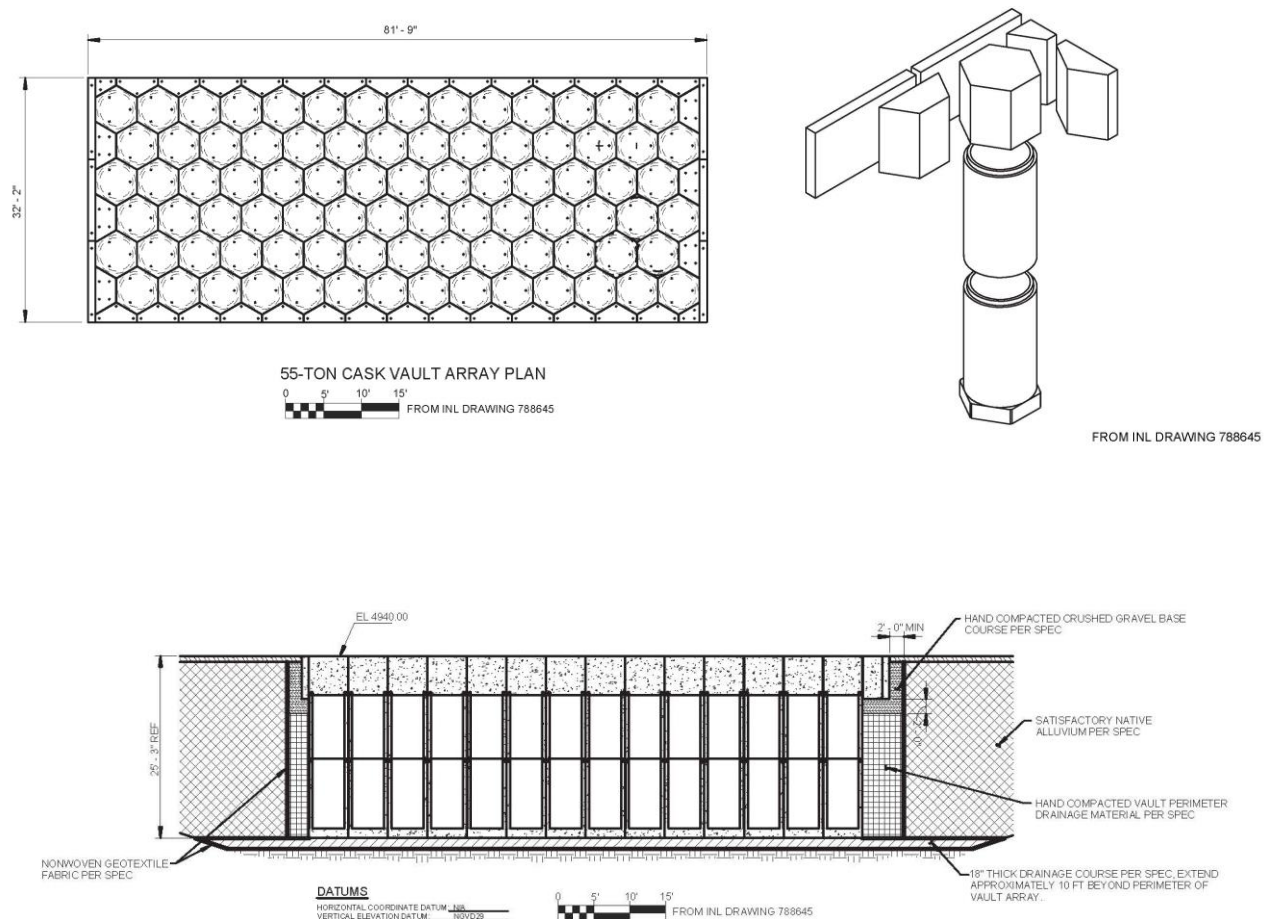
Figure 1. Cross-section through a precast concrete vault array, showing vault bases, riser sections, plugs, drainage course material, vault perimeter drainage material adjacent to the vaults, alluvial fill material throughout the remainder of the excavation area, and the truck access apron (from Drawings 788645, 55-Ton vault array is typical of all vault arrays).

3
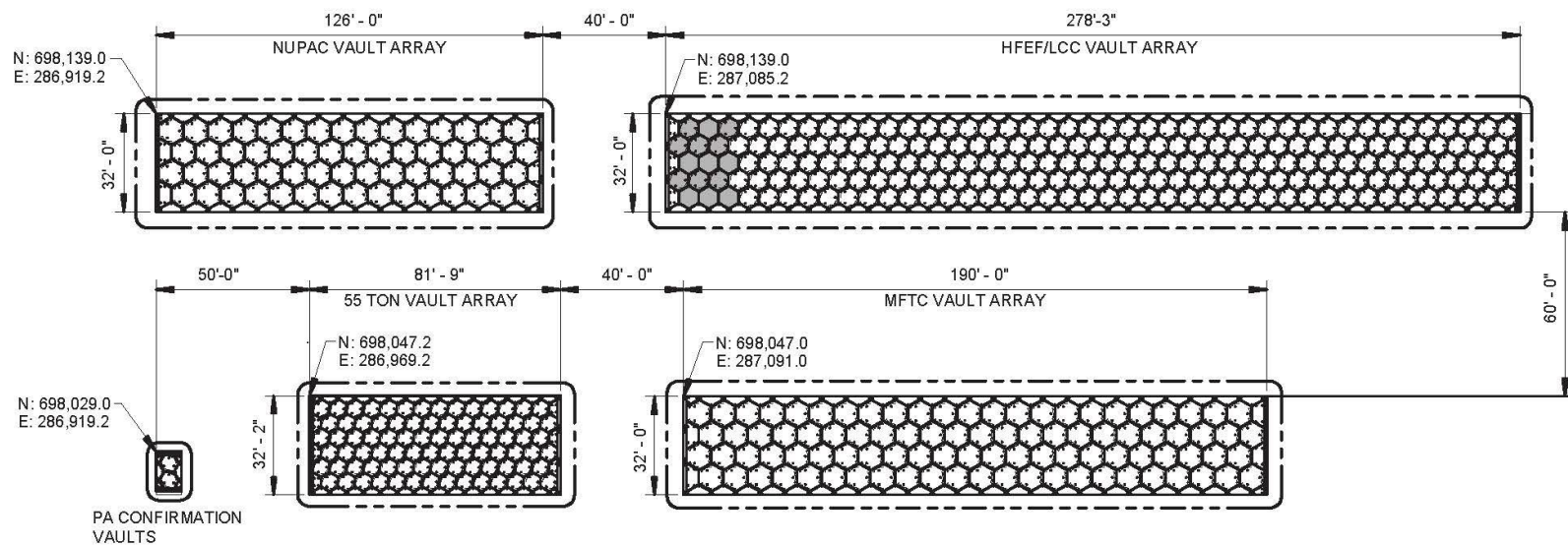
Figure 2. Horizontal layout of the vault arrays (from Drawing 788644). The PA Confirmation Vaults are the two vaults in the southwest corner denoted by C-14.

The Hot Fuel Examination Facility (HFEF) vaults are located at the end of the NRF large concept casks (LCC) array, with this vault array positioned approximately 12.5 m (40-ft) west of the NuPac vault array. The 55-ton and modified fuel transfer cask (FTC) vault arrays are separated by about 18.3 m (60-ft) from the NuPac and LCC vault arrays.

The area containing the vaults was excavated (see Figure 3), leaving a minimum of 5 m of alluvium beneath the vaults (see Figure 2-13 of the PA for vertical cross-sections from the land surface to the aquifer showing the alluvium and underlying basalt-sediment sequences). The extent of soil disturbance beyond the vaults is approximately 21 to 24 m (70 to 80 ft), which is indicated in Figure 3. The excavated area under the vaults was leveled using a thin pit run subbase and covered with a geotextile material to hold the subbase in place (see Figure 1). Over the subbase, a 47-cm (18–in.) thick drainage course was placed, with the drainage course extending 3 m (about 10 ft) beyond the horizontal extent of the vault bases.

During vault construction, the vault bases and integral bottom pipe section was placed on the drainage course, the vault top riser section was added, and volume between the individual vaults was filled with pea gravel. Vault plugs were placed on the vault risers, forming the upper surface hexagonal pattern shown in Figure 1.

The excavation depth and vault height combine to leave the vault plugs above the natural surrounding grade (elevation). This leaves the vault plugs above the frost-line (i.e., 1.4 m [about 4 to 5 ft) and places the vault risers and bases entirely below the frost line. This arrangement allows the road apron to serve as a protective flood-control berm that will prevent ingress of any water, with the exception of direct precipitation on the vault site.

3.   HYDRAULIC PERFORMANCE OF THE VAULT SYSTEM

Hydraulic performance of the vault system is of interest because it determines the amount and duration of water in contact with the concrete vaults. The dimensional and hydraulic performance specifications for the fill materials, including those used adjacent to the vaults, as infill between the vaults, and for the drainage course, were determined using numerical models. Hydraulic performance was numerically simulated using the code TOUGREACT. The code is fully described in Appendix A of the RH-LLW PA. Required input to the code includes model dimensions, material extents, material properties, and infiltration rates. The purpose of this report is to summarize hydraulic performance of the vault system.

3.1   Material Descriptions

The vertical east-west transect through the 55-ton vault array is shown in Section A of Figure 1. The materials represented in the figure are described from land surface downward and include the following:

1.   Surface road base is placed in compacted lifts at the upper most vault surface so the top is even with the top of the concrete plugs. This material is the same as the crushed gravel base course material and is installed a minimum of 12-in. thick (SPC-1860, "General Site Construction Specification").

2.   Crushed gravel base course material beneath and adjacent to the vault perimeter blocks (see inset in the upper left of Figure 1). This material is adjacent to the vault perimeter blocks and tops of the upper vault riser sections. It extends vertically from beneath the surface road base to 2-ft below the base of the perimeter blocks. Per SPC-1910, "Construction Specification - Vault Installation for the RH LLW Disposal Project," this material is a naturally or artificially graded mixture of ¾-in. maximum size natural or crushed gravel, crushed stone, and natural or crushed sand. It meets the requirements of the Idaho Transportation Department Standard Specifications for Highway Construction, Subsection 703.04, Type B material (see Table 3) (SPC-1910).

5
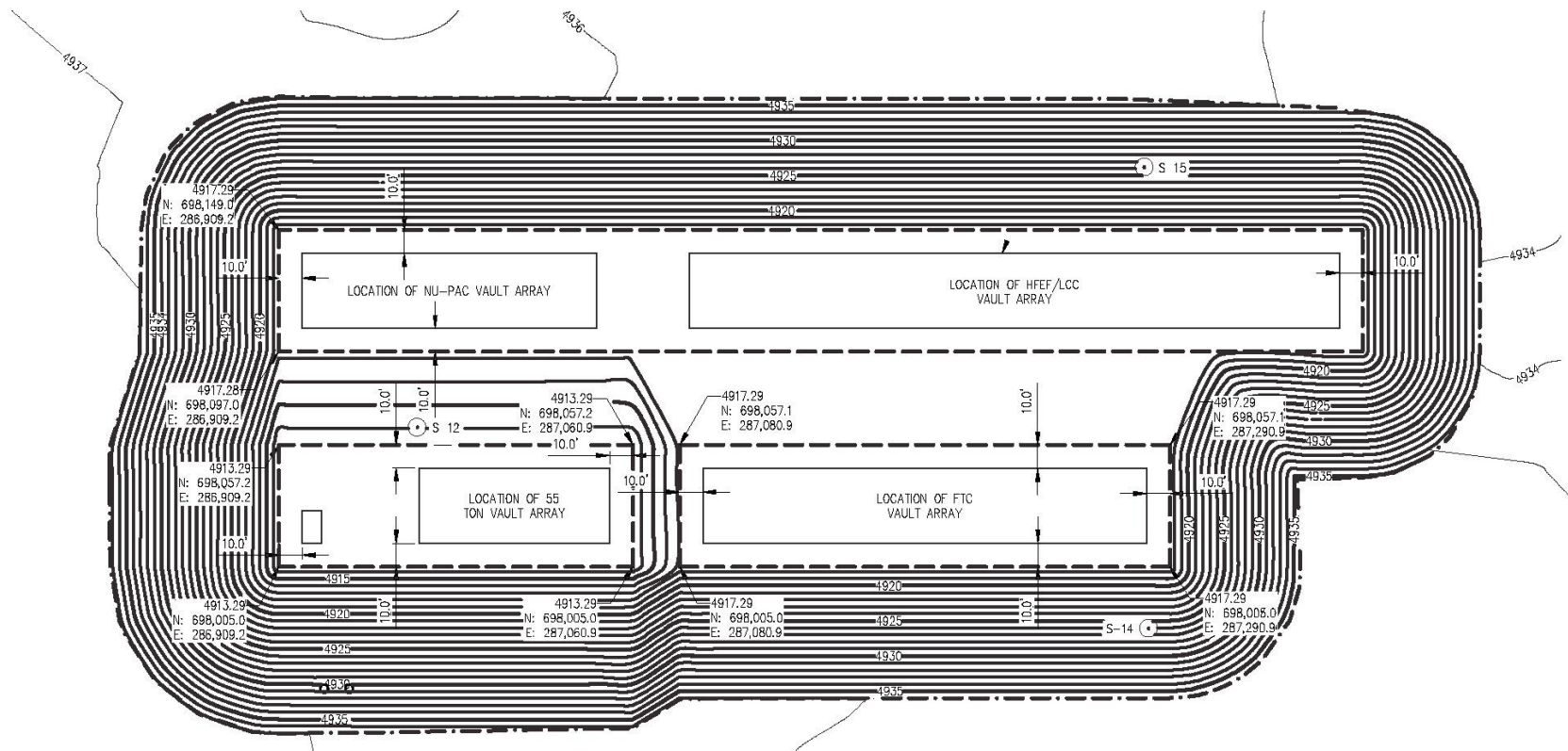
Figure 3. Excavation plan for the vault arrays showing the lateral extent of the excavation area (from Drawing 778766).

3. Vault perimeter drainage material placed below the crushed gravel base course material adjacent to the vault base sections and upper vault risers along each vault array perimeter. This material extends 2-ft beyond the vault perimeter blocks, which are 2 to 3 ft wide. Therefore, the vault perimeter drainage material column is 2 to 3-ft wide and approximately 13 to 17 ft high, depending on the specific vault array height (see Table 2). Per SPC-1910, this material is a narrowly graded mixture of crushed stone or crushed or uncrushed gravel; American Society for Testing and Materials (ASTM) D 448; coarse-aggregate grading Size 67; with 100% passing a 1-1/2-in. sieve and 0 to 5% passing a No. 8 sieve (see Table 3) (SPC-1910).

4. Pea gravel is placed between each of the vaults to fill the inter-vault void space. The hexagonal bases and plugs were sized to minimize the space between the vault risers where they meet. Pea gravel is placed in the areas where the risers do not touch to within approximately 7-in. below the top of the upper riser sections. Per SPC-1910, this material is a naturally or artificially graded mixture of natural or crushed gravel or stone with a nominal size of 1/2-in. and a coefficient of uniformity less than 2 (SPC-1910) (see Table 3).

5. Drainage course material is placed in a 47-cm (18-in.) thick layer beneath each of the vault arrays and extends 10-ft beyond the outer extent of the hexagonal bases along each vault array perimeter. Per SPC-1910, this material is a narrowly graded mixture of crushed stone or crushed or uncrushed gravel; ASTM D 448; coarse-aggregate grading Size 67; with 100% passing a 1-1/2–in. sieve and 0 to 5% passing a No. 8 sieve (see Table 3) (SPC-1910).

6. Non-woven geotextile material placed beneath the drainage course material and between the alluvial fill material and vault perimeter drainage material column is a non-woven needle-punched geotextile, manufactured for separation applications, and complying with American Association of State Highway and Transportation Officials M 288 and the following, measured per-test methods referenced (SPC-1910):

   - Grab Tensile Strength: 180 lbf; ASTM D 4632.
   - Elongation at Break: 50%; ASTM D 4632.
   - Tear Strength: 75 lbf; ASTM D 4533.
   - California Bearing Ratio Puncture Strength: 460 lbf; ASTM D 6241.
   - Apparent Opening Size: No. 70 sieve, maximum; ASTM D 4751.
   - Permittivity: 1.5 per second, minimum; ASTM D 4491.
   - UV Stability: 70% after 500 hours of exposure; ASTM D 4355.

7. Native alluvial sands, gravels, and silty clays extend vertically from the base of the drainage course material to the upper basalt contact. During the geotechnical investigation of the RH-LLW Disposal Facility location (American Geotechnics 2011), 12 borings were advanced to practical refusal on basalt rock or resistant earth material through the surficial sediment. While drilling, the following three strata were identified:

   - Stratum I corresponded to silt with sand (ML), extending from the existing (initial pre-construction excavation) ground surface to depths ranging from about 1 to 5 ft below the existing grade.
   - Stratum II alluvium located below the Stratum I to depths ranging from about 26 to 58 ft below the existing grade was classified as poorly graded sand with gravel (SP), poorly graded gravel with sand (GP), clayey gravel with sand (GC), well graded gravel with sand (GW), well graded gravel with silt and sand (GW-GM), silty, clayey sand (SC-SM), silty sand (SM), and poorly graded sand with clay (SPSC).
   - Stratum III material, classified as lean clay with sand (CL), was encountered below the Stratum II material and varied in thickness from a few inches to about 5 ft.

The Stratum II material predominately underlies the drainage course material, with pockets of Stratum III material found near the PA Confirmation Vaults at the base of the drainage course material.

8. Alluvial fill material is placed adjacent to the vault perimeter drainage material column extending between each of the vault arrays. This material was obtained from the Stratum II alluvium. It is well sorted, free of debris, waste, frozen materials, vegetation, and other deleterious matter. It does not fall in the unsatisfactory soil classifications of clayey gravel with sand (GC, SC) lean clay with sand (CL), silt with sand (ML, OL, CH, MH, OH, and PT) as defined according to ASTM D 2487, or in combinations of these groups (SPC-1910).

9. Bulk of the vadose zone beneath the surficial alluvium. The vadose zone below the surficial alluvium is comprised of a thick sequence of basalt flows separated by thinner sedimentary interbeds. The surficial alluvium is approximately 15-m (50-ft) thick in the vault area and the aquifer is approximately 146 m (480 ft) below land surface.

The vault system materials placed within 5-ft of the vault components were hand compacted with materials further from the vaults machine compacted. SPC-1910 required the materials used in the vault system to be placed in lifts not more than 8 in. in loose depth for material compacted by heavy compaction equipment and not more than 6 in. in loose depth for material compacted by hand-operated tampers. It also required that the surface road base and crushed gravel base course materials are to be compacted to no less than 95% of the maximum dry unit weight according to ASTM D 698. Compaction requirements were not provided for the drainage course material or perimeter drainage course material because of the lack of fines.

Table 3. Mechanical analysis data specifications.

Sieve Size	Surface Road Base and Crushed Gravel Base Course Material Idaho Transportation Department Type B Material	Vault Perimeter Drainage Material and Vault Drainage Course Materials ASTM C33 Size #67 Spec	Pea Gravel Nominal Size 1/2-in. and Coefficient of Uniformity <2
	Percent Passing		
1 1/2 in.		100	
1 in.	100		
¾ in.	90 to 100	90 to 100	
5/8 in.			
1/2 in.			
3/8 in.	40 to 65	20 to 55	
#4	30 to 50	0 to 10	
#8		0 to 5	
# 200	3 to 9		
Coefficient of Uniformity	NA	NA	$Cu=D_{60}/D_{10} < 2$

4. FIELD MECHANICAL TEST DATA

During installation of the vaults and the vault hydraulic drainage system, the RH-LLW Disposal Project required the installation subcontractor to provide material test reports for each material used for the hydraulic drainage system (per SPC-1860 and SPC-1910). The contractor was required to provide the classification according to ASTM D 2487 and the laboratory compaction curves according to ASTM D 698. These data were provided as data into the vendor data system and are summarized in Tables 4 through 8.

The mechanical test data and proctor test data for the surface road base and crushed gravel base course material are provided in Table 4. Comparing the mechanical test data for Sample ID 15-5514 (Column 2) to the required specification (Column 3) show that 75% of this material passes a 3/8-in. opening and 50% of the material can be classified as fine-course sand. The proctor data for the crushed gravel base course material are plotted in Figure 4.

In comparison, data for vault perimeter drainage material and drainage course material (see Table 5) and pea gravel (see Table 6) show that these drainage materials have a very limited fines fraction. Lack of fines makes the drainage materials more difficult to compact; therefore, the proctor data used to obtain the moisture content (θ) that is optimal for compaction was not provided for these materials.

Two soil samples were taken as the vault area was excavated. This material corresponds to the alluvial fill material. Soil classification data are provided in Table 7 and proctor compaction data are provided in Table 8, with the corresponding data plotted in Figure 5. These data indicate that the material between the vaults has a sufficient fines fraction to support traffic in this area. From a hydrogeologic perspective, the data indicate the residual moisture content (θ_r) should be higher than for the vault perimeter drainage material and drainage course material and that the drainage rate through the alluvial fill material should be much slower.

Table 4. Mechanical sieve data and proctor test data for surface road base and crushed gravel base course material.

ASTM D 2487 Classification: Drain Rock Sieve Size	Sample ID 15-5514 Percent Passing	Specification Percent Passing
1-in.		100
3/4-in.	100	90 to 100
1/2-in.	89	
3/8-in.	75	40 to 65
1/4-in.	59	
#4	50	30 to 50
#8	42	
#10	36	
#16	30	
#30	23	
#40	20	
#50	15	
#100	9	
#200	6.6	3 to 9

		Vendor Data Report # VDR-586147 Proctor Data				
	Point #	Percent Moisture (Water Content)	Dry Density (lb/ft^3)		Maximum Dry Density (lb/ft^3)	Optimum Moisture
Assumed Sp. Gr. 2.62	1	5.7	127.8	Uncorrected	134.3	8.3%
	2	7.4	133.5	ASTM D 4718 Correction	NA	NA
	3	9.1	133.8	Ag Found Correction	NA	NA
	4	10.7	129.8			
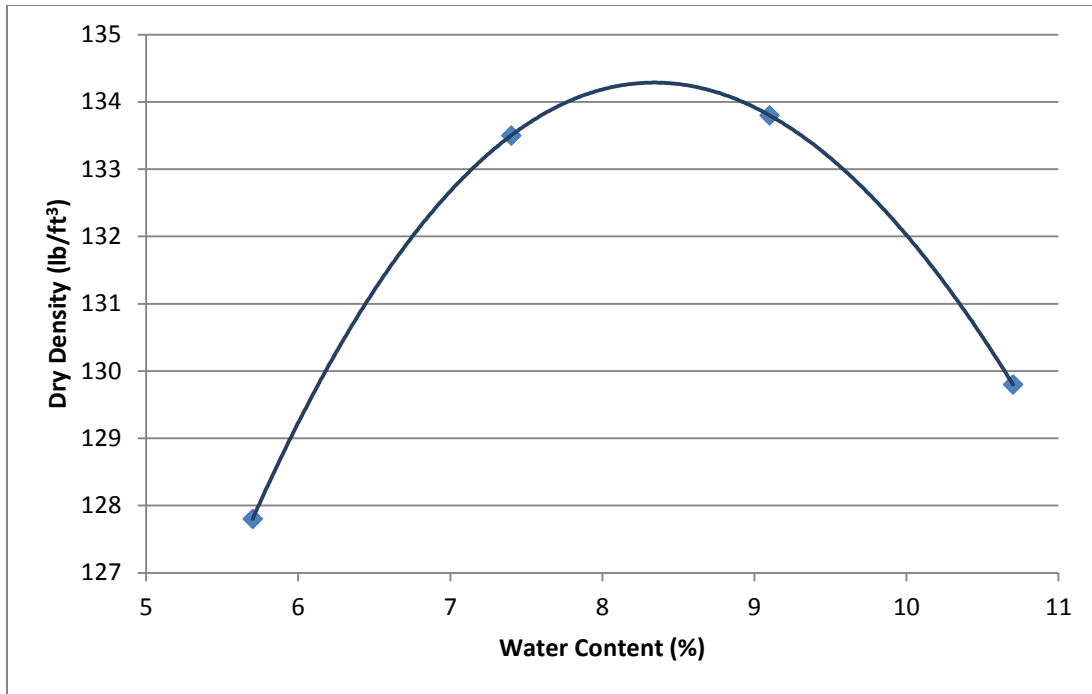
Figure 4. Proctor data for the surface road base and crushed gravel base course material.

Table 5. Mechanical test data for Vault Perimeter Drainage Material and Drainage Course Material used under and adjacent to the RH-LLW Disposal Facility vaults.

ASTM D 2487 Classification: Drain Rock		Sample ID		Specification
	15-5364	15-5374	15-5375	
Sieve Size		Percent Passing		Percent Passing
1-in.	100	100	100	100
3/4-in.	93	91	91	90 to 100
1/2-in.	55	53	53	
3/8-in.	32	33	32	20 to 55
#4	5	5	5	0 to 10
#8	2	3	3	0 to 5
#16	2	2	3	
#30	2	2	3	
#50	2	2	3	
#100	2	2	2	
#200	1.8	1.4	1.7	
Vendor Data Report # VDR-510841				

10

Table 6. Mechanical test data for pea gravel used for infill between the RH-LLW Disposal Facility vaults.

ASTM D 2487 Classification: Pea Gravel VDR-511096	Sample ID				Specification
Sieve Size	15-5372	15-5373	15-5393	15-5396	
	Percent Passing				
3/4-in.	100	100	100	100	100
1/2-in.	96	97	96	97	nominal
3/8-in.	58	61	55	55	
#4	5	7	3	4	
#8	4	4	3	3	
#10	3	4	2	3	
#16	3	4	2	2	
#30	3	4	2	2	
#40	3	4	2	2	
#50	3	4	2	2	
#100	3	3	2	2	
#200	2.5	2.7	2	2	
Coefficient of Uniformity	1.9	1.9	1.8	1.5	<2
Vendor Data Report # VDR-511096					

Table 7. Mechanical test data for alluvial fill material used for infill outside of the vault perimeter drainage material columns.

	Sample ID	
	15-5417	15-5416
	ASTM D 2487 Classification: Poorly Graded Gravel with Silt and Sand	ASTM D 2487 Classification: Poorly Graded Gravel with Sand
Sieve Size	Percent Passing	
6-in.		
5-in.		
4-in.		
3-in.	100	
2-in.	96	100
1.5-in.	92	97
1-in.	79	89
3/4-in.	71	79
1/2-in.	63	63
3/8-in.	57	53
1/4-in.		
#4	44	35
#8	36	27
#10	34	25
#16	30	22
#30	27	19
#40	25	16
#50	21	11
#100	15	4
#200	11.7	2.5
Vendor Data Report # VDR-510949		

Table 8. Proctor test data for alluvial fill material used for infill outside of the vault perimeter drainage material columns.

	Point Number	Percent Moisture (Water Content)	Dry Density (lb/ft^3)		Maximum Dry Density (lb/ft^3)	Optimum Moisture
			Sample # 15-5417			
Assumed Sp. Gr. 2.6	1	6.3	128.3	Uncorrected	130.5	8%
	2	8.1	130.5	ASTM D 4718 Correction	138.4	6.1%
	3	9.7	129.3	Ag Found Correction	NA	NA
	4	11.2	128.2			
			Sample # 15-5416			
Assumed Sp. Gr. 2.6	1	3.1	126.6	Uncorrected	134.5	7.4%
	2	5	129.4	ASTM D 4718 Correction	139.5	6.2%
	3	7.4	134.5	Ag Found Correction	NA	NA
	4	8.8	130.7			
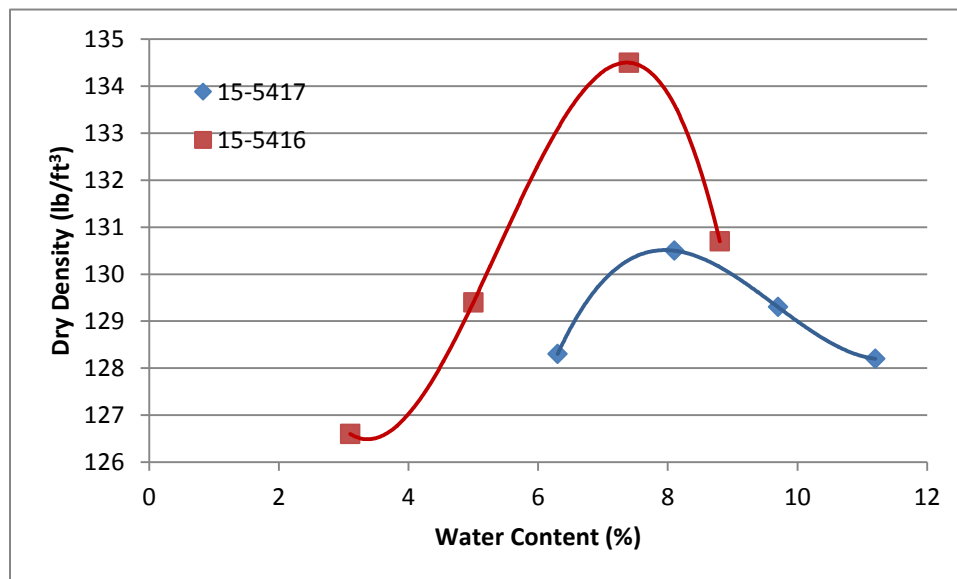
Figure 5. Proctor data for the alluvial fill material used outside of the vault perimeter drainage material columns.

5.   LABORATORY TEST DATA

During installation of the vault system, the RH-LLW Disposal Project required the installation subcontractor to provide information that allowed verification of the hydraulic performance of the drainage materials. Specifically, the subcontractor was required to obtain 10 random samples of the crushed gravel base course material and of the vault perimeter drainage material for hydraulic properties testing. The drainage course material specifications are the same as for the vault perimeter drainage material; therefore, duplicate sample collection and analysis were not required. Grab samples were taken along each of the five vault arrays shown in Figure 2 as the vaults were being installed. The grab samples

were sent to Daniel B. Stephens & Associates, Inc., and their typical hydraulic properties package (HPP) tests were performed to provide the following data:

- Saturated hydraulic conductivity, K_{sat} (cm/sec)

- Water content (volumetric) (a.k.a. moisture content), (θ [L^3L^{-3}]) (volume of water per bulk volume)

- Bulk density (ρ_b [g/cm^3])

- Total porosity, (ϕ=volume of pore space per bulk volume)

- Soil-water characteristic curve

- Unsaturated hydraulic conductivity, K (cm/sec) = $K_{rel} * K_{sat}$

- van Genuchten modeling parameters documented in van Genuchten (1980) and defined as:

$$\Theta(\theta, h) = [1/(1 + (\alpha h)^n]^m \times (\theta_s - \theta_r) + \theta_r \qquad (1)$$

$$K_{rel} = \frac{\{1 - (\alpha h)^n \times [1 + (\alpha h)^n]^{-m}\}^2}{1 + (\alpha h)^{m/2}} \qquad (2)$$

where:

$\Phi(\theta,h)$ = water retention curve [L^3L^{-3}]

h = suction pressure [L] or cm of water

θ_s = saturated water content [L^3L^{-3}]

θ_r = residual water content [L^3L^{-3}]

α = parameter related to the air entry suction, $\alpha > 0$ [L] or (cm^{-1} of water)

n = measure of the pore-size distribution, n>1 (dimensionless)

m = 1-1/n

K_{rel} = relative hydraulic conductivity, $0 \leq K_{rel} \leq 1$, (dimensionless).

Test results are provided in the following subsections for the vault perimeter drainage material, drainage course material, and the crushed gravel base course material.

5.1 Vault Perimeter Drainage and Drainage Course Materials

Laboratory test data for representative vault perimeter drainage material and drainage course material samples are provided in Tables 9 through 12. The material samples were taken along the vault arrays as the vaults were being installed by following the procedure documented in VDR-512339, "Vault Yard Aggregate Processing Field Sampling and Testing Procedure," QA-RHLLW.01, Revision 0, Delhur Industries, Inc. One random sample was obtained on an average of every 2,500 yd^3 of processed drainage course material for gradation testing in accordance with ASTM C 136. Gradation test results for the drainage materials are provided in Table 5 for comparison to the material test requirements in Table 3. Random samples of the vault perimeter drainage material and drainage course materials were sent to Daniel B. Stephens & Associates, Inc. for hydraulic properties testing.

5.1.1 Sample Preparation and Testing Notes

Test instructions required that a portion of each material sample be remolded into a 6-in. diameter testing ring to target 95% of the maximum dry bulk density at the optimum θ, based on the standard proctor compaction test results provided by the project. Because proctor compaction testing was not appropriate for the vault perimeter drainage material or drainage course material samples (due to the coarse particles and lack of fines), a portion of each of these samples was prepared for testing by placing

the material in the 6-in. diameter testing ring while shaking and tapping the test ring in order to encourage compact positioning of the particles.

In preparing the subsamples, particles larger than 3/4-in. were removed from the bulk material prior to remolding the subsamples. Oversized correction calculations were not provided because the removed fraction was less than 5% of the bulk sample mass.

The resultant dry density for the perimeter drainage samples is given in Table 9. This table contains the actual remold data, the volume change achieved after saturating the sample, and the volume change after drying the sample. As indicated in Table 9, no proctor data were provided for these samples and there was no volume change as a result of either saturating or drying the samples after remolding them. The volume change measurements post-saturation were obtained after saturated hydraulic conductivity testing. Volume change measurements were obtained throughout the hanging column and pressure plate testing. The "volume change post drying curve" values represent final sample dimensions after the last pressure plate point, with "---" indicating that no change in volume occurred. These data provide an indication there are relatively few fines in this material and the samples are stable.

The prepared subsamples were then subjected to the hydraulic properties analysis, saturated hydraulic conductivity testing, and the hanging column portion of moisture retention testing. Separate subsamples were obtained for the relative humidity chamber (i.e., high tension) portion of the moisture retention testing.

The saturated moisture content (θ_s) was set equal to the measured porosity for each of the samples. According to the test report, the saturated mass was calculated for sample "LCC North" to match 100% saturation. This sample has anomalously high θ, as indicated in Table 10, which is probably indicative of poor packing of the course particles in the relatively small diameter test ring. This sample was removed from the remaining analyses.

Table 10 contains the remolded θ, the dry bulk density, wet bulk density, calculated porosity (assuming a specific gravity value of 2.65), and the saturated hydraulic conductivity. Bulk density, θ, and calculated porosity were obtained using methods documented in ASTM D 7263 and ASTM D 2216. Hydraulic conductivity was collected using the constant head (i.e., rigid wall) method using the ASTM D 2434 (i.e., modified apparatus) method. For the samples tested, average values are provided with standard deviation and coefficient of variation. These statistical parameters were calculated after removing the LCC North 16-17 sample from the data set because of the anomalously high gravimetric θ.

Table 11 contains moisture retention data for each sample collected using the methods documented in ASTM D 6836 and the relative humidity (box) method developed by Campbell and Gee (1986). These moisture retention data were used to obtain the van Genuchten parameters reported by the testing agency shown in the first four columns of Table 12. The data were fit using unit weighting factors for each of the data sets for Equations 1 and 2 using the RETC code documented in van Genuchten (1991). As indicated by the very high alpha values for these data, these materials should readily drain under the relatively low infiltration conditions typical of INL (about 9 cm/year). The data, van Genuchten fits to the data, and calculated hydraulic conductivity are shown in Figure 6.

The moisture retention data are very consistent for all but one sample corresponding to the LCC North sample (i.e., red circles) as previously discussed. The average θ_s for the remaining samples, average θ_r, and all data were then used to parameterize the RETC code to obtain the fit to the data shown in Figure 6. Figure 6 (lower figure) contains the calculated relative hydraulic conductivity for each of the data sets (dashed lines) and the curve corresponding to the parameters derived for the fit to all data (solid line). The moisture characteristic and hydraulic conductivity relationship based on all data (thick dark line) is shown to adequately represent the remaining data and is used to parameterize the concrete longevity model for the RH-LLW Disposal Facility.

14

Table 9. Bulk density for the vault perimeter drainage material and drainage course materials.[a]

Date	Sample Location	Client Provided Proctor Data		Target Remold Parameters[1]		Actual Remold Data		Volume Change Post Saturation[2]		Volume Change Post Drying Curve[3]		% of Maximum Density
		Optimal Moisture Content (% g/g)	Maximum Dry Density (g/cm³)	Moisture Content (% g/g)	Dry Bulk Density (g/cm³)	Moisture Content (% g/g)	Dry Bulk Density (g/cm³)	Dry Bulk Density (g/cm³)	Percent Volume Change (%)	Dry Bulk Density (g/cm³)	Percent Volume Change (%)	
10/11/2016	LCC North	NA	NA	NA	Shake & Tap	7.8	1.63	1.63	–	1.63	–	NA
10/11/2016	West Center FTC	NA	NA	NA	Shake & Tap	1	1.66	1.66	–	1.66	–	NA
10/11/2016	West Center LCC	NA	NA	NA	Shake & Tap	1.4	1.72	1.72	–	1.72	–	NA
10/20/2015	Drain Rock (used near the PA Confirmation Vaults)	NA	NA	NA	Shake & Tap	0.6	1.61	1.61	–	1.61	–	100%
7/8/2016	55-Ton Vaults, SW Corner 3rd and 4th Rows	NA	NA	NA	Shake & Tap	0.7	1.67	1.67	–	1.67	–	100%
7/8/2016	PA Confirmation Vaults, NW Corner	NA	NA	NA	Shake & Tap	1	1.64	1.64	–	1.64	–	100%
7/8/2016	NUPAC Vaults, NW Corner, 5th Row	NA	NA	NA	Shake & Tap	1.5	1.67	1.67	–	1.67	–	100%
6/28/2017	Large Concept South	NA	NA	NA	Shake & Tap	1.4	1.60	1.60	–	1.60	–	100%
6/28/2017	FTC North	NA	NA	NA	Shake & Tap	2.0	1.63	1.63	–	1.63	–	100%
6/28/2017	FTC South	NA	NA	NA	Shake & Tap	1.1	1.68	1.68	–	1.68	–	100%
Average Dry Density										1.65		
Standard Deviation										0.036		
Coefficient of Variation										0.022		

a. Data from Vendor Data Report (VDR-521511 2016).
1. Target remold parameters: The material was remolded into a ring while shaking and tapping the test ring in order to encourage particles at the "as received" moisture content.
2. Volume change post saturation: volume change measurements were obtained after saturated hydraulic conductivity testing.
3. Volume change post drying curve: Volume change measurements were obtained throughout the hanging column and pressure plate testing. The volume change post-drying curve values represent the final sample dimensions after the last pressure plate point. "—" indicates no volume change occurred.

Table 10. Hydraulic properties and saturated hydraulic conductivity of the vault perimeter drainage material and drainage course material.

Sample Location	Remolded θ		Dry Bulk Density (g/cm³)	Wet Bulk Density (g/cm³)	Calculated Porosity (%)	Ksat (cm/sec)
	Gravimetric (%, g/g)	Volumetric (%, g/g)				
LCC North	7.8	12.7	1.63	1.76	38.5	1.1E-01
West Center FTC	1.0	1.7	1.66	1.68	37.4	9.3E-02
West Center LCC	1.4	2.4	1.72	1.74	35.1	7.8E-02
Drain Rock (used near the PA Confirmation Vaults)	0.6	1.0	1.61	1.62	39.4	1.2E-01
55-Ton Vaults, SW Corner 3rd and4th Rows	0.7	1.1	1.67	1.68	37.1	9.0E-02
PA Confirmation Vaults, NW Corner	1	1.7	1.64	1.66	38	9.1E-02
NUPAC Vaults, NW Corner, 5th Row	1.5	2.6	1.67	1.69	37	8.4E-02
ed	1.4	2.2	1.60	1.62	39.6	8.4E-02
FTC North	2.0	3.2	1.63	1.66	38.6	4.9E-02
FTC South	1.1	1.9	1.68	1.70	36.6	8.0E-02
Average Values[1]	1.19	1.98	1.65	1.67	37.64	8.5E-02
Standard Deviation	0.43	0.71	0.04	0.04	1.43	1.8E-02
Coefficient of Variation	0.37	0.36	0.02	0.02	0.04	2.2E-01

1. The statistical summary values were calculated after removing the LCC North sample because the high gravimetric moisture content indicates this sample was not adequately compacted into the sample ring during sample preparation.

Table 11. Moisture content and pressure head for the vault perimeter drainage material and drainage course material.

Sample Location	Pressure Head (-cm water)	θ (%, cm³/cm³)	θ (fraction)	Sample Location	Pressure Head (-cm water)	θ (%, cm³/cm³)	θ (fraction)
LCC North	0	38.6	0.386	PA Confirmation Vaults, Northwest Corner	0	38	0.38
	6	14.0	0.14		7	6.3	0.063
	15	13.2	0.132		14	3.9	0.039
	56	12.8	0.128		58	3.5	0.035
	160	12.7	0.127		176	3.1	0.031
	854,159	0.7	0.007		851,293	0.6	0.006
West Center FTC	0	36.7	0.367	NUPAC Vaults, Northwest Corner, 5th Row	0	37	0.37
	6	4.1	0.041		7	4.8	0.048
	14	3.4	0.034		15	4.1	0.041
	56	3.1	0.031		60	3.6	0.036
	167	3.0	0.03		180	3.3	0.033
	854,159	0.7	0.007		851,293	0.7	0.007
West Center LCC	0	33.9	0.339	Large Concept South	0	38.4	0.38
	6	6.2	0.062		6	4.0	0.04
	13	4.3	0.043		15	3.7	0.04
	55	3.8	0.038		60	3.2	0.03
	166	3.5	0.035		184	2.9	0.03
	854,159	0.8	0.008		848,426	1.0	0.01
Drain Rock (used near the PA Confirmation Vaults)	0	41.5	0.415	FTC North	0	39.6	0.40
	6	6.8	0.068		6	5.7	0.06
	10	3.4	0.034		14	3.7	0.04
	55	2.9	0.029		61	3.2	0.03
	187	2.6	0.026		182	2.9	0.03
	846,993	0.6	0.006		848,426	0.8	0.01
55-Ton Vaults, SW Corner 3rd and 4th Rows	0	36.6	0.366	FTC South	0	41.1	0.41
	7	7.4	0.074		6	8.7	0.09
	11	4.7	0.047		13	5.0	0.05
	59	4	0.04		58	4.4	0.04
	175	3.5	0.035		184	3.9	0.04
	851,293	0.7	0.007		848,426	0.9	0.01

Table 12. van Genuchten fits to the vault perimeter drainage and drainage course materials moisture retention data.

Sample Location	RETC fitted van Genuchten Parameters (by D.B Stephens) Using Uniform Weighting Across the Moisture Content Range				Correction for Oversize Fractions	
	α (cm^{-1})	n	θ_r (%vol)	θ_s (%vol)	θ_r (%vol)	θ_s (%vol)
LCC North	215.7519	1.1276	0	38.52	---	---
West Center FTC	19,638.2911	1.1834	0	37.37	---	---
West Center LCC	33,985.6743	1.1515	0	35.12	---	---
Drain Rock (used near the PA Confirmation Vaults)	19.0383	1.4413	0.85	41.45	NA	NA
55-Ton Vaults, SW Corner 3rd and4th Rows	514.0667	1.2128	0	36.61	---	---
PA Confirmation Vaults, NW Corner	1,000.8122	1.2168	0	38.07	---	---
NUPAC Vaults, NW Corner, 5th Row	8,697.2212	1.1806	0	37	0	35.23
Large Concept South	6,317.1	1.1998	0.00	38.00	0	35.99
Mod FTC North	8,318.1	1.1894	0.00	39.96	---	---
Mod FTC South	168.0	1.2417	0.00	41.06	---	---
RETC fitting parameters using all of the data except the LCC North sample and average θ_r and θ_s values	10,532.27524	1.17514	0.085	0.3733		
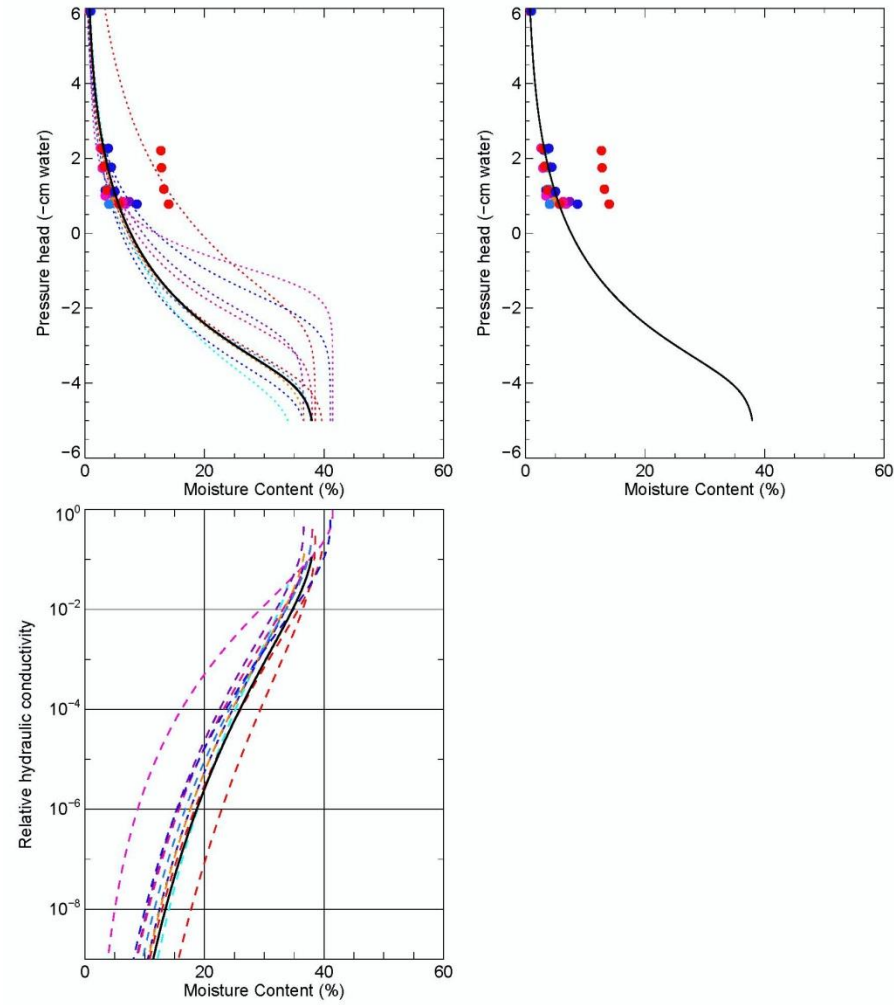
Figure 6. Vault perimeter drainage and drainage course material moisture retention data and van Genuchten parameter fit to each of the data sets (upper left), van Genuchten parameter fit to all (except outlier dataset) of the data (upper right), and calculated hydraulic conductivity (lower inset) for each data set (dashed) and for all data combined (solid line).

5.2   Crushed Gravel Base Course Material

Laboratory test data for representative crushed gravel base course material samples are provided in Tables 13 through 16. Material samples were taken along the vault arrays as the vaults were being installed following the procedure documented in VDR-512339. One random sample was obtained on an average of every 2,500-yd^3 of processed drainage course material for gradation testing in accordance with ASTM C136. Gradation test results for the drainage materials are provided in Table 5 for comparison to the material test requirements in Table 3. All random samples of the crushed gravel base course material were sent to Daniel B. Stephens & Associates, Inc. for hydraulic properties testing.

5.2.1   Sample Preparation and Testing Notes

Test instructions required that a portion of each material sample be remolded into a 6-in. diameter testing ring to target 95% of the maximum dry bulk density at the optimum θ, based on the standard proctor compaction test results provided by the project. The proctor test results for this material are shown in Table 13, Columns 3 and 4. The target remold parameters, shown in Columns 5, 6, and 7 correspond to 95% of the maximum density and optimal θ to be consistent with installation requirements for this material at the RH-LLW Disposal Facility vaults.

In preparing the subsamples, particles larger than 3/4-in. were removed from the bulk material prior to remolding the subsamples. Oversized correction calculations were not provided because the removed fraction was less than 5% of the bulk sample mass. After preparation of the subsamples, the target remold parameters were met as shown in Columns 8, 9, and 10 of Table 13.

Even though this material contains a higher volume percent of fine material than the vault perimeter drainage material and drainage course material did, the volume change measurements shown in Table 13 are equal to the "volume change post drying curve" values. This similarity provides an indication that the material contains very little clay fraction and remold of the material resulted in a stable sample.

The prepared subsamples were then subjected to the hydraulic properties analysis, saturated hydraulic conductivity testing, and hanging column portion of the moisture retention testing. Separate subsamples were obtained for the relative humidity chamber (i.e., high tension) portion of moisture retention testing.

Table 14 contains the remolded θ, the dry bulk density, wet bulk density, calculated porosity (assuming a specific gravity value of 2.65), and the saturated hydraulic conductivity. Bulk density, θ, and calculated porosity were obtained using methods documented in ASTM D 7263 and ASTM D 2216. Hydraulic conductivity was collected using the constant head (i.e., rigid wall) method using the ASTM D 2434 (i.e., modified apparatus) method. For the samples tested, average values are provided with standard deviation and coefficient of variation. These statistical parameters were calculated using all available data for this material.

Table 15 contains moisture retention data for each sample collected using the methods documented in ASTM D 6836 and the relative humidity (box) method developed by Campbell and Gee (1986). These moisture retention data were used to obtain the van Genuchten parameters reported by the testing agency shown in the first four columns of Table 16. The data were fit by D.B. Stephens & Associates, Inc. using unit weighting factors for each of the data sets for Equations 1 and 2 using the RETC code documented in van Genuchten (1991) (see Columns 2 through 5).

In contrast to the vault perimeter drainage material and drainage course material, the α values for these data are much more reflective of a sandy-soil type material. However, they are still high enough that this material should readily drain under the relatively low infiltration conditions typical of INL (about 9 cm/year). Therefore, weighting the low end of the retention curve is appropriate. The data and the fits to the data are shown in the upper left inset of Figure 7.

The data are very consistent for all tested samples as indicated by the closely aligned data in Figure 7 for both moisture retention, calculated hydraulic conductivity, and variance and coefficient of variation for data given in Tables 12 through 15. The average θ_s and θ_r (i.e., near zero for these samples) and all data were then used to parameterize the RETC code to obtain the fit to the data shown by the dark line in the insets of Figure 7. This fit to the data will be used to parameterize the concrete longevity model for the RH-LLW Disposal Facility.

Figure 7 (lower figure) contains the calculated hydraulic conductivity for each data set (dashed lines) and the average curve corresponding to the parameters derived for the fit to all data (solid line). The calculated hydraulic conductivity relationship using the average end-point θ is shown to adequately represent the crushed gravel base course material data.

5.3   Pea Gravel

Laboratory test data were not obtained for the pea gravel infill between the vaults. Because the pea gravel contains no fine textured sand or clay (see Table 6) and the upper size fraction is similar to that of the vault perimeter drainage material and drainage course material (see Table 5), it will be assumed that the hydraulic characteristics, including Ksat and the van Genuchten relationships, are the same.

5.4   Alluvial Fill Material

Laboratory test data were not obtained for the alluvial fill material placed between the vault perimeter drainage material columns. As indicated in Table 7, there is a significant proportion of this material is sized in excess of 3/4-in. This material would be difficult to test and obtain representative data for using the 6-in. testing ring. Data for this material were collected using a combination of advanced tensiometers (ATs) to measure the water tension and water content reflectometer (WCR) probes to measure the corresponding θ during infiltration tests. These data are discussed in Section 6.

5.5   Non-Woven Geotextile Material

Laboratory test data were not obtained for the very thin non-woven geotextile material. However, the product specifies a permittivity of 1.5 per second. Permittivity refers to the cross-plane coefficient of permeability when applied to geotextiles. It is equal to cross-plane hydraulic conductivity under a unit gradient divided by thickness. For the material used, the water flow rate under a unit gradient is 110 gallon/minute/ft^2, which is equal to a hydraulic conductivity of 7.5 cm/second (product data sheet for US 160NW by Construction Geosynthetics, https://www.usfabricsinc.com/products/us-160nw, visited January 2017).

Table 13. Bulk density for the crushed gravel base course material.

Vendor Data Report	Sample Location	Contractor-Provided Proctor Data		Target Remold Parameters			Actual Remold Data			Volume Change Post Saturation		Volume Change Post Drying Curve	
		Optimal Moisture Content (% g/g)	Maximum Dry Density (g/cm3)	Moisture Content (% g/g)	Dry Bulk Density (g/cm3)	Percent of Maximum Density	Moisture Content (% g/g)	Dry Bulk Density (g/cm^3)	Percent of Maximum Density	Dry Bulk Density (g/cm^3)	Percent of Maximum Density	Dry Bulk Density (g/cm^3)	Percent of Maximum Density
10/11/2016	NUPAC West Center	6.6	1.97	6.6	1.87	95	7	1.86	94.6	1.86	94.6	1.86	94.6
10/11/2016	NUPAC East Center	6.6	1.97	6.6	1.87	95	6.5	1.87	95.1	1.87	95.1	1.87	95.1
10/11/2016	55-Ton North	6.6	1.97	6.6	1.87	95	6.8	1.87	95.0	1.87	95.0	1.87	95.0
1/8/2016	Road Base	6.6	1.97	6.6	1.87	95	6.3	1.88	95.4	1.88	95.4	1.88	95.4
8/16/2017	NuPac North #1			AR			1.9	1.81		1.93	106.4	1.92	105.9
8/16/2017	NuPac North #2			AR			2.9	1.95		1.95	100.0	1.95	100.0
8/16/2017	NuPac South #1			AR			2.7	1.76		1.94	110.3	1.92	109.1
8/16/2017	NuPac South #2			AR			3.1	1.98		1.98	100.0	1.98	100.0
8/16/2017	LCC North #1			AR			3.3	1.71		1.91	112.0	1.89	111.0
8/16/2017	LCC North #2			AR			3.1	1.91		1.91	100.0	1.91	100.0
8/16/2017	LCC South #1			AR			6.8	1.74		1.89	108.1	1.87	107.0
8/16/2017	LCC South #2			AR			6.3	1.94		1.94	100.0	1.94	100.0
8/16/2017	LCC East #1			AR			4.5	1.74		1.87	107.6	1.87	107.7
8/16/2017	LCC East #2			AR			4.0	1.99		1.99	100.0	1.99	100.0
8/16/2017	FTC North #1			AR			2.3	1.78		1.95	109.1	1.94	108.6
8/16/2017	FTC North #2			AR			3.1	1.97		1.97	100.0	1.97	100.0
8/16/2017	FTC South #1			AR			2.3	1.75		1.94	110.6	1.94	110.6
8/16/2017	FTC South #2			AR			2.9	1.82		1.82	100.0	1.82	100.0
Average												1.91	102
Standard Deviation												0.05	5.7
Coefficient of Variation												0.02	0.1

AR = as received.

Table 14. Saturated hydraulic conductivity and porosity for the crushed graved base course.

Sample Location	Remolded θ Gravimetric (%, g/g)	Volumetric (%, g/g)	Dry Bulk Density (g/cm³)	Wet Bulk Density (g/cm³)	Calculated Porosity (%)	Ksat (cm/sec)
NUPAC West Center	7	13.1	1.66	1.99	29.8	7.0E-02
NUPAC East Center	6.5	12.2	1.87	1.99	29.5	8.8E-02
55-Ton North	6.8	12 .7	1.87	1.99	29.5	7.1E-02
Road Base	6.3	11.9	1.88	1.99	30.5	1.1E-01
NuPac North #1	1.9	3.5	1.81	1.85	31.6	5.6E-02
NuPac North #2	2.9	5.6	1.95	2.01	26.3	3.0E-02
NuPac South #1	2.7	4.7	1.76	1.81	33.6	6.1E-02
NuPac South #2	3.1	6.2	1.98	2.04	25.3	3.0E-02
LCC North #1	3.3	5.7	1.71	1.76	35.6	5.7E-02
LCC North #2	3.1	6.0	1.91	1.97	28.0	6.0E-02
LCC South #1	6.8	11.9	1.74	1.86	34.2	3.9E-02
LCC South #2	6.3	12.3	1.94	2.07	26.7	7.1E-02
LCC East #1	4.5	7.9	1.74	1.82	34.3	5.7E-02
LCC East #2	4.0	8.0	1.99	2.07	24.9	6.4E-02
FTC North #1	2.3	4.1	1.78	1.83	32.6	7.9E-02
FTC North #2	3.1	6.0	1.97	2.03	25.8	2.8E-02
FTC South #1	2.3	4.0	1.75	1.79	34.0	8.0E-02
FTC South #2	2.9	5.3	1.82	1.88	31.2	6.1E-02
Average Values	4.2	7.6	1.8	1.9	30.2	6.2E-02
Standard Deviation	1.8	3.4	0.1	0.1	3.4	2.1E-02
Coefficient of Variation	0.4	0.4	0.1	0.1	0.1	3.4E-01

Table 15. Moisture content and pressure head for the crushed gravel base course material.

Sample Location	Pressure Head (-cm water)	θ (%, cm³/cm³)	θ (fraction)	Sample Location	Pressure Head (-cm water)	θ (%, cm³/cm³)	θ (fraction)
NUPAC West Center	0	31.2	0.312	LCC North #1	0	27.9	0.279
	6	15.3	0.153		7	18.0	0.180
	13	12.8	0.128		20	13.5	0.135
	52	9.6	0.096		54	9.2	0.092
	161	7.5	0.075		215	7.9	0.079
	854,159	0.9	0.009		1,122	5.4	0.054
NUPAC East Center	0	30.2	0.302		4,283	2.8	0.028
	6	16.5	0.165		28,656	1.7	0.017
	12	12.3	0.123		149,095	1.1	0.011
	51	8.8	0.088		855,592	0.4	0.004
	165	6.8	0.068	LCC North #2	0	28.0	0.280
	854,159	1	0.01		9	18.8	0.188
55-Ton North	0	28.5	0.285		16	14.6	0.146
	6	15.0	0.15		49	8.9	0.089
	14	12.9	0.129		195	6.7	0.067
	49	10.1	0.101		1,530	4.4	0.044
	164	7.9	0.079		8,158	2.4	0.024
	854,159	1.0	0.01		92,700	1.2	0.012
Road Base	0	33.0	0.33		675,210	0.8	0.008
	6	13.4	0.134		855,592	0.4	0.004
	12	10.5	0.105	LCC South #1	0	28.8	0.288
	53	7.5	0.075		7	18.9	0.189
	53	7.5	0.075		15	14.4	0.144
	185	5.7	0.057		53	10.4	0.104
	918	1.7	0.017		195	7.9	0.079
	15,093	0.9	0.009		816	3.3	0.033
	151,134	0.4	0.004		6,017	1.4	0.014
	841,261	0.3	0.003		30,798	0.8	0.008
					95,555	0.6	0.006
					855,592	0.2	0.002

Sample Location	Pressure Head (-cm water)	θ (%, cm^3/cm^3)	θ (fraction)	Sample Location	Pressure Head (-cm water)	θ (%, cm^3/cm^3)	θ (fraction)
NuPac North #1	0	27.2	0.272	LCC South #2	0	26.7	0.267
	7	20.7	0.207		6	14.1	0.141
	17	18.2	0.182		14	11.9	0.119
	51	11.3	0.113		53	10.0	0.100
	200	8.3	0.083		201	7.8	0.078
	2,040	4.8	0.048		918	2.8	0.028
	7,750	3.0	0.030		7,139	1.2	0.012
	54,355	1.7	0.017		67,001	0.7	0.007
	172,346	1.3	0.013		790,243	0.4	0.004
	855,592	0.4	0.004		855,592	0.2	0.002
NuPac North #2	0	26.3	0.263	LCC East #1	0	29.4	0.294
	8	19.9	0.199		7	16.3	0.163
	14	17.5	0.175		13	12.8	0.128
	43	10.3	0.103		52	8.6	0.086
	200	7.1	0.071		205	6.8	0.068
	3,059	3.7	0.037		1,122	2.9	0.029
	13,563	2.5	0.025		3,671	1.7	0.017
	85,765	1.5	0.015		31,104	0.8	0.008
	671,946	1.1	0.011		181,422	0.5	0.005
	855,592	0.4	0.004		855,592	0.2	0.002
NuPac South #1	0	26.8	0.268	LCC East #2	0	24.9	0.249
	7	20.6	0.206		5	14.7	0.147
	13	16.1	0.161		13	10.2	0.102
	51	10.1	0.101		57	7.7	0.077
	210	7.5	0.075		205	6.5	0.065
	1,530	4.4	0.044		1,530	2.4	0.024
	6,221	2.8	0.028		6,425	1.2	0.012
	50,786	1.5	0.015		51,398	0.7	0.007
	179,791	1.1	0.011		430,967	0.4	0.004
	855,592	0.4	0.004		855,592	0.2	0.002

Sample Location	Pressure Head (-cm water)	θ (%, cm³/cm³)	θ (fraction)	Sample Location	Pressure Head (-cm water)	θ (%, cm³/cm³)	θ (fraction)
NuPac South #2	0	25.3	0.253	FTC North #1	0	26.5	0.265
	6	18.9	0.189		7	19.4	0.194
	13	15.4	0.154		17	16.3	0.163
	45	10.1	0.101		54	11.8	0.118
	195	7.4	0.074		200	8.3	0.083
	1,734	4.0	0.040		2,142	5.3	0.053
	8,668	2.6	0.026		5,915	2.7	0.027
	93,108	1.3	0.013		23,761	1.7	0.017
	601,070	0.9	0.009		91,782	1.2	0.012
	855,592	0.4	0.004		855,592	0.3	0.003
LCC North #1	0	27.9	0.279	FTC North #2	0	25.8	0.258
	7	18.0	0.180		7	19.5	0.195
	20	13.5	0.135		13	16.9	0.169
	54	9.2	0.092		46	10.6	0.106
	215	7.9	0.079		202	7.0	0.070
	1,122	5.4	0.054		2,855	3.9	0.039
	4,283	2.8	0.028		7,139	2.5	0.025
	28,656	1.7	0.017		42,832	1.5	0.015
	149,095	1.1	0.011		608,719	0.9	0.009
	855,592	0.4	0.004		855,592	0.3	0.003
LCC North #2	0	28.0	0.280	FTC South #1	0	26.9	0.269
	9	18.8	0.188		7	20.7	0.207
	16	14.6	0.146		15	16.3	0.163
	49	8.9	0.089		55	10.9	0.109
	195	6.7	0.067		195	7.8	0.078
	1,530	4.4	0.044		816	3.5	0.035
	8,158	2.4	0.024		6,935	2.0	0.020
	92,700	1.2	0.012		43,647	1.2	0.012
	675,210	0.8	0.008		123,702	0.9	0.009
	855,592	0.4	0.004		855,592	0.3	0.003

Sample Location	Pressure Head (-cm water)	θ (%, cm³/cm³)	θ (fraction)	Sample Location	Pressure Head (-cm water)	θ (%, cm³/cm³)	θ (fraction)
LCC South #1	0	28.8	0.288	FTC South #2	0	31.2	0.312
	7	18.9	0.189		6	15.6	0.156
	15	14.4	0.144		13	11.1	0.111
	53	10.4	0.104		51	7.5	0.075
	195	7.9	0.079		198	5.8	0.058
	816	3.3	0.033		1,224	2.9	0.029
	6,017	1.4	0.014		12,748	1.7	0.017
	30,798	0.8	0.008		79,748	1.0	0.010
	95,555	0.6	0.006		620,752	0.6	0.006
	855,592	0.2	0.002		855,592	0.3	0.003
LCC South #2	0	26.7	0.267				
	6	14.1	0.141				
	14	11.9	0.119				
	53	10.0	0.100				
	201	7.8	0.078				
	918	2.8	0.028				
	7,139	1.2	0.012				
	67,001	0.7	0.007				
	790,243	0.4	0.004				
	855,592	0.2	0.002				

Table 16. van Genuchten fits to the moisture retention data for the crushed gravel base course material.

Sample Location	RETC Fitted van Genuchten Parameters (by D.B Stephens) Using Uniform Weighting Across the Moisture Content Range				Correction for Oversize Fractions	
	α (cm^{-1})	n	θ_r (%vol)	θ_s (%vol)	θ_r (%vol)	θ_s (%vol)
NUPAC West Center	3.2806	1.2228	0	29.83	—	—
NUPAC East Center	1.3493	1.2975	0.65	29.45	—	—
55-Ton North	4.2864	1.2035	0	29.54	—	—
Road Base	3.1994	1.3008	0	33.05	—	—
NuPac North #1	0.2430	1.3102	0.25	27.20	—	—
NuPac North #2	0.1925	1.4043	1.02	26.30	—	—
NuPac South #1	0.2782	1.3414	0.49	26.76	—	—
NuPac South #2	0.3669	1.3042	0.23	25.26	—	—
LCC North #1	0.6750	1.2745	0.00	27.92	—	—
LCC North #2	0.3128	1.3870	0.78	27.97	—	—
LCC South #1	0.4426	1.3344	0.00	28.83	—	—
LCC South #2	1.4800	1.2599	0.00	26.68	—	—
LCC East #1	0.8785	1.3201	0.00	29.35	—	—
LCC East #2	1.2823	1.2837	0.00	24.88	—	—
FTC North #1	0.3293	1.2781	0.00	26.52	—	—
FTC North #2	0.2513	1.3428	0.46	25.80	—	—
FTC South #1	0.2273	1.3528	0.00	26.94	—	—
FTC South #2	1.6183	1.3197	0.23	31.22	—	—
Fitting parameters using all data and average θ_r and θ_s values	2.24323	1.26302	0.002	0.28		
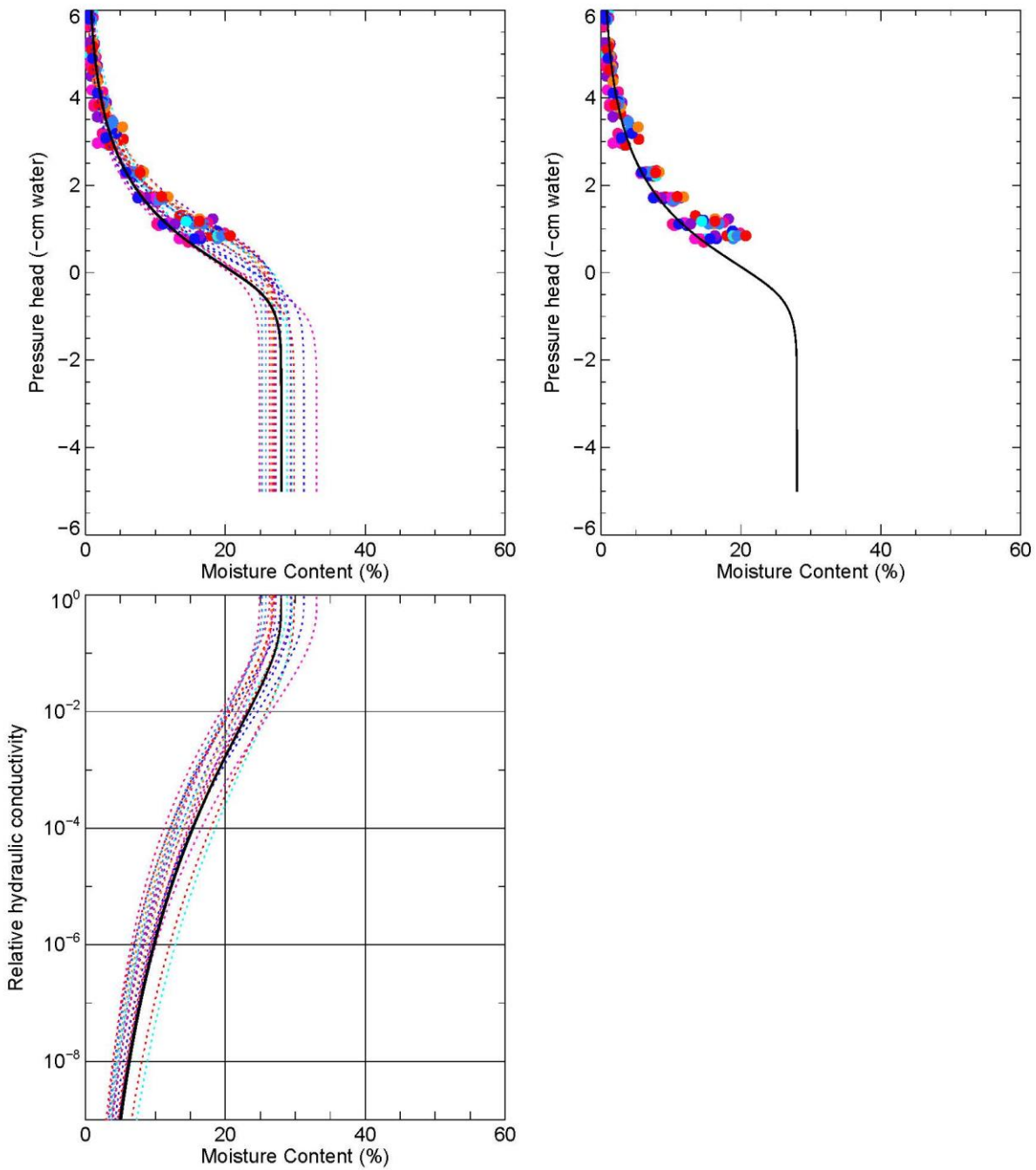
Figure 7. Moisture retention data for crushed gravel base course material and van Genuchten parameter fit to each of the data sets (upper left), van Genuchten parameters fit to all data (upper right), and calculated hydraulic conductivity (lower inset) for each data set (dashed) and for all data combined (solid line).

6. FIELD CHARACTERIZATION TEST RESULTS

This section provides the field characterization test results obtained for the PA confirmation vault array. The PA confirmation vaults were installed specifically to enable monitoring and collection of hydraulic and concrete performance data. As shown in the as-built monitoring system document (INL 2017) and in the following sections, the instrumentation at this vault array is provided along the entire height of the vaults and to the depth of the upper basalt contact allowing vertical resolution of infiltrating water. Field characterization tests were conducted initially at this array because of the high data collection capability and because during construction, the vault arrays were installed beginning at the west end of the vault yard and ending with installation of the MFTC and LCC vaults on the east end of the vault yard. Instruments installed at the other vault arrays (INL 2017) are focused on compliance monitoring for the groundwater exposure pathway. Field characterization tests were conducted at locations along the vault arrays that will receive waste as the monitoring system was installed at those locations. Those tests were conducted to determine the overall variability in the vault system hydraulic drainage system performance as opposed to focusing on detailed performance. This objective of determining system variability was met by determining the time-arrival of infiltration fronts and residual moisture content in the drainage course and Stratum II alluvium as opposed to higher resolution data provided at the PA Confirmation vault array. These courser-resolution test data are provided in Appendices A and B.

6.1 Characterization Test Overview

This section describes two characterization tests conducted near the PA Confirmation Vaults at the RH-LLW Disposal Facility. The characterization tests were designed to apply water uniformly over a 64-ft^2 area at a constant rate for application periods of 24 hours and 8 hours. During the tests and for several months following the end of water application, subsurface instruments installed in instrumented tubes and an instrumented borehole were used to collect moisture retention data in the vault perimeter drainage material, drainage course material, alluvium fill material, and Stratum III alluvium just above the first basalt layer in the vadose zone. Data were stored during the tests using onsite data loggers. This report provides the test design description and infiltration characterization test data.

6.2 Test Location

Characterization tests were conducted adjacent to the PA Confirmation Vaults that are located in the southwest corner of the vault array area (see Figure 2 and Figure 8). These vaults are approximately 7.76 m (25-ft-3-in.) tall from the top of the plug to the bottom of the hexagonal base plate (see Figure 1). The vaults sit on a 45.72 cm (18-in.) thick layer of the drainage course material. The width of a side perimeter block at the narrowest point is 30.5 cm (12-in.) and at the widest point it is 78.74 cm (2-ft-7 in.).

The surface road base starts at the top of the plug and is 30.5-cm (12-in.) thick and extends laterally well beyond the area influenced by the characterization test. The crushed gravel base course material below the surface road base is 2.1-m (7-ft thick) and extends a minimum of 2 ft (61.96 cm) beyond the outer edge of the perimeter block where it meets the geotextile material separating the crushed gravel base course material from the alluvial fill material. Therefore, while adjacent to the vault perimeter block, the crushed gravel base course material is approximately 61-cm (2-ft) wide; below the block it ranges from 91.5 to 140-cm (3-ft to 4-ft-7-in.) wide. The vault perimeter drainage material extends from the edge of the vault wall to a minimum width of 2-ft beyond the outer edge of the perimeter block. Therefore, the width of the vault perimeter drainage material ranges from 91.5 to 140-cm (3-ft to 4-ft-7-in.) wide. Below the vaults, the drainage course material extends 3.05 m (10 ft) beyond the edge of the hexagonal base plate where it meets the alluvial fill material.
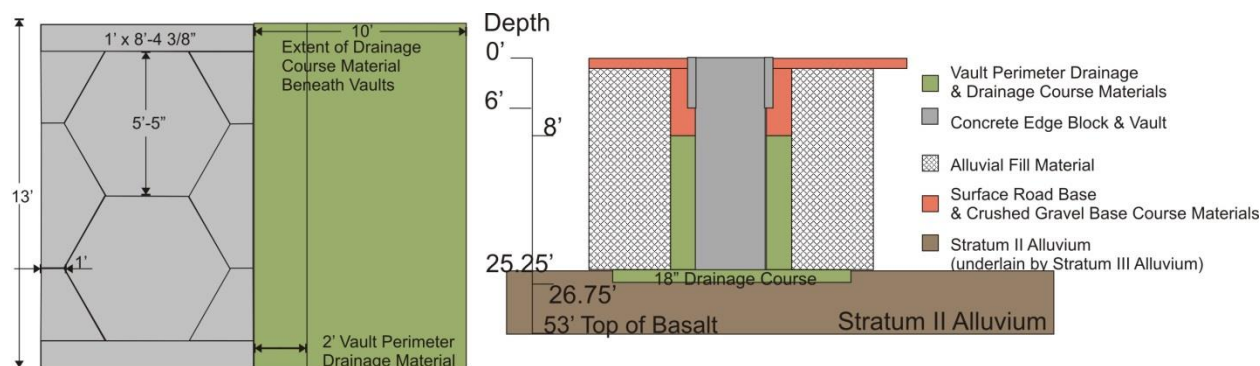
Figure 8. Layout of the PA Confirmation Vaults showing the extent of surface road base, crushed gravel base course material, vault perimeter drainage material, drainage course material, alluvial fill material, and surficial alluvium.

6.3   Test Design

During the first 24-hour test, approximately 1,900 gallons of potable water was applied to an 8-ft-×-8-ft area using a constant volume 12-volt direct current (VDC) pump and a series of low volume spray heads. The pump was selected to provide the necessary volume of water over a 24-hour period, reducing the time onsite. The volume of water to be applied was determined based on model simulations using approximate parameters for the geologic materials and characterization requirements. During the second 8-hour test, approximately 1,000 gallons of water was applied. The difference in application duration was selected based on infiltration behavior observed during the first longer-duration test.

The same test apparatus and configuration was used for both tests. The equipment used is summarized in Table 17. The configuration of the pump, spray heads, and connecting hardware is shown in Figure 9. The test apparatus consisted of two poly tubes forming separate water supply loops connected to a water inlet hose using a "Y" connector that was connected to a 12-VDC Shurflo 2080 diaphragm pump (agricultural spray pump). The pump was used to pump unfiltered water from a 2,000-gallon stock tank that was filled using a water truck. The 12-VDC pump was supplied with power from 12-volt batteries that were recharged using a gas generator. The test apparatus was protected from the weather (e.g., wind/rain) by placing it in a 2-ft tall plywood box that was open at the bottom and covered with strips of plywood to minimize water loss via evaporation.

6.4   Characterization Test Procedure

1. The subsurface instruments were previously installed as the vaults were being backfilled (illustrated in Section 6.5). The cabling was brought from the instruments through instrumented tubes into the protective box mounted on top of the surface casing. The data loggers were placed in the protective box and connected to the instrument leads and a solar panel providing power to the data loggers.

2. Prior to the characterization test, the data loggers were inspected to ensure the batteries were charged, the on-logger memory was empty, and they were ready to receive data from the instruments.

3. The test area was cleared of debris (see Figure 10 for the test area).

4. The test area was scarified to a depth of approximately 6-in. in order to allow ready infiltration of water. Scarification was performed over a 9 x 9-ft area encompassing the 8 x 8-ft test area. The test area was leveled during this process to minimize the potential for surface run-off or local ponding in the test area.

5. An 8 x 8 x 2-ft high test box made of plywood was placed over the test area encompassing the instrumented tubes and borehole. The test box was set into a shallow (about 2-in. deep) trench to allow the box to sit level on the surface road base. The test box was leveled at this time.

6. The outer loop containing the pre-assembled tubing and four 180-degree spray heads was centered in the box (Figure 10), with the spray directed into the box. The outer loop sits 3 to 4-in. from the inner perimeter of the wood box. The loop was secured in place using metal stakes.

7. The inner loop containing the pre-assembled tubing and 360-degree spray heads was then centered in the box (Figure 10). The loop was secured in place using the supplied metal stakes.

8. Water was obtained from the INL Central Facilities Area potable water supply. This water supply was used throughout the backfill of the PA Confirmation Vaults during construction for dust suppression. The truck was parked close enough to the test area to allow siphon hoses to be used to fill the stock tank. Water levels in the stock tank were regulated using a float valve.

9. The two water loops were connected to the 12-VDC pump outlet fitting using the supplied "Y" connector. The pump inlet side was connected to a hose placed in the stock tank.

10. A garden hose was inserted into the top of the tank truck with the hose weighted to keep it from floating in the water. A siphon was started from the tank truck, and connected to a float valve mounted on the side of the stock tank. The stock tank was then filled to the float level.

11. A plywood lid was placed over the test box and screwed on using supplied screws to keep the water in the test area.

12. The pump was connected to the 12-VDC battery using the supplied cable. The pump is self-priming and water arrived almost immediately at the spray heads. The time was noted in the logbook.

13. As the test was started, and periodically throughout the test, the following occurred:

    - Orientation of the spray was visually inspected to ensure optimal spray uniformity across the box and tubing leaks were stopped if any were found.
    - The battery charge was measured and, if necessary, the battery was recharged using a generator.
    - Water flow rate was measured to ensure the pumps were functioning at the expected rate and replaced if necessary. Use of the siphon/float valve system allowed turning the water supply off periodically during the test to allow measurement of the water discharge rate. First the hose was kinked to stop flow to the valve without losing the siphon. The water level in the stock tank was measured and the water depth was recorded. The pump continued to apply water to the test apparatus for a recorded time period, typically 1/2-hour. The stock tank water level was re-measured and recorded in order to calculate the water application rate. Then, the hose was unkinked, allowing the water level to rise back to the float level in the stock tank.

14. The pumps were operated for 24 hours during the first test and for 8 hours during the second test. At the end of the test period, the test apparatus was carefully disassembled, allowing it to be reused for the subsequent characterization tests.

15. Data collection continued until the drain out was observed at the deepest monitoring location and the θ achieved a steady-state background condition in the vault perimeter drainage material, drainage course material, and alluvial fill material.

Table 17. Test apparatus components.

Part	Purpose	Part #	Quantity	Specifications
180-degree spray heads	Provide water along perimeter of test area	DIG B10C (pack of 5)	4	180-degree spray pattern 0 to 15.7 GPH 0 to 2.7-ft diameter at 30 psi
360-degree spray heads	Provide water across interior of test area	DIG B05B (pack of 5)	5	180-degree spray pattern 0 to 15.7 GPH 0 to 2.7-ft diameter at 30 psi
1/2-in. poly tubing	Connect sprayers to pump and filters	B36	100-ft roll	1/2-in. diameter 60-psi operating pressure 2-gpm, 4.2-psi head loss
1/2-in. compression fittings	Connect sprayers to pump and filters		20	0.45-in. outer diameter
3/4-in. swivel compression fitting	Connect tubing to pump		1	
90-degree elbows	Connect tubing		7	
12-VDC pump	Provide water at constant rate	Shurflo 2088-343-135	1	
Y-connector	Split flow into the two tubing circuits	D52B 3/4-in. heavy duty "Y" plastic hose end splitter	1	Shut-off valve controls two outlets from a 3/4-in. faucet or garden hose
4,000-gallon water truck	Provide water			
Generator	Recharge batteries			
1/2-in. plywood 2-ft × 8-ft	Contain water		24 ft	
1/2-in. plywood sheets for roof	Contain water		Two 4 x 8 sheets	
Screws	Screw box together	3-in. deck screws	20	
Steel stakes	Hold tubing in place		40	4-in. stakes for 1/2-in. tubing
Electrical adaptor	Connect pump to battery		1	Eliminates direct battery connections
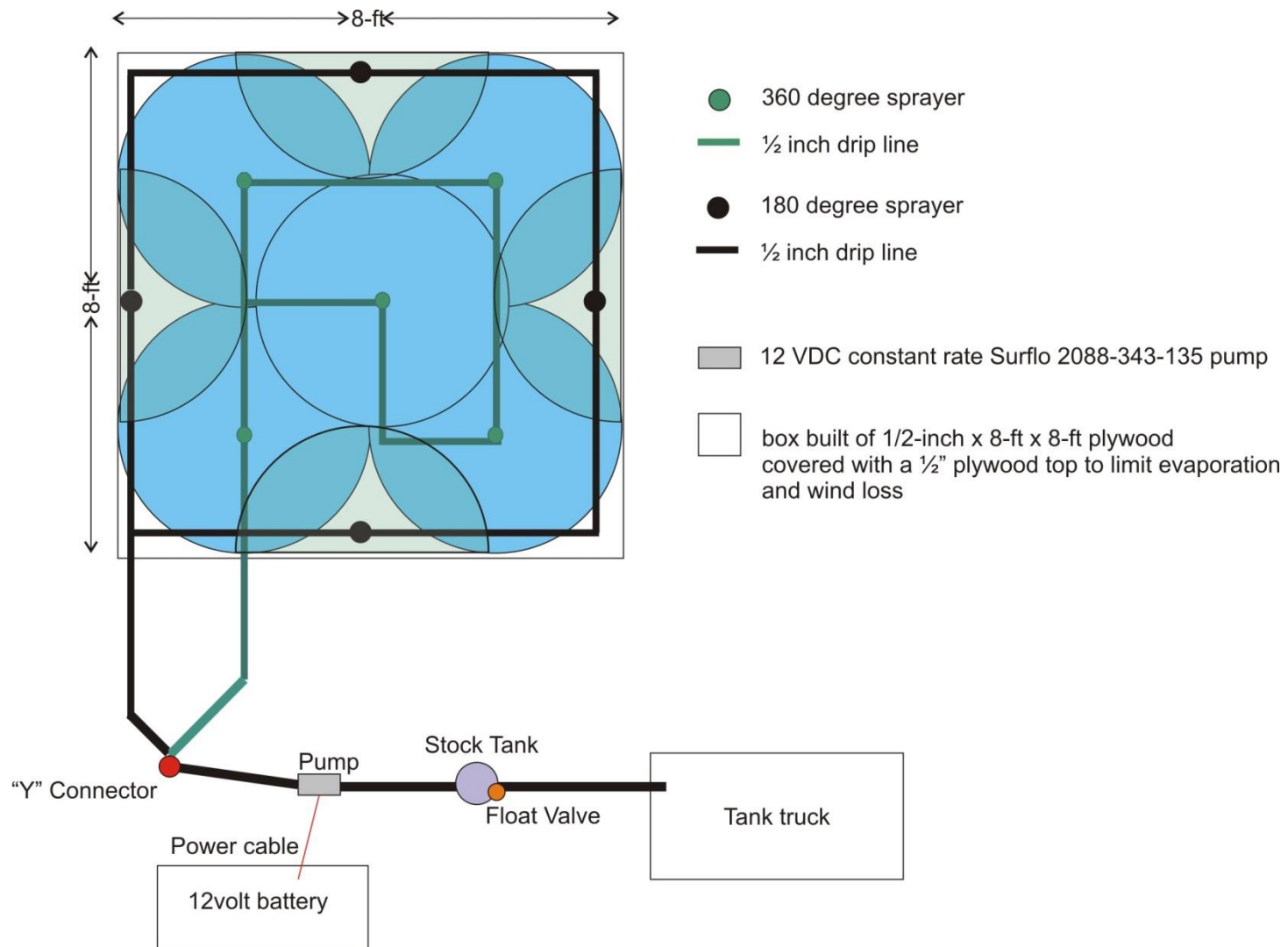
Figure 9. Water supply layout. Sprayer lines are connected to the pump using a "Y" connector and 1/2-in. polyline. Pump takes water from the stock tank through the float valve, which receives it via siphon from 4,000-gallon tank truck. Pump power supplied using a 12-volt battery.

6.5 Monitoring System Used for Field Characterization

6.5.1 Physical Layout

There are two instrumented tube sets and one drilled borehole adjacent to the PA Confirmation Vaults (Figure 10). The PA south instrumented tubes are installed within the vault perimeter drainage material just beyond the perimeter edge block. The PA north instrumented tubes are about 2-ft further to the east, penetrating the alluvial fill material. At land surface, the drilled borehole is located within the vault perimeter drainage material on the northeast corner of the PA Confirmation Vault perimeter block and drilled to a total depth of 45-ft. The locations relative to the vault base section, vault upper riser section, vault plug, and perimeter block are illustrated in Figures 11, 12, and 13.

6.5.2 Monitoring Instruments and Depths

Instruments installed at the PA south and PA north instrumented tube set locations are listed in Table 18. They include ATs and WCR probes installed at depths of 12-ft, 18-ft, 26-ft, and 29-ft measured from the top of the vault plugs at the PA south location and ATs and WCR probes installed at depths of 26-ft and 29-ft at the PA north instrumented tube location.

The instruments were installed as the vault backfill material was emplaced, beginning with the instruments placed in the Stratum II alluvium and drainage course materials. For the AT installations, porous cups were attached to 2-in. diameter PVC tubes and the electrical cables for the WCR probes were placed in 1-in. diameter PVC tubes. The PVC tubes were extended in 10-ft sections as the vault perimeter drainage material was brought upward in lifts around the vaults. Shallower instruments were set in place as the vault perimeter drainage material reached the target installation depth.
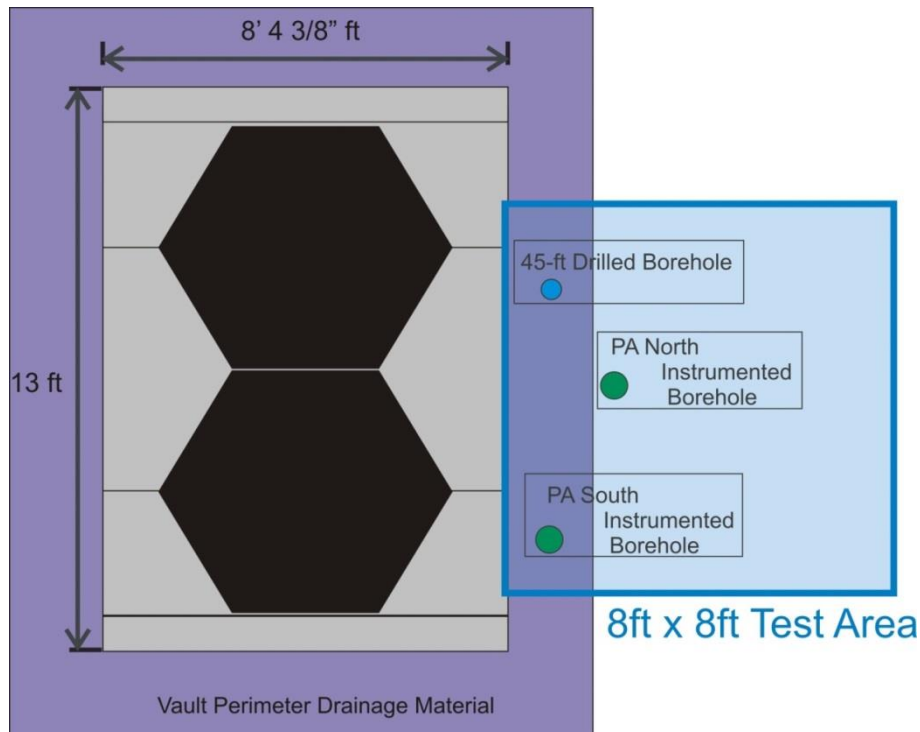
Figure 10. Plan view showing the location of the 8 x 8-ft test area (blue box) relative to the two instrumented boreholes, drilled borehole, and PA Confirmation Vaults.
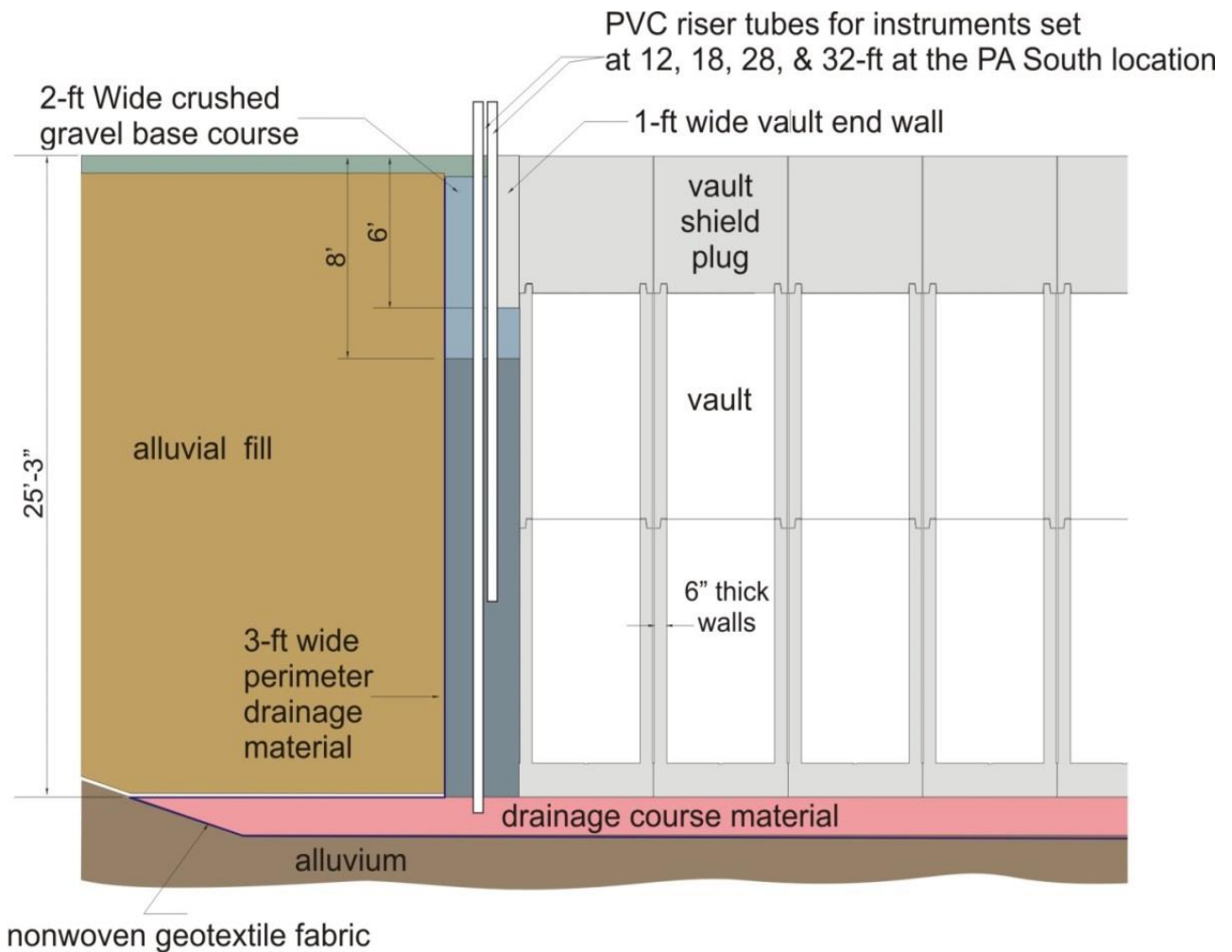
Figure 11. Vertical view of the PA south instrumented tube set showing the polyvinyl chloride (PVC) risers located within the vault perimeter drainage material.
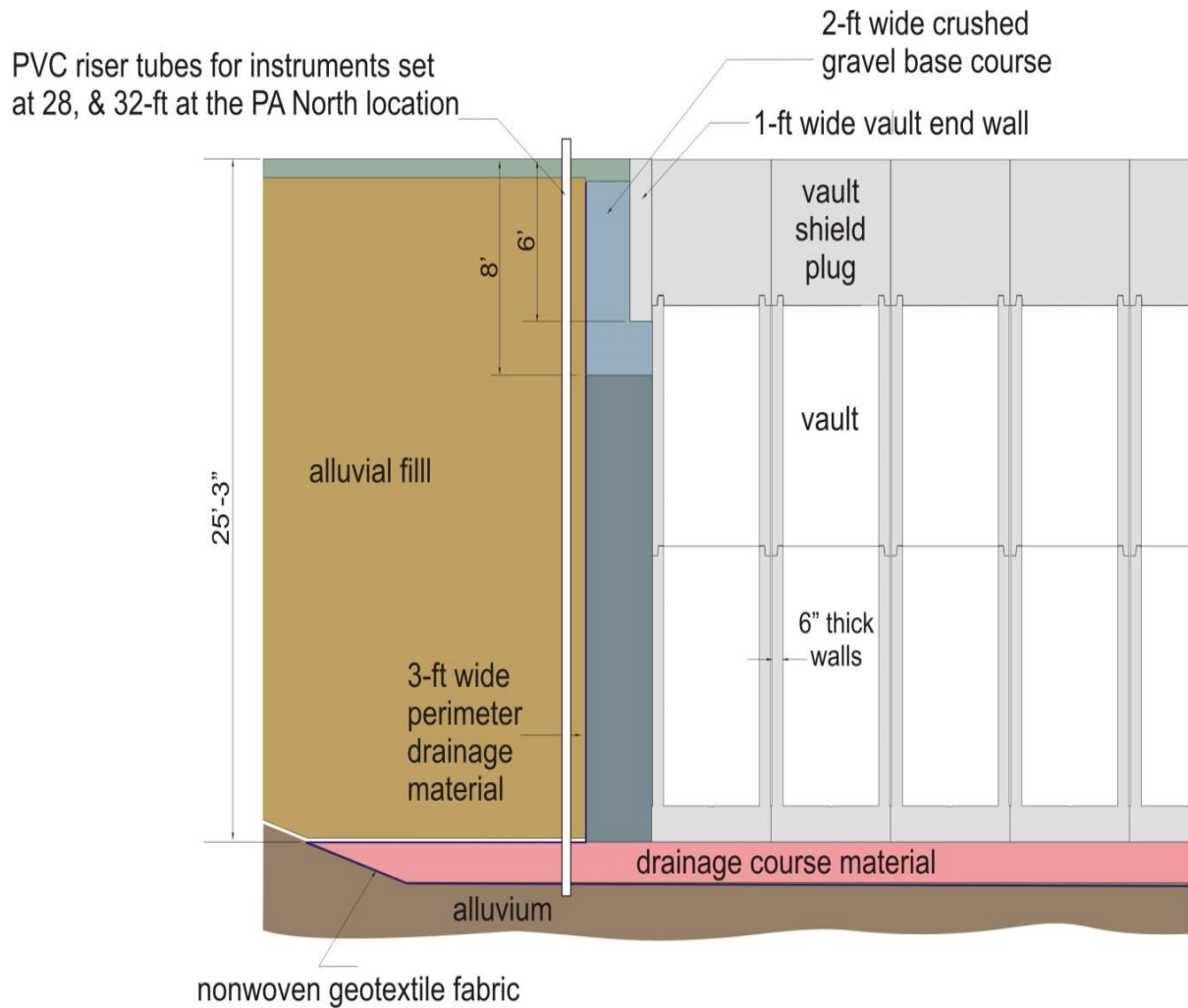
Figure 12. Vertical view of the PA north instrumented tube set showing the PVC risers located within the alluvial fill material.

Once the vault perimeter drainage material reached a depth of 8-ft from the vault plug top surface, a 10-in. Schedule 80 PVC pipe was set as a surface casing, allowing a surface weather proof enclosure to be placed 2-ft above the vault surface. The PVC riser tubes were terminated within the 10-in. Schedule 80 PVC pipe, and the cabling for the ATs and WCR probes were connected to the enclosed Campbell Scientific data logger. The data loggers were powered by a nearby solar panel, allowing continuous data collection.

The instruments installation depths for the PA drilled borehole are given in Table 19.
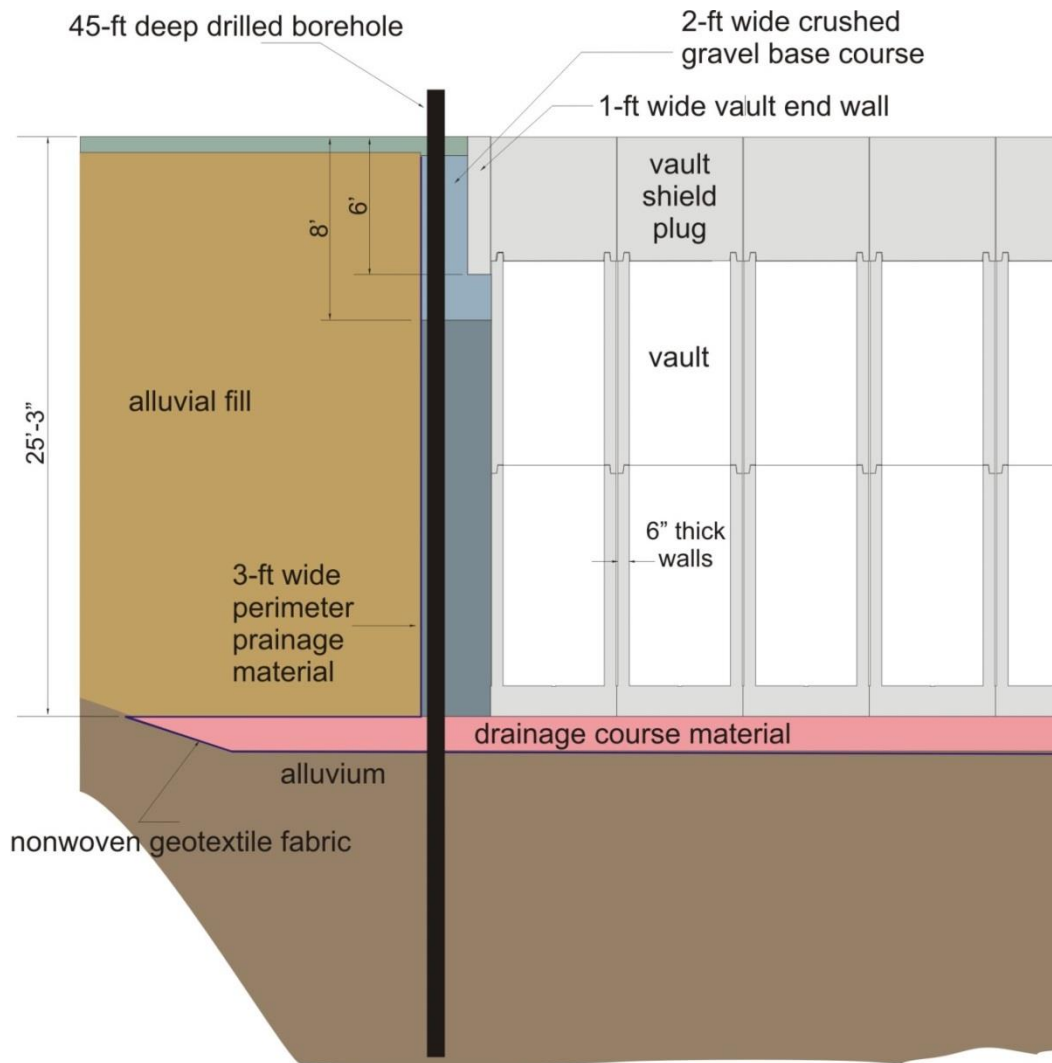
Figure 13. Vertical view of the PA drilled borehole located within the vault perimeter drainage material adjacent to the vaults and drilled to a total depth of 45-ft.

Table 18. Sensors, locations, and installation depths for the PA south and PA north instrumented tube locations.

| Sensor Type | Depths of Instrument Installation Relative to Top of the Vault Plug | | Material Instrumented |
	PA South Location	PA North Location	
ATs and WCR probes	12 ft	NA	Vault perimeter drainage material
	18 ft	NA	Vault perimeter drainage material
	26 ft	26 ft	Drainage course material
	29 ft	29 ft	Stratum II alluvium just below the drainage course material

Table 19. Sensors, locations, and installation depths for the PA 45-ft drilled borehole.

Sensor Type	Depths of Instrument Installation in Drilled Borehole (Relative to Top of the Vault Plug)
Advanced tensiometer	43 ft
WCR probe	43 ft
Suction lysimeter	NA
Thermocouple	12 ft
	18 ft
	26 ft
	34 ft
	43 ft

6.6 Calibration of Advanced Tensiometers and Water Content Reflectometer Probe

The ATs and WCR probes installed in the instrumented tube sets and drilled borehole at the PA Confirmation Vaults are illustrated in Figure 14 and 15. The ATs used in the characterization tests were supplied by Soil Water Monitoring Systems, Inc. based on the design patented by Dr. James "Buck" Sisson. The WCR probes were supplied by Campbell Scientific and are model CS-655 WCR with 12-cm probes.

6.6.1 Calibration of the Advanced Tensiometer

The ATs are essentially a pressure transducer placed inside a porous ceramic cup. The porous ceramic cup allows water to be drawn into it or out of it from the materials in which they are embedded through capillary action, the pressure (tension) is measured with the pressure transducer, and the signal is transmitted to land surface via the PVC tube. Calibration of the pressure transducers is required to convert the electrical signal to a water pressure or suction tension.

The calibration apparatus consists of a water-filled U-tube manometer, where one side is connected to an adjustable pressure and the other side of the manometer is connected to the sensor being calibrated. The water level (i.e., the hydraulic head) in the U-tube manometer is sequentially cycled through a range of values and the corresponding voltages output from the sensor are recorded and loaded into an Excel spreadsheet for processing.

The pressure values and voltages were fit using straight lines with the linest() function in an Excel spreadsheet. The resulting R^2 values exceeded 0.999 in all cases, indicating the straight line fit was more than adequate for all the sensors tested. The slope and intercepts obtained for each sensor were written on heavy plastic tags and attached to each sensor. Thus, the individual slopes and intercepts were used as unique identifiers for each of the sensors. The data and fitting parameters are found in Table 20.
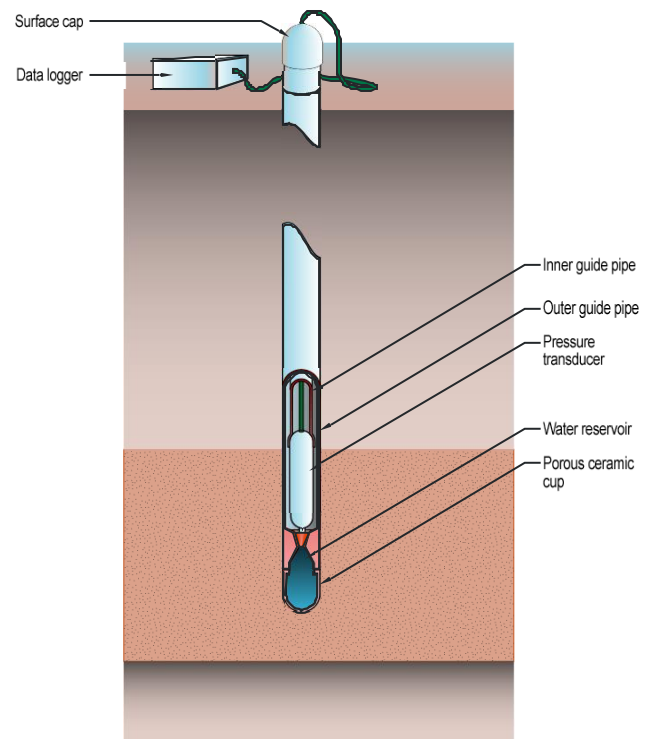
Advanced Tensiometer showing porous ceramic cup, pressure transducer and inner/outer guide pip
The instrument cable from the transducer to data logger is not shown. Outer pipe ID is 1 1/2".

Figure 14. Advanced tensiometer.
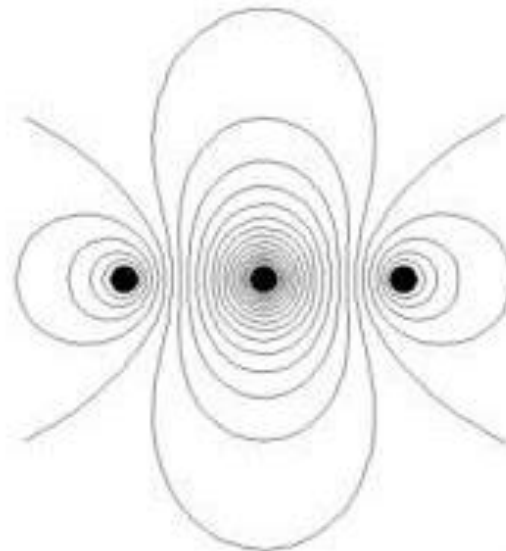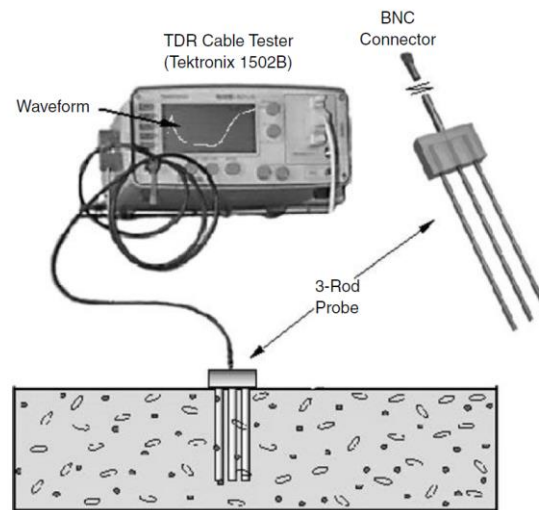
Figure 15. WCR probe showing example three-rod probe embedded vertically in surface soil layer and corresponding electric field lines.

Table 20. Calibration data and first order fitting parameters for the ATs used in the PA instrumented tube sets and drilled borehole.

Installation Location	PA South Instrumented Tube Set				PA North Instrumented Tube Set		PA Drilled Borehole
	29 ft	26 ft	18 ft	12 ft	29 ft	26 ft	18 ft
Tension (cm of water)	mV	mV	mV	mV	mV	mV	mV
0	1,234	1,245	1,248	1,238	1,241	1,240	1,239
-20	1,222	1,233	1,236	1,226	1,229	1,228	1,227
-40	1,210	1,221	1,225	1,214	1,217	1,217	1,215
-60	1,199	1,209	1,213	1,203	1,206	1,206	1,203
-80	1,187	1,197	1,201	1,191	1,194	1,194	1,192
-100	1,176	1,185	1,189	1,180	1,182	1,182	1,180
Slope	1.7237	1.6670	1.6991	1.7237	1.7030	1.7364	1.6987
Intercept	-2,126.5	-2,075	-2,121	-2,133	-2,113	-2,153	-2,104

6.6.2 Calibration of the Water Content Reflectometer Probe

WCR is a highly precise and automated method for determining porous media θ and electrical conductivity. Water content is inferred from the dielectric permittivity of the medium, whereas electrical conductivity is inferred from WCR signal attenuation. Empirical and dielectric mixing models are used to relate θ to measured dielectric permittivity. A WCR probe is essentially a pair of probes or wave guides that can be embedded in soil and connected to an electromagnetic signal generator (Figure 15).

The main advantages of an WCR probe over other soil θ measurement methods are: (1) automated data collection; (2) calibration requirements are minimal—in many cases, soil-specific calibration is not needed; (3) lack of radiation hazard associated with neutron probe or gamma-attenuation techniques; (4) WCR probes have excellent spatial and temporal resolution; and (5) measurements are simple to obtain and the method is capable of providing continuous measurements through automation and multiplexing.

6.6.2.1 ***Basic Water Content Reflectometer Theory.*** The bulk dielectric constant (ε), otherwise known as the dielectric permittivity, of a non-magnetic cable of length L is related to the signal propagation velocity (V) according to:

$$\epsilon = \left(\frac{c}{V}\right)^2 = \left(\frac{ct}{2L}\right)^2 \tag{3}$$

where c is the speed of light (velocity of electromagnetic waves) in vacuum (3×10^8 m/s), and t is the travel time for the pulse to traverse the length of the cable (down and back). This equation simply states that the dielectric constant of a porous medium is the ratio squared of the propagation velocity in vacuum relative to that in a medium. A WCR probe embedded in soil is basically a pair of cables separated by the porous media soil (e.g., the soil-air-water system), or an effectively "heterogeneous cable". Therefore, using Equation (3), given a WCR-generated electromagnetic ramp, the travel time required to traverse the net probe length can be determined. In this case, the travel time reflects the 'apparent' electromagnetic length of the probe-soil system.

The bulk dielectric constant of a soil (ε_b) is dominated by the dielectric constant of liquid water, $\varepsilon_w = 81$ @ 20°C, because the dielectric constants of other soil constituents are much smaller (e.g., soil minerals $\varepsilon_s = 3$ to 5, frozen water $\varepsilon_i = 4$, and air $\varepsilon_a = 1$). This large disparity of dielectric constants makes the method relatively insensitive to soil composition and texture; this is a good method for 'liquid' water measurement in soils.

In practice, several factors influence dielectric constant measurements, including soil porosity and bulk density, measurement frequency, temperature, water status (bound or free), and dipole moments induced by mineral, water, and air shapes. This gives rise to the need to relate θ to ε_b and has resulted in a variety of empirical and 'dielectric mixing' models, the most common takes the form proposed by Topp et al. (1980):

$$\theta = -5.3 \times 10^{-2} + 2.92 \times 10^{-2}\epsilon_b - 5.5 \times 10^{-4}\epsilon_b^2 + 4.3 \times 10^{-6}\epsilon_b^3 \qquad (4)$$

This equation provides an adequate description of θ for $0.05 < \theta < 0.5$, which covers the range of interest in most mineral soils, with θ estimation error of 0.013.

While the standard calibration equation relating to the measured permittivity to θ is the Topp Equation, the WCR probe manufacturer (i.e., Campbell Scientific) recommends developing user-derived calibrations to optimize accuracy of the θ measurement. These recommendations are made because the Topp Equation has been found to underestimate the θ of some organic, volcanic, and fine textured soils and the Topp Equation was not developed or tested for media with porosity greater than 0.5 or bulk densities greater than 1.5 g/cm³. Therefore, because Equation (4) was not developed or tested for use in the perimeter drainage and drainage course materials comprising the vault hydraulic drainage system, where the typical range of θ would be less than 0.05, media-specific calibration relationships were developed.

6.6.2.2 *Calibration of the Water Content Reflectometer Probes to the Perimeter Drainage and Drainage Course Materials.* The WCR probes were calibrated to the perimeter drainage gravel, drainage course material, and alluvial fill materials by Dr. James "Buck" Sisson at Soil Water Monitoring Systems, Kennewick, Washington. The following sections provide the methodology used in calibrating the WCR probes to the materials at the sensor installation depths given in Tables 17 and 18 and the resultant calibration curves.

Determination of the θ versus Permittivity Calibration Curve

To determine the appropriate calibration curve to apply to materials used for fill at the RH-LLW Disposal Facility vault system, a test system was constructed using 10-in. ID schedule 40 PVC pipe, perimeter drainage gravels, WCR probes, and a Campbell Scientific CR1000 data logger. A 6-in. section of the PVC pipe was set vertically on a test bench. The tests were conducted by placing 3-in. of drainage gravel in the bottom of the pipe. The WCR probe was then installed and covered with another 3-in. layer of the drainage gravel.

Prior to conducting tests, the oven-dried bulk density of the drainage gravel sample was first determined by weighing a known volume of the material yielding a value of 1.6 g/cm³. The initial test calibration point ($\theta=1\%$) recorded in Figure 16 was determined using the same material that was first wetted, air dried, and weighed prior to layering it into the test apparatus. The test sample weight and volume were used to determine the sample density, which was then used with the oven-dried sample density to determine the test sample θ. After recording the corresponding permittivity using the built in function in the CR1000 data logger, a sufficient quantity of water was added to the test apparatus to increase the θ to 2.1% and the permittivity was recorded. Subsequent data points were obtained by simply increasing the θ and recording the permittivity. Recorded θ and permittivity data for the perimeter drainage and drainage course material are provided in Table 21.

These data points are represented by the solid squares in Figure 16. The data were then fitted with a straight line for comparison to the Topp polynomial given in Equation (4). The two relationships are reflective of the differences between the drainage gravel system and soil system used to derive the coefficients in Equation (4). Of note is the θ range limit of the Topp equation. Below a permittivity of 2, the modeled θ becomes negative. In the RH-LLW disposal vault system, θ on the order of 2 to 5% are

expected based on the calibration apparatus and data. Therefore, it is recommended that the fitted calibration curve be used instead of the Topp equation for the drainage gravels.

Table 21. Water content and permittivity for perimeter drainage and drainage course materials.

Water Content θ (m³/m³)	Permittivity (Dimensionless)
0	1.018
0.021	1.26
0.043	2.65
0.013	1.028
0.053	3.582
0.040	3.393517
0.047	4.046552
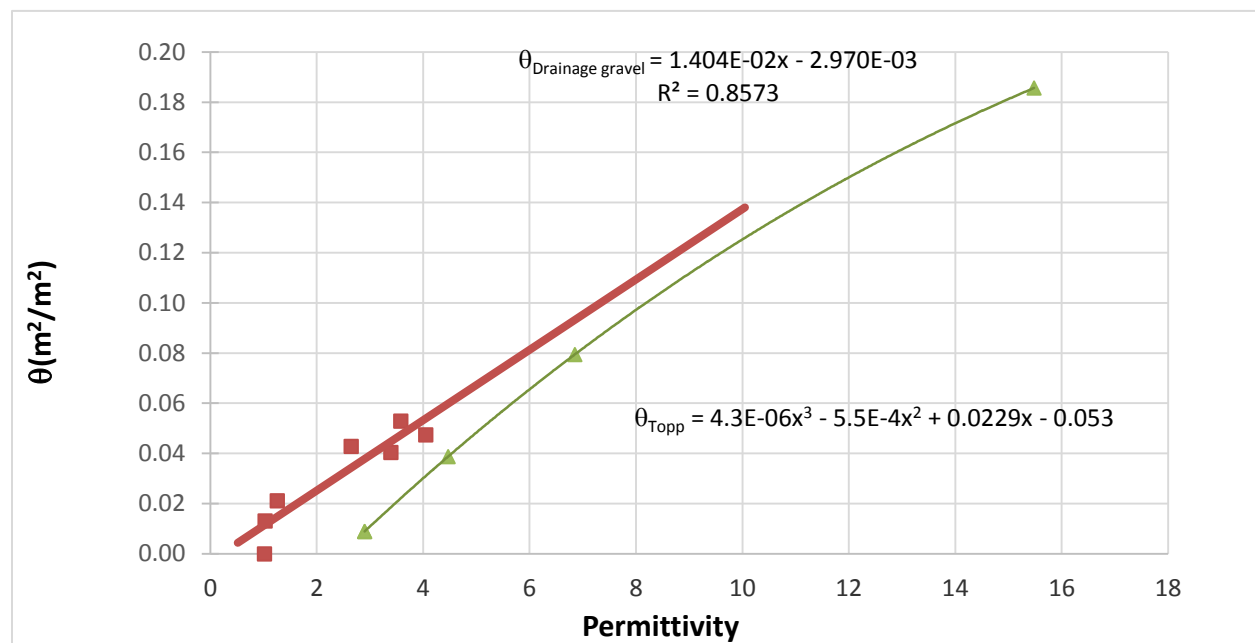
Figure 16. θ versus permittivity for the drainage gravels with the fitted calibration curve and the Topp calibration curve used by the CR 1000 data logger.

During the process of obtaining the data shown in Figure 16, it was noted that the gravels drained rapidly, suggesting there would be a gradation in θ as a function of depth. To test this hypothesis, the test was re-conducted with θ measured on vertical 2-in. layers removed after the permittivity was recorded for the 6-in. sample. Data obtained by the stratified sampling are shown in Figure 17 by the blue dots. The figure shows that even though the 2-in. layers were removed rapidly from the 10-in. PVC pipe and weighed, there was a significant difference in θ as a function of depth. At a θ of 0.01, the different test samples resulted in a more consistent measurement of permittivity. At higher θ, there is more variability in measured permittivity. These differences in θ demonstrate that the water is held loosely in the gravel and moves by gravity to the bottom of the column as opposed to being held by capillary forces.
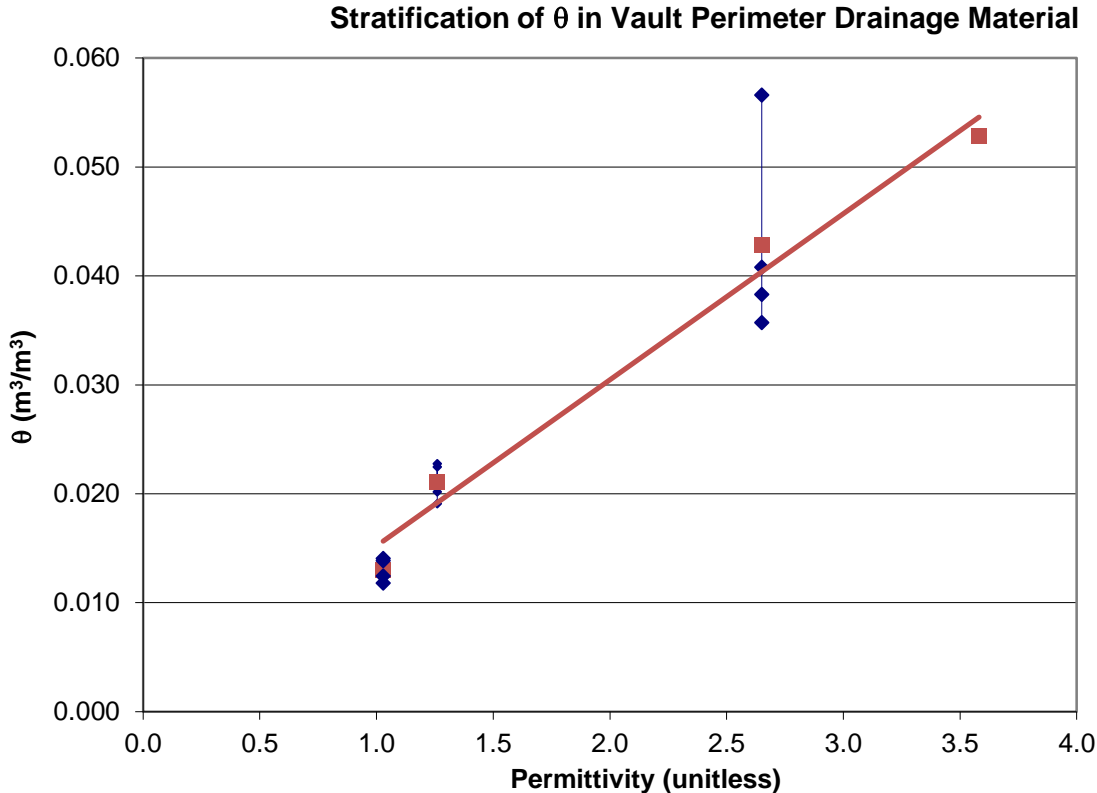
Figure 17. θ (solid squares) as a function of permittivity values obtained using the built in functions by the CR1000 data logger with a straight line fit to the data. Blue diamonds represent the data collected using vertically stratified sampling.

Dynamic Water Content Reflectometer Probe Response Testing

The responsiveness of WCR probes in gravels was tested to determine their potential for use in monitoring the expected wetting front behavior in the RH-LLW Disposal Facility drainage gravels under field conditions. Expected field conditions correspond to those encountered during an infiltration test and during normal precipitation events. During these infiltration events, a steady-state drainage condition would be exposed to a rapidly applied water source, resulting in the dynamic propagation of a wetting front.

During the dynamic test, a 60-cm column was constructed of the 10-in. PVC pipe. The pipe was filled with drainage gravel to within 5 cm of the top with a WCR probe installed 15 cm from the top (see Figure 18). The bottom of the column was open and provided unimpeded drainage of water. The test column was equipped with an infiltration plate designed to apply a uniform distribution of water at a constant rate over the surface of the column. This plate was installed 5 cm from the top of the column (i.e., 10 cm above the WCR probe) and covered with 2 cm of gravel to prevent evaporation and to keep the plate in place. The plate is shown in Figure 19.

For the responsiveness test, the water application rate was 30.5 ml/minute for 60 minutes, which is equivalent to 28 cm/day over the 10-in. PVC pipe area. The calibration curve determined for the drainage gravel was used to convert the measured permittivity to θ and the fitted θ data is plotted in Figure 20. The figure shows that the wetting front reached a distance of 10 cm from the water supply plate within 3 minutes, with the θ reaching a near steady-state within 5 minutes. The drainout period after the end of

the 60-minute water application period is much longer, exceeding 250 minutes. At no time did the θ exceed 6% at the application rate.

Calibration of WCR sensors was accomplished over a 0.01 to 0.05 range of θ in the Vault Perimeter Drainage and Drainage Course Materials. The range of the calibration was restrained by the inability of the relatively course materials to retain water against the force of gravity. The inability of the drainage materials to retain water indicates that water will be kept away from the vaults. This test indicates that changes in θ, while relatively small, will be observable during vault characterization tests.

Figure 18. Photograph of the infiltration column showing gravel covering the infiltration plate.

Figure 19. Infiltration (constant flux) plate made from 1/4-in. porous tubing coiled in a spiral pattern to provide nearly uniform distribution of the infiltrating water.
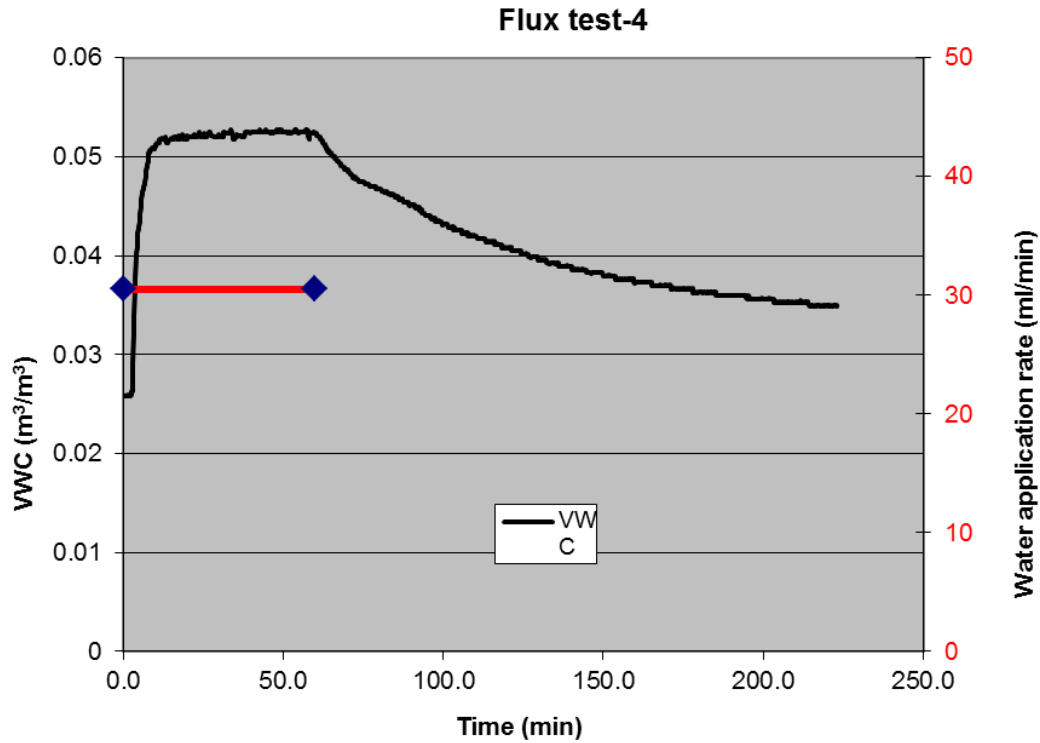
Figure 20. θ (black line using left axis) and application rate (right axis) during the WCR probe responsiveness test.

6.6.2.3 Calibration of Water Content Reflectometer Probes for the Alluvial Fill Material.

Calibration of the WCR probes in the alluvial fill material was similar to that for the drainage gravels. The first 3-in. of the alluvial fill material was packed into the 6-in. tall 10-in. diameter PVC column. The WCR probe was inserted and then covered with 3-in. of packed alluvial fill material. The permittivity was measured, then the alluvial fill material was removed from the column, weighed, dried, and weighed again to obtain the oven dry bulk density and the θ corresponding to the measured permittivity. In subsequent steps, an increment of water was added to the alluvial fill material and mixed by hand. Once mixed, the rewetted alluvial fill material was packed back into the column with the WCR probe and the permittivity output recorded. The process was repeated over the range of θ shown in Table 22 and on Figure 21 with the fitted calibration curve and the Topp default calibration curve for comparison. To mimic the field installation process, where the WCR probes were installed in finer materials, the Stratum II alluvium used in calibration was material that passed a 1/2-in. sieve. Only about 25% of the bulk non-sieved alluvial fill material passed the 1/2-in. openings.

Table 22. Water content and permittivity for alluvial fill material.

Water Content θ (m³/m³)	Permittivity (Dimensionless)
0.027107	2.898
0.027081	2.897
0.066919	4.47
0.122595	6.85
0.28317	15.48

48

Differences between the Topp calibration curve and the fitted Stratum II alluvium calibration curve increase with higher θ. Deviations from the Topp calibration curve have been reported in literature for sand materials, but the large deviation observed for Stratum II alluvium was not expected. The $θ_s$ for the Stratum II alluvium materials is approximately 35%; therefore, deviation occurs near saturation. It is possible that the alluvial materials could reach saturation near the vault perimeter and the location of the WCR sensors. If that occurs, there should be a significant difference between the θ calculated using the Topp equation and the Stratum II alluvium calibration curve, in which case, the measured calibration equation should be used.
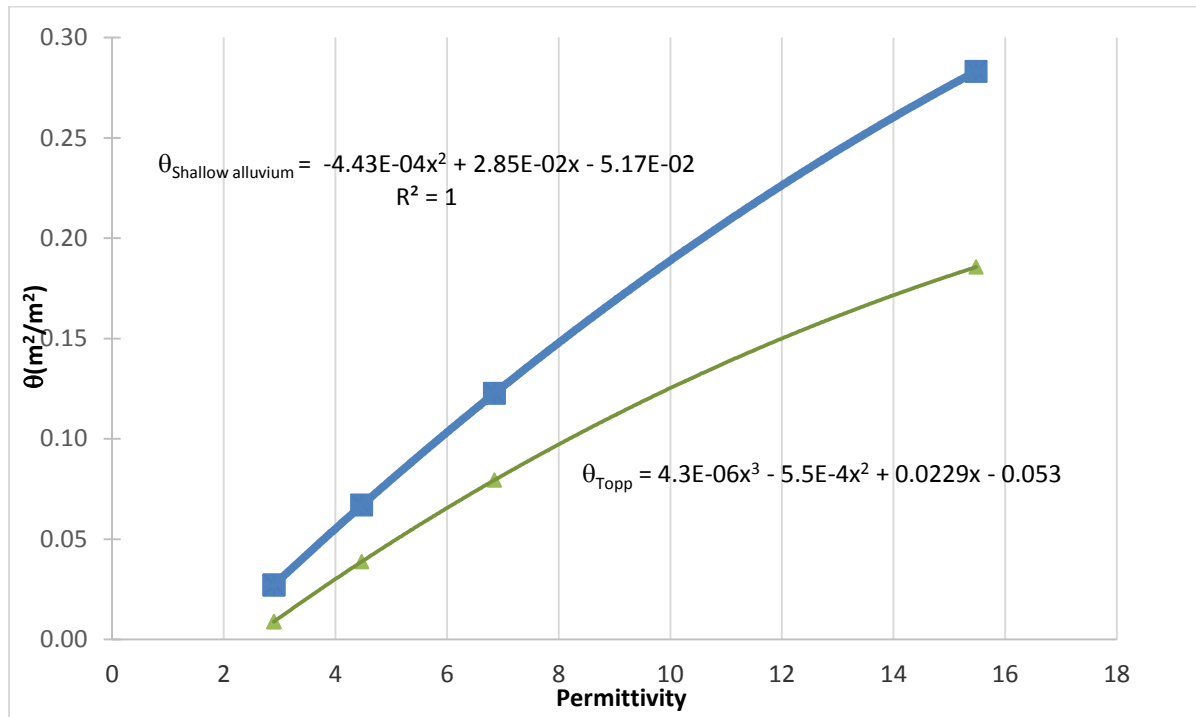
Figure 21. Calibration data and results for the WCR probe in Stratum II alluvium.

The plot shows θ(m²/m²) versus Permittivity with two curves:

$$θ_{Shallow\ alluvium} = -4.43E\text{-}04x^2 + 2.85E\text{-}02x - 5.17E\text{-}02$$
$$R^2 = 1$$

$$θ_{Topp} = 4.3E\text{-}06x^3 - 5.5E\text{-}4x^2 + 0.0229x - 0.053$$

6.7   Characterization Test Data and Interpretation

This section provides data collected during the two characterization tests conducted during the summer and early fall at the PA Confirmation Vault location and includes the following:

- Volumetric rates and durations of water application for two characterization tests and a natural precipitation event

- Uncalibrated (i.e., raw) data collected prior to the first characterization test through complete drainout of both characterization tests and a natural precipitation event

- Calibrated data corresponding to the uncalibrated raw data

- Data interpretation, including a discussion of the following:

  - Sensor response. The uncalibrated and AT data did not respond well in the vault perimeter drainage and drainage course materials while the WCR responded extremely well. The converse was observed in the 45-ft drilled borehole because of installation issues (as discussed in this section).
  - Interpretation of data that is representative of the first characterization test.
  - Interpretation of data that is representative of the second characterization test.

- Interpretation of natural precipitation event data.

6.7.1 Water Application Rates

Volumetric rates recorded during the two characterization tests are given in Table 23. The rates were recorded periodically throughout both tests and, based on the pump discharge rates, the pumps were replaced when the volumetric rate decreased below a value of 1.2 gpm.

Table 23. Volumetric rates applied during the two characterization tests.

First Characterization Test Conducted 7/22/2016-7/23/2016							
			Water Depth in Tank				
Time Start	Time End	Delta Time (minutes)	Start (inches)	End (inches)	Height Loss (inches)	Volume Loss (gallons)	Flow Rate (gpm)
8:30am	Test Start						
9:07:00 AM	9:37:00 AM	30.00	19.50	13.00	6.50	44.75	1.49
2:20:00 PM	2:50:00 PM	30.00	19.00	13.00	6.00	41.31	1.38
3:50:00 PM	4:20:00 PM	30.00	19.00	13.00	6.00	41.31	1.38
8:30:00 PM	9:00:00 PM	30.00	18.13	13.88	4.25	29.26	0.98
9:45:00 PM	10:15:00 PM	30.00	19.25	16.50	2.75	18.93	0.63
10:30:00 PM	11:00:00 PM	30.00	19.13	12.88	6.25	43.03	1.43
1:15:00 AM	1:45:00 AM	30.00	19.50	13.44	6.06	41.74	1.39
3:10:00 AM	3:40:00 AM	30.00	18.75	12.75	6.00	41.31	1.38
5:45:00 AM	6:15:00 AM	30.00	19.56	13.56	6.00	41.31	1.38
7:50:00 AM	Test end						
Test duration	23.33 (hours)						
Total volume of water						1,905 gallons	
Average rate							1.4 gpm
Infiltration rate over an 8 × 8-ft area							2.9E-3 ft/min
							3.5E-2 in./min
							1.8E4 in./year
Second Characterization Test Conducted 9/30/2016							
			Water Depth in Tank				
Time Start	Time End	Delta Time (minutes)	Start (inches)	End (inches)	Height Loss (inches)	Volume Loss (gallons)	Flow Rate (gpm)
6:20:00 AM	Test Start						
7:32:00 AM	7:52:00 AM	20.00	17.75	11.63	6.13	42.17	2.11
10:00:00 AM	10:30:00 AM	30.00	16.50	10.00	6.50	44.75	1.49
2:15:00 PM	2:45:00 PM	30.00	18.00	11.00	7.00	48.19	1.61
4:00:00 PM	4:30:00 PM	30.00	21.00	14.75	6.25	43.03	1.43
4:50:00 PM	5:20:00 PM	30.00	17.88	11.25	6.63	45.61	1.52
5:20:00 PM	5:50:00 PM	30.00	11.25	4.38	6.88	47.33	1.58
6:16:00 PM	Test End						
Test duration	11.93 (hours)						
Total volume of water						1,056 gallons	
Average rate							1.6 gpm
Infiltration rate over an 8 × 8-ft area							3.4E-3 ft/min
							4.1E-2 in./min
							2.1E4 in./year

The precipitation record obtained from the ATR Complex weather station for the month preceding the first infiltration test extending through the 3 months following the second test are given in Table 24 and is summarized by the following:

- During the first test, the average flow rate was approximately 1.38 gpm over the test duration of 23 hours, resulting in a total discharge of approximately 1,900 gallons of water.

- During the second test, the average flow rate was approximately 1.62 gpm over the test duration of 11 hours, resulting in a discharge of approximately 1,055 gallons of water.

- There was 0.16 in. of precipitation during the month preceding the first characterization test, but no rainfall occurred during the entire month of August (the month following the first characterization test).

- There was approximately 3/4 in. of rain in the 2 weeks prior to the second characterization test.

- After the end of the second characterization test, it rained, resulting in total precipitation of approximately 3/4 in. during the next 20 days.

- During the last 2 weeks of October, the rainfall was more significant/ with almost 2 in. recorded during the last 10 days of the month.

Table 24. Precipitation record for the June through December period taken from the Advanced Test Reactor Complex weather station.

Date	Cumulative Precipitation (inches)	Date	Cumulative Precipitation (inches)	Date	Cumulative Precipitation (inches)
Month Prior to First Test		Month Following Second Test		November	
7/1/16	0.06	10/1/16	0.01	11/9/16 8:55	0.01
7/9/16	0.01	10/2/16	0.23	11/14/16 12:50	0.02
7/10/16	0.09	10/3/16	0.05	11/23/16 12:05	0.01
No Rain Observed in August		10/4/16	0.01	11/27/16 0:25	0.08
Month Prior to Second Test		10/5/16	0.22	11/29/16 12:45	0.25
9/2/16	0.01	10/14/16	0.02		
9/4/16	0.11	10/15/16	0.15		
9/5/16	0.01	10/16/16	0.1		
9/12/16	0.17	10/17/16	0.04		
9/14/16	0.15	10/24/16	0.74		
9/21/16	0.12	10/27/16	0.01		
9/22/16	0.13	10/28/16	0.42		
9/23/16	0.42	10/29/16	0.09		
9/29/16	0.02	10/30/16	0.5		
Conducted Second Test 9/30/16					

6.7.2   Uncalibrated Characterization Test Data

6.7.2.1   Performance Assessment South Instrumented Tube Set. The data recorded for the sensors of the PA south instrumented tube set are listed in Table 18 and shown in Figures 22 and 23. The figures contain the uncalibrated voltage recorded for the ATs and the permittivity recorded for the WCR probes. Data are color coded by instrumentation depth with red lines corresponding to the deepest instruments installed in the Stratum II alluvium at 29 ft, green lines corresponding to the instruments

installed in the drainage course material at 26 ft, purple lines corresponding to the instruments installed in the vault perimeter drainage material at a depth of 18 ft, and the blue lines corresponding to the instruments installed in the vault perimeter drainage material at a depth of 12 ft. Calibrated data are provided in Section 6.6.3.1.

6.7.2.2 ***Performance Assessment North Instrumented Tube Set.*** Data recorded for the PA north instrumented tube set listed in Table 18 is shown in Figures 24 and 25, which contain the uncalibrated voltage recorded for the ATs and the permittivity recorded for the WCR probes. The PA north instrumented tube set penetrates the crushed gravel base course material near land surface, the alluvial fill material that extends downward to the top of the drainage course material, and the drainage course material that extends 10-ft horizontally beyond the edge of the vault base and penetrates into the Stratum II alluvium. Instruments are installed at depths of 29 ft, corresponding to the alluvial fill material, and at a depth of 26 ft, corresponding to the drainage course material. Data are color coded by instrumentation depth, with red lines corresponding to the deepest instruments installed in the Stratum II alluvium at 29 ft and green lines corresponding to instruments installed in the alluvial fill material at 26 ft. The alluvial fill material is somewhat heterogeneous; therefore, shallower instruments were not installed in the PA north location. Calibrated data are provided in Section 6.6.3.2.

6.7.2.3 ***Performance Assessment 45-ft Borehole.*** Data recorded for the PA 45-ft drilled borehole listed in Table 19 are shown in Figures 26 and 27 and contain the uncalibrated voltage recorded for the single AT and the permittivity recorded for the single WCR probe. The PA 45-ft borehole was augered through the crushed gravel base course material near the land surface, the vault perimeter drainage material, the drainage course material, the Stratum II alluvium, and the Stratum III alluvium. These instruments are installed at a depth of 43 ft in the Stratum III alluvium. Calibrated data are provided in Section 6.7.3.2.

In addition to the AT and the WCR probe, thermocouples were installed at depths of 12, 18, 26, 34, and 43 ft. These data are provided in Section 6.6.3.3 because temperature is output directly by the data logger and requires no calibration.

6.7.3   Calibrated Characterization Test Data

6.7.3.1 ***Performance Assessment South Instrumented Tube Set.*** Using the parameters discussed in Section 6.6, data provided for the PA south instrumented tube set in Section 6.7.2.1 were adjusted by calibration equations. Straight line formulas in Table 20 for the four ATs were applied to the data shown in Figure 22. Resultant calibrated data are given in Figure 28.

The first order calibration relationship for the WCR probes derived for the vault perimeter drainage course and drainage course materials (Figure 16) were applied to permittivity data for sensors installed at depths of 12, 18, and 26 ft. The second order calibration relationship for the Stratum II alluvium (Figure 21) was applied to WCR probe data for the sensor installed at a depth of 29 ft. The resultant calibrated θ is shown in Figure 29. For completeness, the Topp relationship provided by Equation (4) was also applied to the WCR probe permittivity data and the resultant calibrated θ is shown in Figure 30. Comparison of Figures 29 and 30 indicate that use of the Topp equation for drainage materials would have slightly underestimated θ_r in the shallow sensors, but there would have been relatively little difference if it had been used for the sensor placed in the Stratum II alluvium.
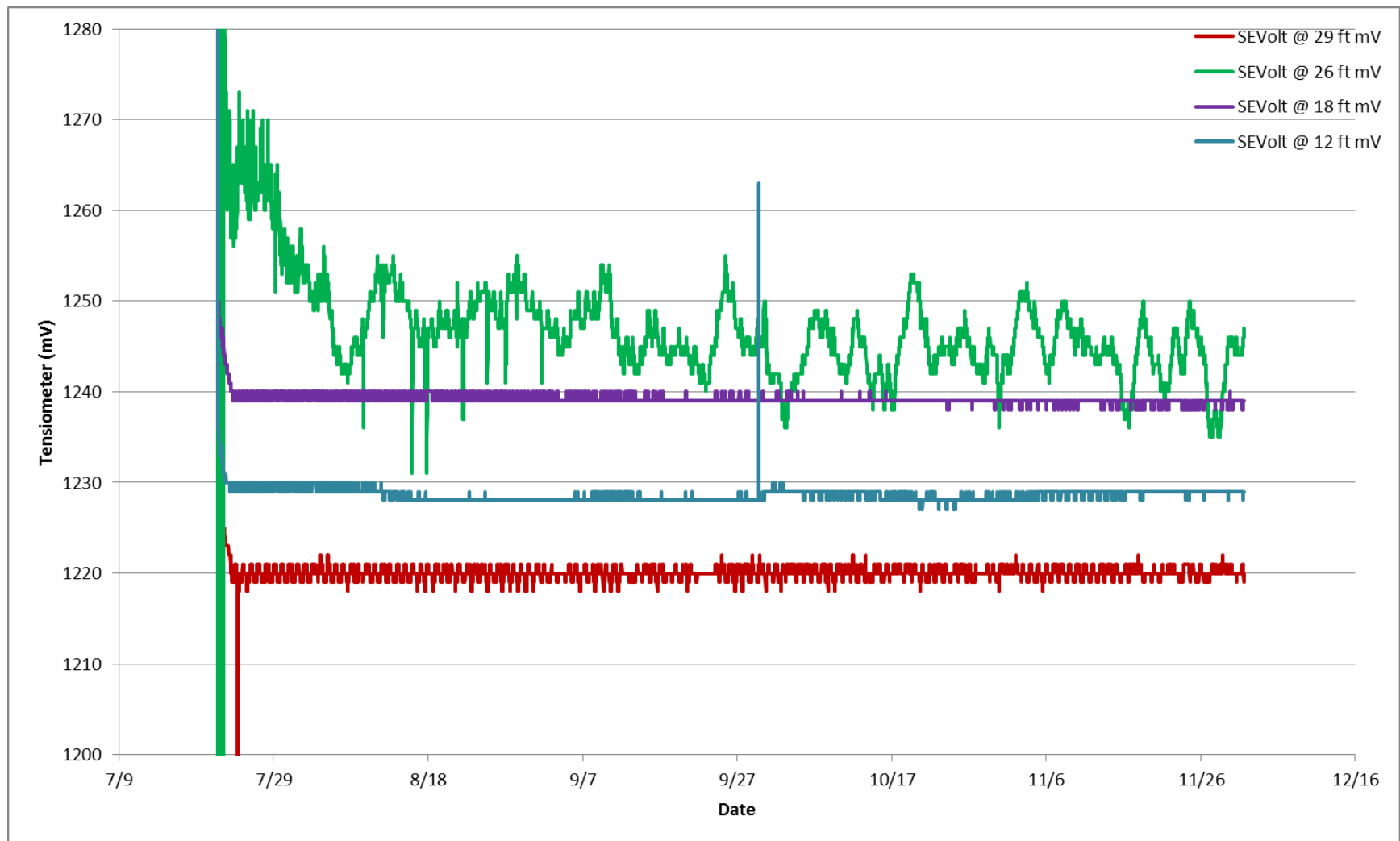
Figure 22. Voltage recorded for the ATs in the PA south instrumented tubes.
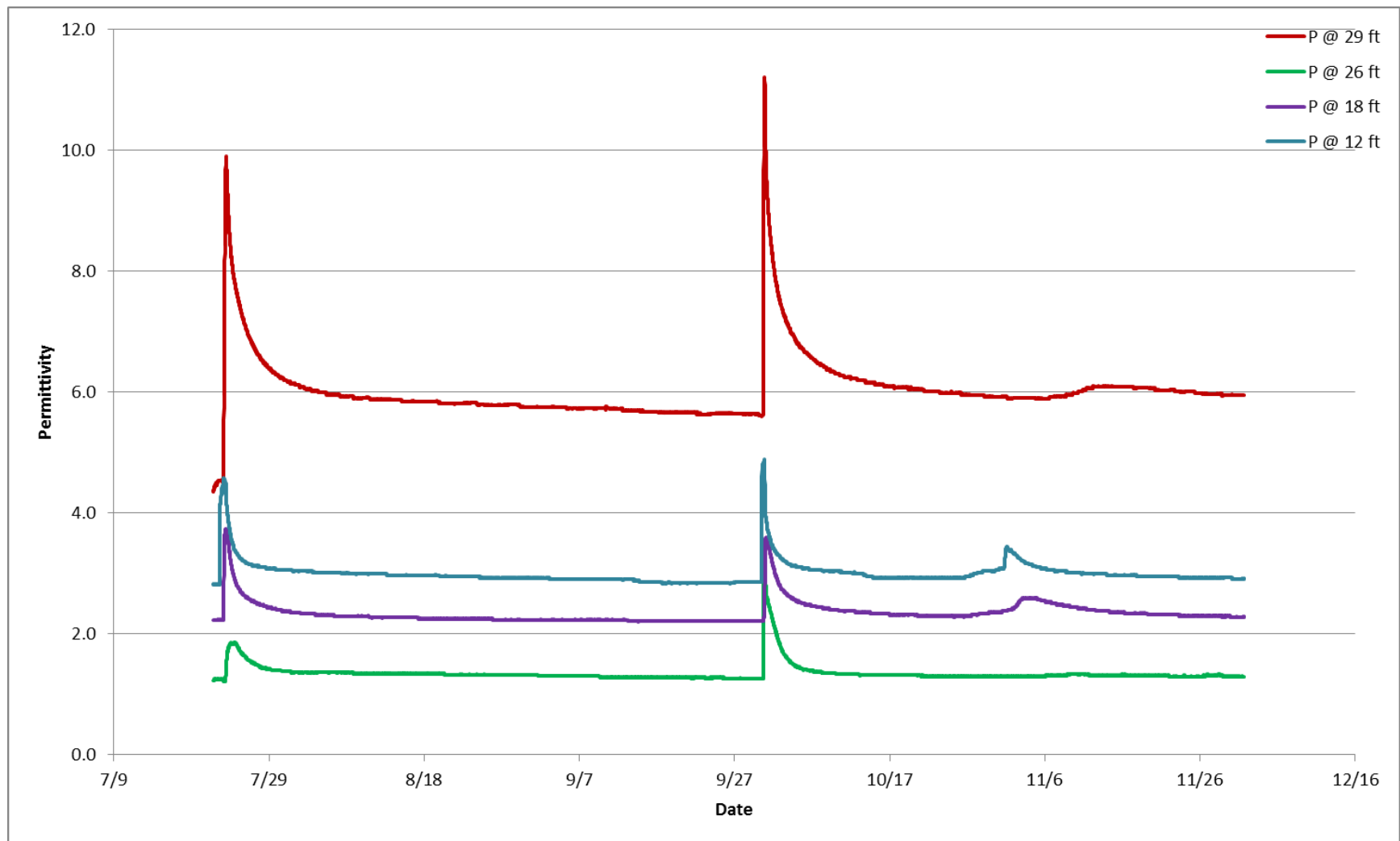
Figure 23. Permittivity recorded by the WCR probes in the PA south instrumented tubes.
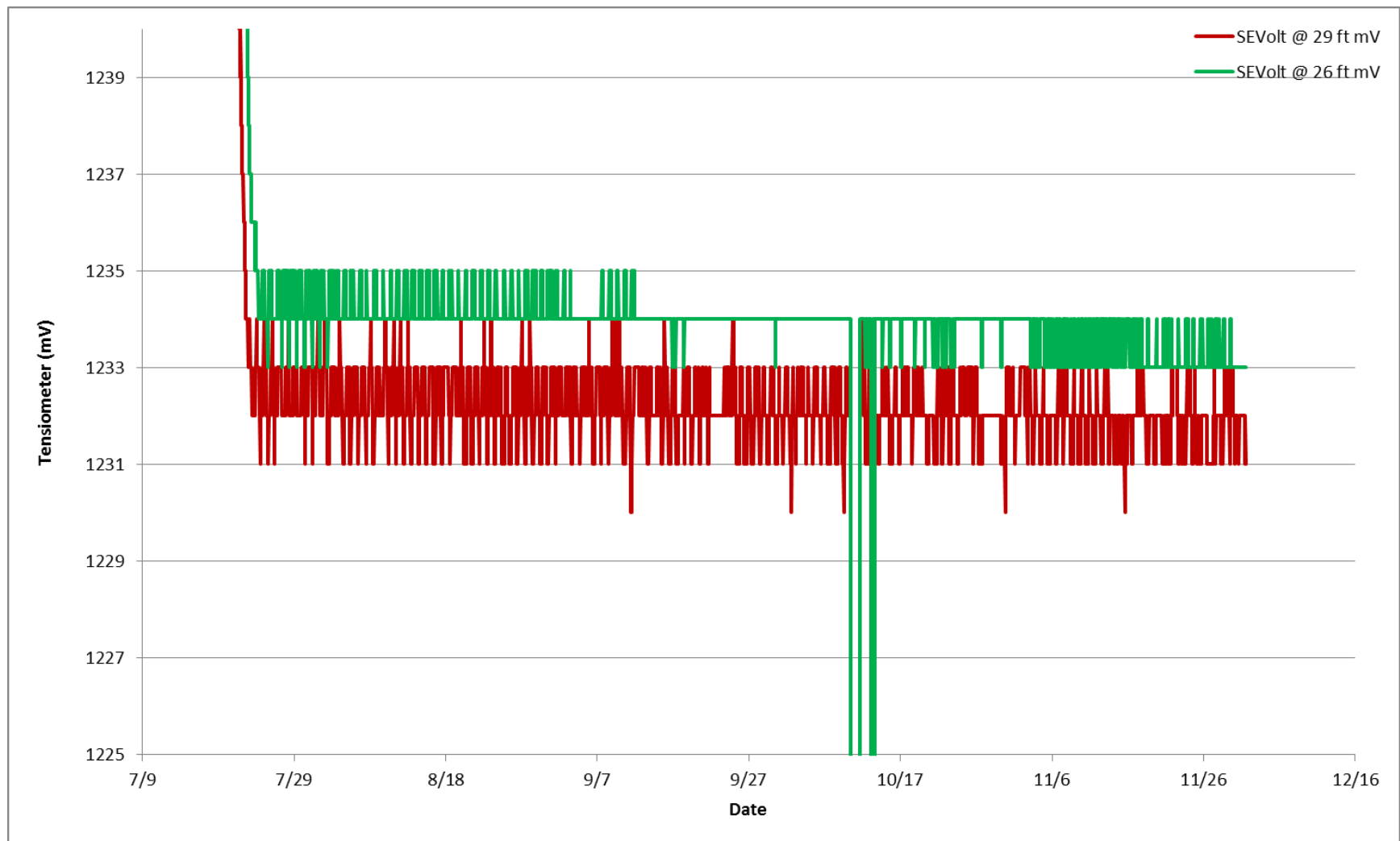
Figure 24. Voltage recorded for the ATs in the PA north instrumented tubes.
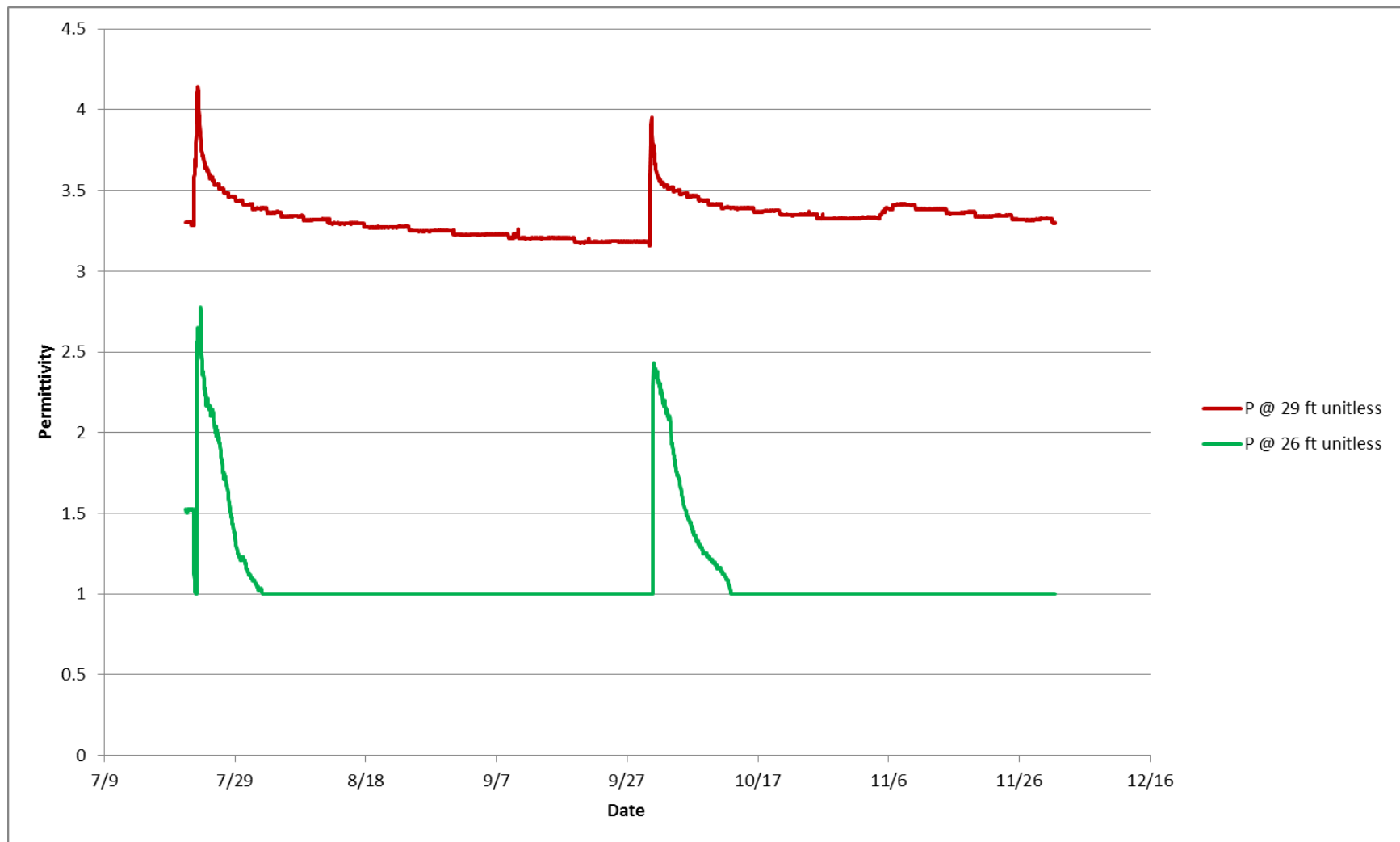
Figure 25. Permittivity recorded by the WCR probes in the PA north instrumented tubes.
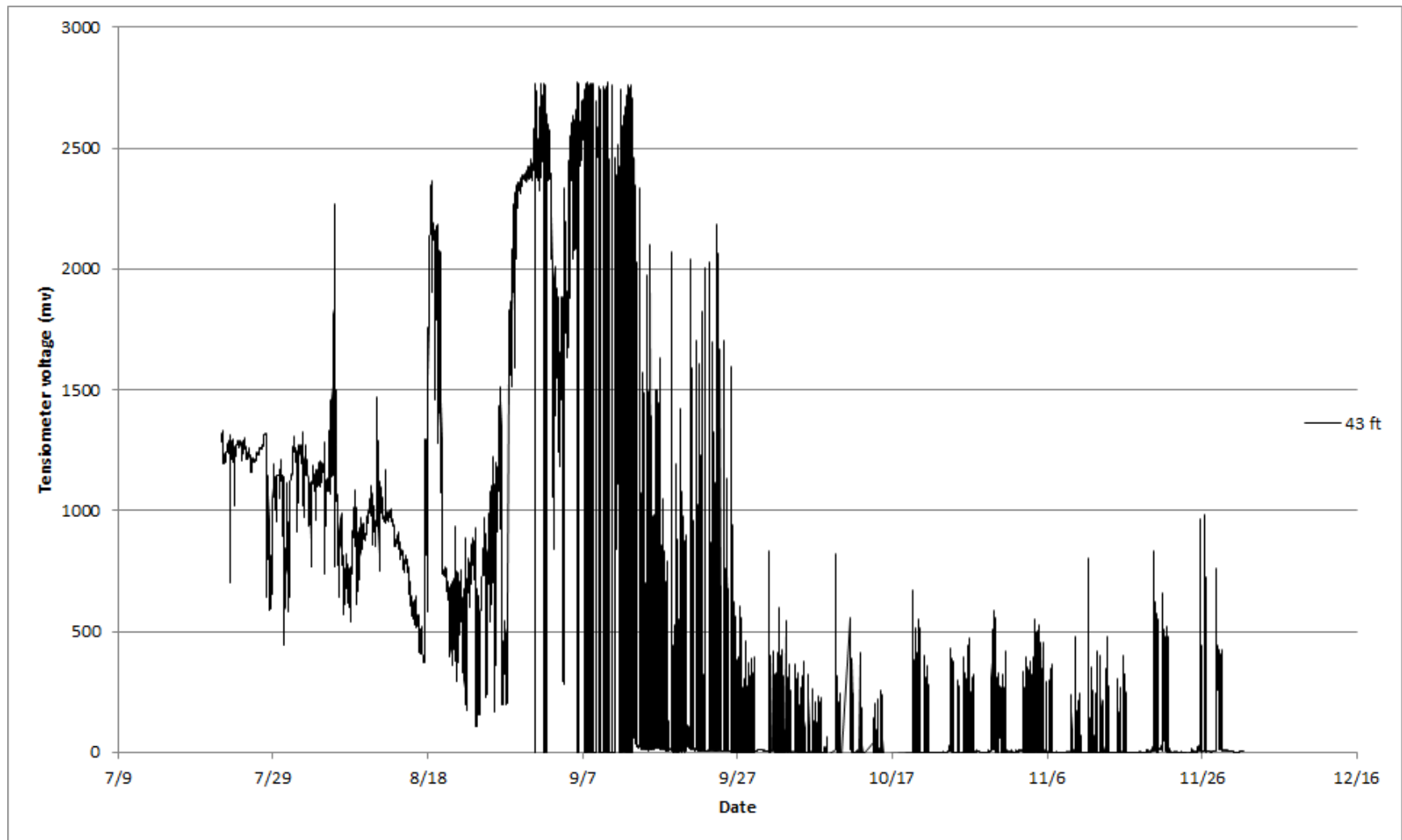
Figure 26. Voltage recorded for the AT in the PA 45-ft borehole.
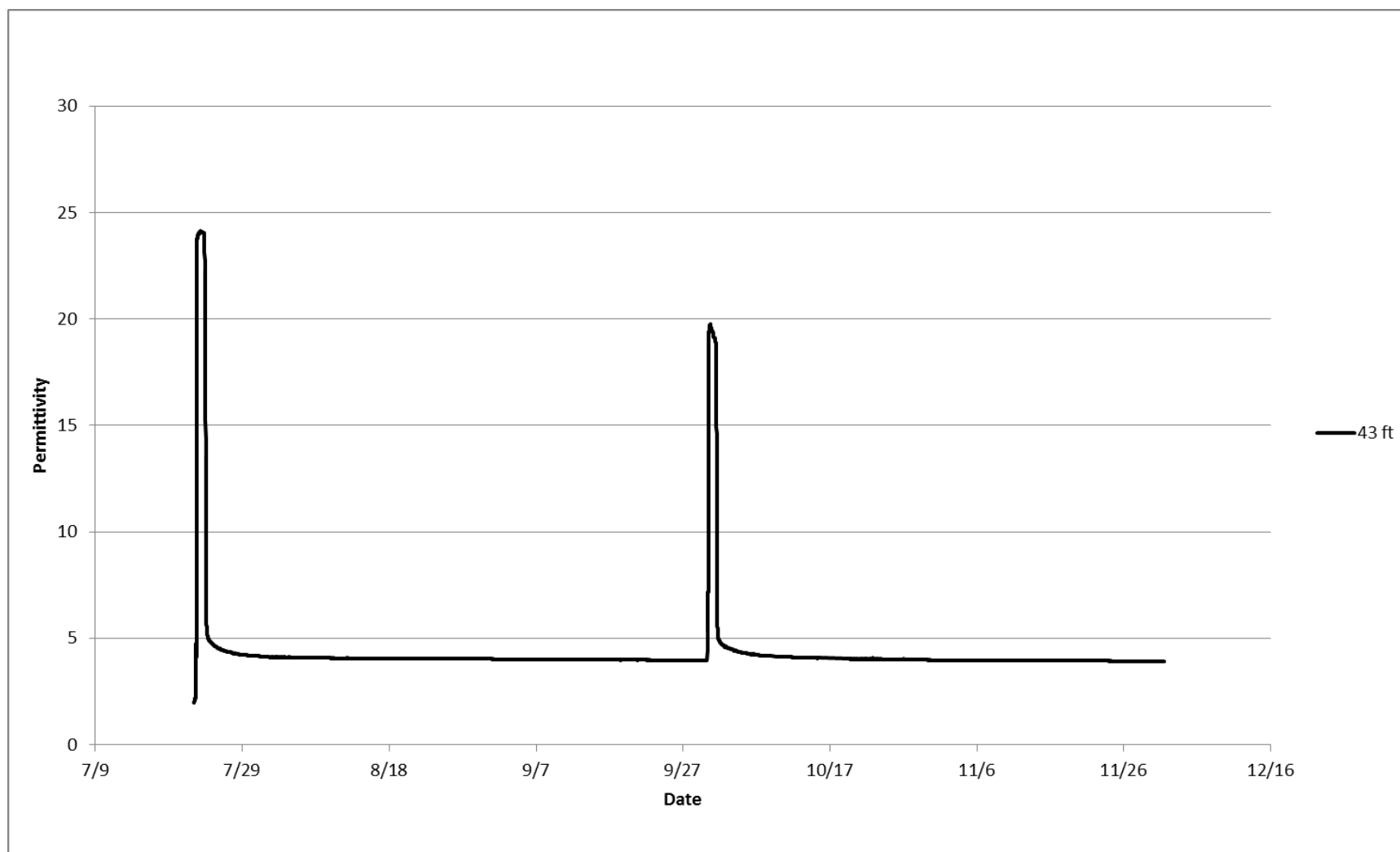
Figure 27. Permittivity recorded by the WCR probe in the PA 45-ft borehole.
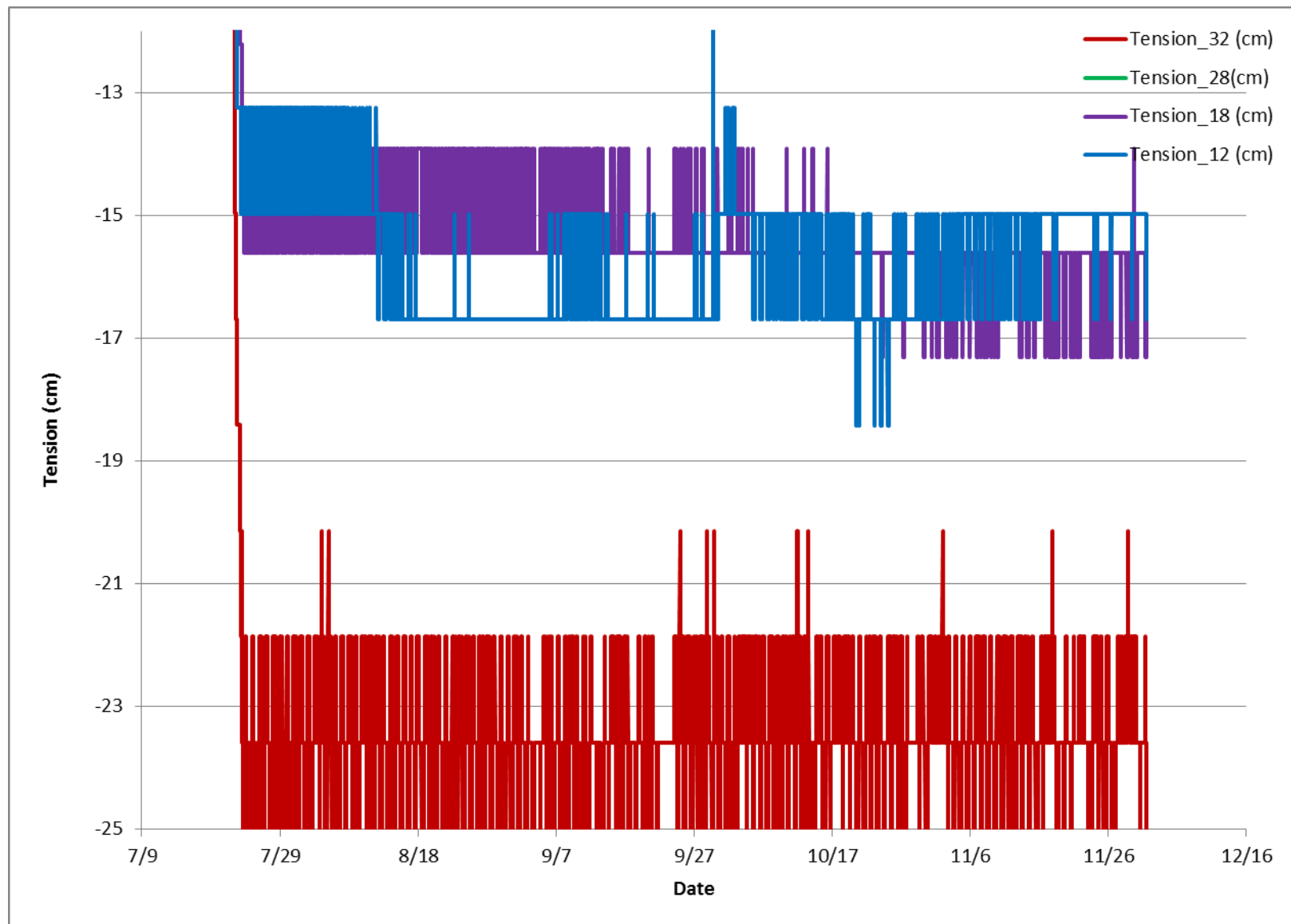
Figure 28. Tension calculated using measured AT voltage and calibration curve for ATs in the PA south instrumented tubes.
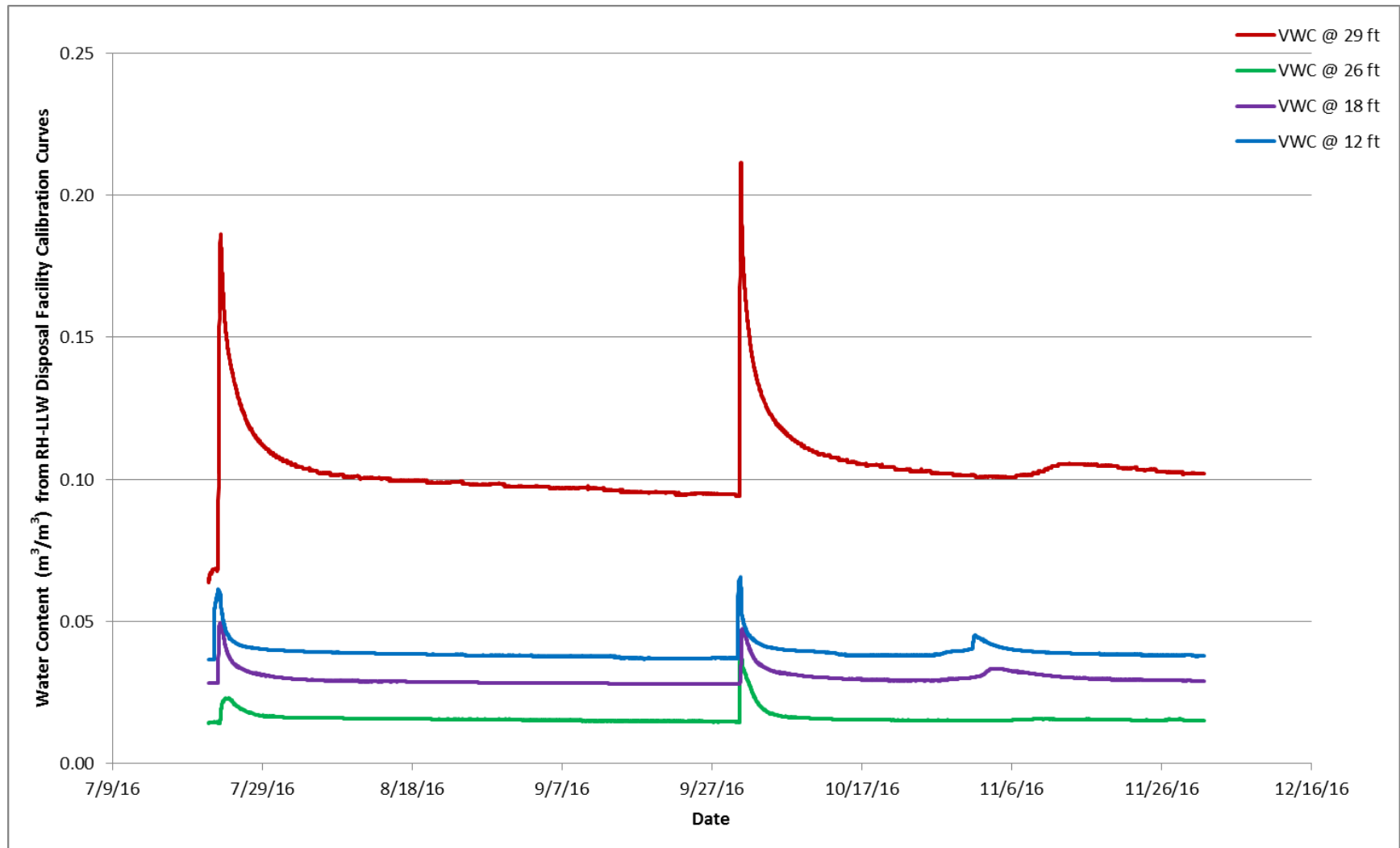
Figure 29. θ calculated using measured permittivity, first order calibration curve for data at 12, 18, and 26-ft depths and second order calibration curve for data at 29 ft in the PA south instrumented tubes.
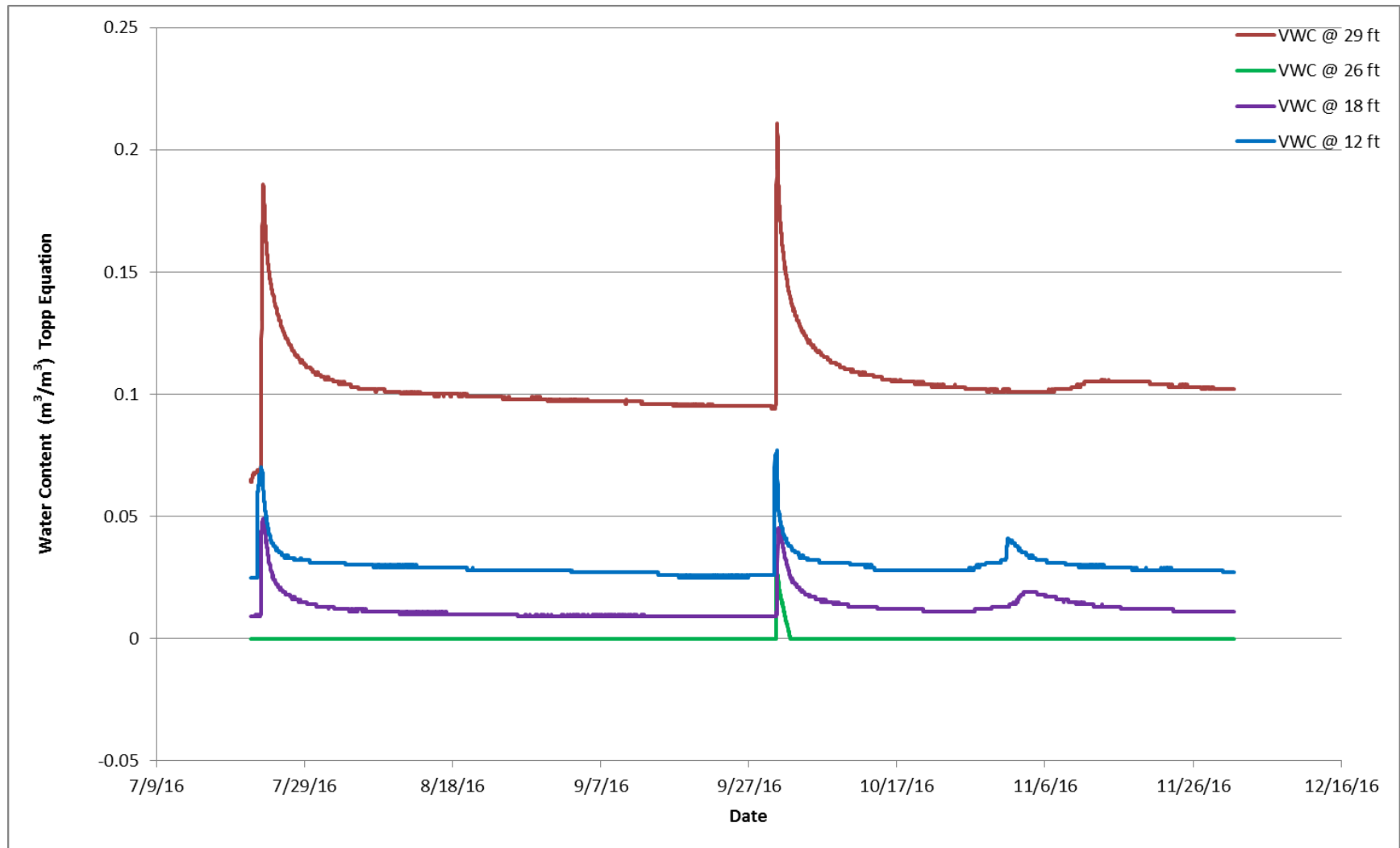
Figure 30. θ calculated using the Topp equation for the calibration curve applied to the measured permittivity at all depths in the PA south instrumented tubes.

6.7.3.2 ***Performance Assessment North Instrumented Tube Set.*** Using the parameters discussed in Section 6.6, data provided for the PA north instrumented tube set in Section 6.7.2.2 were adjusted with the calibration equations. The straight line formula in Table 20 for the ATs was applied to data shown in Figure 24. Resultant calibrated data are given in Figure 31.

The first order calibration relationship for the WCR probes derived for the vault perimeter drainage course and drainage course materials shown in Figure 16 were applied to the permittivity data shown in Figure 27 for the WCR probe installed at a depth of 26 ft. The second order calibration relationship for the Stratum II alluvium shown in Figure 21 was applied to the WCR probe data for the WCR probe installed at a depth of 29 ft. The resultant calibrated θ is shown in Figure 32.

For completeness, the Topp relationship provided by Equation (4) was also applied to the WCR probe permittivity data and is given in Figure 33. The minimum θ in Figure 33 has been truncated at a zero value, where the Topp relationship would have yielded negative θ. A negative θ is non-physical. In comparison, the calibration curves provided in Section 6.6 yield θ_r values of about 1.8%, which are still very low.

6.7.3.3 ***Performance Assessment 45-ft Drilled Borehole.*** The calibration curve for the AT installed in the PA 45-ft drilled borehole given in Table 20 was applied to the data shown in Figure 26. The resultant tension is shown in Figure 34, with all data plotted using the light blue dotted line and over plotted using a 100-point moving average. The ATs are very sensitive to barometric pressure changes and can be influenced by small changes in temperature. A 100-point moving average fitted to the data provides a better indication of the wetting front propagation at this depth.

Figure 35 contains the results of applying the Topp relationship (Equation 4) to the data shown in Figure 27 for the WCR probe installed at this location. The Topp relationship was used instead of providing media-specific calibration data to material at this depth because no soils were available. However, based on the American Geotechnics report and increased resistance during drilling, the alluvium at this depth is a fine material containing a large fraction of sand, silt, and clay, corresponding to the Stratum III alluvial material. Therefore, the Topp relationship should provide an adequate interpretation of θ.

Temperature data for thermocouples installed at depths of 12 ft (black line), 18 ft (blue line), 26 ft (purple line), 34 ft (green line), and 43 ft (red line) are given in Figure 36.

6.7.4 Test Interpretation

Data collected during the July through December timeframe will be discussed in the context of sensor behavior, θ_r, wetting front arrival sequence, and estimated hydraulic conductivity in the following subsections. These discussions are meant to inform the model used to assess the expected longevity of the concrete vault system and will be used to inform future monitoring efforts.

6.7.4.1 Sensor Behavior

Water Content Reflectometer Probe Response

The Campbell Scientific WCR probes provided very robust and accurate θ measurements in the coarse vault perimeter drainage materials, drainage course materials, and alluvial fill material. These sensors were hand installed at target depths because the materials were emplaced during vault backfill operations. This ensured the sensors were oriented horizontally with the probes fully embedded perpendicular to the expected wetting front direction. Wires were extended to the land surface using small diameter PVC tubing, and the PVC tubing was sufficiently backfilled to prevent preferential flow down to the tubes. An excellent signal response was observed for all of sensor locations and depths above 30 ft.
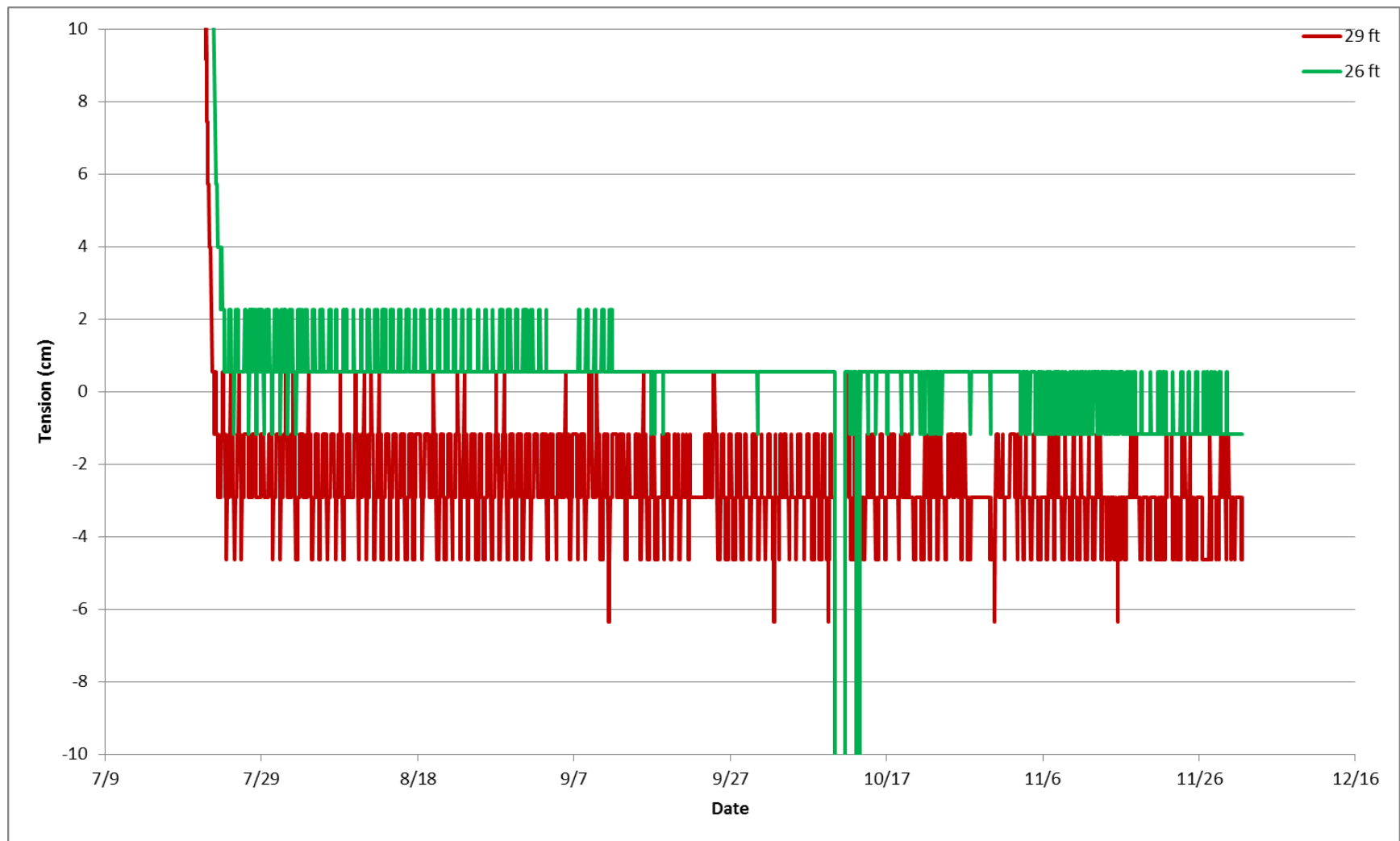
Figure 31. Tension calculated using a measured AT voltage and calibration curve for ATs in the PA north instrumented tubes.
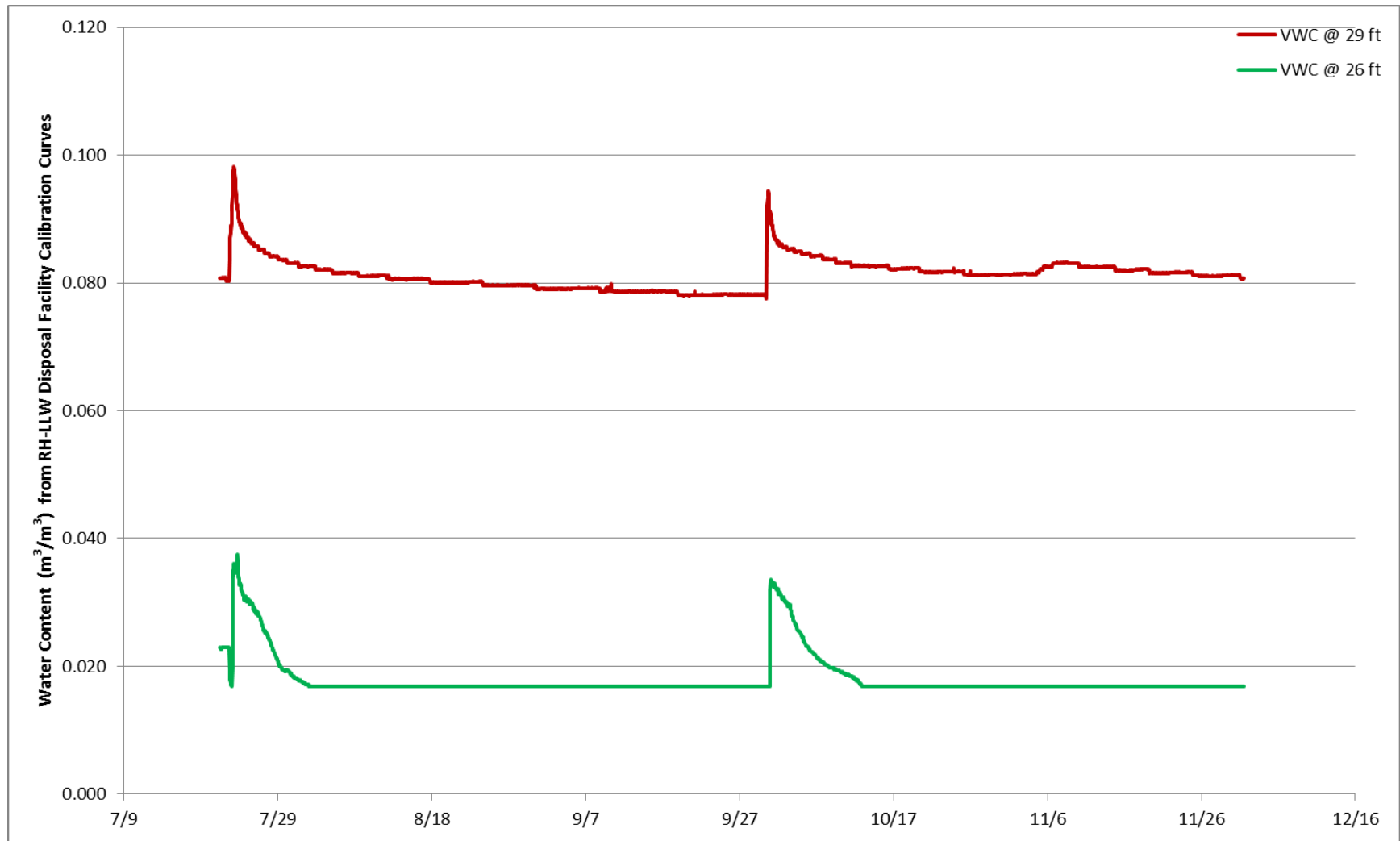
Figure 32. θ calculated using measured permittivity, first order calibration curve for data at 26-ft depths, and a second order calibration curve for data at 29 ft in the PA north instrumented tubes.
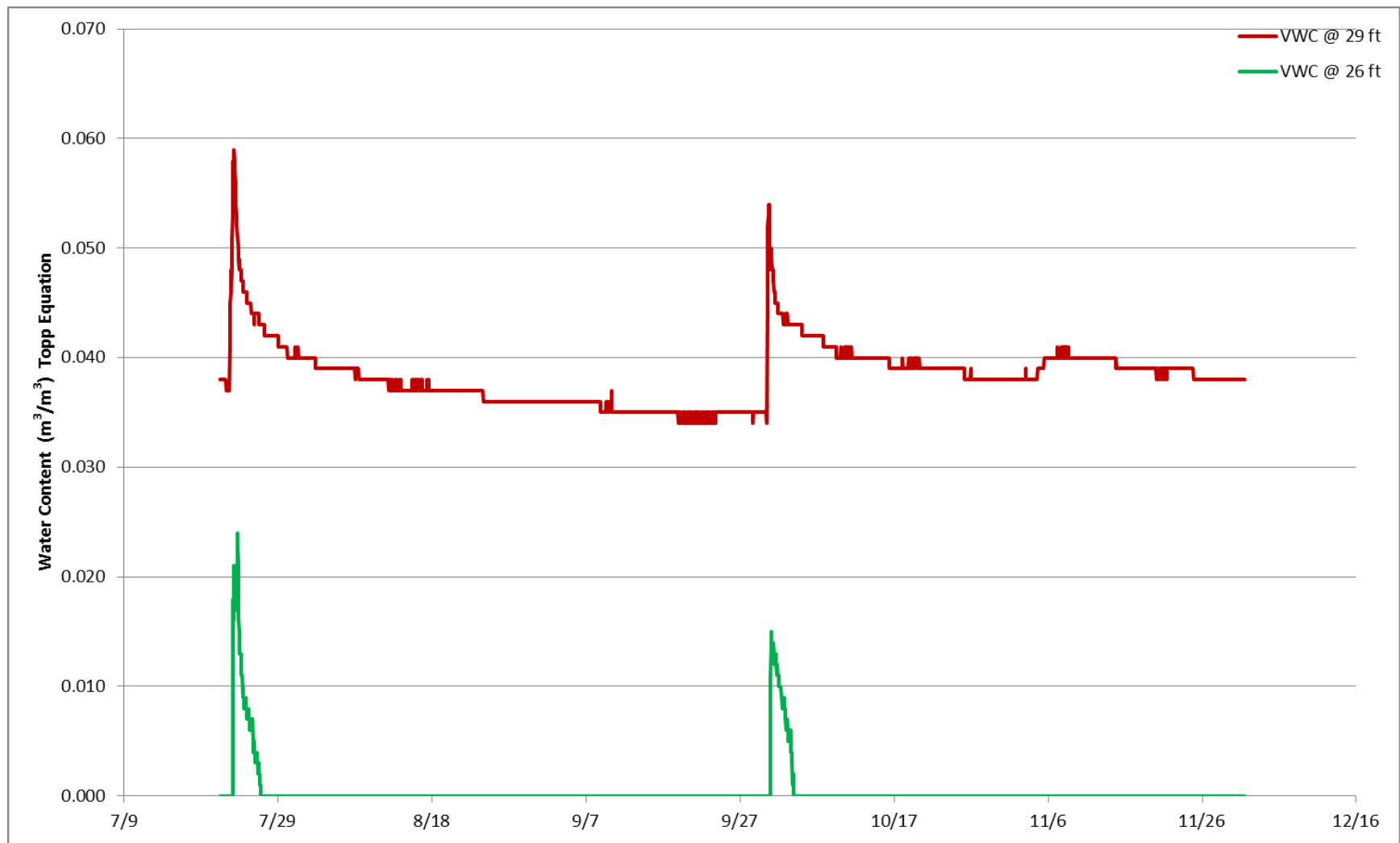
Figure 33. θ calculated using the Topp equation for a calibration curve applied to the measured permittivity at all depths in the PA north instrumented tubes.
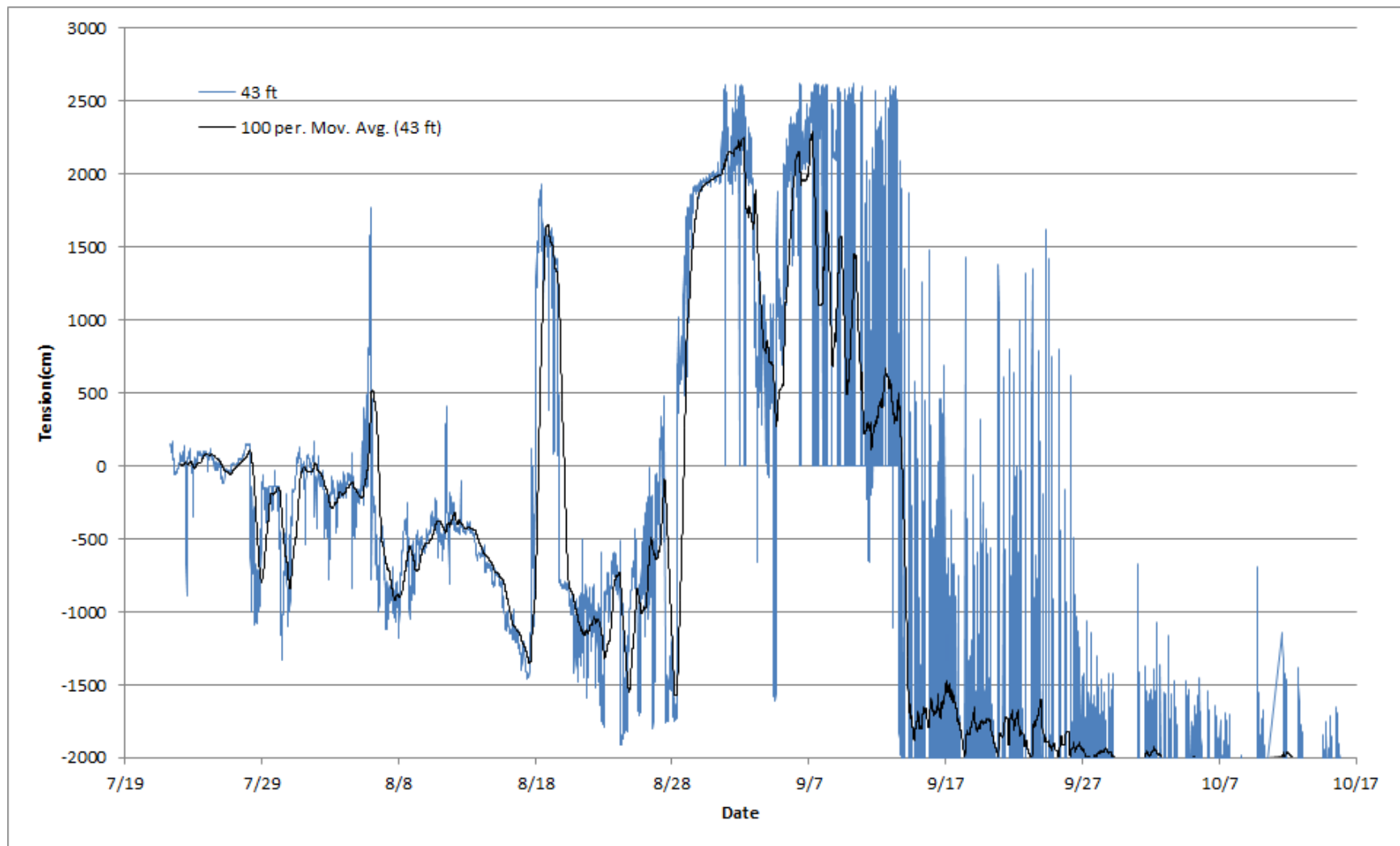
Figure 34. Tension calculated using a measured AT voltage and calibration curve for AT in the PA 45-ft borehole with a 100-point moving average overlying the data.
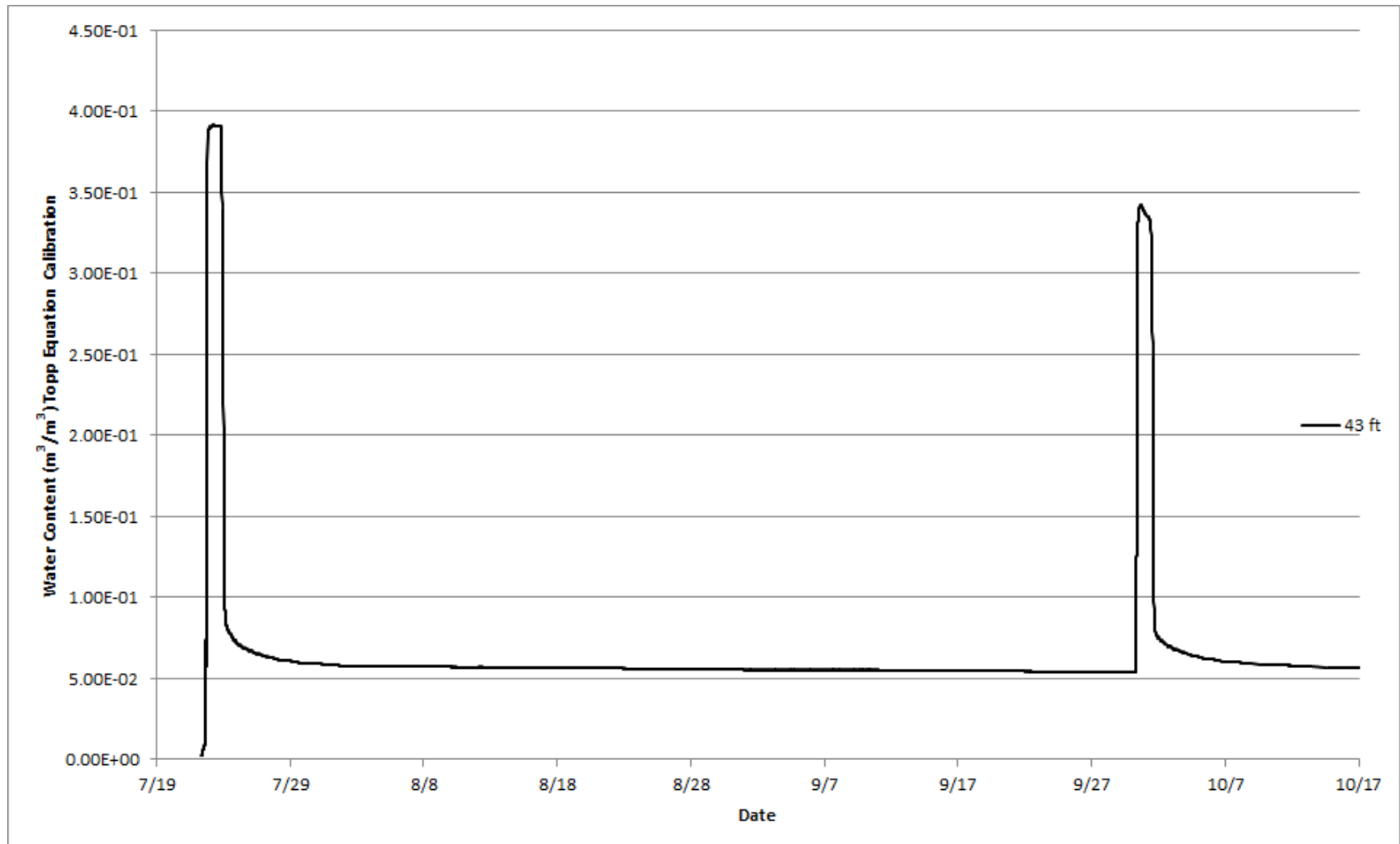
Figure 35. θ calculated using measured permittivity and the Topp Equation calibration curve for data at 43 ft in the PA 45-ft borehole.
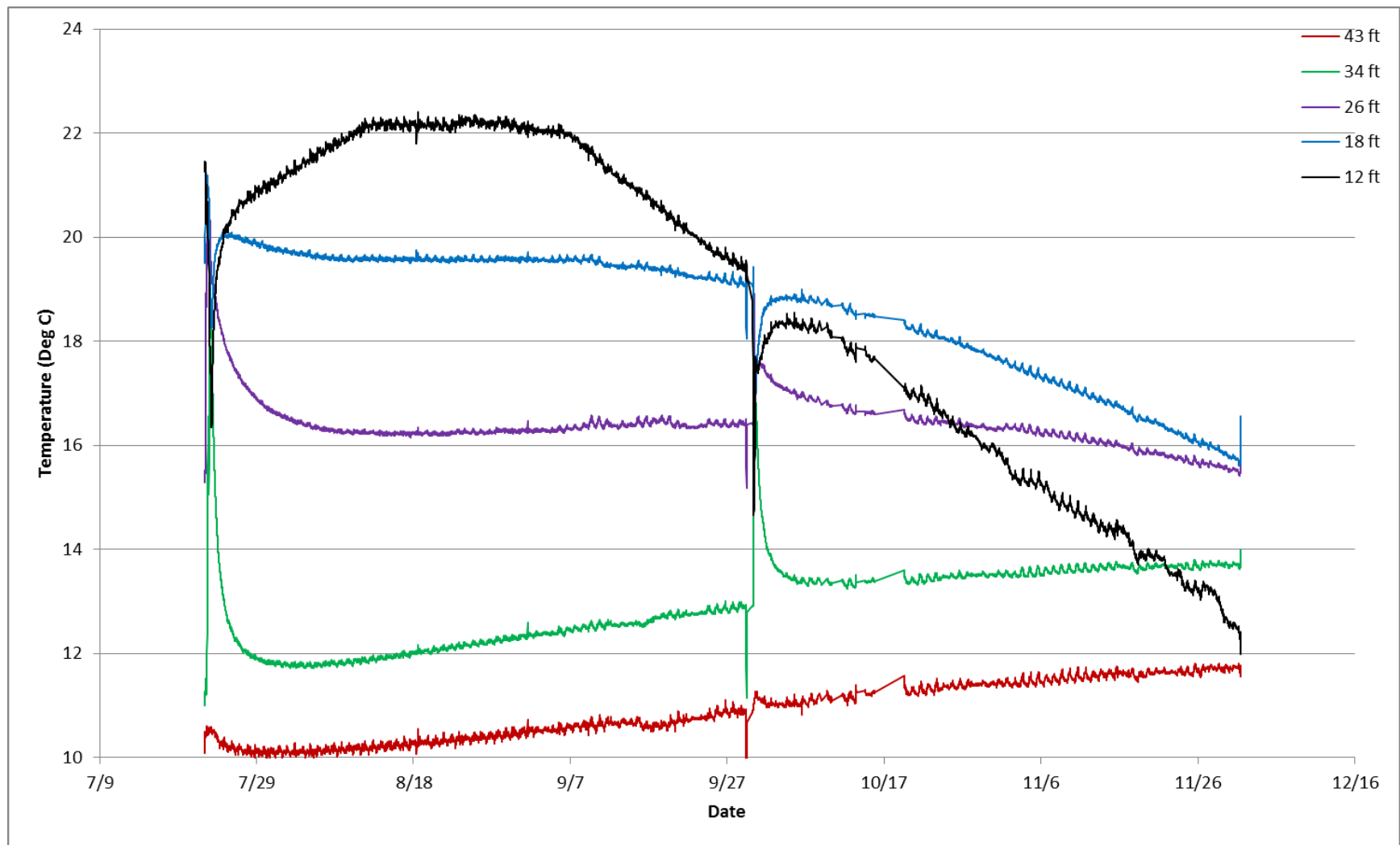
Figure 36. Temperature in the PA 45-ft borehole.

Auguring in the 45-ft drilled borehole required the WCR probe be installed with the probes oriented vertically instead of horizontally. The wires were brought to land surface using the same small diameter PVC tubing, but the in-auger material could not be hand compacted around it as the auger was reversed to land surface. Based on data shown in Figure 34 compared to the AT signal response shown in Figure 35, it is very likely the WCR probe in the 45-ft drilled borehole responded to moisture infiltrating down the sides of the PVC tubing. Over time, it is likely soils around this PVC tube will self-consolidate and the signal response will be more reflective of the actual θ at a depth of 45 ft.

Advanced Tensiometer Response

The signal response observed in the AT installed in the 45-ft drilled borehole is unexpected. While the early (i.e., prior to August) signal might be reflective of several small wetting fronts, the calculated tensions are well out of range of the expected values.

ATs installed in the PA south and PA north instrumented tube sets are not correctly recording water tension. Initially, it appears as though sensor readings were reflective of water tension, but, after several hours, the signal in all sensors shallower than 26-ft appear to reflect simple white noise. The AT installed at a depth of 26-ft in the PA south location appears to be recording barometric pressure fluctuations. There are no discernable trends in either of the two ATs installed in the PA north instrumented tube set. This behavior is very uncharacteristic of a sensor design that has proven to be extremely robust when installed in very dry conditions existing in deep vadose zones. It is very uncharacteristic that a measurable, discernable signal would not be observed during the relatively high θ characterization infiltration events.

As shown in Figure 16a, components of AT include an outer guide pipe and a flexible inner guide pipe that contain a pressure transducer apparatus. The outer guide pipe of the AT consists of a porous ceramic cup, a water reservoir, a gasket throat, and the outer 1.5-in. PVC guide pipe. The inner pressure transducer apparatus is comprised of an inner flexible pipe, the pressure transducer, and a rubber stopper (i.e., gasket) that seals in the gasket throat. Through the inner flexible pipe, an air line is run to allow maintenance of the AT by providing the ability to refill the water reservoir. The electrical leads are also run through the flexible inner guide pipe.

The installation process for the monitoring system used at the PA Confirmation Vault location was modified to allow acceleration of vault perimeter drainage course material installation. Instead of pre-setting the outer guide pipes at depths of 29-ft and 26-ft and backfilling with the vault perimeter drainage course material to a height of about 7 ft, adding the next extension section of the outer guide pipe, and continuing backfill to the surface, a different installation method was used. First, an 18-in. deep hole was dug into the Stratum II alluvium beneath the drainage course material. Then a 10-ft tall section of 10-in. Schedule 80 PVC pipe was placed into the hole and stabilized with the Stratum II alluvium removed from the hole. Then, the drainage course material and vault perimeter drainage course material were packed around the 10-in. PVC pipe to a total depth of 9 ft. The AT and WCR to be installed at a total depth of 29 ft were lowered into the pipe and backfilled with 18-in. of Stratum II alluvium, then the AT and WCR to be installed at a total depth of 26 ft were lowered into the pipe and the 10-in. PVC pipe was backfilled nearly to the top (about 9 ft). The pipe was pulled from the ground using a front-end loader. This left the tops of the outer guide pipe for the ATs and the 1-in. diameter PVC tubes carrying the WCR electrical wires available for extension to land surface. These tubes were extended by adding couplers, stringing the air line and electric leads through the next PVC sections, and backfilling the guide tubes following the expected procedure. Use of the 10-in. PVC pipe did not affect installation of the sensors at either 18 ft or 12 ft in the PA south location.

After the guide pipes were brought clear to the surface, the flexible inner guide pipe containing the very sensitive pressure transducers were placed into the outer guide pipes and the electric leads were connected to the data loggers. At this time, an initial reading indicated the ATs were functioning correctly; however, they failed shortly after.

It is not known whether pulling the 10-in. PVC pipe from around the installed sensors disrupted the seal between the porous ceramic cup and the outer guide pipe at the 26 and 29-ft locations. It is also not known if the ground motions and largely fluctuating ground pore pressures caused by nearby mechanical vibratory compactors being used at the vault installation area resulted in damage to the pressure transducers. The inner guide pipe will be pulled from these installations, the pressure transducer checked using the calibration procedure, and replaced if necessary. As part of monitoring system maintenance, the ATs will be refilled to check the inner seals at the top of the ceramic cup. If the ceramic cups or inner seal have been damaged, no further data will be collectable using the ATs. Inability to collect data from the PA vault ATs will not affect facility compliance and performance monitoring.

Thermocouple Response

The 45-ft borehole was augered from land surface to the total depth, with the auger hole within 2-ft of the vault perimeter block. Therefore, this hole penetrates the crushed gravel base course material, the vault perimeter drainage material, the drainage course material, and the Stratum II alluvium to a total depth of 45 ft. The sensors at depths of 12, 18, and 26 ft are installed in media, presumably representing the vault perimeter drainage course and drainage course materials. The sensor at 34 ft is likely installed in a gravely sandy Stratum II alluvium material and the deep sensor is installed in the Stratum III sandy, silty clay alluvium material (American Geotechnics 2011). These sensors were installed by first augering the hole using a hollow stem auger, placing the AT and WCR probe at a 43-ft depth, and reversing the auger to the target depth for thermocouple installation. This process will result in some inter-depth material mixing as the auger is reversed to the surface. Initially, the materials in this auger hole were highly disturbed, but over time, they will consolidate under their own weight. Therefore, the absolute temperatures taken within a week of augering the hole may not represent the final at-depth temperature, and temperatures taken during the first and second characterization test may not reflect wetting front propagation that would be reflective of a consolidated condition.

6.7.4.2   *Residual Moisture Content θ_r*

Vault Perimeter Drainage Material and Drainage Course Material

Figures 28 and 31 show that θ_r at 26 ft is approximately 0.015 (1.5%). The θ_r at 18 ft at the PA south location is approximately 0.028 (2.8%) and, at a depth of 12 ft in the PA south location (Figure 30), it is approximately 0.035 (3.5%).

The laboratory data reported $\theta_r = 0.0\%$. The differences between field data and laboratory data are related to increased consolidation of the drainage materials achieved using vibratory hand compactors during material installation.

For the purposes of estimating concrete longevity, a value of 3.5% is appropriate. This can be compared to θ_s (also equal to the porosity) of 37.3%, resulting in a residual saturation of approximately 9%.

Stratum II Alluvium at a 29-ft Depth

Figures 28 and 31 show that θ_r in the alluvium at a depth of 29 ft is approximately 0.09 (9%). There are no corresponding laboratory data for this material, but based on the similarity to the crushed gravel base course material, this range is appropriate.

Stratum III Alluvium at a 43-ft Depth

Assuming the WCR probes are in contact with the Stratum III alluvium in the 45-ft borehole, Figure 36 indicates that θ_r in the Stratum III alluvium is 0.05 (5%). This seems an unlikely low value for Stratum III alluvium given the sandy-silty clay material type. The sensor is likely installed in Stratum II alluvium.

70

6.7.4.3 *First Characterization Test.* Figures 37 and 38 contain the calibrated θ for instruments installed in the PA south and PA north instrumented tube sets. These data are replotted from Figures 29 and 32 with the time-scale expanded to show the first arrival of water at the sensor depths and the re-equilibration to background θ. The arrival information and peak θ is summarized in Table 25.

- Sensors installed in the vault perimeter drainage material and drainage course material. At the PA south location, the infiltrating water arrived at the 12-ft sensor first, followed by near simultaneous water arrival at depths of 18 and 29-ft. The last sensor to respond was the sensor located at a depth of 26-ft. At the PA north location, infiltrating water arrived at the 26 and 29-ft depths, almost at the same time the 12-ft sensor in the PA south instrumented tube responded.

  At the PA South location, the peak θ recorded in the vault perimeter drainage material and drainage course material was 6%, with this value achieved at a depth of 12 ft and with content decreasing with depth to a value of 1.5% at 26 ft. A similar peak θ was observed at 26 ft in the PA north instrumented tube set, where a peak θ of 3.4% was observed.

  Other significant differences are apparent in the widths of the θ peaks where the PA north instruments at a depth of 26 ft are much more pronounced in width and peak value compared to the subdued response observable in the PA south location. At the PA south location, the very low θ response shows very little water reached a depth of 26 ft, while in the PA north location, the larger signal response shows more water arrived at the 26-ft depth.

- Sensors installed in the Stratum II Alluvium. The peak θ observed in the Stratum II alluvium located below the drainage course material at the PA south and PA north locations were much higher at 18.6% and 9.7%, respectively, than observed in any of the drainage materials. This was expected given a larger fines fraction compared to the negligible fines in the drainage materials.

There are at least three different explanations for the differences in the very low peak θ observed in the vault perimeter drainage material and to the early arrival of water in the Stratum II alluvium, with the possibility that a combination of the following three mechanisms are contributory:

1. It is possible that water flowed preferentially down the geotextile material, separating the vault perimeter drainage material and the alluvial fill material. Earlier arrival at the deeper PA north sensors could indicate that a portion of the water applied on the surface road base traveled down a preferential flow path created by the geotextile material placed between the vault perimeter drainage material and the alluvial fill material. If this occurred, the width of the peak θ response and very long tail-off in the PA north location indicates that the bulk of the water likely moved through the lower transmissivity alluvial fill material with a much smaller volume moving through the path created by the geotextile material.

2. It is possible that a capillary barrier was created between the crushed gravel base course and the vault perimeter drainage material, diverting the infiltrating water into the alluvial fill material. Based on the van Genuchten parameters provided in Tables 11 and 15, this is possible, even though all of these materials are relatively course.

   During this first characterization test, approximately 1,900 gallons (7.2 m^3) of potable water were applied within the 8×8-ft (2.7 m x 2.7 m) test box during the 23-hour test period. The average porosity of the surface road base, crushed gravel base course material, and vault perimeter drainage material is on the order of 35% (see Tables 9 and 13). Assuming a water column over the vault perimeter drainage material of $2 \times 8 \times 25$ft (403 ft^3, 11.4m^3), the pore volume below the test box is approximately 3.4 m^3. The total volume of water applied to this area, assuming equal distribution across the test box, is 1.8 m^3. If the applied water migrated directly into the pore space and had not exited into the drainage column, the applied water volume was high enough to result in a water

71

saturation of approximately 50%. However, the observed peak θ at a depth of 12 ft was only 6% (Sw = 16%).

The lower than expected peak θ implies that the bulk of the water applied to the surface road base did not pass through the vault perimeter drainage material, but was diverted around it instead. This would account for the very broad and long-lasting θ distribution observable in the PA north instrument set at 26 ft, the higher peak θ at 12-ft depth than at the 18-ft depth in the PA south location, and the lack of significant water at 26 ft in the PA south location.

3. It is possible horizontal hydraulic conductivity is significantly larger than vertical hydraulic conductivity in the surface road base, crushed gravel base course, vault perimeter drainage material, drainage course material, and alluvial fill material. Anisotropic hydraulic conductivity in these materials would be associated with requirements for achieving 95% compaction at the optimal θ as the materials were installed in 6-in. lifts.

Evidence of higher-than-anticipated horizontal conductivity was observed during the first test (Figure 39). The measured extent of the relatively high saturated surface road base shown in the photograph ranges from several centimeters to as much as 1.5 m on three sides of the test box. When looking down the gaps between the vault perimeter edge blocks, it was apparent that water had reached the crushed gravel base course material at the bottom (i.e., depth of 6 ft) of the vault perimeter edge blocks.

Accounting for the larger horizontal test area (approximately $14 \times 11 \times 25$ ft) observed in Figure 39 would reduce the predicted saturation from 50 to 20%, which is still higher than the observed peak θ at a depth of 12 ft. However, this calculation accounts for a full 25-ft vault height, which still results in large over-predictions of peak θ.

- Sensors in the PA 45-ft drilled borehole. Figures 40, 41, and 42 contain data collected in the PA 45-ft drilled borehole. The AT data contain a large broad peak in water tension, beginning on approximately August 23, 2016, and continuing through September 2, 2016. The timing of this peak starts approximately 30 days after the pumps were turned off and ends prior to beginning the second characterization test. The corresponding WCR shows an instantaneous response during both tests, probably caused by water infiltrating along the PVC tubes that extend to land surface. Over time, the materials adjacent to the WCR could seal and the WCR could provide useful data in the future; however, presently, the WCR data are not useful.

The thermocouples respond to the wetting front as it passes through the perimeter drainage gravel. The first characterization test was started at 6:30 a.m. July 22, 2016. The water truck supplying the infiltrating water was delivered to the site the previous night and the water temperature had equilibrated with the overnight ambient air temperature. The arrival of the cold water is observable at the 12-ft location. As the daytime temperature increased, the water in the truck warmed and the signal at depth was damped. By the time the infiltrating water reached the depth of 34 ft, the water was much warmer than the ambient soil temperature, and the signal is very pronounced. While temperature data are not directly correlatable to θ, they provides a reliable indication of wetting front arrival times.

Table 25. Summary of arrival times and peak moisture content for the first characterization test.

Sensor Location	Time of First Arrival	Time When Moisture Content Rises Rapidly	Time When Peak θ Decreases Significantly	Peak Moisture Content Percent	Date θ Approaches θr	Comments
PA South 12-ft	7/22/2016 14:50	7/22/2016 16:20	7/23/2016 10:00	6.0	7/29/2016	Width of "peak" reflective of the 24-hour test period
PA South 18-ft	7/23/2016 02:30	7/23/2016 2:30	7/23/2016 14:20	5.3	7/29/2016	
PA South 26-ft	7/23/2016 09:30	7/23/2016 9:40		1.5	7/27/2016	Rapid return to θr
PA South 29-ft	7/23/2016 02:20	7/23/2016 10:40	7/23/2016 10:40	18.6	9/27/2016	Narrow steep peak with long tail
PA North 26-ft	7/22/2016 xxx	7/23/2016 04:00	7/23/2016 21:00	3.4	8/2/2016	First arrival questionable---see figure
PA North 29-ft	7/22/2016 14:00	7/23/2016 04:00	7/23/2016 06:00	9.7	8/3/2016	
PA 45-ft	8/23/2016	8/28/2016	9/2/2016			Based on first large peak in the AT data
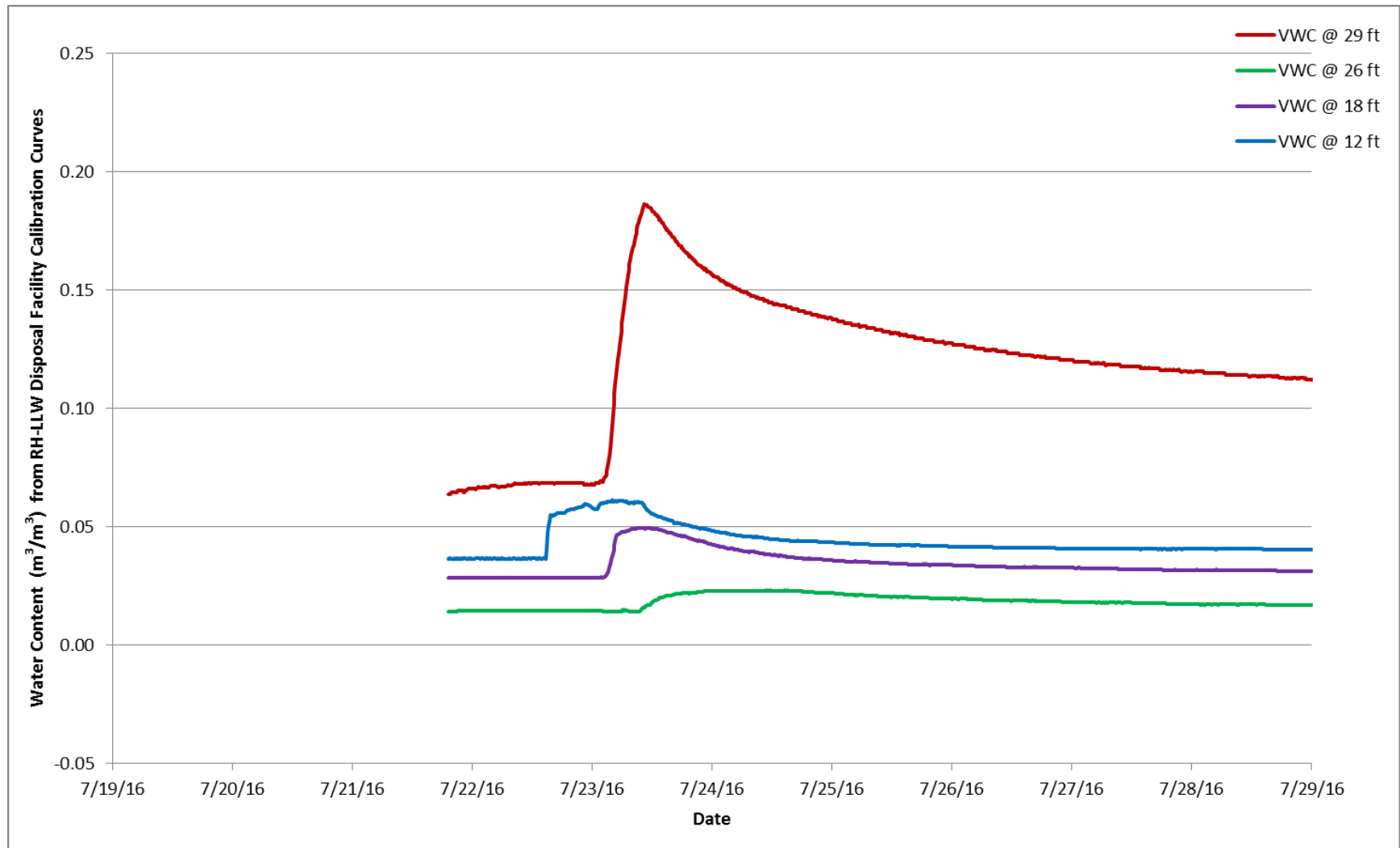
Figure 37. θ calculated using measured permittivity, first order calibration curve for data at 12, 18, and 26-ft depths and second order calibration curve for data at 29 ft during the first characterization test in the PA south instrumented tubes.
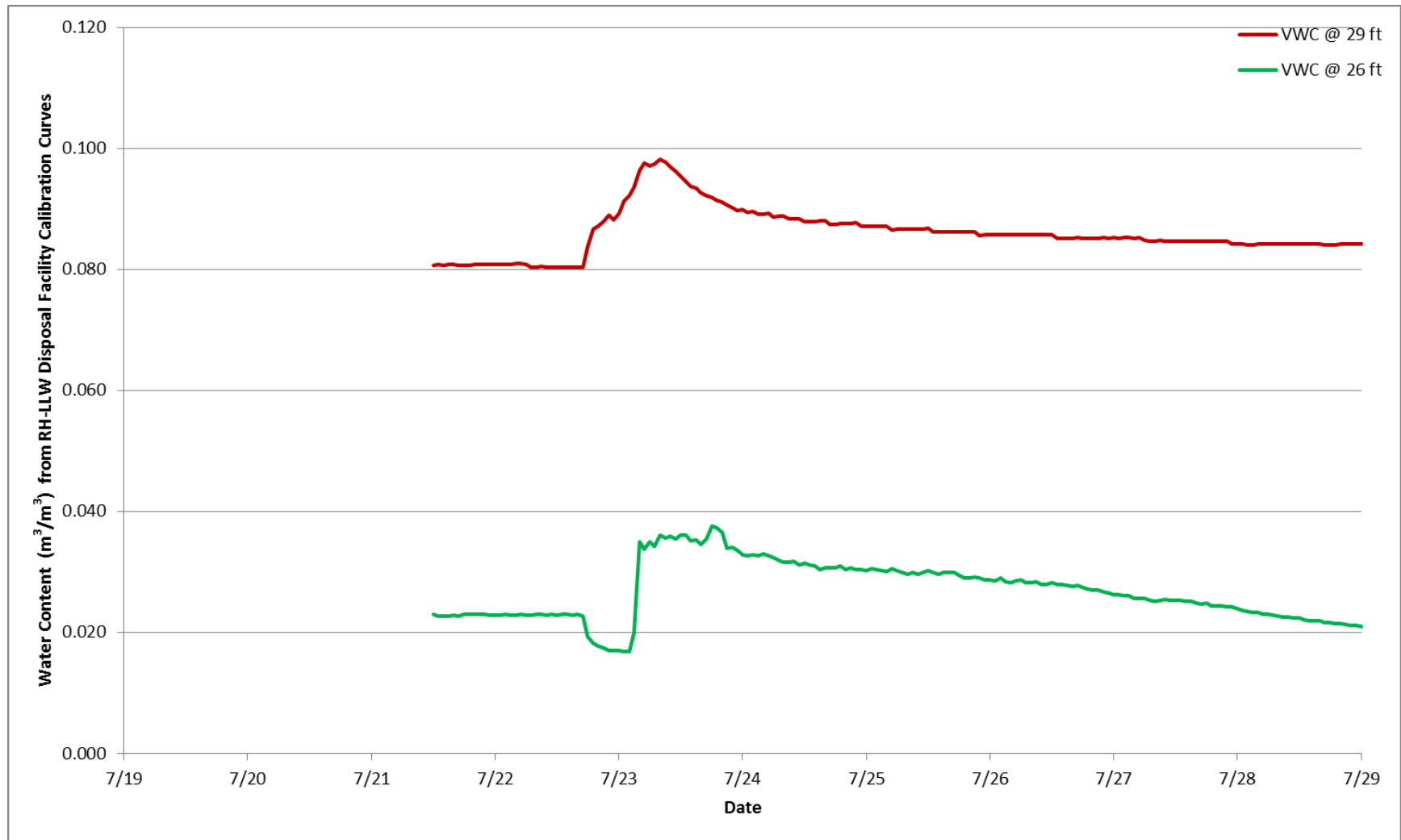
Figure 38. θ calculated using measured permittivity, first order calibration curve for data at 26-ft depth, and second order calibration curve for data at 29 ft during the first characterization test in the PA north instrumented tubes.

Figure 39. Observed extent of lateral water migration away from the water application area at the end of the first characterization test.

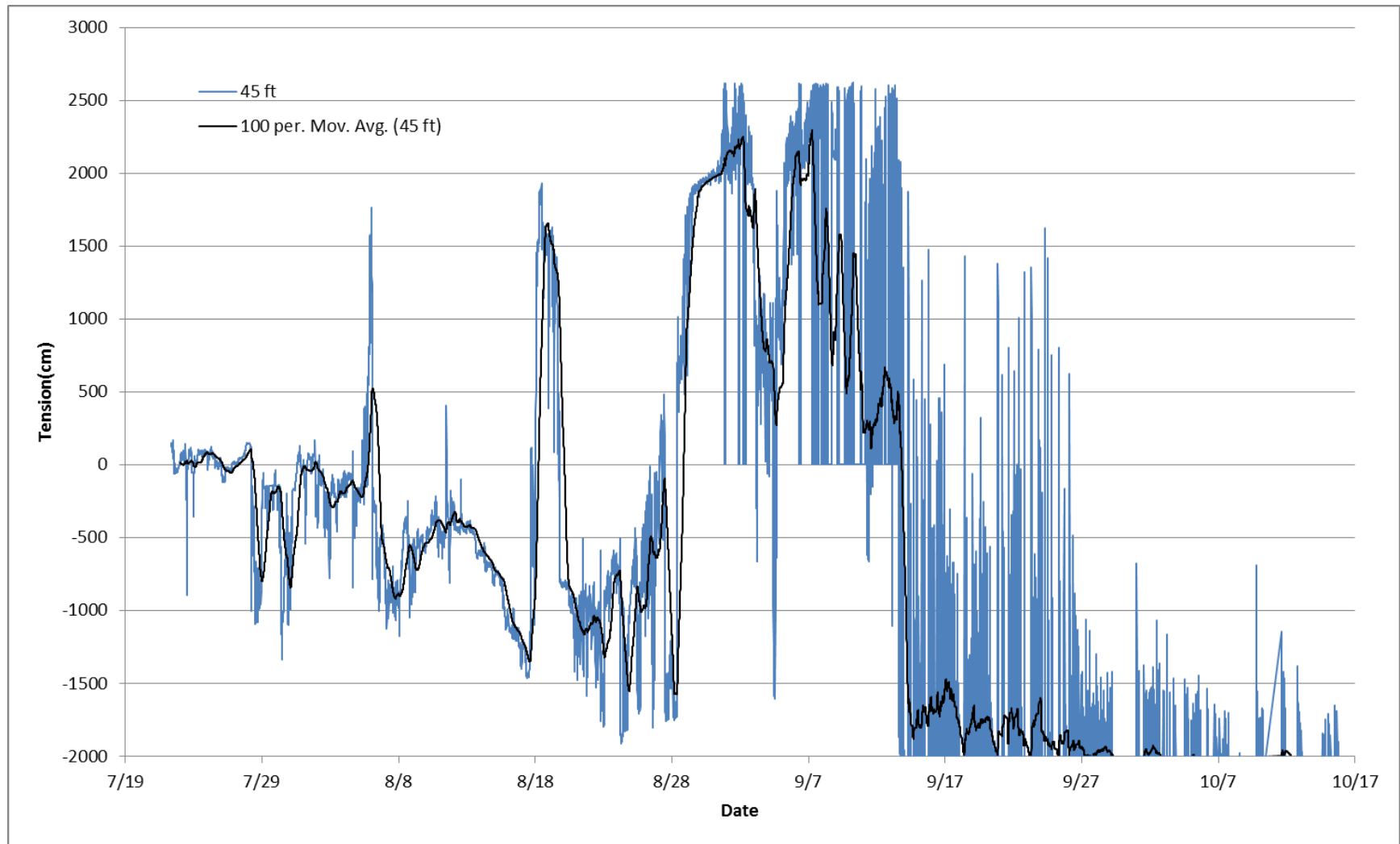Figure 40. Tension calculated using the measured AT voltage and calibration curve for the AT in the PA 45-ft borehole.
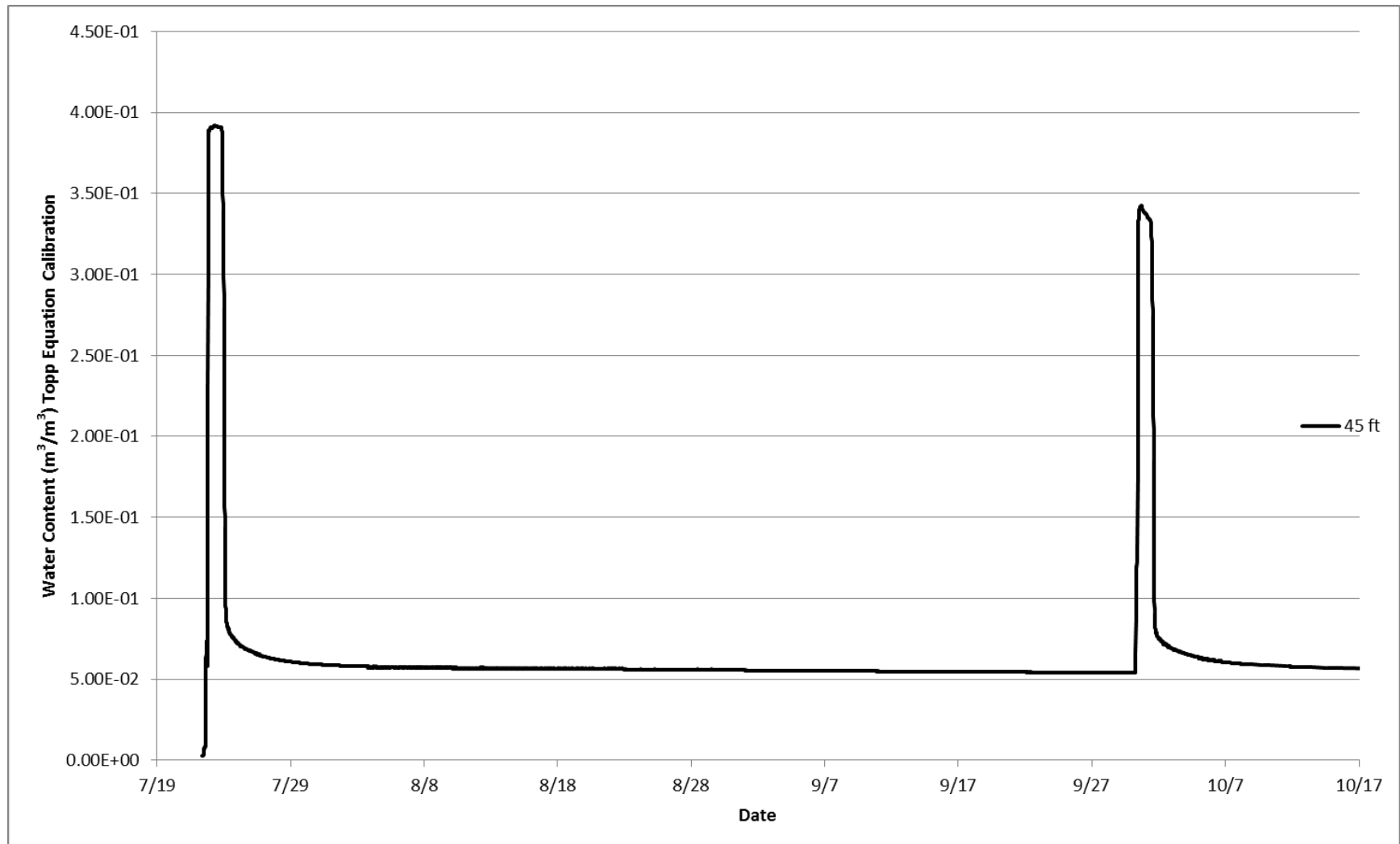
Figure 41. θ calculated using measured permittivity and the Topp Equation calibration curve for data at 43 ft in the PA 45-ft borehole during the two characterization tests.
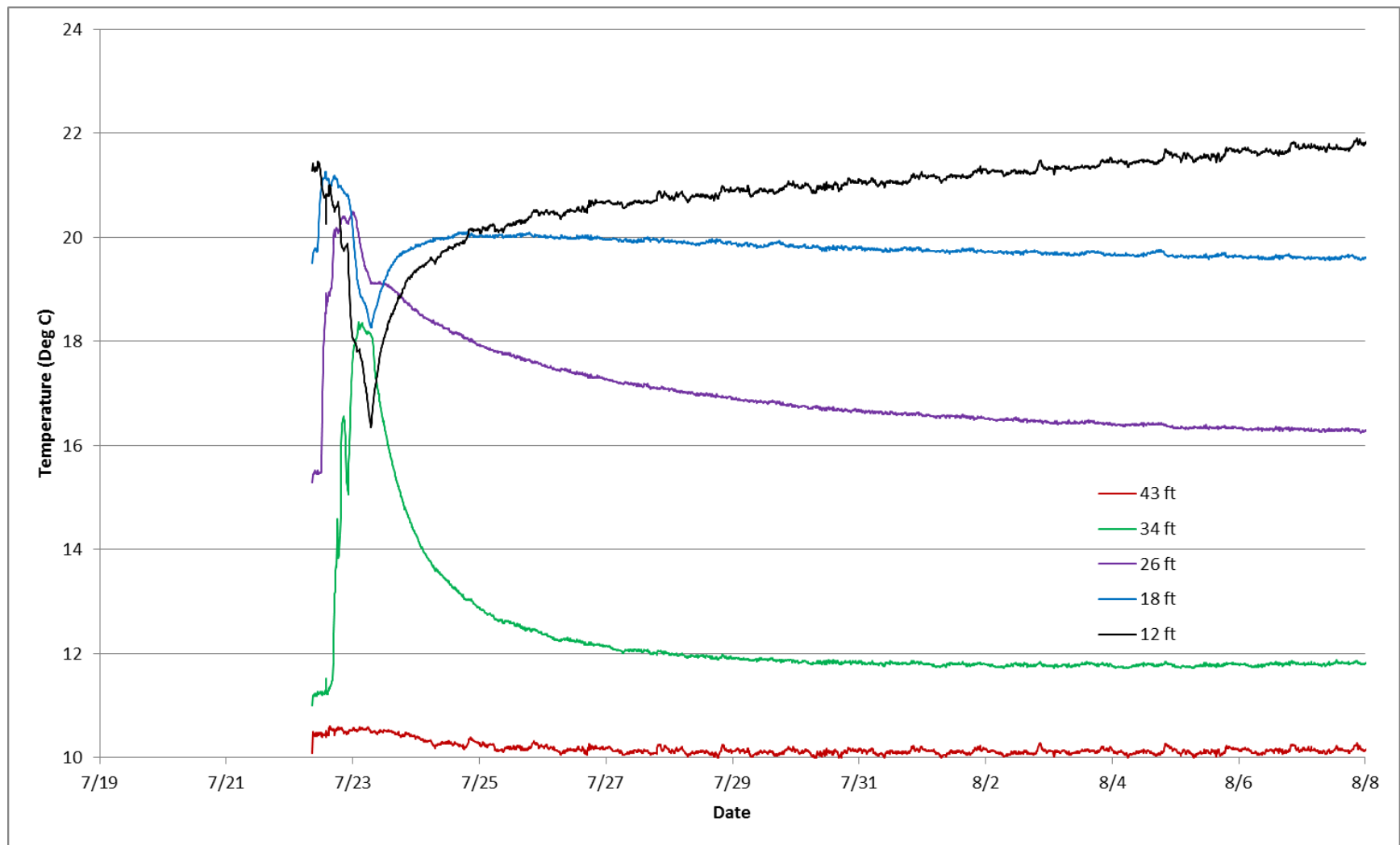
Figure 42. Temperature in the PA 45-ft borehole during and after the first characterization test.

6.7.4.4 **_Second Characterization Test._** Figures 43 and 44 contain the calibrated θ for instruments installed in the PA south and PA north instrumented tube sets. These data are replotted from Figures 29 and 32 with the time scale expanded to show the first arrival of water at the sensor depths and re-equilibration to background θ. The arrival information and peak θ are summarized in Table 26.

At the PA south location, the infiltrating water arrives out of sequence at the 18-ft depth as indicated by earlier arrival at the PA south 26-ft sensor. Although the arrival order is out of sequence, the order in peak θ is consistently decreasing within the perimeter drainage gravel, with highest θ at 12 ft and lowest θ at 26 ft. At the PA north location, the first arrival occurs first at the 29-ft depth, followed by arrival at the 26-ft depth.

The observed wetting front behavior during the second characterization test is consistent with the first characterization test. As explained in Section 6.7.4.3, it likely caused by a combination of preferential infiltration along the geotextile material, formation of a capillary barrier between the crushed gravel base course material and vault perimeter drainage material, and anisotropic hydraulic conductivity of drainage materials and alluvial fill material.

The data plotted in Figure 45 show that the AT installed in the PA 45-ft drilled borehole responds about 20 days after the start of the second characterization test. The sensor shows a response for a period of about 10 days. The longer-term response is expected and it is likely that the later set of peaks corresponds to a natural infiltration event that occurred about 48 hours after the end of the second characterization test.

During this much shorter duration test, the thermocouples do not show an appreciable response (Figure 46).

6.7.4.5 **_Natural Precipitation Event._** Figures 47 and 48 represent the calibrated θ for the PA south and PA north instrumented tube sets for the late October to early November time period. These data were extracted from Figures 29 and 32.

The observed θ response is a result of the natural precipitation events that occurred during October 2016 (see Table 24) when approximately 2 in. of rain was recorded at the ATR Complex weather station over a 2-week period. During this time, 3/4-in. fell on October 24, 2016; 0.42-in. fell on October 28, 2016; 0.09 in. fell on October 29, 2016; and 0.5-in. fell on October 30, 2016, with smaller amounts during that 2-week period. At INL, the annual average precipitation rate is 8.4 in. and the average monthly rainfall is less than 1.2 in. (http://niwc.noaa.inel.gov/climate/precip/table22.txt, visited February 9, 2016), making this series of rainfall events abnormally high.

The peak θs resulting from natural precipitation at depths of 12 and 18 ft in the PA south instrumented tubes occurred on October 31, 2016, and November 3, 2016, respectively, and were 4.5% and 3.3%. The corresponding background θ at these depths is 3.5% and 2.8%. The θ response in the drainage gravel material at depths of 26 ft is negligible. The θ increased approximately 1% in the Stratum II alluvium beneath the drainage course material.

These data show the vault perimeter drainage and drainage course materials are performing as designed. It also shows the time period during which lysimeters should be sampled following a rainfall event in order to capture potential contaminants or other chemical indicators from the vault array.

Table 26. Summary of arrival times and peak moisture content for the second characterization test.

Sensor Location	Time of First Arrival	Time When Moisture Content Rises Rapidly	Time When Peak θ Decreases Significantly	Peak Moisture Content Percent	Date θ Approaches θr	Comments
PA South 12-ft	9/30/2016 11:10	9/30/2016 11:20	9/30/2016 20:40	6.4	10/3/2016	Width of "peak" reflective of the 8-hour test period
PA South 18-ft	9/30/2016 18:40	9/30/2016 19:40	10/1/2016 1:40	4.7	10/4/2016	
PA South 26-ft	9/30/2016 16:40	9/30/2016 17:20	9/30/2016 23:50	3.7	10/6/2016	Very slow return to θr
PA South 29-ft	9/30/2016 14:30	9/30/2016 15:30	9/30/2016 21:10	21.1	10/7/2016	Very slow return to θr
PA North 26-ft	9/30/2016 21:00	9/30/2016 21:00	10/1/2016 14:00	3.3	10/12/2016	
PA North 29-ft	9/30/2016 12:00	9/30/2016 12:00	9/30/2016 19:00	9.4	10/12/2016	2 peaks show second water arrival at 10/1/2016
PA-45 ft	11/19/2016	11/19/2016	11/28/2016			Based on 4 "peaks" in the AT data

Figure 43. θ calculated using measured permittivity, first order calibration curve for data at 12, 18, and 26-ft depths, and second order calibration curve for data at 29 ft during second characterization test in the PA south instrumented tubes.

Figure 44. θ calculated using measured permittivity, first order calibration curve for data at 26-ft depth, and second order calibration curve for data at 29 ft during second characterization test in the PA north instrumented tubes.
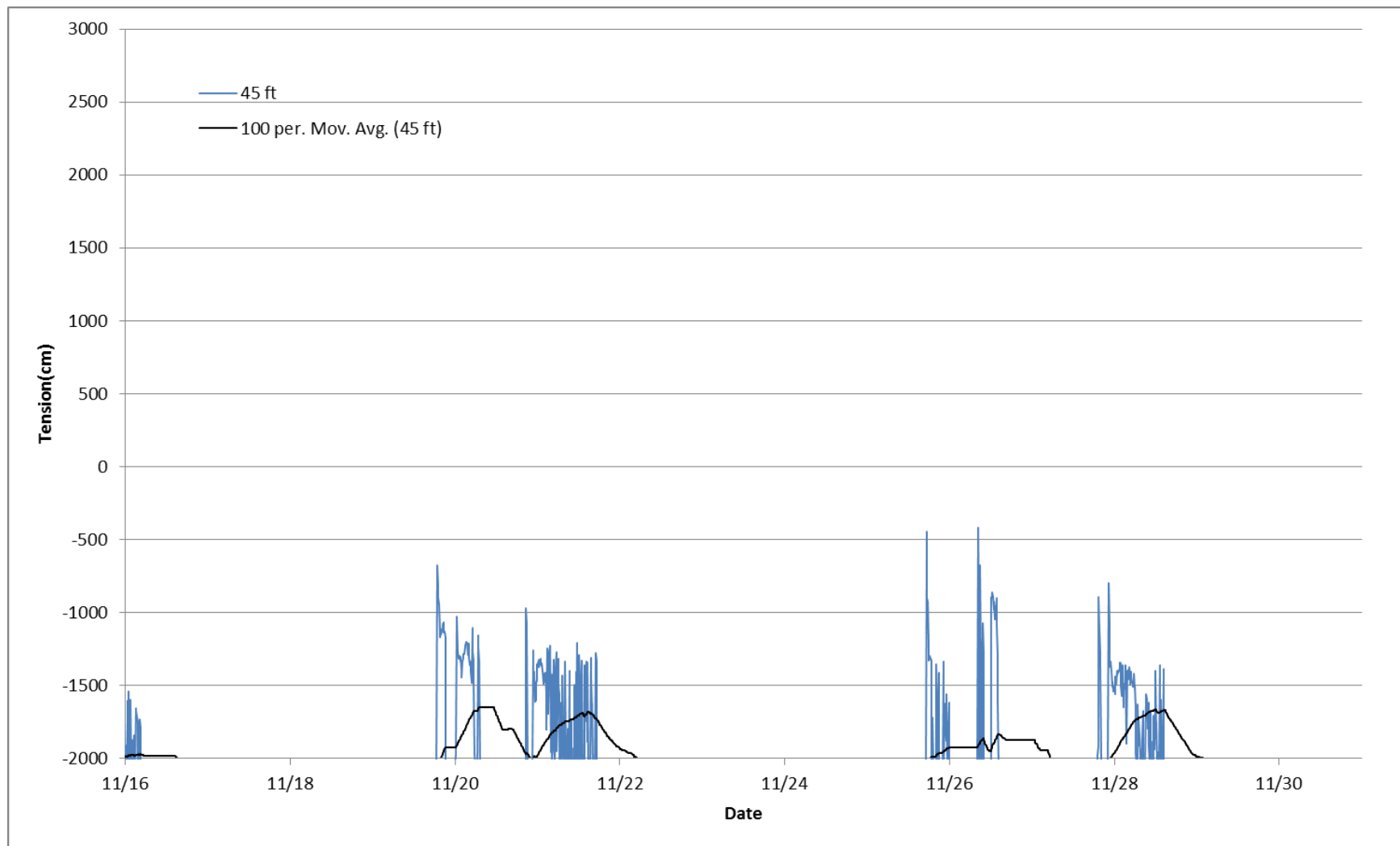
Figure 45. Water tension in the PA 45-ft drilled borehole following the second characterization test.
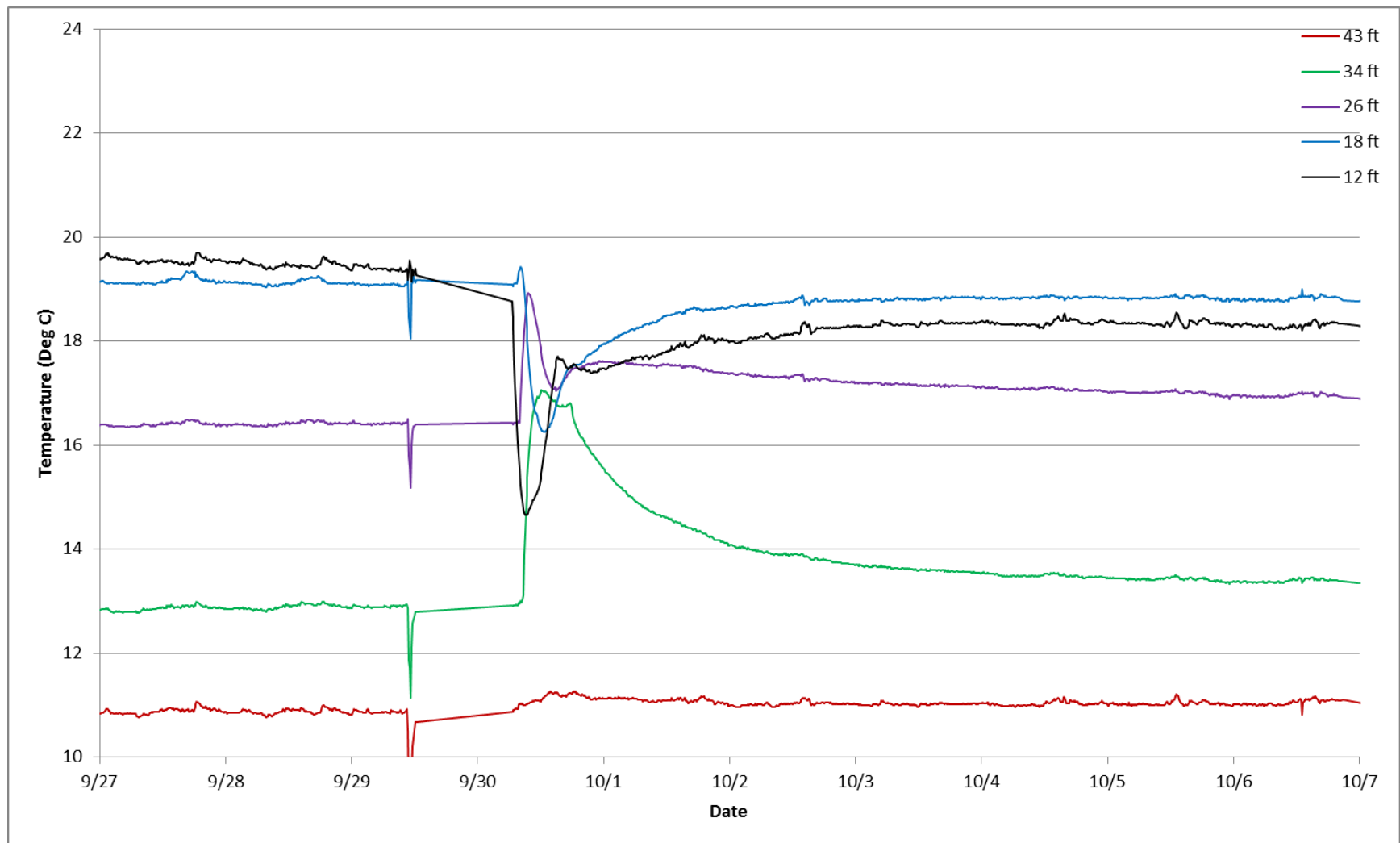
Figure 46. Temperature in the PA 45-ft borehole during and after the second characterization test.
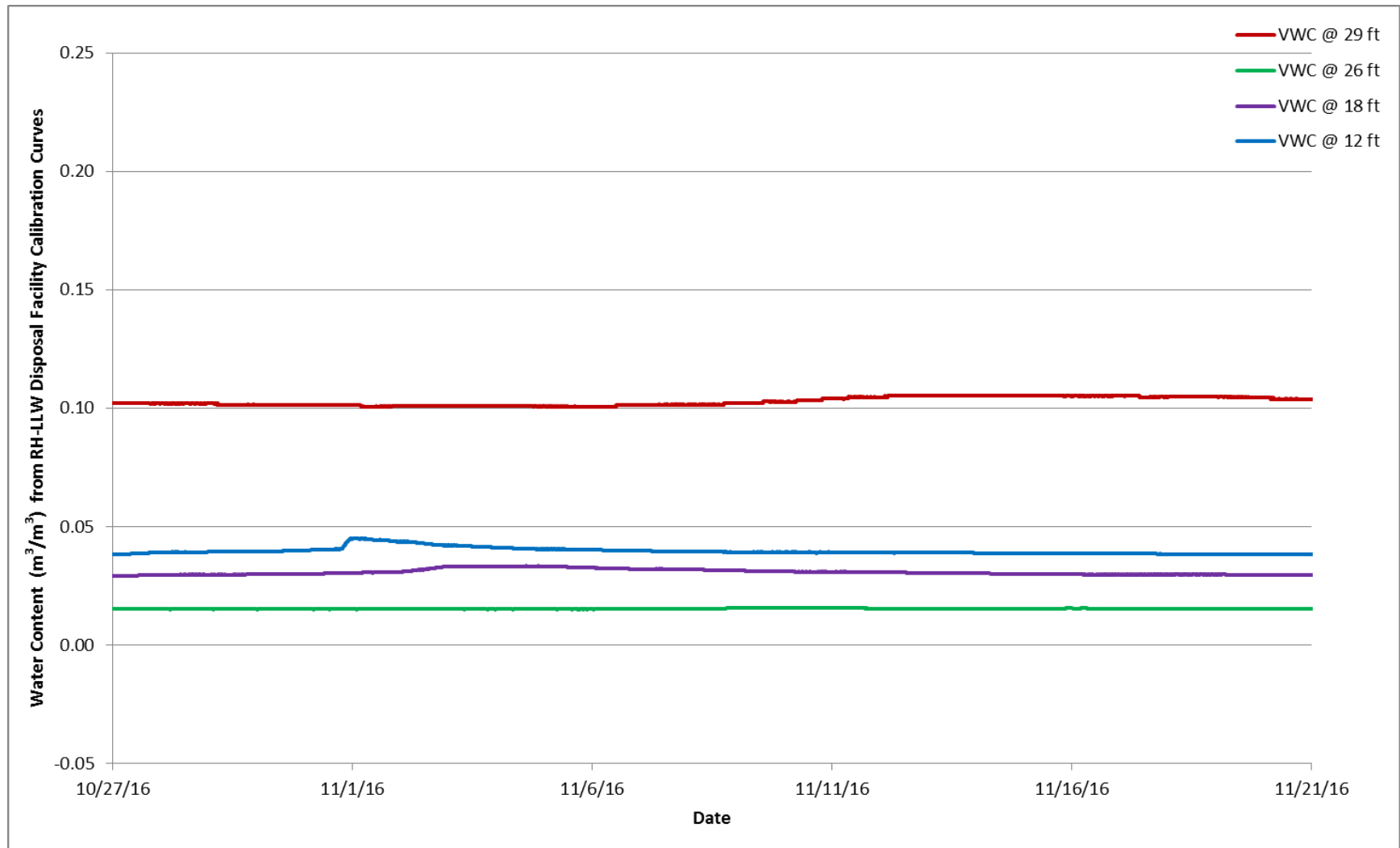
Figure 47. θ calculated using measured permittivity, first order calibration curve for data at 12, 18, and 26-ft depths, and second order calibration curve for data at 29 ft during late October to early November in the PA south instrumented tubes.
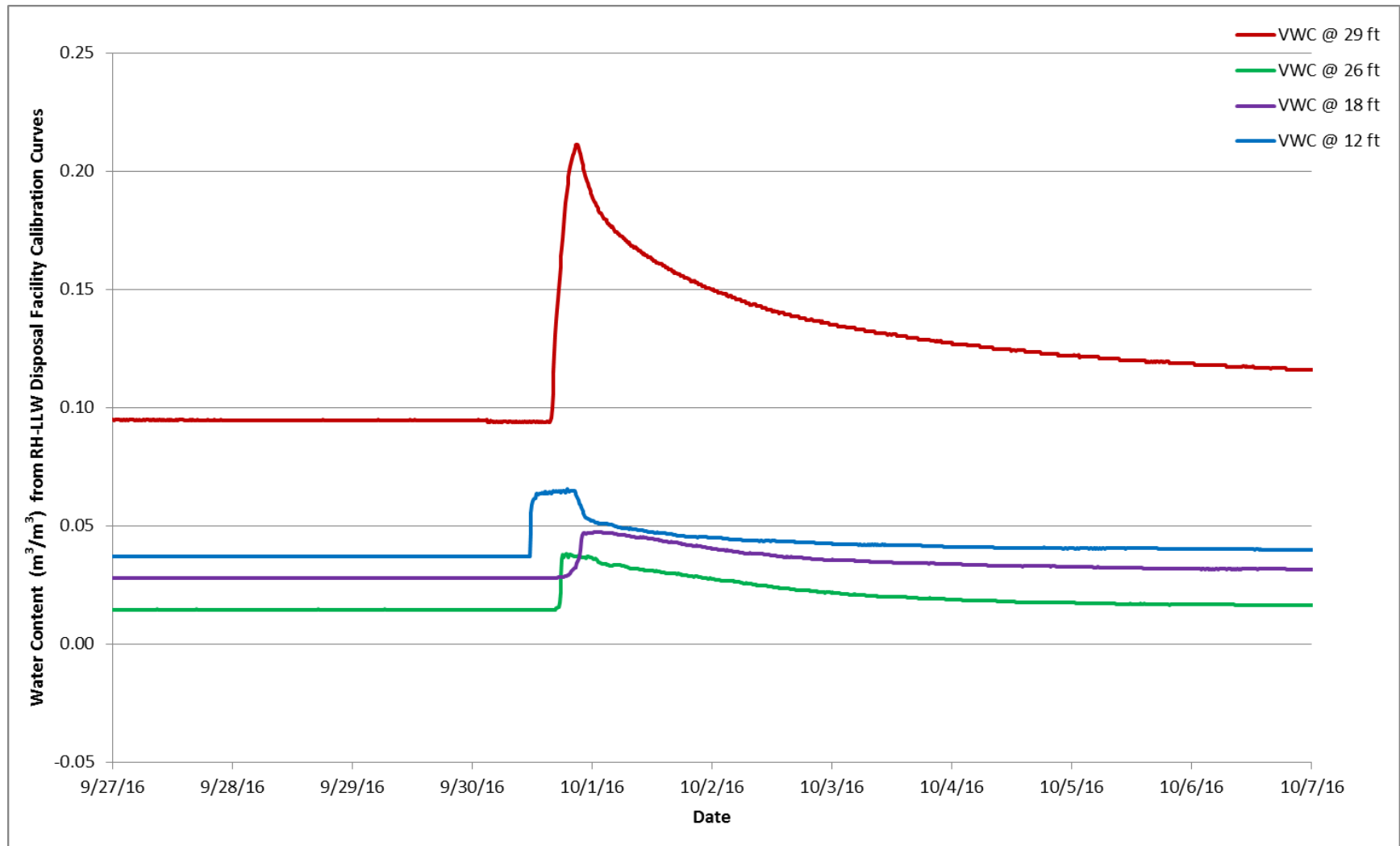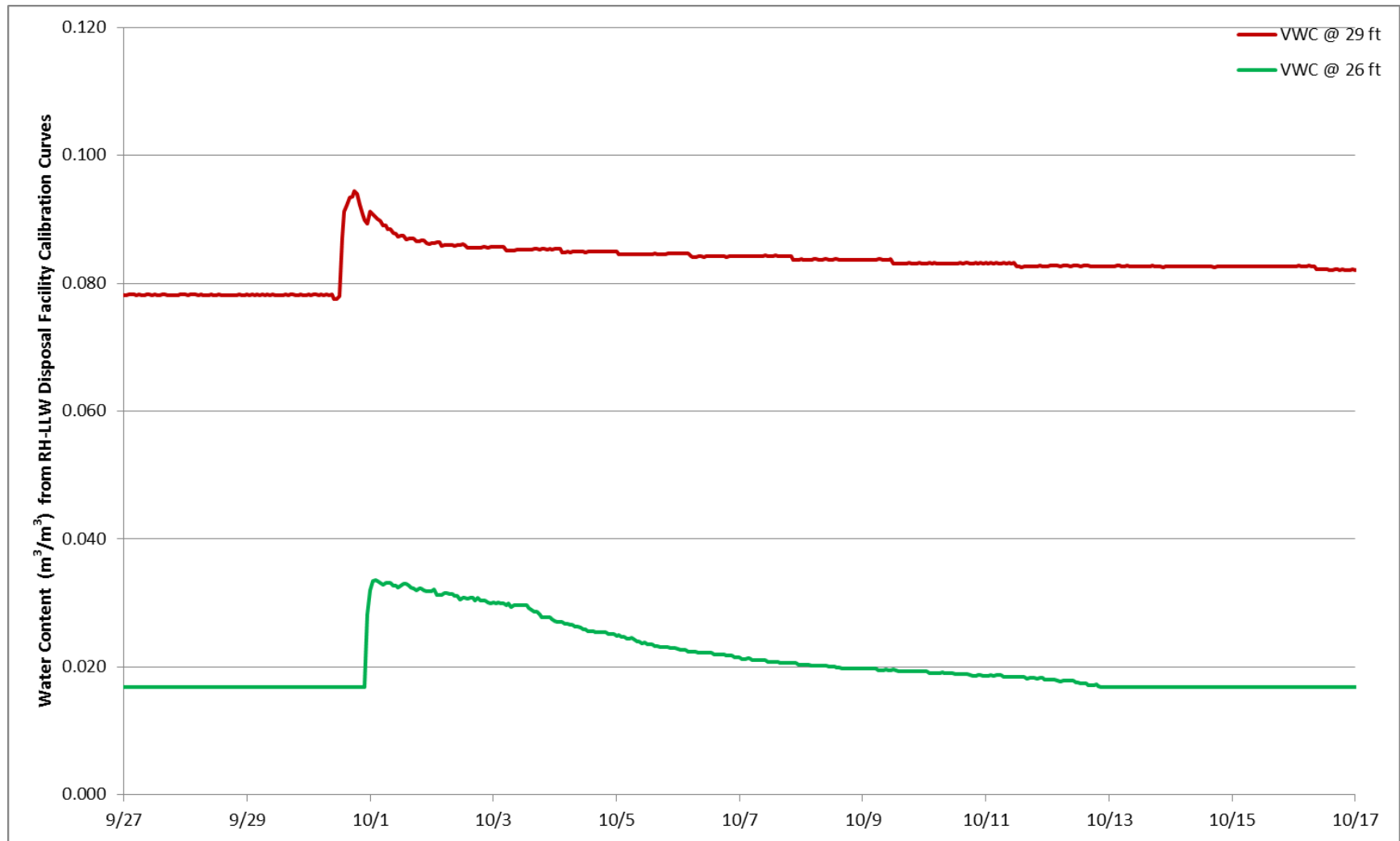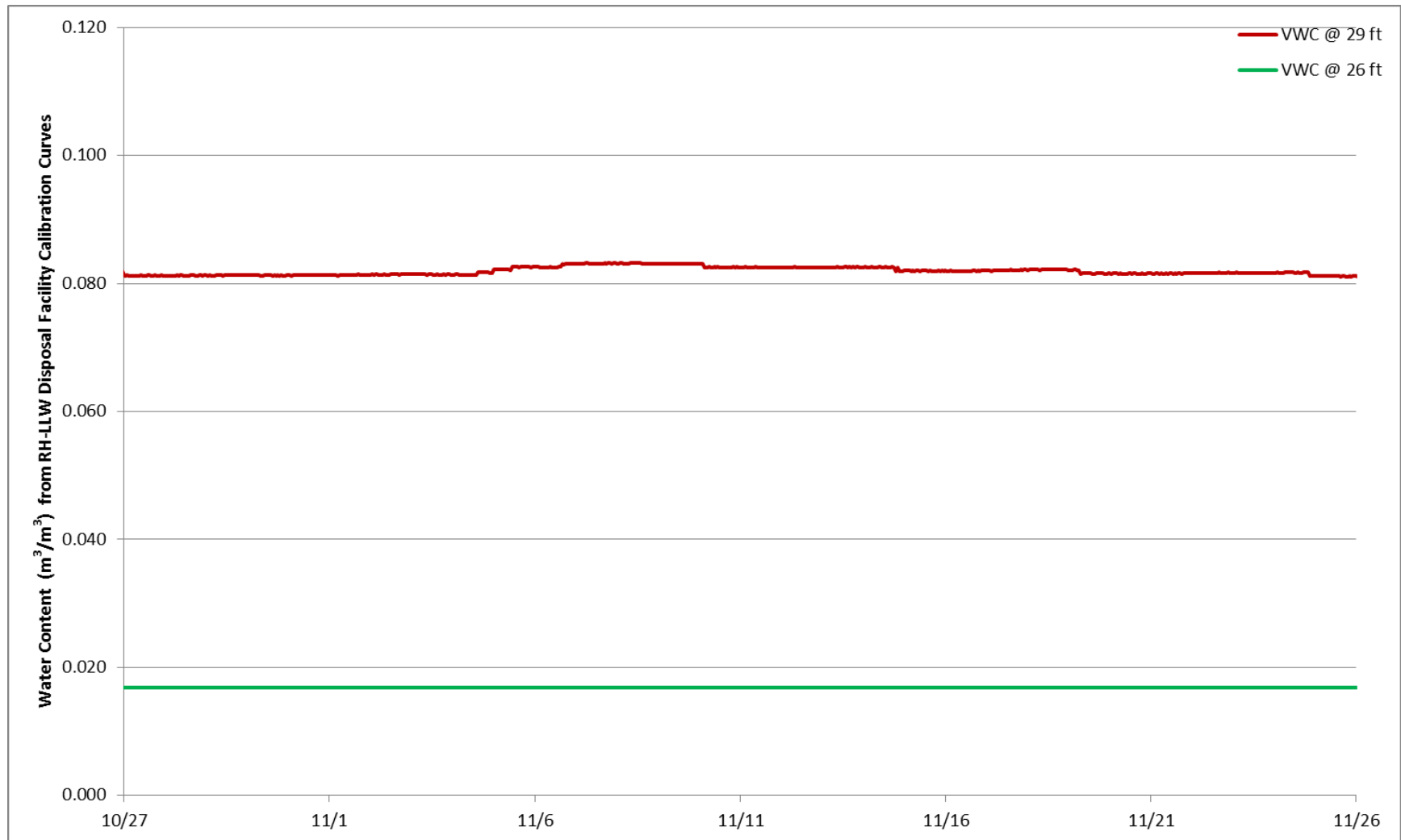
Figure 48. θ calculated using measured permittivity, first order calibration curve for data at 26-ft depth, and second order calibration curve for data at 29 ft during late October to Early November in the PA north instrumented tubes.

7. HYDRAULIC MODEL

The TOUGH2 ("Transport of Unsaturated Groundwater and Heat") code was used to simulate the characterization tests and natural precipitation event discussed in Section 6. TOUGH2 is a multi-dimensional numerical model developed to simulate the coupled transport of water, vapor, non-condensable gas, and heat in porous and fractured media by the Lawrence Berkeley National Laboratory in the early 1980s. In this application, it is used to simulate transport of water in unsaturated media comprising the vault hydraulic drainage system.

7.1 Model Dimensions and Parameters

The hydrologic model was developed to represent the excavated area and vaults shown in Figure 8 and 10. The model (shown with material types and discretization in Figure 49) extends vertically from the top of the vault plugs and surface road base through the drainage course material underlying the vault base section, the Stratum II and Stratum III alluvium, and a basalt layer. The materials represented in Figure 49 are as follows: impermeable concrete components (grey), surface road base and crushed gravel base course material (light blue), alluvial fill material (dark blue), vault perimeter drainage material (light green), drainage course material (dark green), Stratum II alluvium (pink), Stratum III alluvium (purple), and basalt (olive green).

The model domain is 4 m in the y-direction, representing the 13-ft vault extent that includes the vault end blocks and plugs shown in Figure 49. It is 7 m in the x-direction to allow inclusion of 0.6 m (2 ft) of the concrete vault wall, 0.3-m (1-ft) wide perimeter block, and 0.6-m (2-ft) wide column of crushed gravel base course at the surface. In the model, the drainage course material extends beyond the required 3 m (10-ft) lateral extent in order to make up the total 7-m model width. In the z-direction, the model height allows representation of construction and geologic materials shown, while not impacting drainage by a bottom boundary condition.

The hydrologic parameters assigned to materials are given in Table 27. As indicated in Table 27, parameters assigned to the surface road base and crushed gravel base course are equivalent and those assigned to the vault perimeter drainage material and the drainage course materials are equivalent. They are equal to the laboratory derived values. The pore space parameter (n) assigned to the vault perimeter drainage material and drainage course material is slightly higher than the value obtained by fitting all of the laboratory data (i.e., the average n value) to increase the drainage rate to match that observed in the field data. This model n is within the overall range provided for the laboratory data. All other parameters for these materials correspond to those shown in Tables 12 and 16. The basalt layer is included in this model to simulate a free draining bottom boundary, which is simulated by a saturated zone. Alluvium properties were taken largely from the Remedial Investigation/Feasibility Study for the Idaho Nuclear Technology and Engineering Center (DOE-ID 2006), with the exception of the alluvial fill material, which was assumed to be similar to the crushed gravel base course based on the textural characteristics and method of installation.

Infiltration rates and areas used in simulation of the characterization tests and natural precipitation event are given in Table 28. Boundaries on the model sides were no-flow. The model top boundary was assigned the annual average infiltration rate. The region-assigned aquifer blocks at the bottom of the model were set to "fixed-state." The fixed-state fully saturated aquifer allows accumulation of drainage from the upper model regions, allowing the model to reach a steady-state saturation based on the infiltration rate assigned to each of the top cells of the model domain.

Simulations for the transient infiltration condition were initiated from the steady-state condition corresponding to the material installation requirements to achieve 95% compaction at optimal moisture content.
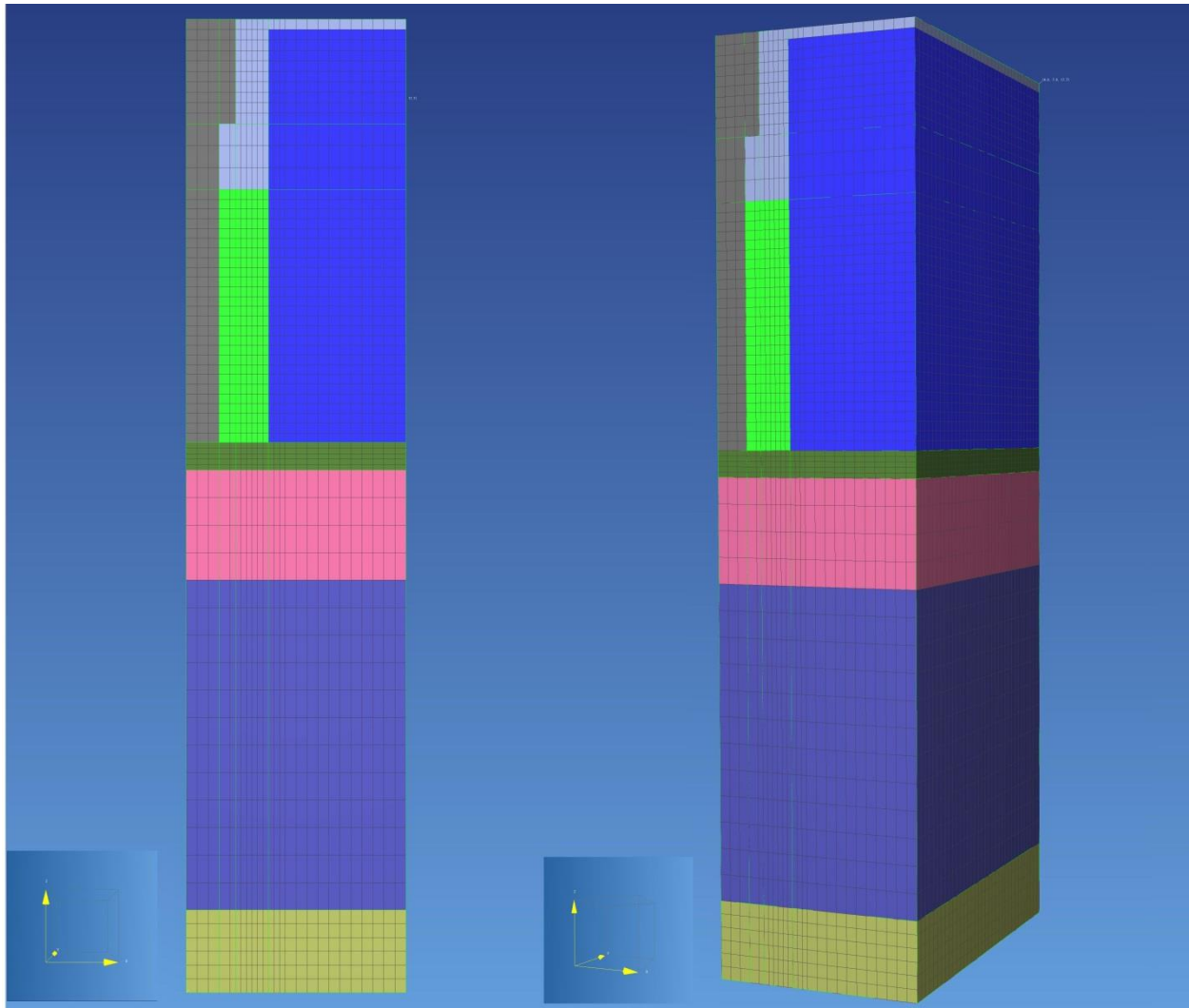
Figure 49. Hydraulic model domain showing the impermeable concrete components (grey), surface road base and crushed gravel base course material (light blue), alluvial fill material (dark blue), vault perimeter drainage material (light green), drainage course material (dark green), Stratum II alluvium (pink), Stratum III alluvium (purple), and basalt (olive green).
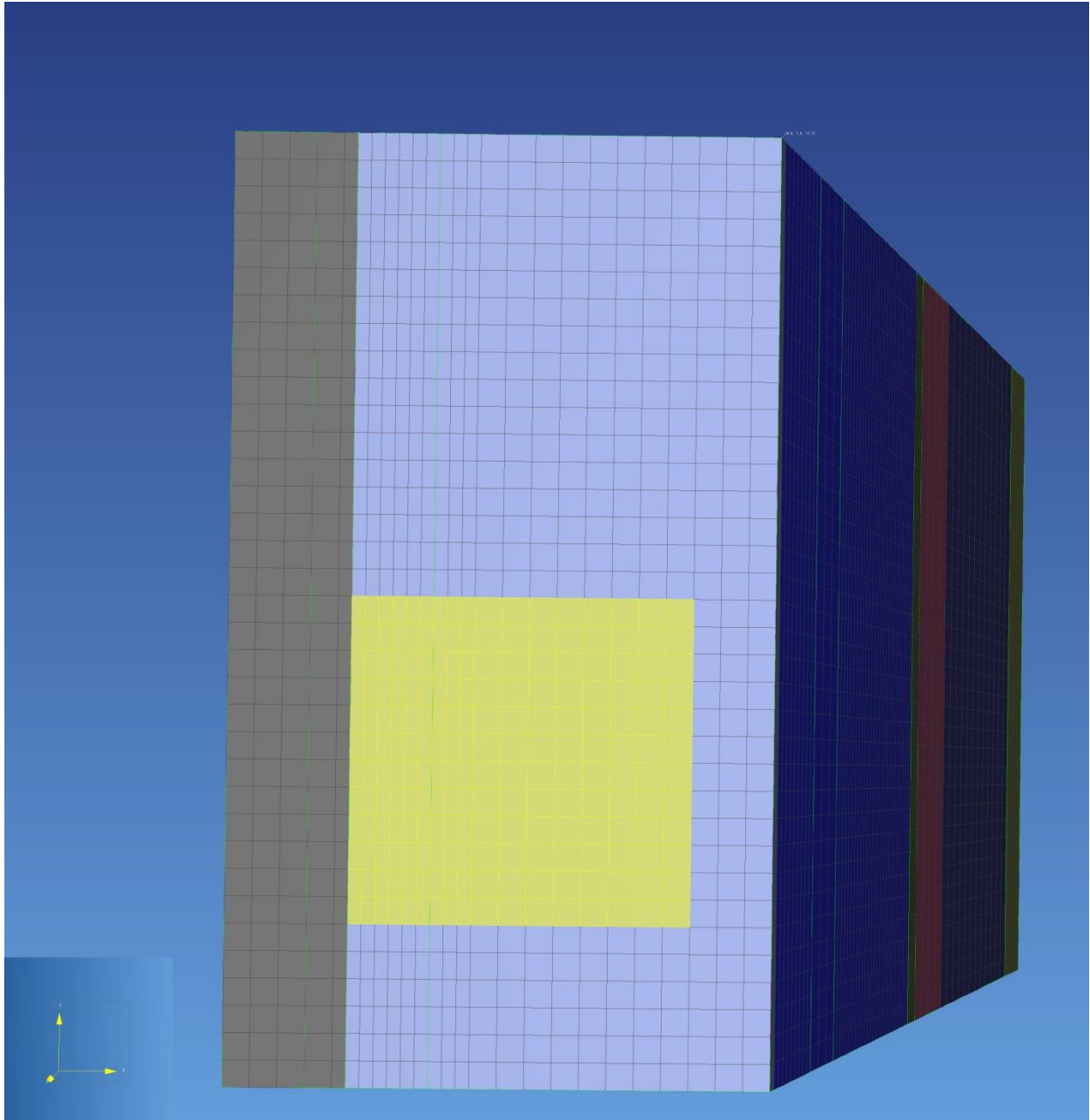
Figure 50. Horizontal plan view at the top of the surface road base (light blue) and impermeable concrete plugs and perimeter blocks (grey), showing the cells representing the 8 x 8-ft test area (yellow).

Table 27. Hydraulic properties of the porous materials in the vault system.

Material	Horizontal Permeability[a] (m²)	Vertical Permeability[a] (m²)	Porosity (φ) = Sw_{sat}[b]	λ[c]	Sw_{res}[d]	$1/P_0$ (Pa^{-1})[e]
Surface Road Base	1.3E-10	8.64E-12	0.298	0.208	0.0054	0.0229
Crushed Gravel Base Course	1.3E-10	8.64E-12	0.298	0.208	0.0054	0.0229
Vault Perimeter Drainage	2.37E-10	9.48E-12	0.37	0.33	1.0E-5	107.363
Drainage Course	2.37E-10	9.48E-12	0.37	0.33	1.0E-5	107.363
Alluvial Fill[f]	1.3E-10	8.64E-11	0.298	0.208	0.0054	0.0229
Strata II Alluvium[g]	2.84E-11	2.84E-11	0.32	0.286	6.25E-4	0.0102
Strata III Alluvium[h]	3.7E-13	3.7E-13	0.39	0.324	0.256	6.01E-4
Basalt[i]	2.94E-13	2.94E-13	0.05	0.9	0.021	2.5E-4

All values are based on the laboratory test data provided in Tables 12 and 16 for vault drainage materials and backfill.

a. Horizontal permeability was assigned a value 15 times higher than vertical permeability to match the extent of wetted area at land surface during the first characterization test for the crushed gravel base course material, surface road base, vault perimeter drainage material, and drainage course material.

b. Porosity (φ) assigned a value equal to the saturated moisture content equivalent from the laboratory test data.

c. λ calculated from the van Genuchten n-Mualem model parameter (λ=1-1/n) adjusted based on model results for the vault perimeter drainage course material and drainage course material to promote rapid drainage observed during the first characterization test where: $(k_{rel} = S_*^{0.5} \left(1 - \left(1 - S_*^{1/\lambda}\right)^\lambda\right)^2$.

d. Residual water saturation calculated from corresponding residual moisture content.

e. Air entry parameter calculated from the van Genuchten function α parameter $(CP = -P_0 \left((S^*)^{-1/\lambda} - 1\right)^{1-\lambda})$.

f. Alluvial fill material assumed to be similar to the crushed gravel base course material based on textural data for the Stratum II alluvium found in the vault area and method of installation.

g. Stratum II alluvium values are based on the data provided for similar materials at the nearby Idaho Nuclear Technology and Engineering Center (DOE-ID 2006).

h. Stratum III alluvium values are based on a sandy-silty clay from the RETC database and the textural data in the American Geotechnics Report (American Geotechnics 2011).

i. Basalt values are based on the analyses provided for similar materials at the nearby Idaho Nuclear Technology and Engineering Center (DOE-ID 2006).

Table 28. Infiltration conditions simulated and provided for reference.

Infiltration Condition	Water Infiltration Rate	When/Why of Interest
First characterization test	7.2 kg (1,905 gal) applied to a 2.4 ×2.4 m (8 ×8 ft) area for 24 hours.	4.6E4 cm/year. Pre-test calculated value to achieve greater than 50% moisture content in the test area.
Second characterization test	4.0E3 kg (1,056 gal) applied to a 2.4 ×2.4 m (8 ×8 ft) area for 12 hours.	5.4E4 cm/year. Increased pump rate compared to the first characterization test.
Natural precipitation event	5 cm (2 in.) applied over the entire model surface covered by surface road base for a period of 10 days. Within the 2.4 ×2.4 m test area. This is equivalent to 288 kg in 10 days.	For comparison to the precipitation event where approximately 2 in. of water fell over 10 days in late October (see Table 24).
Annual average infiltration	10 cm/year.	Long-term conditions in the backfilled areas not covered by the final engineered cover. This value is the typical background infiltration rate through disturbed alluvial materials at INL, and not necessarily representative of an infiltration rate expected through the vault plugs or through the pea gravel between them.
Annual transient infiltration	70% of the annual average infiltration occurring in 30 days, with the remainder distributed throughout the rest of the year,	Spring and fall when most of the precipitation in Idaho occurs.
Maximum precipitation infiltration	9 in. in 1 hour corresponding to the probable maximum precipitation event at INL.	This infiltration rate is thought to bound extreme rain events or potential flood events.

7.2 Simulation Results for the First Characterization Test

The simulated water saturation and corresponding moisture content histories for depths of 12, 18, and 26 ft using the infiltration rates for the first characterization test are given in Figures 51 and 52, respectively. The moisture content was calculated for depths of 12 and 18 ft using model-predicted water saturations and a porosity of 37% from Tables 10 and 27 for the vault perimeter drainage and drainage course materials. The moisture content at a depth of 26 ft was calculated using a porosity of 0.32 (Strata II Alluvium). Vertical profiles of the wetting front at elapsed times of 5, 15, 22, 30, and 80 hours, starting with the first application of water, are given in Figures 53 through 57. The vertical profile shown extends from the edge of the vaults to the east through the position of the PA south instrumented tube set (see Figure 10).

Figure 52 can be compared to data shown in Figure 37. The predicted peak θ values at depths of 12, 18, and 26 ft are approximately 33, 34, and 27%, respectively. These moisture contents are about a factor of five higher than observed in field data for the vault perimeter drainage material (i.e., 12-ft and 18-ft sensor depths), and a factor of ten higher than observed in the drainage course material at 26 ft. The model predicted higher than observed θ and longer drainout times can be explained, in part, by higher than actual porosity values and, more likely, by small differences in the laboratory van Genuchten properties determined through laboratory testing compared to the highly compacted field conditions. This is demonstrated by the time-sequence of wetting front propagation shown in Figures 53 through 57 as follows:

- Figure 53, captured 5 hours after the start of the application of water, shows that the wetting front is predicted to migrate rather quickly and uniformly through the surface road base and crushed gravel base course material until the wetting front reaches the bottom of the perimeter block shown by the recessed area in the upper left of the figure.

- Figure 54, captured 15 hours after the start of the application of water, shows that as the wetting front reaches the top of the vault perimeter drainage material, the difference in unsaturated characteristic properties (i.e., the van Genuchten parameters) allows the wetting front to move preferentially through the alluvial fill material. Essentially, the vault perimeter drainage material is acting like a capillary barrier, diverting the water into the alluvial fill material.

- At 20 hours (see Figure 55), near the end of water application, the region closest to the vault perimeter block is saturated. This is consistent with field observations of water ponding between the perimeter block and the vault plug at the base of the vault plug.

- Figure 52 shows that overall predicted moisture contents are higher than observed in field data at depths of 12 and 18 ft. As indicated in Figure 56, high saturations are never propagated deep into the vault perimeter drainage material, instead showing a preference for moving into the alluvial fill material. This figure shows that the long return period (compared to observations) required to reach residual saturation is being caused by water retained in the surface road base and crushed gravel base course. In the field, these materials are draining much more rapidly than predicted using the laboratory-derived van Genuchten parameters used in the model. If the van Genuchten parameters for these materials were adjusted to allow more rapid drainage (i.e., if the n-parameter were increased), it is likely that less water would have been predicted to enter the vault perimeter drainage material and that the vault perimeter drainage material would have returned to residual saturation faster than shown in this sequence of simulations.

While the model may be overpredicting moisture content with respect to field observations, the model is predicting the general behavior observed in the field. Namely the following:

- Observed moisture content is very low in the vault perimeter drainage material and drainage course material. Any of the infiltrating water that does enter these materials passes very rapidly through the vault perimeter drainage material and drainage course material.

- Water tends not to accumulate or be retained against the vault walls in part due to the following:

  - Unsaturated moisture content property differences between the vault perimeter drainage material and alluvial fill

  - Rapid drainage characteristics of the vault perimeter drainage material

  - In part, because of the "umbrella" effect caused by the perimeter block.

- Water does not accumulate significantly in the drainage course material, but instead it infiltrates into the underlying Stratum II alluvium.
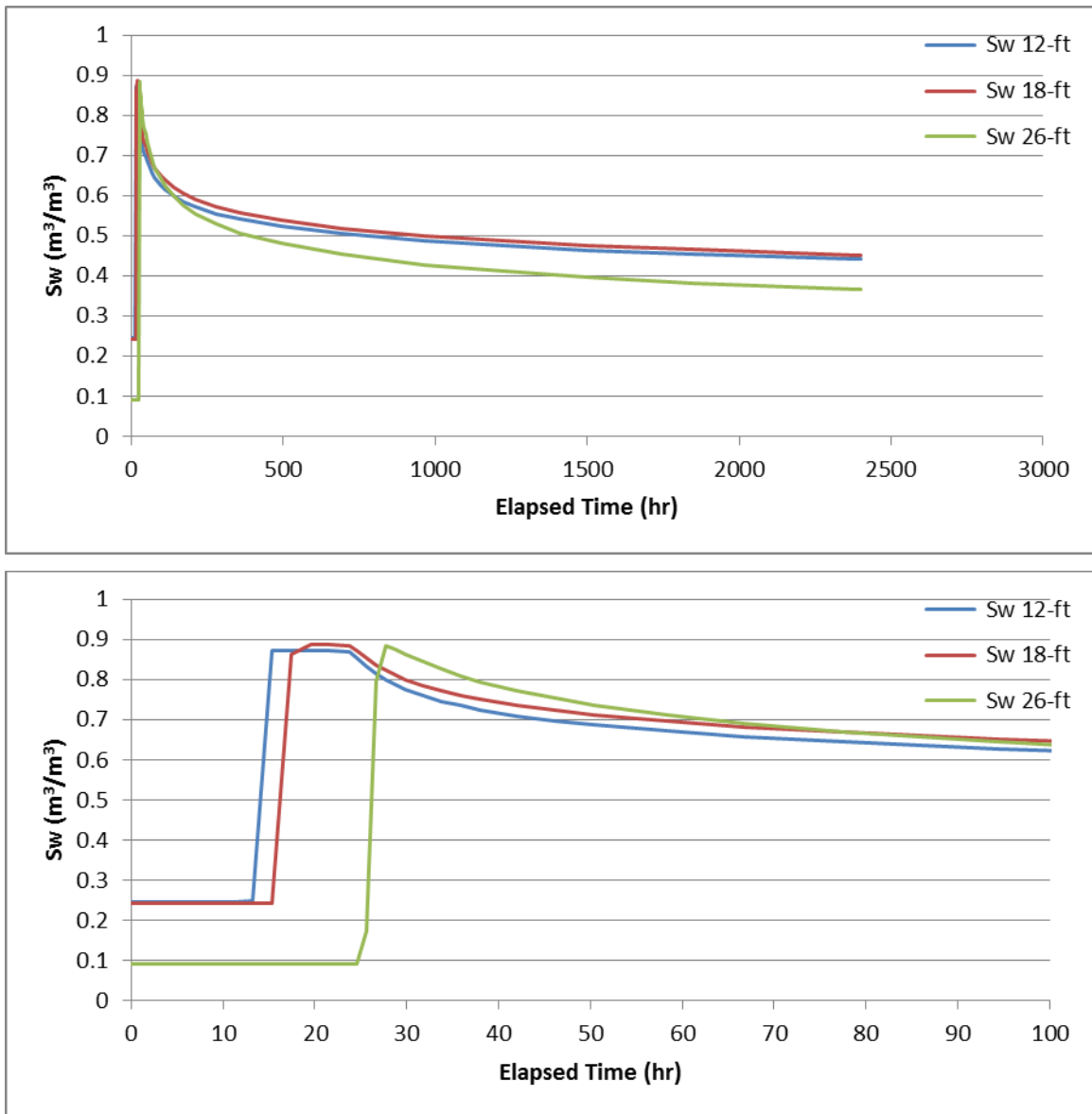
Figure 51. Water saturation time history predicted for the first characterization test. Time begins with the first application of water.
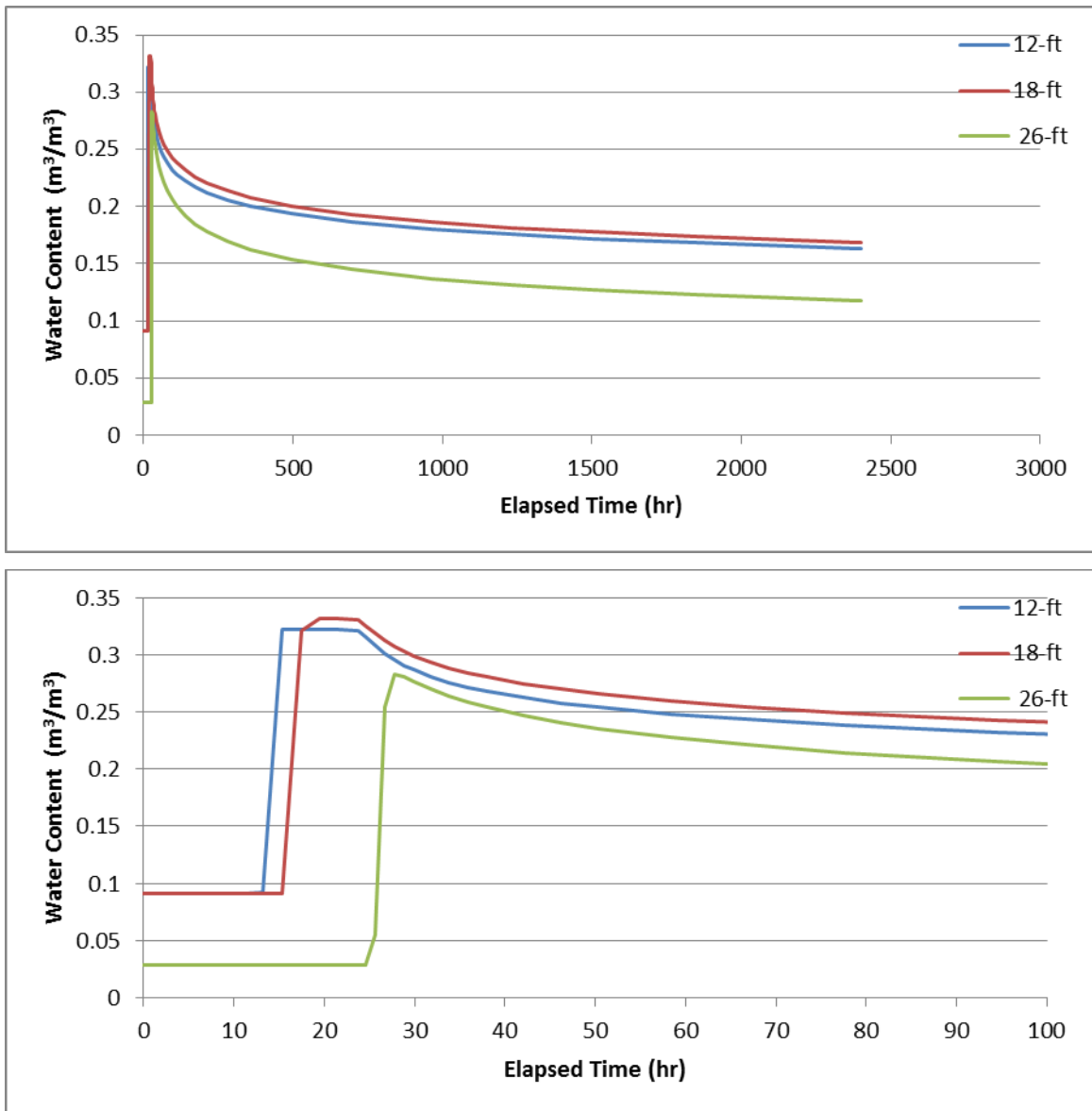
Figure 52. Moisture content time histories corresponding to water saturation given in Figure 51 for the first characterization test. Time begins with the first application of water.

95
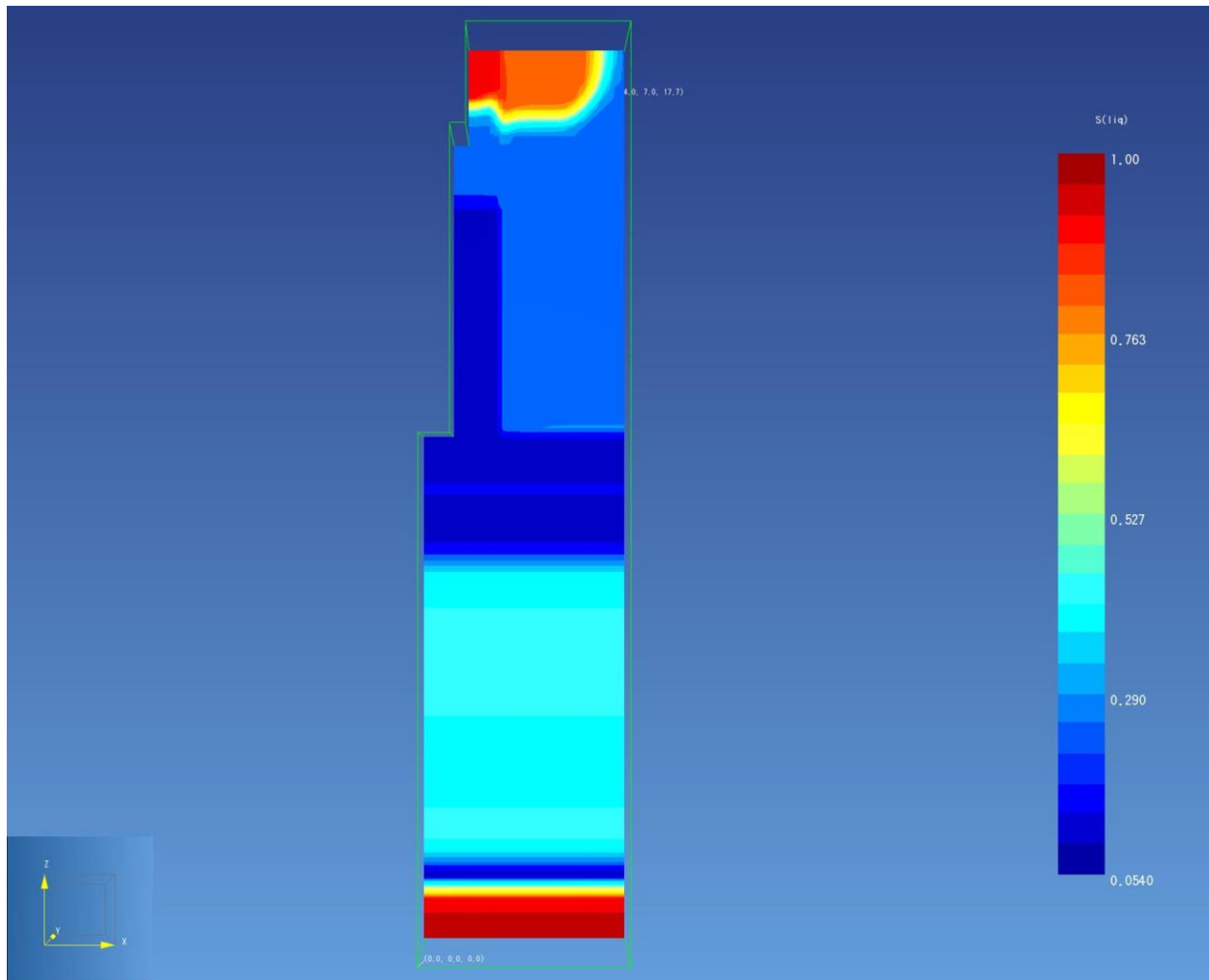
Figure 53. Predicted water saturation 5 hours after start of the first characterization test. The vertical slice runs west to east through the PA south instrument tube and the left side of the domain corresponds to the edge of the vault perimeter blocks (top), vault edges (middle), and below the vaults (bottom).

Figure 54. Predicted water saturation 15 hours after start of the first characterization test. The vertical slice runs west to east through the PA south instrument tube and the left side of the domain corresponds to the edge of the vault perimeter blocks (top), vault edges (middle), and below the vaults (bottom).

Figure 55. Predicted water saturation 22 hours after start of the first characterization test. The vertical slice runs west to east through the PA south instrument tube and the left side of the domain corresponds to the edge of the vault perimeter blocks (top), vault edges (middle), and below the vaults (bottom).

Figure 56. Predicted water saturation 30 hours after start of the first characterization test. The vertical slice runs west to east through the PA south instrument tube and the left side of the domain corresponds to the edge of the vault perimeter blocks (top), vault edges (middle), and below the vaults (bottom).

Figure 57. Predicted water saturation 80 hours after start of the first characterization test. The vertical slice runs west to east through the PA south instrument tube and the left side of the domain corresponds to the edge of the vault perimeter blocks (top), vault edges (middle), and below the vaults (bottom).

7.3 Simulation Results for the Second Characterization Test

Simulated water saturation and corresponding moisture content time histories for depths of 12, 18, and 26 ft using the infiltration rates for the second characterization test are given in Figures 58 and 59, respectively. The moisture content was calculated for depths of 12 and 18 ft using model-predicted water saturations and a porosity of 37% from Tables 10 and 27 for the vault perimeter drainage and drainage course materials. The moisture content at a depth of 26 ft was calculated using a porosity of 0.32 (Stratum II Alluvium). Vertical profiles of the wetting front at elapsed times of 5, 15, 22, 30, and 80 hours (beginning with the first application of water) are given in Figures 60 through 64. The vertical profile shown extends from the edge of the vaults to the east through the PA south instrumented tube set (see Figure 10).

Figure 59 can be compared to the data shown in Figure 43. The predicted peak θ values at depths of 12, 18, and 26 ft are approximately 31, 27, and 15, respectively. While these moisture contents are higher than the observed values (similar to the first test), they are slightly lower than predicted for the first characterization test even though the water application rate was slightly higher. During the first characterization test, approximately 1,900 gallons of water were applied over a 23.3-hour period

100

(i.e., 82 gallons/hour) compared to 1,056 gallons of water over a period of 11.9 hours
(i.e., 89 gallons/hour) for the second characterization test (see Table 23). The slightly higher rate of application over a shorter time period resulted in lower saturations in the vault perimeter drainage material, as indicated by the following:

- Figure 60 can be compared to Figure 53, captured 5 hours after the start of the application of water for both tests. The comparison shows that the wetting front in the second test through the first 5 hours migrates very uniformly through the surface road base and crushed gravel base course materials, reaching nearly complete saturation near the perimeter block, and extending to the east (i.e., right side of figure) about as far. This is consistent with field data that showed slightly less lateral migration of water near the surface outside of the 8×8-ft test box.

- Figure 61 compared to Figure 54, captured 15 hours after the start of the application of water, shows much more rapid drainage of the surface road base and crushed gravel base course at the slightly higher water-application rate and much shorter duration test. This shows that following a relatively high infiltration event (due to high precipitation or rapid snowmelt) water will dissipate relatively rapidly. As during the first characterization test, the vault perimeter drainage material appears to be acting like a capillary barrier, diverting the water into the alluvial fill material.

- At 20 hours (see Figure 61), 8 hours after the end of water application during the second characterization test, the wetting front in the alluvial fill further from the vault wall is nearly stagnant with very little change between the position at 15 hours versus 30 hours (see Figures 62 and 63). However, the wetting front in the alluvial fill nearer the vault perimeter drainage material has extended deeper. During this time period, very little water was predicted to penetrate into the vault perimeter drainage material. During the second characterization test, personnel were not on sight to ascertain whether or not water was visibly ponding between the perimeter block and the vault plug at the base of the vault plug as was observed during the first characterization test. However, the model indicates that no water should have been observable.

- After 80 hours (see Figure 64), the saturation and moisture content adjacent to the vaults should remain relatively dry and near the residual moisture content for the vault perimeter drainage material. The highest saturations are in the alluvial fill adjacent to the vault perimeter drainage material. Eighty hours after the application of water ceased, a very thin layer of slightly higher water saturation is predicted to form above the drainage course material.
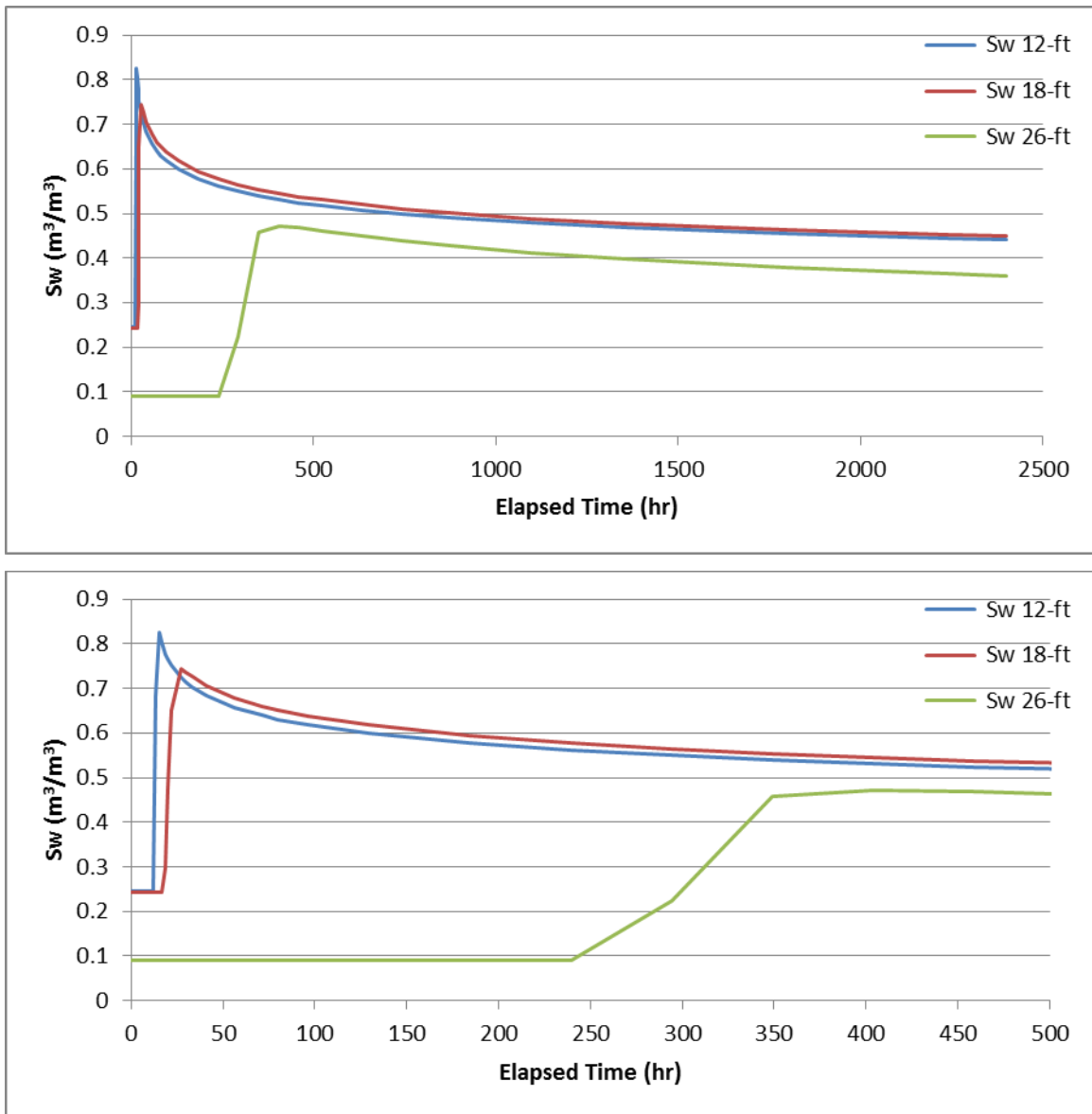
Figure 58. Water saturation time history predicted for the second characterization test. Time begins with the first application of water.
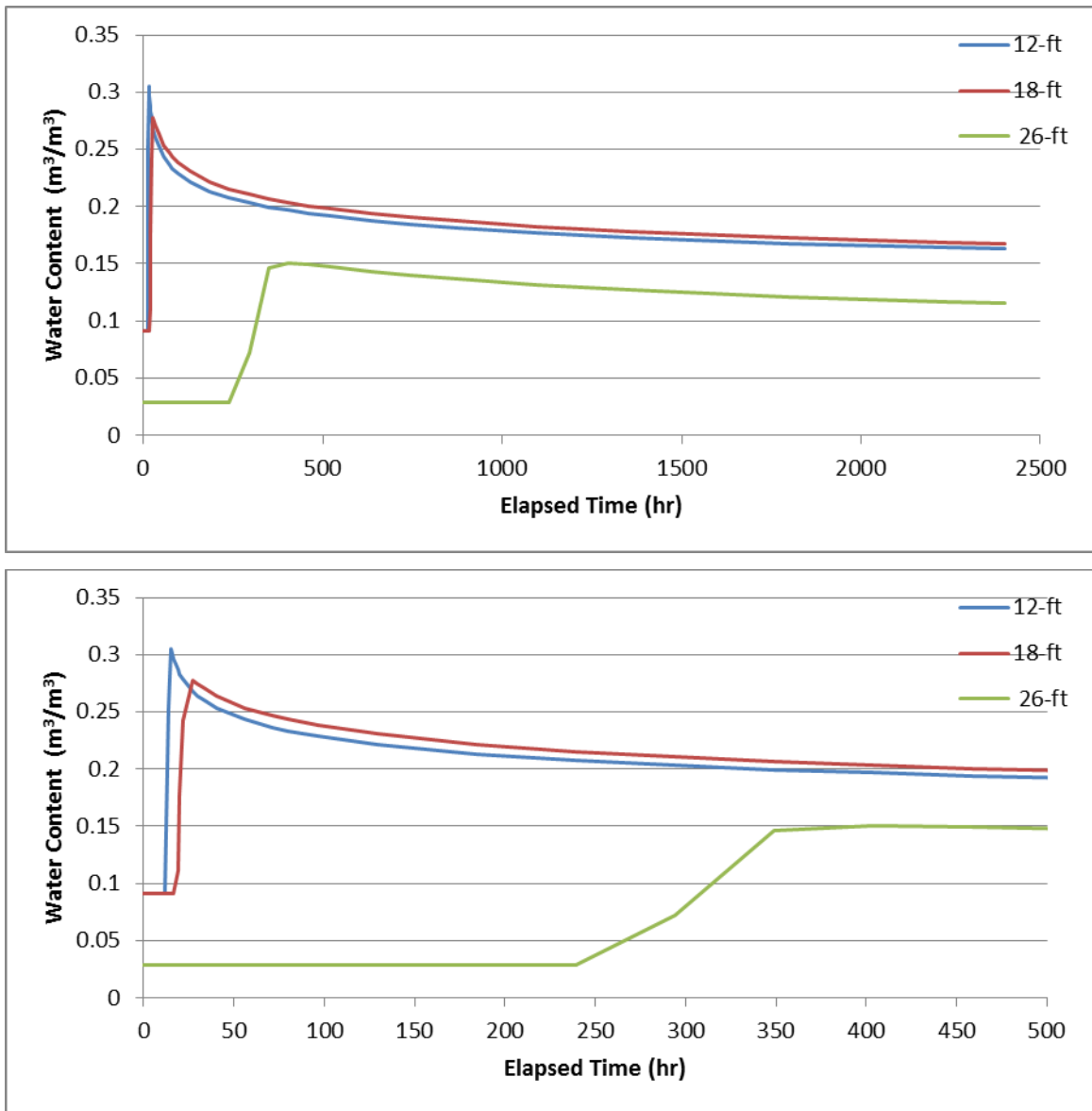
Figure 59. Moisture content time history corresponding to the water saturation given in Figure 58 for the second characterization test. Time begins with the first application of water.
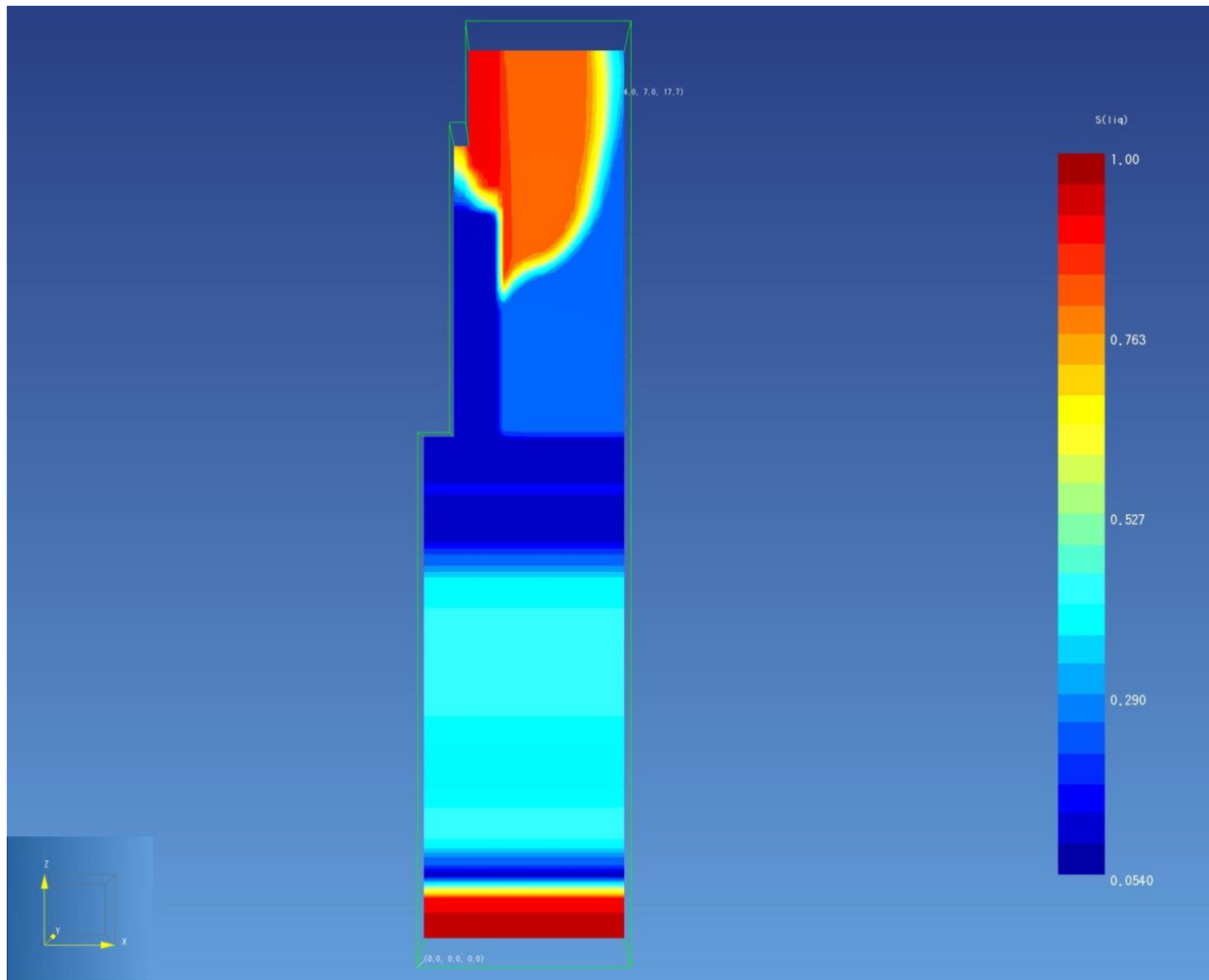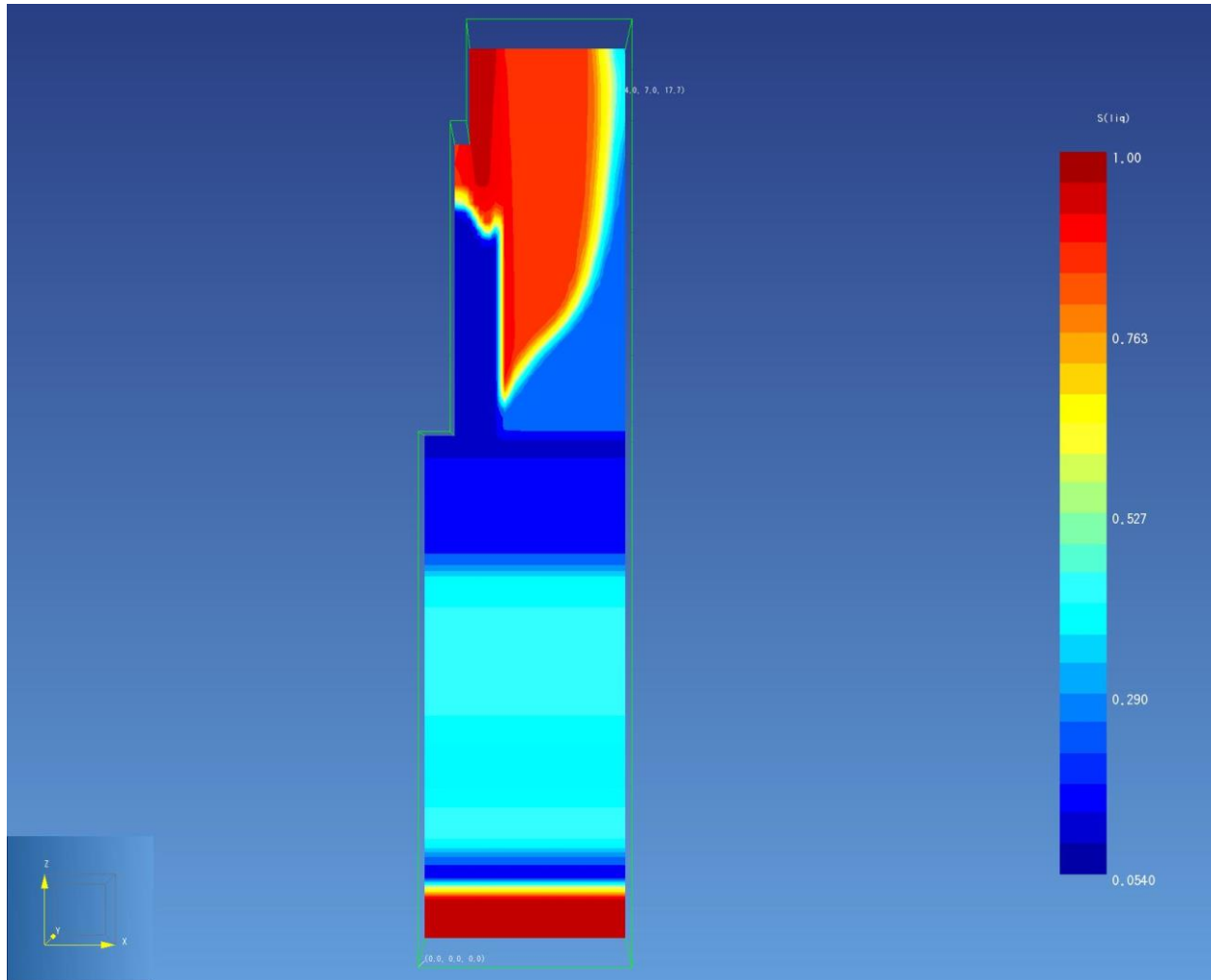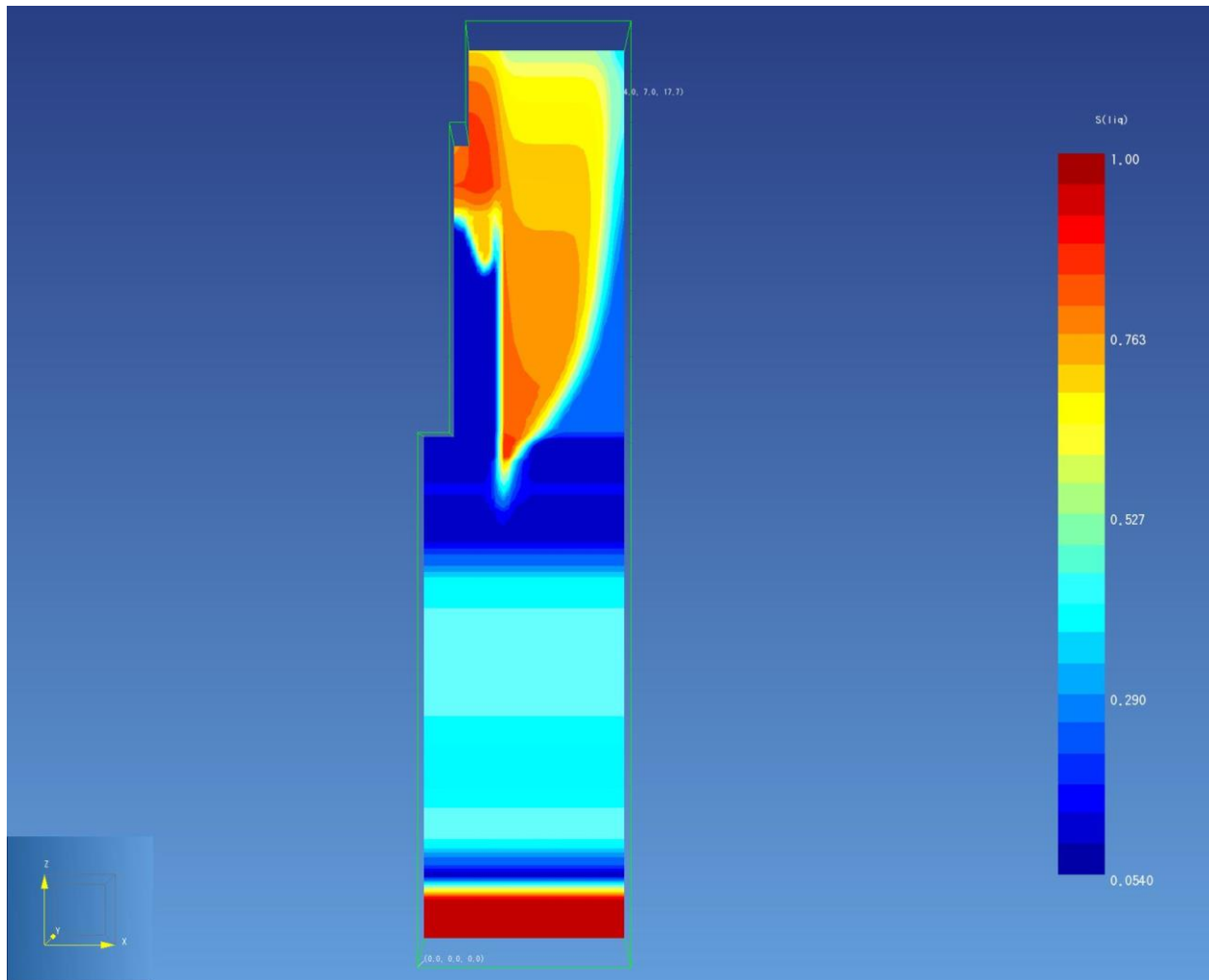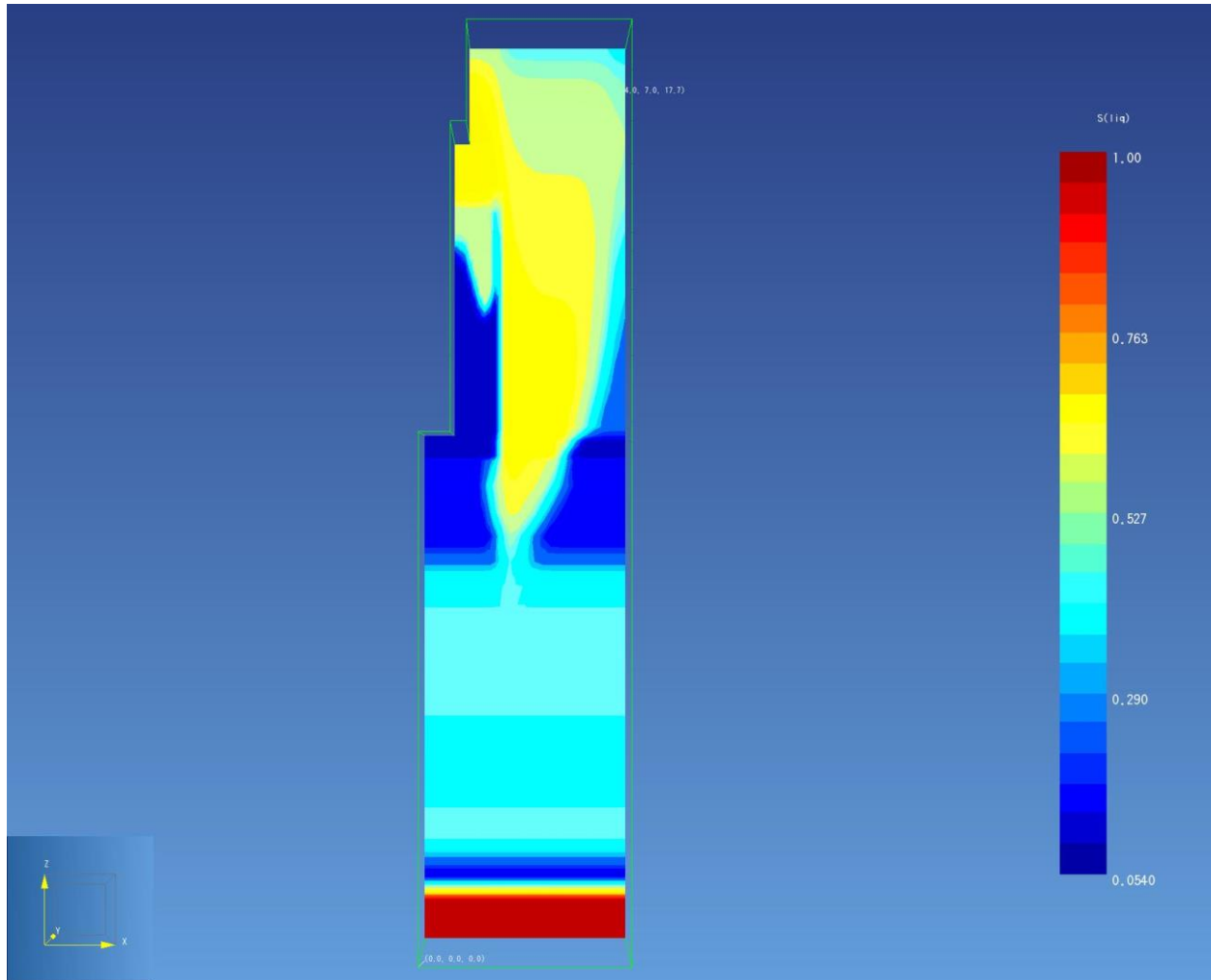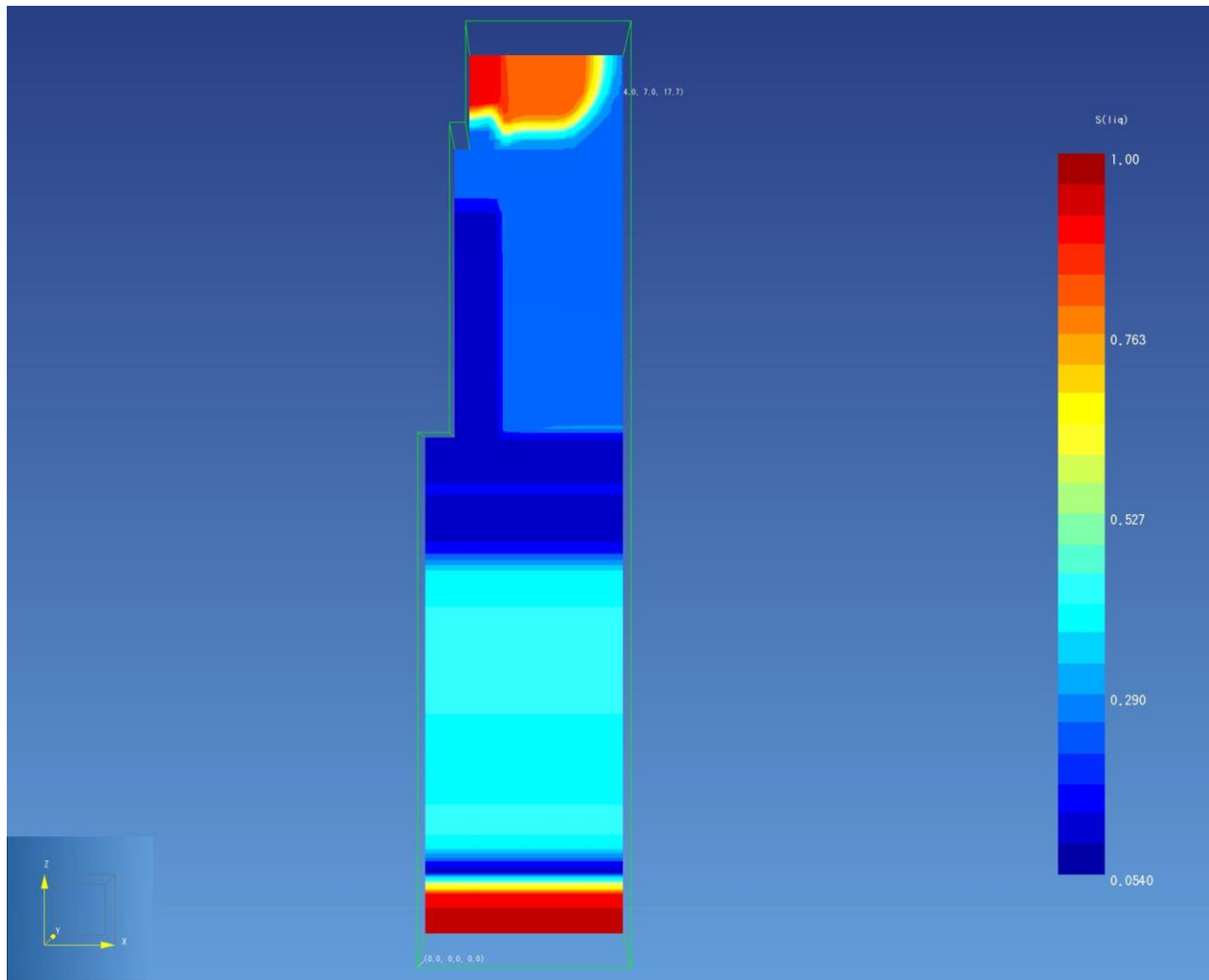
Figure 60. Predicted water saturation 5 hours after start of the second characterization test. The vertical slice runs west to east through the PA south instrument tube and the left side of the domain corresponds to the edge of the vault perimeter blocks (top), vault edges (middle) and below the vaults (bottom).

Figure 61. Predicted water saturation 15 hours after start of the second characterization test. The vertical slice runs west to east through the PA south instrument tube and the left side of the domain corresponds to the edge of the vault perimeter blocks (top), vault edges (middle) and below the vaults (bottom).

Figure 62. Predicted water saturation 22 hours after start of the second characterization test. The vertical slice runs west to east through the PA south instrument tube and the left side of the domain corresponds to the edge of the vault perimeter blocks (top), vault edges (middle) and below the vaults (bottom).
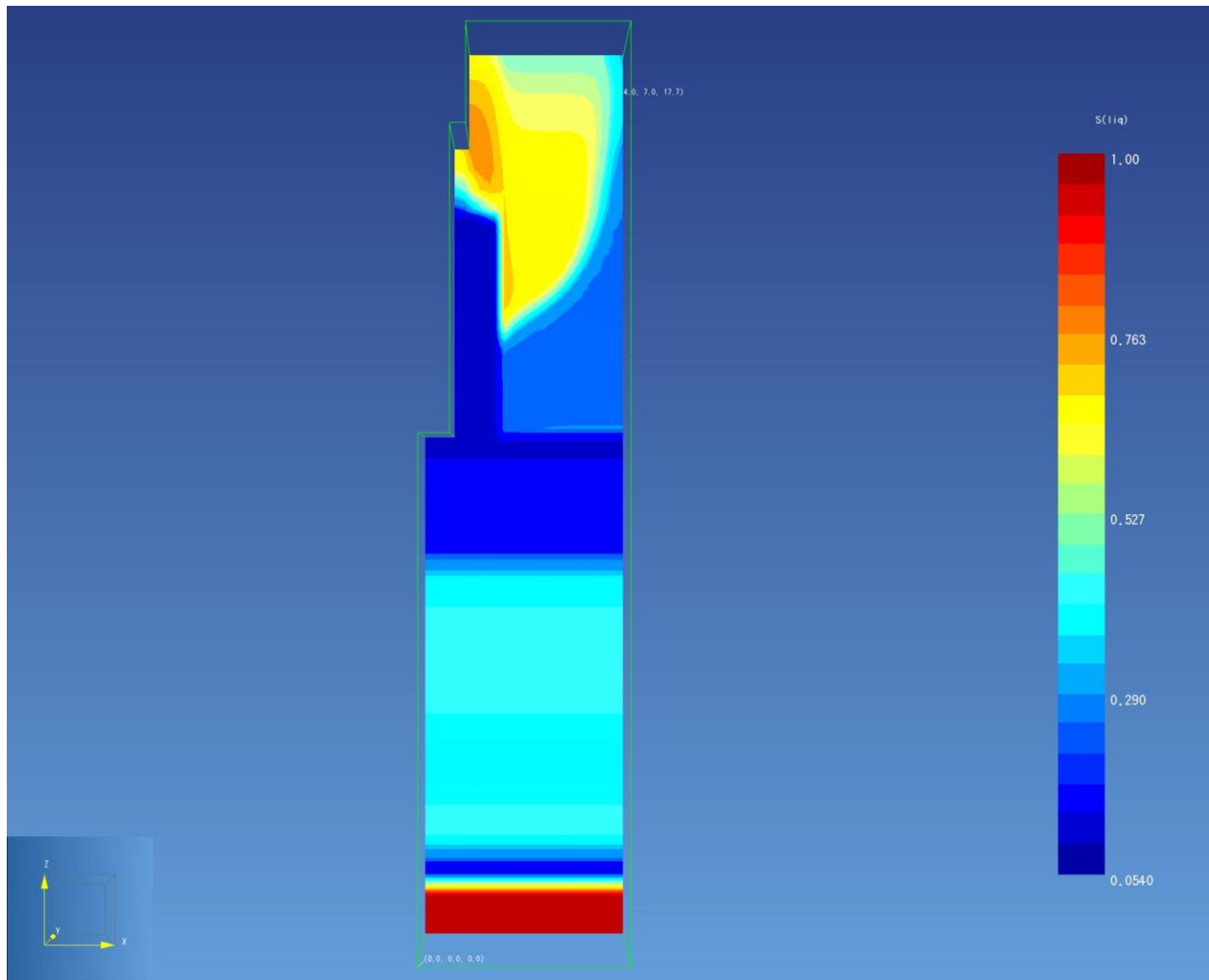
Figure 63. Predicted water saturation 30 hours after start of the second characterization test. The vertical slice runs west to east through the PA south instrument tube and the left side of the domain corresponds to the edge of the vault perimeter blocks (top), vault edges (middle) and below the vaults (bottom).
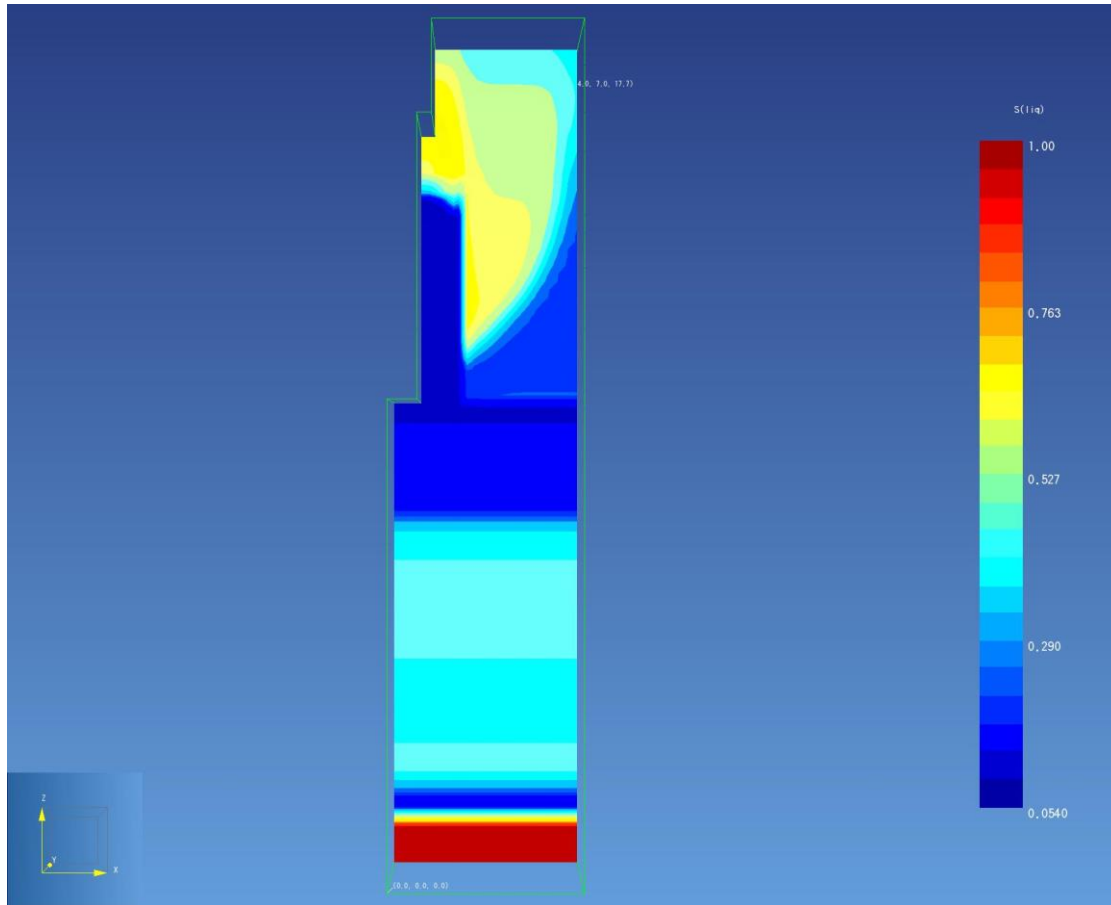
Figure 64. Predicted water saturation 80 hours after start of the second characterization test. The vertical slice runs west to east through the PA south instrument tube and the left side of the domain corresponds to the edge of the vault perimeter blocks (top), vault edges (middle) and below the vaults (bottom).

7.4   Simulation Results for the Natural Precipitation Event

In addition to simulating the first and second characterization tests, the model was used to simulate the natural precipitation event discussed in Section 6.7.4.5. The predicted moisture content time history for a depth of 12 ft is given in Figures 65; it shows a less than a 1% increase in moisture content following the abnormally high precipitation event (2 in. over 2 weeks). Negligible increases in saturation were predicted at all other depths. Vertical profiles of the wetting front at the end of the 10-day precipitation event and 117 days after the precipitation event are given in Figures 66 and 67. The vertical profiles shown correspond to the northern position of the PA south instrumented tube set, with the profile extending from the vaults to the east. Figure 66 shows that most of the precipitation water is held very high in the surface road base and crushed gravel base course at 10 days. At 117 days, the wetting front has migrated to the top of the vault perimeter drainage material, where it is again diverted into the alluvial fill along a narrow strip where the two different textual materials meet. This behavior is consistent with the original hypothesis made at the end of the first characterization test, where it was thought that water could be bypassing the vault perimeter drainage material and preferentially flowing down the geotextile between the alluvial fill and vault perimeter drainage material. However, in all simulations, no geotextile was used. The wetting front behavior shown in Figure 67 is purely a result of textural material contrasts and the effective capillary barrier between the crushed gravel base course and the vault perimeter drainage material. This simulation and corresponding field data show that very little water from precipitation events at INL would be expected to reach the concrete vault walls.
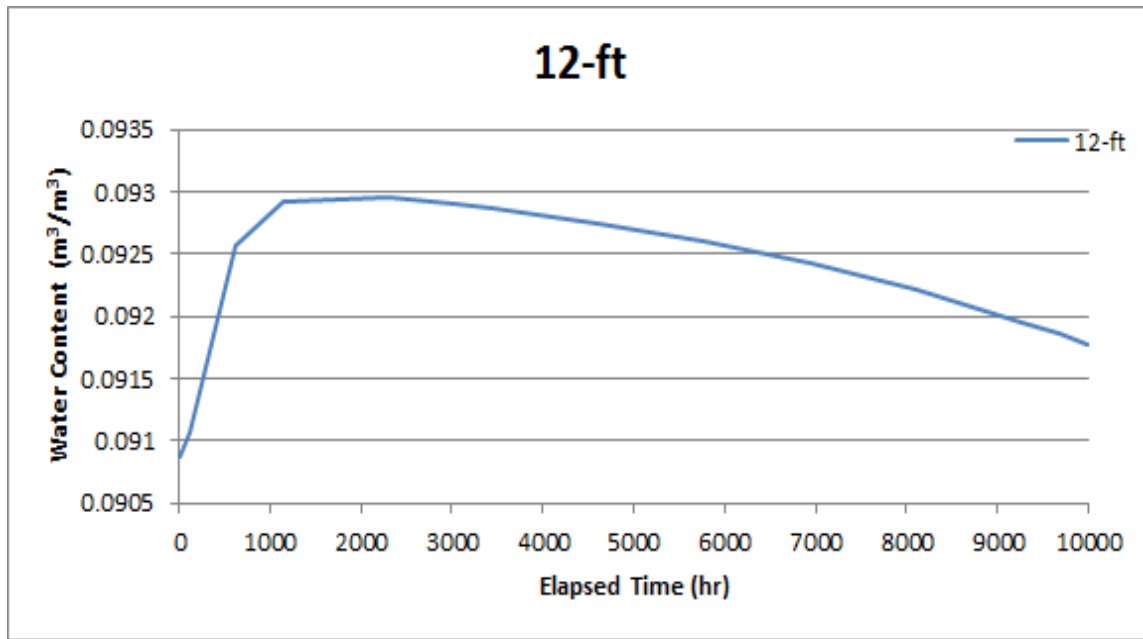
Figure 65. Model-predicted moisture content corresponding to model-predicted water saturation for the natural precipitation event.
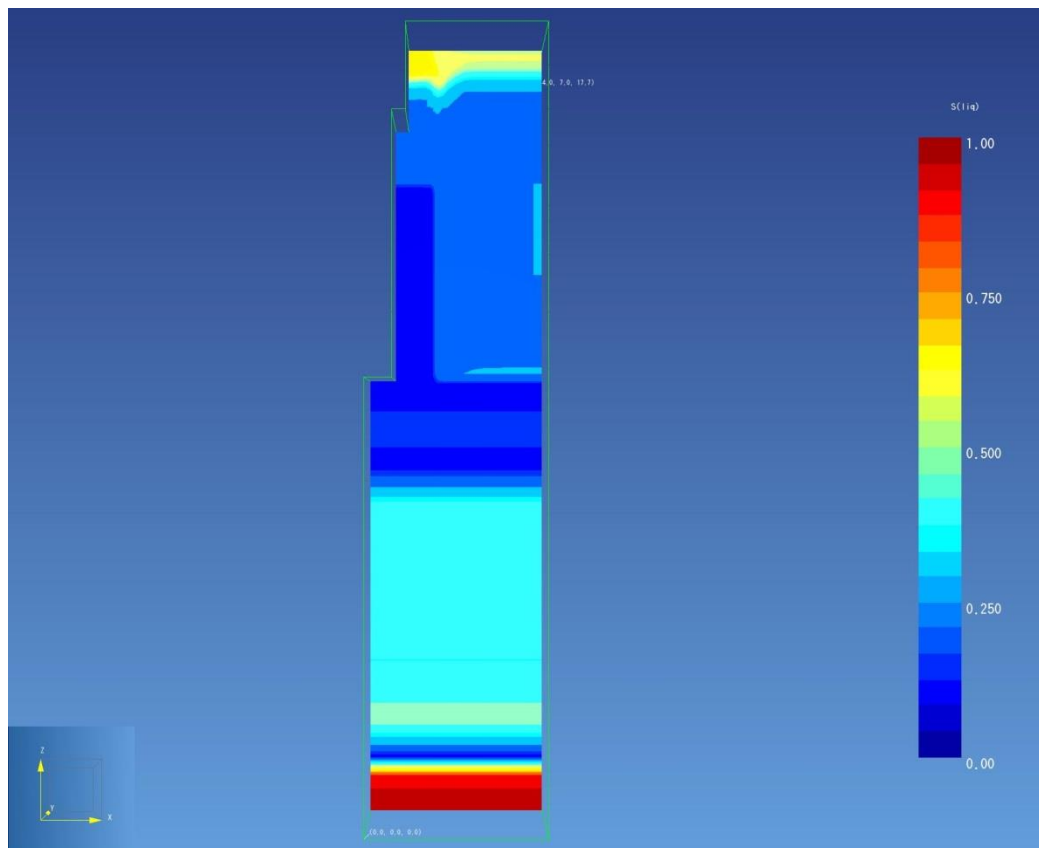
Figure 67. Predicted water saturation 10 days after start of the natural precipitation event. The vertical slice runs west to east through the PA south instrument tube and the left side of the domain corresponds to the edge of the vault perimeter blocks (top), vault edges (middle) and below the vaults (bottom).
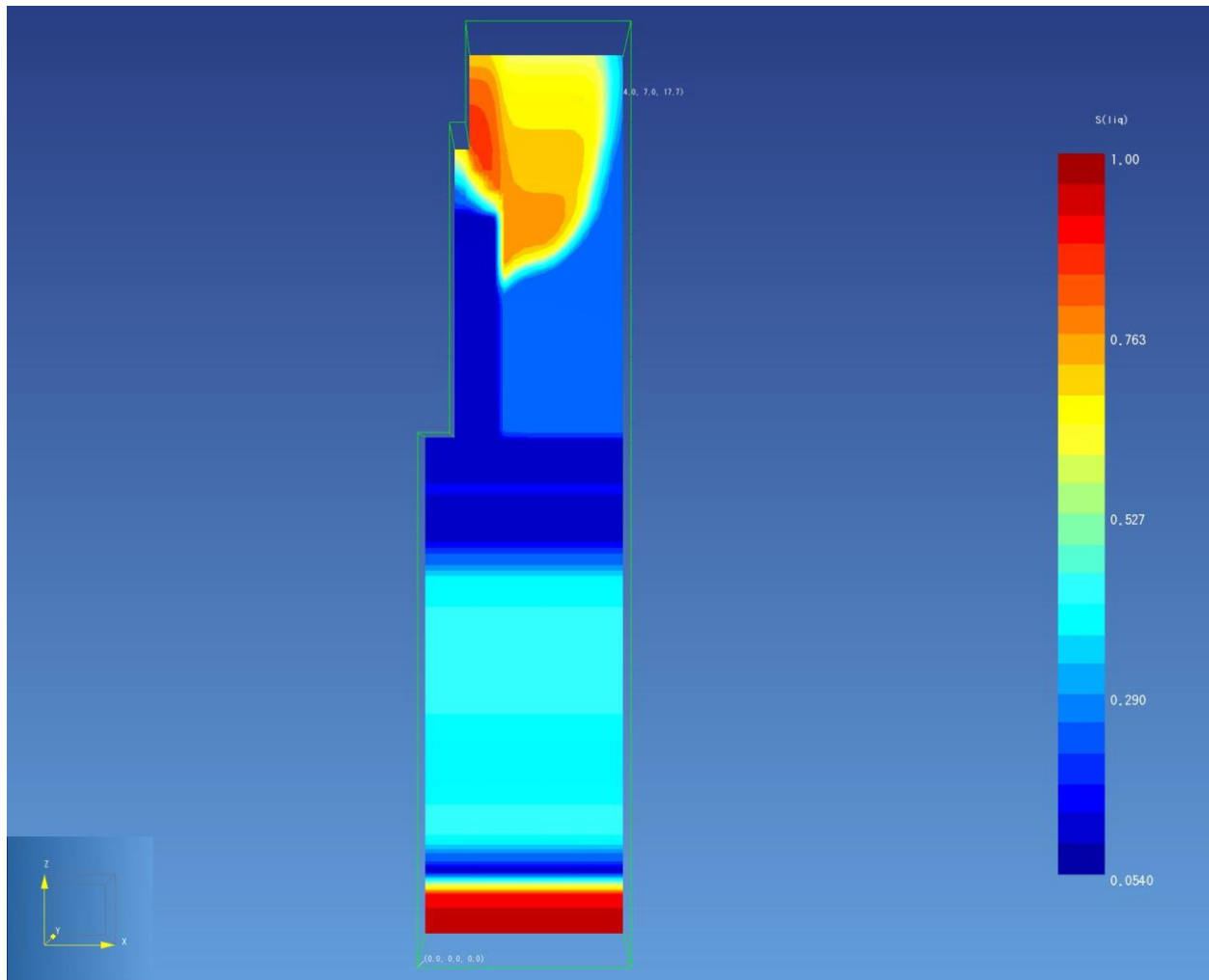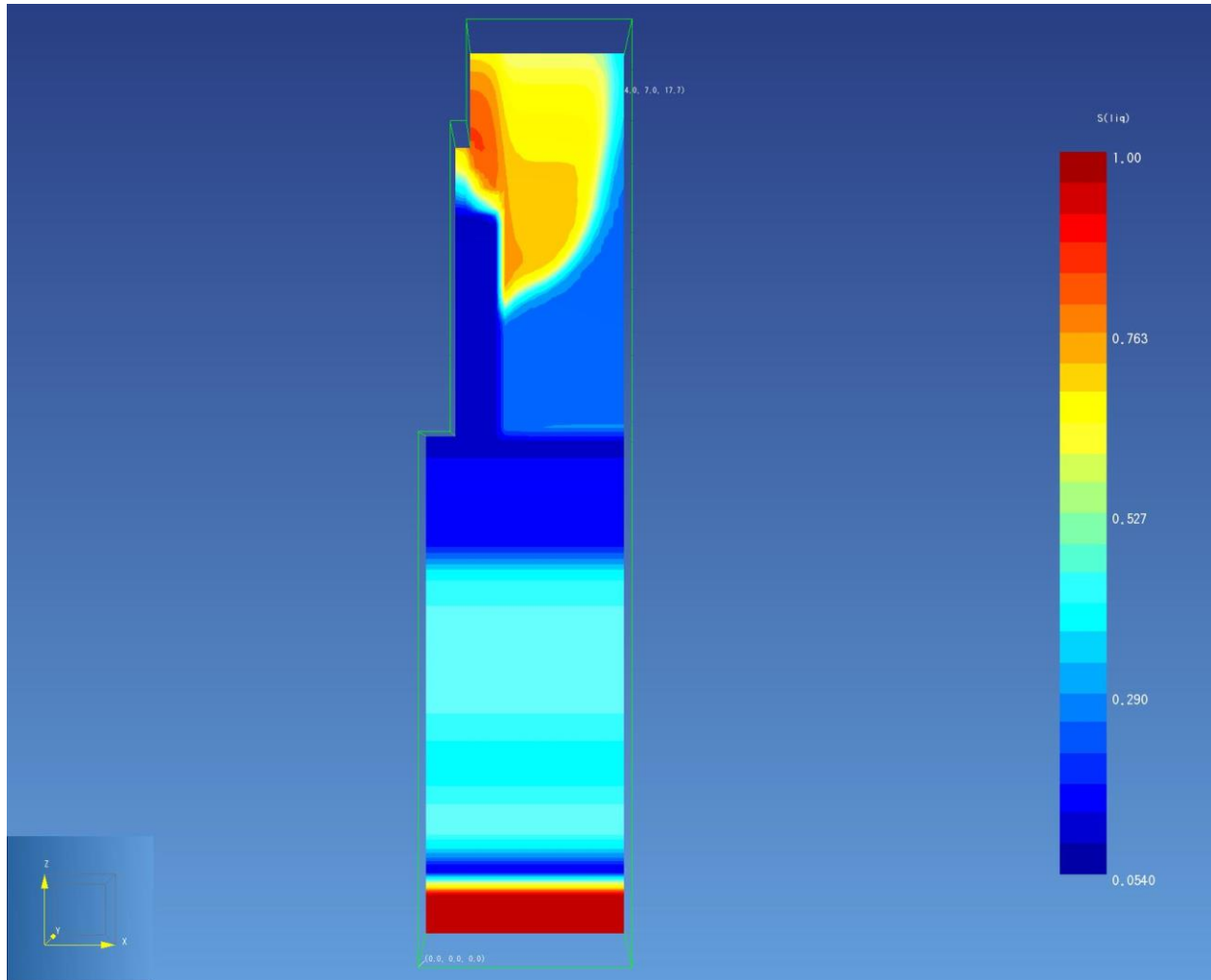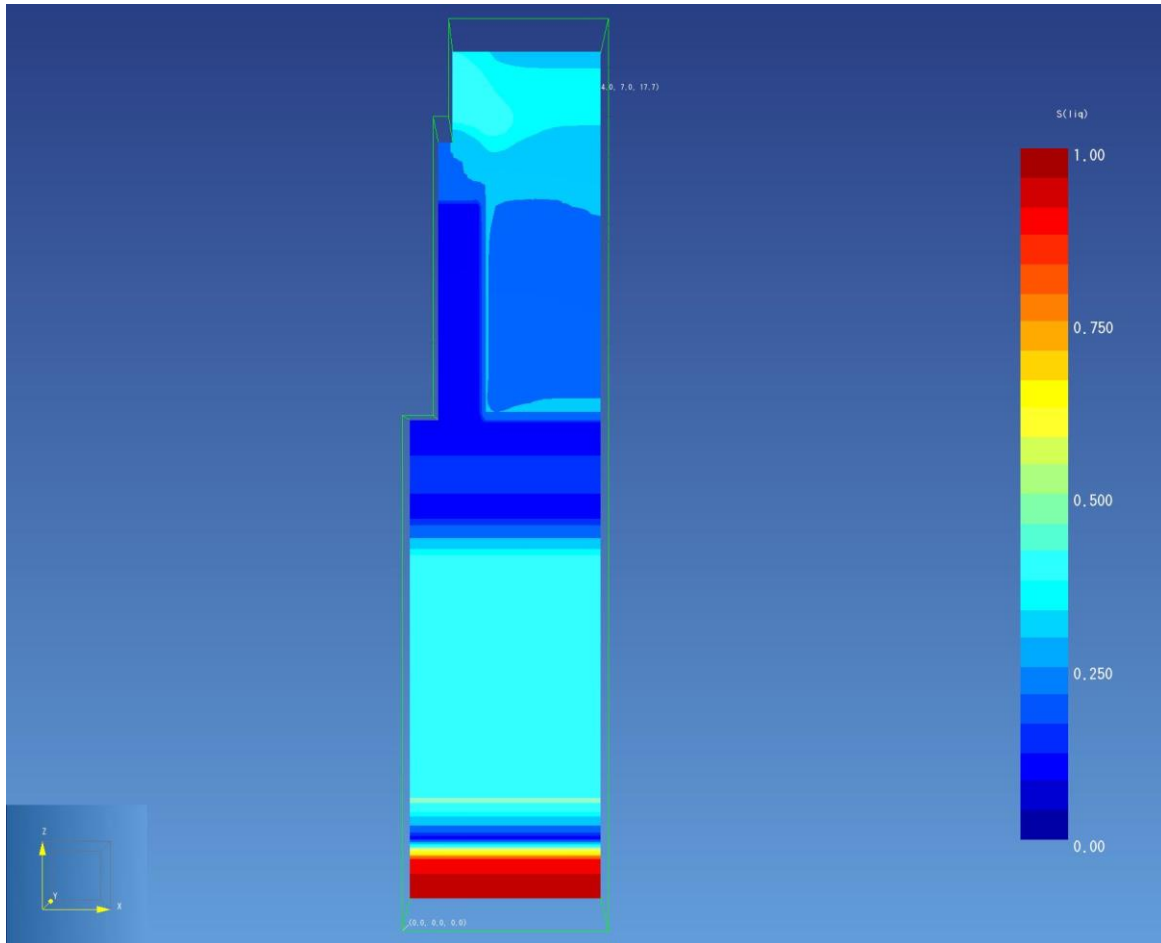
Figure 68. Predicted water saturation 117 days after the end of the natural precipitation event. The vertical slice runs west to east through the PA south instrument tube and the left side of the domain corresponds to the edge of the vault perimeter blocks (top), vault edges (middle) and below the vaults (bottom).

8.   SUMMARY OF HYDRAULIC PERFORMANCE

This document provides a summary of the expected hydraulic performance of the vault drainage system installed at INL's RH-LLW Disposal Facility. The hydraulic performance was assessed through analysis of mechanical properties of the drainage system and backfill materials, including material gradation and proctor data; laboratory data, including bulk density, porosity, unsaturated hydraulic conductivity, moisture-retention data, and van Genuchten parameters; and field-data collected using in-situ instrumentation during vault-scale infiltration characterization tests conducted at the PA vaults. Appendices A and B provide the data collected along the vaults that will contain waste. The purpose of conducting the east-side and west-side field characterization test was to assess the net performance of the perimeter drainage material and drainage course material following high rate infiltration for relatively high water application times. The overall hydraulic drainage system performance was evaluated using the field characterization tests conducted at the PA vault array. The PA vaults and all vaults on the east-side arrays were installed using the same materials and installation methods. The data from the west-side and east-side field characterization tests are given in Table 29. The maximum θ reached during and after these tests is shown in Column 3 and the elapsed time to return to θ_r is given in Column 4. These values are somewhat lower than observed during the PA vault array field characterization tests because of the shorter water application times and smaller total water volumes applied. The results support the conclusions of the PA vault array field characterization tests that were conducted at higher rates and for

longer application times. The maximum θ would not be expected to ever exceed the values shown in Table 29 under normal precipitation infiltration rates and durations.

Table 29. Summary of east-side vault array field characterization test results.

Location	Material	Maximum θ	Elapsed time to return to θ_r
NuPac-West	Drainage Course	3.5%	1-3 days for the peak, ~10 days to reduce to within 90% of θ_r
	Stratum II Alluvium	28%	1-3 days for the peak, ~2 months to reach θ_r
	45-ft Stratum II/III	<2%	
NuPac-East	Drainage Course	4.5%	1-3 days for the peak, ~10 days to reduce to within 90% of θ_r
	Stratum II Alluvium	19%	1-3 days for the peak, ~2 months to reach θ_r
	45-ft Stratum II/III	AT not WCR	> 3 months
55-Ton	Drainage Course	1.7%	1 day
	Stratum II Alluvium	20%	~10 days then the NuPac West peak arrives
	45-ft Stratum II/III	AT not WCR	> 3 months
LCC-West	Drainage Course	<1%	Unobservable increase
	Stratum II Alluvium	8%	<1 month
	45-ft Stratum II/III	AT not WCR	> 1 months
MFTC-West	Drainage Course	2%	1 day
	Stratum II Alluvium	22%	~1 month
	45-ft Stratum II/III	<2%	10-15 days
MFTC-East	Drainage Course	7%	Unobservable increase
	Stratum II Alluvium	1.5%	~15 days
	45-ft Stratum II/III	AT not WCR	~10 days

The predicted hydraulic performance is, in part, a function of materials used in construction of the vault drainage system, sequencing of the drainage materials, and the as-built condition of the materials following compaction necessary to ensure vault stability. Specifying specific as-built hydraulic properties is exceedingly difficult at the facility specification/design phase. Instead, material mechanical properties were specified and confirmed early during the construction process. As the drainage materials were installed, samples were sent to a laboratory for hydraulic property testing and, after the drainage system installation was complete around the PA vaults, two field-scale characterization tests were conducted with data collection to verify the as-built hydraulic performance. Conducting field-scale infiltration tests with collection of moisture retention data and wetting front propagation data allows extension of the laboratory data to as-installed conditions of the vault drainage system. These combined data types were integrated using a numerical simulation of the infiltration characterization test to refine model parameters. The infiltration characterization model and supporting laboratory data will be used to support the hydraulic and concrete performance of the vault system provided in the facility PA. This is summarized as follows:

- Hydraulic properties have been determined from mechanical and laboratory test data of backfill materials.

- A monitoring system is in place to demonstrate the hydraulic performance of the vault system.

- The efficacy of the monitoring system was demonstrated during two characterization tests.

- The tests demonstrated that significant amounts of water can be transmitted relatively rapidly through the vault drainage system (backfill materials) and moisture contents in the vault perimeter drainage material next to vaults are low, demonstrating little opportunity for moisture to enter the concrete.

- A model parameterized with hydraulic properties determined from mechanical and laboratory test data of the backfill materials was used to simulate the characterization tests and a natural precipitation event. The model demonstrated the general hydraulic behavior of the vault system.

- The characterization tests and model results provide data that can be used to support expectations regarding hydraulic performance and concrete longevity expectations in the PA.

The expected vault drainage behavior can be summarized as follows:

- During natural precipitation events, very little moisture would be expected to migrate from the alluvial fill material into the vault perimeter drainage material.

- The vault perimeter drainage material is expected to limit water contact with the concrete vault walls, resulting in near-residual moisture content for this material equal to the values obtained from laboratory data.

- Precipitation (i.e., rain or snow melt) falling on the perimeter blocks and vault plugs is expected to migrate through the pea gravel between the plugs or through the gap between the perimeter block and vault plug:

  - Precipitation moving through the pea gravel will drain rapidly into the underlying drainage course material. The pea gravel has very few fine sands in it and is predominantly 3/8-in. gravel pieces; therefore, it is expected to drain more rapidly than the vault perimeter drainage material. The pea gravel is between the riser sections of the vault upper riser and vault base section. There is a gap between the hexagonal base sections which allows free drainage into the gap from the pea gravel. The underlying drainage course material has some fine material, which will wick the water from the gap as opposed to acting like a capillary barrier.

  - Precipitation moving between the perimeter block and plug will enter the crushed gravel base course. This water is not expected to migrate into the vault perimeter drainage material as shown in the simulation results for the first and second characterization test and for the simulation of the natural precipitation event.

  - The drainage course material underlying each vault array footprint is 18-in. thick, extending 10 ft beyond the outer perimeter of the footprint. At a porosity of 33%, the drainage course material can accommodate approximately 6 in. of rain prior to filling the pore space of the drainage course material. This is more than adequate to prevent water from backing up into the vaults and is sufficient to accommodate all natural precipitation events.

  - Once the precipitation water reaches the drainage course material, it will drain into the underlying Stratum II alluvium through a combination of capillary suction into the finer material and gravitational forces.

9.   REFERENCES

American Geotechnics, 2011, *Geotechnical Investigation of the Proposed RH-LLW Facility,* Butte County, Idaho, American Geotechnics, File No. 10B-G2163, Revision 1.

ASTM C33, "Standard Specification for Concrete Aggregates," *American Society for Testing and Materials*.

ASTM C136, "Standard Test Method for Sieve Analysis of Fine and Coarse Aggregates," *American Society for Testing and Materials*.

ASTM D448, "Standard Classification for Sizes of Aggregate for Road and Bridge Construction," *American Society for Testing and Materials*.

ASTM D698, "Standard Test Methods for Laboratory Compaction of Soil Standard Effort," *American Society for Testing and Materials*.

ASTM D2216, "Standard Test Methods for Lab Determination of Water Content of Soil," *American Society for Testing and Materials*.

ASTM D2434, "Standard Test Method for Permeability of Granular Soils (Constant Head)," *American Society for Testing and Materials*.

ASTM D2487, "Standard Practice for Classification of Soils for Engineering Purposes (Unified Soil Classification System)," *American Society for Testing and Materials*.

ASTM D4355, "Standard Test Method for Deterioration of Geotextiles by Exposure to Light, Moisture, and Heat in a Xenon Arc Type Apparatus," *American Society for Testing and Materials*.

ASTM D4491, "Test Methods for Water Permeability of Geotextiles by Permittivity," *American Society for Testing and Materials*.

ASTM D4533, "Standard Test Method for Trapezoid Tearing Strength of Geotextiles," *American Society for Testing and Materials*.

ASTM D4632, "Standard Test Method for Grab Breaking Load and Elongation of Geotextiles," *American Society for Testing and Materials*.

ASTM D4718, "Standard Practice for Correction of Unit Weight and Water Content for Soils Containing Oversize Particles," *American Society for Testing and Materials*.

ASTM D4751, "Standard Test Methods for Determining Apparent Opening Size of a Geotextile," *American Society for Testing and Materials*.

ASTM D6241, "Standard Test Method for Static Puncture Strength of Geotextiles and Geotextile-Related Products Using a 50-mm Probe," *American Society for Testing and Materials*.

ASTM D6836, "Standard Test Methods for Determination of the Soil Water Characteristic Curve for Desorption Using Hanging Column, Pressure Extractor, Chilled Mirror Hygrometer, or Centrifuge," *American Society for Testing and Materials*.

ASTM D7263, "Standard Test Methods for Laboratory Determination of Density (Unit Weight) of Soil Specimens," *American Society for Testing and Materials*.

Campbell, G. and G. Gee, 1986, "Water Potential: Miscellaneous Methods," Chapter 25, pp. 631-632, in A. Klute (ed.), *Methods of Soil Analysis. Part 1, American Society of Agronomy*, Madison, Wisconsin.

Campbell Scientific, Inc. CS650 and CS655, "Water Content Reflectometers," Revision February 2016.

DOE-ID, 2006, *Operable Unit 3-14 Tank Farm Soil and Groundwater Remedial Investigation/Baseline Risk Assessment*, DOE/NE-ID-11227, U.S. Department of Energy Idaho Operations Office, April 2006.

DOE Order 435.1, "Radioactive Waste Management," *U.S. Department of Energy*.

INL, 2017, *As-Built Characterization and Monitoring System for the RH-LLW Disposal Facility*, INL/EXT-17-43081, Idaho National Laboratory.

SPC-1860, "General Site Construction for Remote-Handled Low-Level Waste Disposal Project."

SPC-1910, "Vault Installation for the Remote-Handled Low-Level Waste Disposal Project."

Topp, G. C, J. L. Davis, and A. P. Annan, 1980, "Electromagnetic Determination of Soil Water Content: Measurements in Coaxial Transmission Lines," *Water Resources Research* 16(3): 574–582.

van Genuchten, M. T., 1980, "A Closed-Form Equation for Predicting the Hydraulic Conductivity of Unsaturated Soils," SSSAJ 44:892-898.

van Genuchten, M. T., F. J. Leij, and S. R. Yates, 1991, "The RETC Code for Quantifying the Hydraulic Functions of Unsaturated Soils," Robert S. Kerr Environmental Research Laboratory, Office of Research and Development, U.S. Environmental Protection Agency, Ada, Oklahoma. EPA/600/2091 /065, December 1991.

VDR-510303, 2016, "Earth Moving, Material Test Reports, Drain Gravel," Revision 0, Areva Federal Services, contains the following individual reports: DHI-Vault – 8-01 MTI sieve analysis for samples: Drain Gravel 15-5364 and 15-5375.

VDR-510841, 2015, "Earth Moving, Material Test Reports, Perimeter Drainage Material," Revision 1, Areva Federal Services, contains the following individual report: DHI-Vault – 8-01. MTI sieve analysis for samples: Drain Gravel 15-5364, 15-5374, and 15-5375.

VDR-510949, 2017, "Earth Moving, Material Test Reports, Sub-base Proctor and Classification for Alluvial Fill," Areva Federal Services, contains the following individual reports: DHI-Site-26-06.

VDR-511096, 2015, "Earth Moving, Materials Test Reports: Pea Gravel Gradations," Revision 0, Areva Federal Services, contains the following individual report: DHI-Vault – 8-02 MTI sieve analysis for samples: Drain Gravel 15-5372, 15-5373, 15-5393, and 15-5396.

VDR-512339, "Vault Yard Aggregate Processing Field Sampling and Testing Procedure," QA-RHLLW.01, Revision 0, Delhur Industries, Inc.

VDR-521511, 2016, "Earth Moving – Hydraulic Properties Package Report (HPP)," Revision 2, Areva Federal Services, contains the following individual reports: DHI-Vault-09-01A. Hydraulic Properties Package – Drain Gravel and Base Course Samples 1 of 10 each; DHI-Vault-09-03. Samples 2, 3, 4 of 10 – Hydraulic Properties Package – Vault Perimeter Drainage Gravel; and DHI-Vault-09-04. Samples 5, 6, 7 of 10 – Hydraulic Properties Package – Vault Perimeter Drainage Gravel. Samples 1, 2, 3 of 10 Crushed Gravel Base Course (Revision 2).

VDR-544834, 2016, "Earth Moving – Hydraulic Properties Package Report (HPP)," Areva Federal Services, contains the following data report: DHI-Vault-8-03, Proctor Results for Performance Assessment Array Subgrade.

VDR-586147, 2017, "Vendor Data Report, Earthwork – Base Course Proctor and Classification," Areva Federal Services, contains the following individual report: DHI-Site-26-09: Base Course Proctor and Classification.

Appendix A

Characterization Test Data for the West-Side Vault Arrays

Appendix A

Characterization Test Data for the West-Side Vault Arrays

A-1. CHARACTERIZATION TEST OVERVIEW

This appendix contains characterization test data obtained for the NuPac and 55-Ton vault arrays located on the west-side of the RH-LLW Disposal Facility vault system. The test procedure followed the procedure outlined in Section 6.4 and used the test apparatus discussed in Section 6.3. Differences in the characterization tests compared to the test conducted at the PA Confirmation Vaults (see Section 6) are as follows:

- **Test Location.** Three test apparatuses were assembled for use adjacent to the NuPac-West, NuPac-East, and 55-ton monitoring system locations (see Figure A-1). The three test apparatuses are similar to the apparatus discussed in Section 6.3.
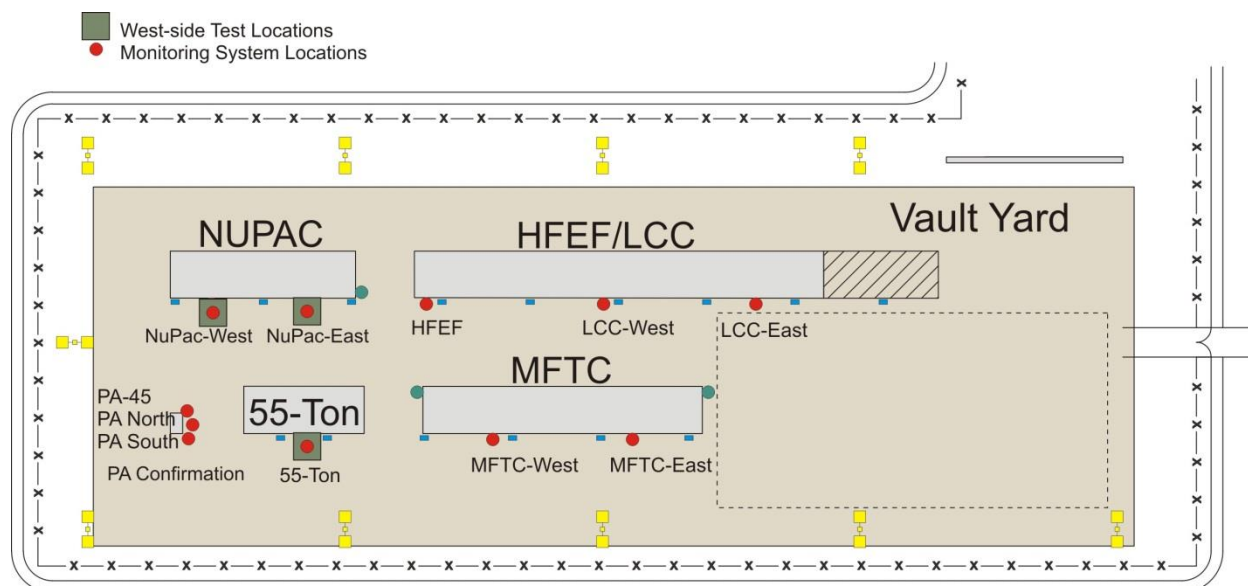
Figure A-1. Locations for the west-side vault array characterization tests.

- **Test Design.** The test was conducted to obtain moisture content history in the drainage course material and Stratum II alluvium (below the drainage course) at the test locations for comparison to test data collected at the PA vaults.

- **Test Procedure.** The test procedure outlined in Section 6.4 was used at all three of the west-side vault test locations.

- **Monitoring System.** The monitoring and characterization system at the test locations is presented in INL/EXT-17-43081 (INL 2017).

- **Calibration Data.** WCR calibration data are discussed in Section 6.6.2. Calibration used for the drainage course material and perimeter drainage course materials is provided in Figure 16 and for the

shallow alluvium in Figure 21. The Topp calibration relationship was used for the Stratum III alluvium. The AT calibration data are provided in Table A-1.

Table A-1. AT calibration data for the west-side vault array characterization tests.

Location	Stratum II Alluvium (deep) (U1 Data Logger Connection)			Perimeter Drainage Material (shallow) (U2 Data Logger Connection)		
	Depth	Slope	Offset	Depth (ft)	Slope	Offset
NuPac-West	26	1.7090	-2147	22	1.6980	-2085
NuPac-East	26	1.6670	-2054	22	1.6950	-2088
55-Ton East	29	1.6670	-2034	26	1.6950	-2085

Location	Stratum III Alluvium (45-ft depth) (U1 Data Logger Connection)		
NuPac-45-West	42.5	No AT at this location	
NuPac-45-East	41	1.6390	-2019
55-Ton-45	40	1.6810	-2051

A-2. CHARACTERIZATION TEST DATA AND INTERPRETATION

The west-side vault array characterization tests were conducted on May 12, 2017. The infiltration tests were conducted over a period of approximately 10.5 hours, keeping the infiltration rates roughly constant as shown in Table A-2. Data were collected using the monitoring instruments in the instrumented tubes and 45-ft drilled boreholes at each of the three locations. The raw data were calibrated as indicated in the following subsections.

Table A-2. Volumetric rates applied during the west-side vault array characterization tests.

		Characterization Test Conducted 5/12/2017 at the NuPac-West Location		
		Water Depth in Tank		Flow Rate
Time	Elapsed Time (minutes)	Water Level (inches)	Water Used (inches)	(in./hour)
7:00 a.m.				
8:36		24		
9:06	0:30	18	6	12
10:31		23.5		
11:01	0:30	19.125	4.375	8.75
11:21		16.875		
11:51	0:30	11.125	5.75	11.5
12:19		22.875		
12:49	0:30	20.75	2.125	4.25
1:08		17.75		
1:38	0:30	11	6.75	13.5
2:10		23.5		
2:40	0:30	16.75	6.75	13.5
4:22		16.5		
5:22	1:00	4	12.5	12.5
17:35	Test end			
Test duration	10.58 (hours)			
Tank diameter (in)		50		
Total volume of water		225,615 (in.^{3})		
Total volume of water		977 (gallons)		

117

Characterization Test Conducted 5/12/2017 at the NuPac-East Location				
		Water Depth in Tank		Flow Rate (in./hour)
Time	Elapsed Time (minutes)	Water Level (inches)	Water Used (inches)	Flow Rate (in./hour)
7:06 a.m.				
8:18		23.5		
8:48	0:30	15.5	8	16
10:22		23.375		
10:52	0:30	15.25	8.125	16.25
12:09		22.375		
12:39	0:30	14.375	8	16
1:58		23.75		
2:28	0:30	15.25	8.5	17
4:28		22.5		
5:28	1:00	6.25	16.25	16.25
17:29	Test end			
Test duration	10.38 (hours)			
Tank Diameter (in)		44.5		
Total volume of water		263,229 (in.^{3})		
Total volume of water		1,140 (gallons)		
Characterization Test Conducted 5/12/2017 at the 55-Ton Location				
		Water Depth in Tank		Flow Rate (in./hour)
Time	Elapsed Time (minutes)	Water Level (inches)	Water Used (inches)	Flow Rate (in./hour)
7:10 a.m.				
8:40		23		
9:10	0:30	15.5625	7.4375	14.875
10:37		24		
11:07	0:30	16.375	7.625	15.25
12:29		23		
12:59	0:30	15.25	7.75	15.5
2:15		24		
2:45	0:30	16.25	7.75	15.5
4:15		22.75		
5:15	1:00	7.5	15.25	15.25
17:45	Test end			
Test duration	10.58 (hours)			
Tank Diameter (in)		44.5		
Total volume of water		251,428 (in.^{3})		
Total volume of water		1,088 gallons		
Average rate		1.4 gpm		

A-2.1   Calibrated Characterization Test Data

A-2.1.1   NuPac-West Instrumented Tube and 45-ft Drilled Borehole

The calibrated θ data for the NuPac-West instrumented tube are given in Figure A-2. Data collected in the drainage course material shows a single peak value, while data in the Stratum II alluvium show a second smaller peak. This behavior is expected given the PA Confirmation Vault test data and the model used to fit it. There are two early peaks occurring at the Stratum II sensor depth. The first peak is probably representative of faster water being transmitted along the material interface between the vault perimeter

drainage material and the alluvial fill. The second peak likely represents the arrival of water transmitted just through the alluvial fill.

These data show the maximum θ in the drainage course material was 3.5% and 28% in the Stratum II alluvium. As with the data shown in Section 6 for the PA Confirmation Vault tests, the return to θ_r occurs within days in the drainage course material. The return to θ_r in the Stratum II alluvium takes on the order of 2 months, reflecting the much slower drainout through the alluvial fill material.

The water tension shown in Figure A-3 in the drainage course material is positive, indicating saturated conditions. This is not born out by WCR data that shows the system is less than 30% moisture content. Tension data are computed from the recorded voltage; it is likely the calibration equation used is erroneous. The tension data in the Stratum III alluvium responded to the arrival of water in May and that it is still draining from the sandy-silty material in October.

The θ data computed from permittivity for the NuPac-West 45-ft drilled borehole are shown in Figure A-4. These data are negative, indicating that the θ is less than 2, which is a characteristic of the Topp Equation applied to very low permittivities as indicated in Figures 16 and 21. Although the calibrated θ is negative, the permittivity used to calculate θ is clearly decreasing, showing the instrument is connected correctly and the data logger is recording the permittivity.

Figure A-5 contains the temperature obtained for sensors installed at depths of 12, 18, 26, 34, and 43 ft. These data do not require calibration; therefore, they represent the "raw" signal. Data at depths shallower than 34-ft clearly indicate the arrival of the wetting front in the early to mid-May timeframe. Temperature data in these sensors are increasing from late May through August, reflecting higher day-time temperatures at land surface in Idaho. It is expected that these data will decrease over the winter months. The temperature data collected using the sensors installed at 34-ft and 43-ft reflect the same overall trend. Because these data are excessively noisy, they were tested for continuity and the measured resistance is within the general range. This probably indicates the wires or sensors may have been damaged during installation.
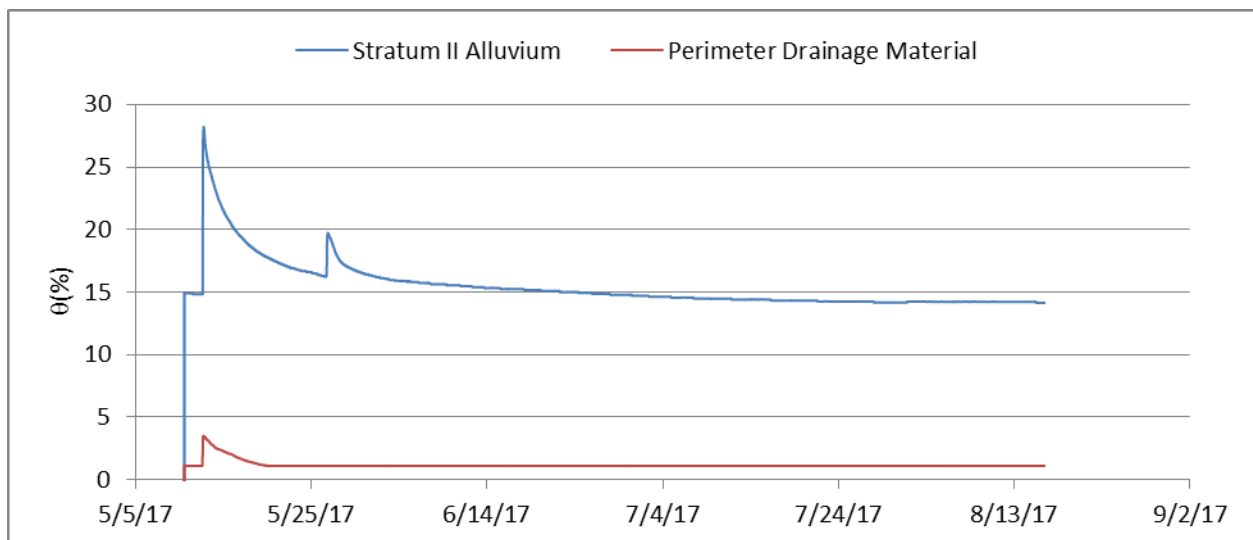

Figure A-2. θ calculated using measured permittivity, first order calibration curve for data at a 22-ft depth, and a second order calibration curve for data at 26 ft in the NuPac-West instrumented tube.
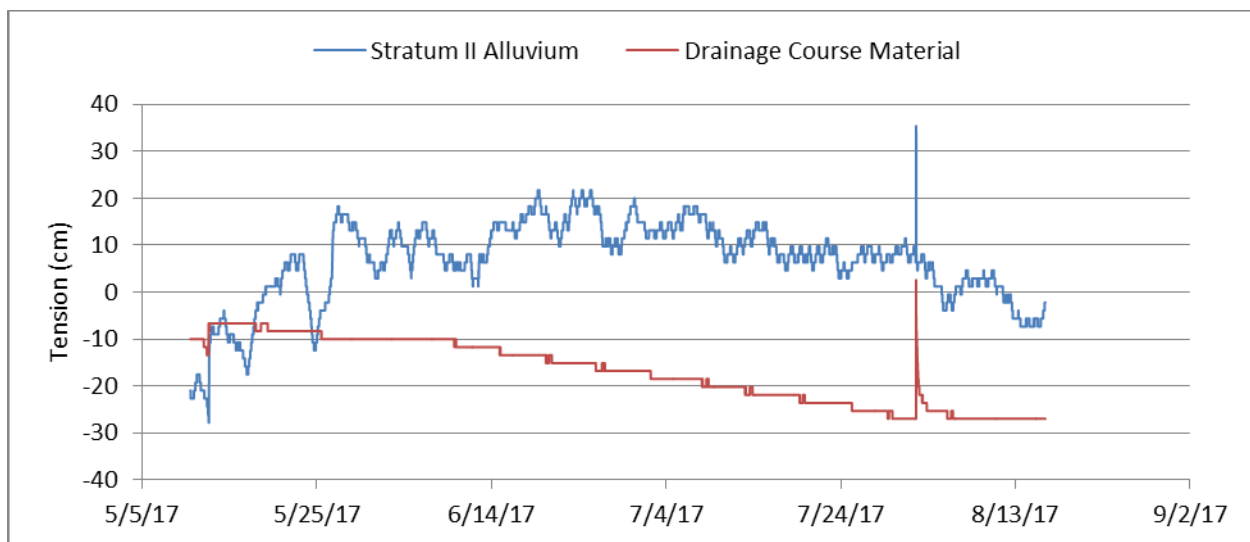
Figure A-3. Water tension in the NuPac-West instrumented tube at 22 and 26-ft depths.
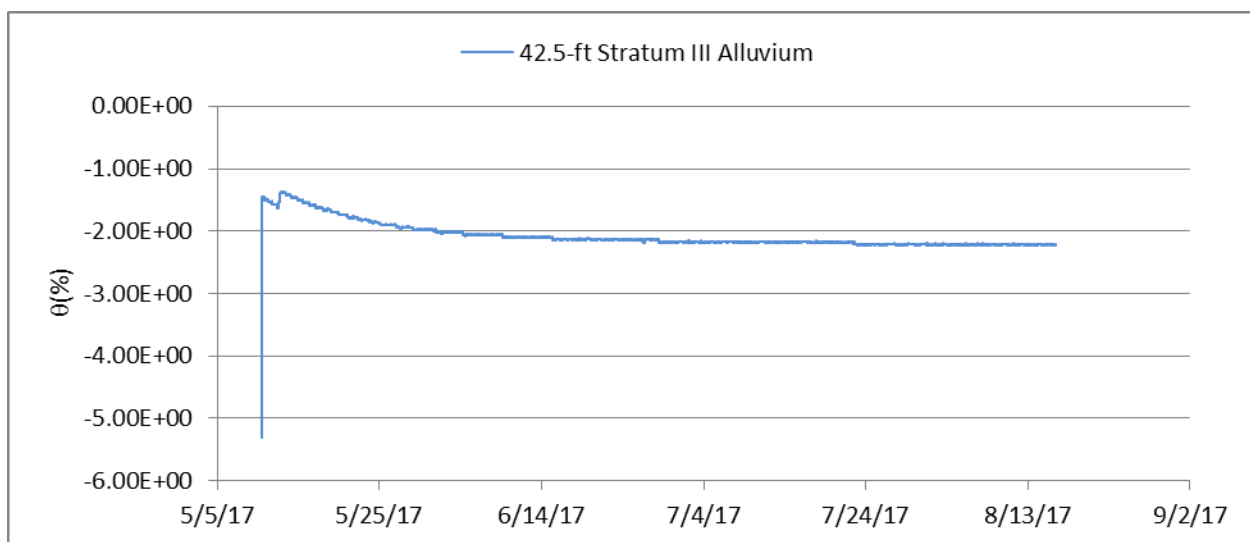

Figure A-4. θ calculated using measured permittivity and the Topp equation in the NuPac-West 45-ft drilled borehole.
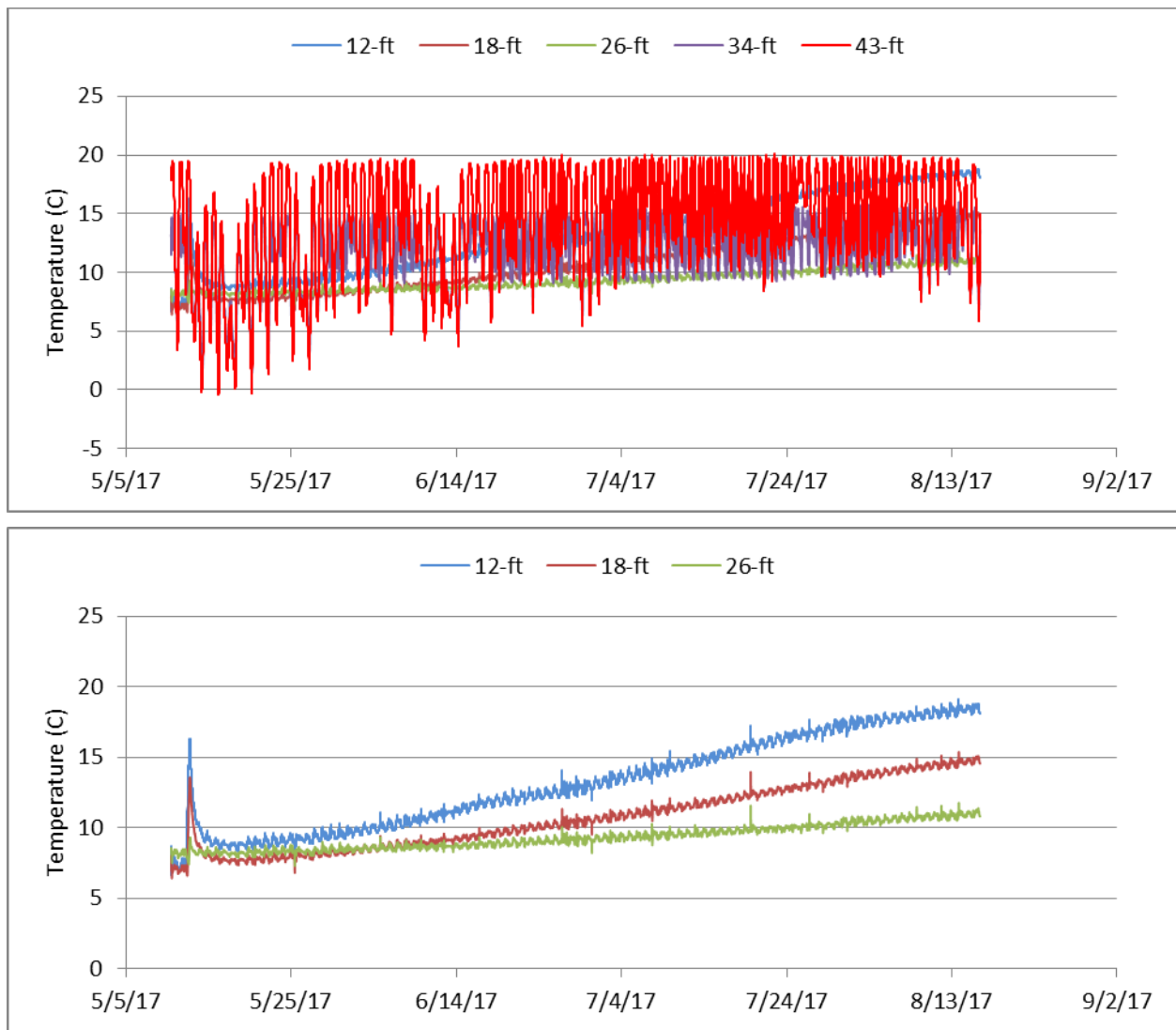
Figure A-5. Temperature in the NuPac-West 45-ft drilled borehole. Upper figure shows all data and lower figure removes the noisy data obtained using the sensors installed at depths of 34 and 43-ft.

A-2.1.2   NuPac-East Instrumented Tube and 45-ft Drilled Borehole

The calibrated θ data for the NuPac-East instrumented tube are given in Figure A-6. There is a single peak in θ for both the drainage course material and the Stratum II alluvium. This is in contrast to the NuPac-West data shown in Figure A-2. In the NuPac-East location, the applied water tended to spread out at land surface instead of being infiltrated within the 8-ft x 8-ft area. The lack of a defined second peak was expected in these data because of the lateral spread of water observed at this location at land surface.

The data show that the vault perimeter drainage material behaves similarly to the NuPac-West data, with the maximum θ in the drainage course material equal to 4.5% and equal to 19% in the Stratum II alluvium. As with the data shown in Section A-2.1.1, the return to $θ_r$ occurs within days in the drainage course material. The return to $θ_r$ in the Stratum II alluvium takes on the order of 2 months, reflecting the much slower drainout through the alluvial fill material.

121

Water tension shown in Figure A-7 is extremely small, showing that the data logger is recording millivolt changes. In this figure, the calculated water tension for both sensors is slightly positive. Given the very low recorded voltage changes, the absolute value of these data is not meaningful.

Water tension in the NuPac-East 45-ft drilled borehole is shown in Figure A-8. These data show good response to the infiltration characterization test and the very long slow drain out that would be expected in the Stratum III material. The spike in tension data in early October is a result of refilling the AT.

Figure A-9 contains the temperature obtained for sensors installed at depths of 12, 18, 26, 34, and 43-ft. These data do not require calibration; therefore, they represent the "raw" signal. Data clearly indicate the arrival of the wetting front in the early to mid-May timeframe. The temperature at depths less than 26 ft reflects the day-time temperature increase that occurs from late May through August. At a depth of 26 ft, the increase is very small it is unobservable at depths below 34 ft. It is expected the sensors will reflect the colder winter air temperatures.
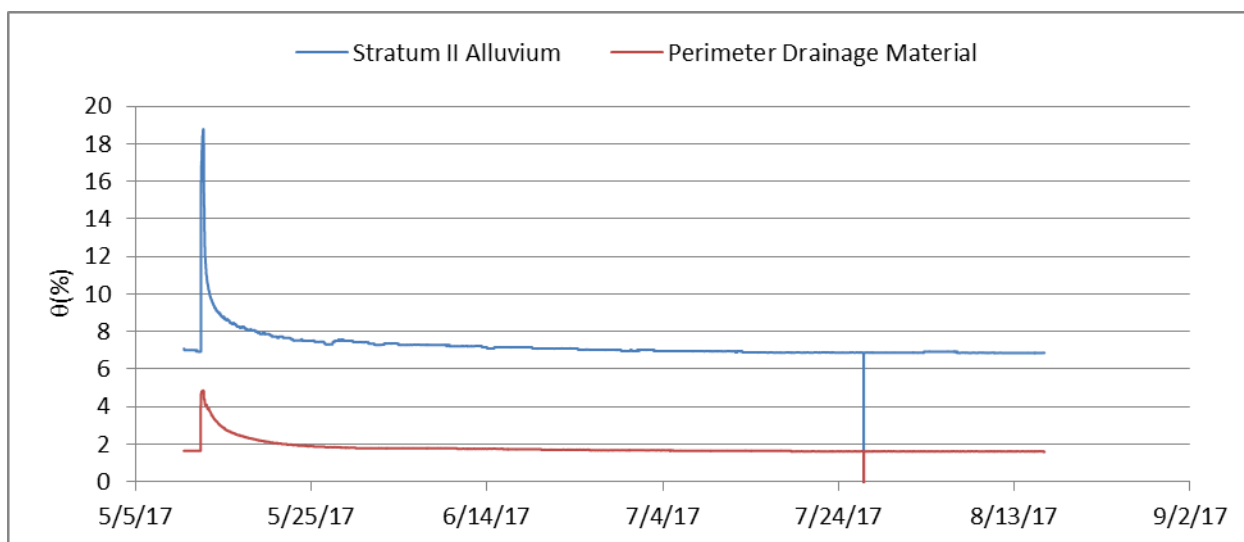

Figure A-6. θ calculated using measured permittivity, a first order calibration curve for data at 22-ft depth, and a second order calibration curve for data at 26 ft in the NuPac-East instrumented tube.
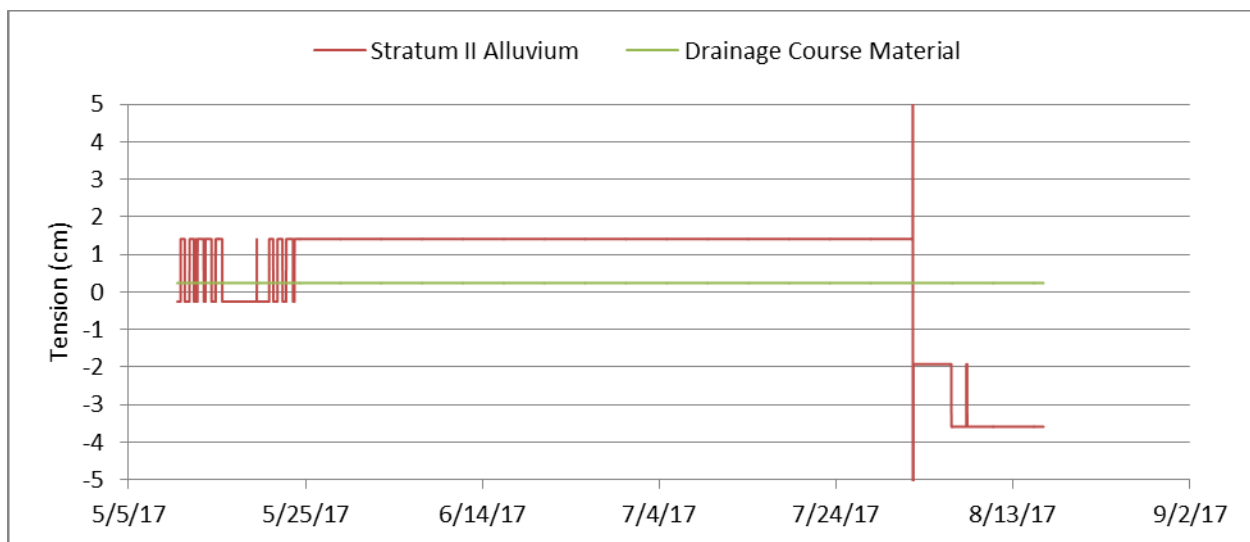
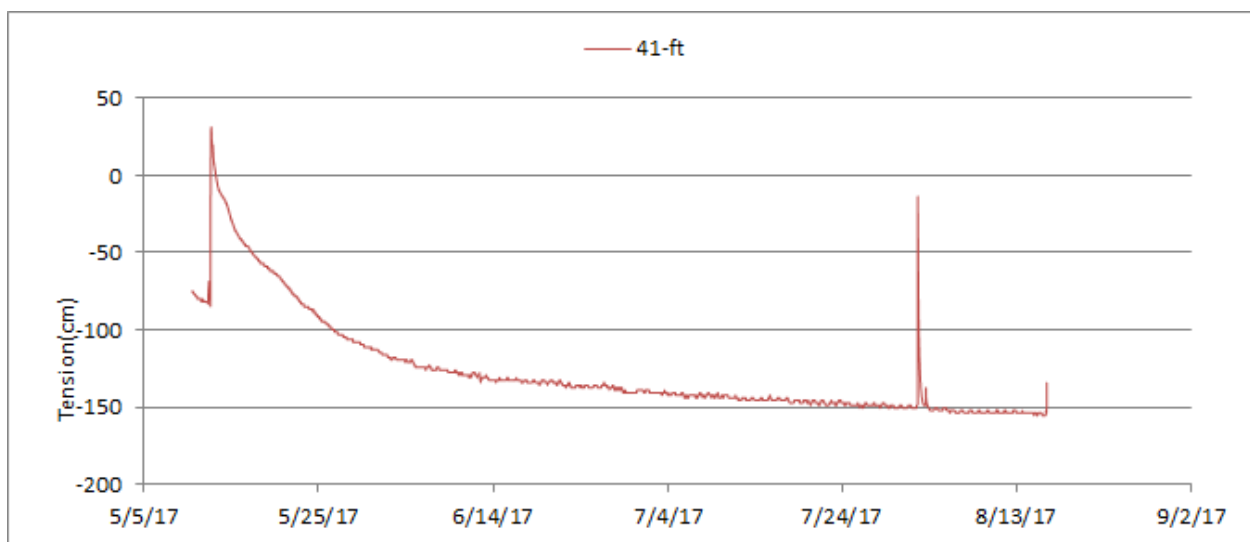Figure A-7. Water tension in the NuPac-East instrumented tube at 22 and 26-ft depths.

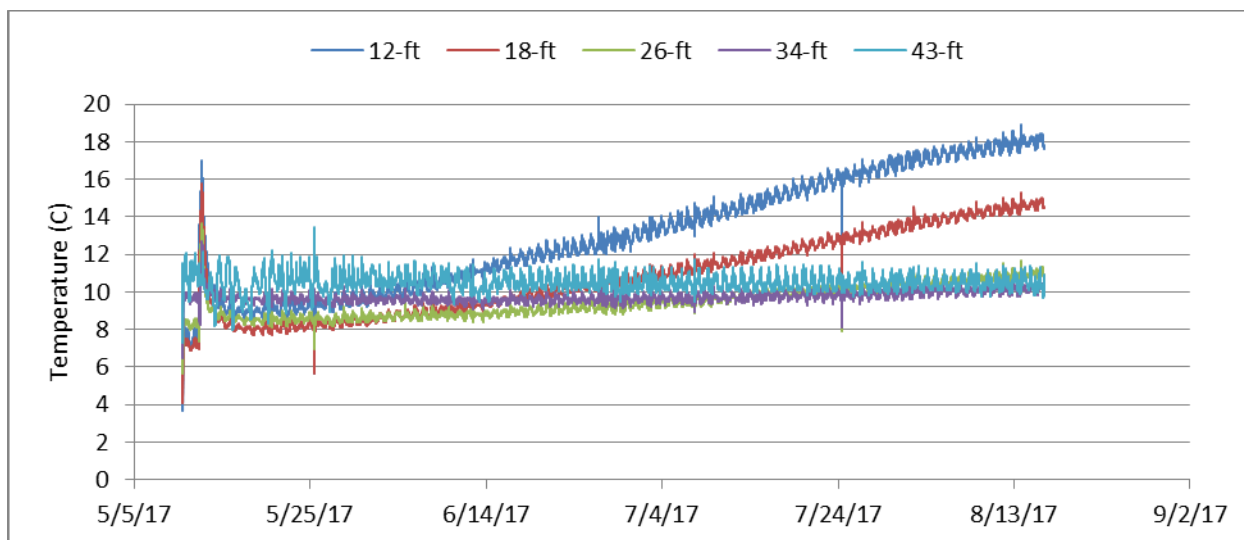Figure A-8. Water tension in the NuPac-East 45-ft drilled borehole.

Figure A-9. Temperature in the NuPac-East 45-ft drilled borehole.

A-2.1.3 55-Ton Instrumented Tube and 45-ft Drilled Borehole

The calibrated θ data for the 55-ton instrumented tube are given in Figure A-10. These data exhibit the typical bi-modal arrival of water in the perimeter drainage material following the May 12, 2017, characterization test with a maximum θ in the drainage course material of 1.7% and 20% in the Stratum II alluvium. The return to θ_r after the May bi-modal peak occurs within days in the drainage course material. The return to θ_r in the Stratum II alluvium takes on the order of 2 months, reflecting the much slower drainout through the alluvial fill material. The water tension shown in Figure A-11 is essentially zero prior to the first of October when the ATs were re-filled with water, showing the data logger is recording millivolt changes.

Water tension in the 55-ton 45-ft drilled borehole is shown in Figure A-12. These data show good response to the infiltration characterization test and the very long slow drain out that would be expected in the Stratum III material. Again, the spike in tension data in early October is a result of refilling the AT.

Figure A-12 contains the temperature obtained for sensors installed at depths of 12, 18, 26, 34, and 43-ft. These data are very similar to the temperature data collected with the NuPac-East monitoring system. The data all clearly indicate the arrival of the wetting front in the early to mid-May timeframe. The temperatures at depths less than 26 ft reflect the daytime temperature increase that occurs from late May through August. At a depth of 26 ft, the increase is very small and it is unobservable at depths below 34 ft. It is expected the sensors will reflect the colder winter air temperatures.
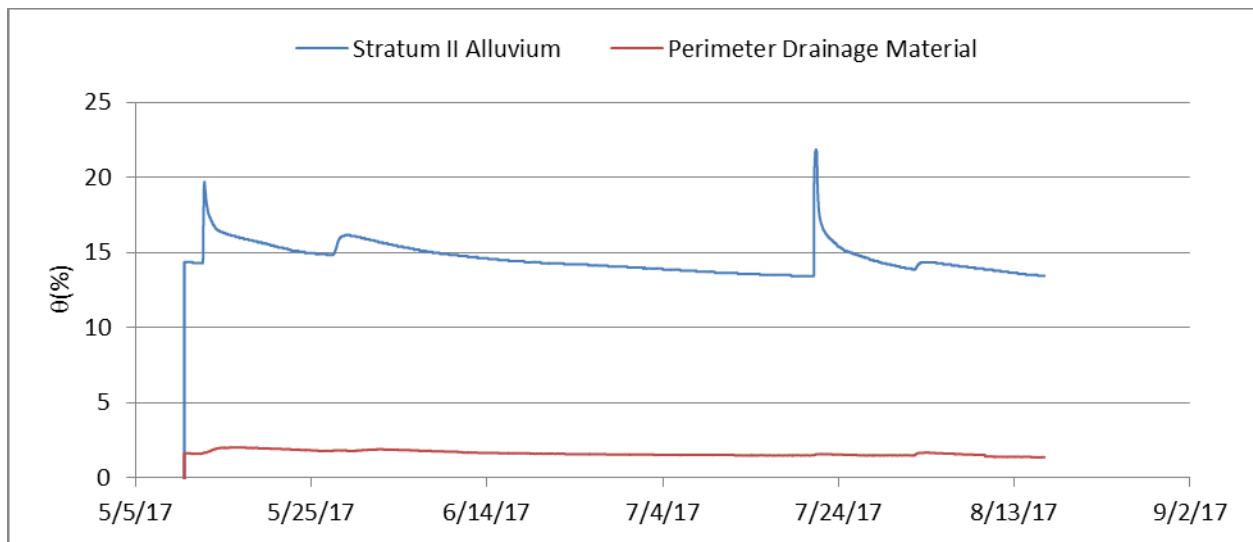
124

Figure A-10. θ calculated using measured permittivity, first order calibration curve for data at a 26-ft depth, and second order calibration curve for data at a 29-ft depth in the 55-ton instrumented tube.
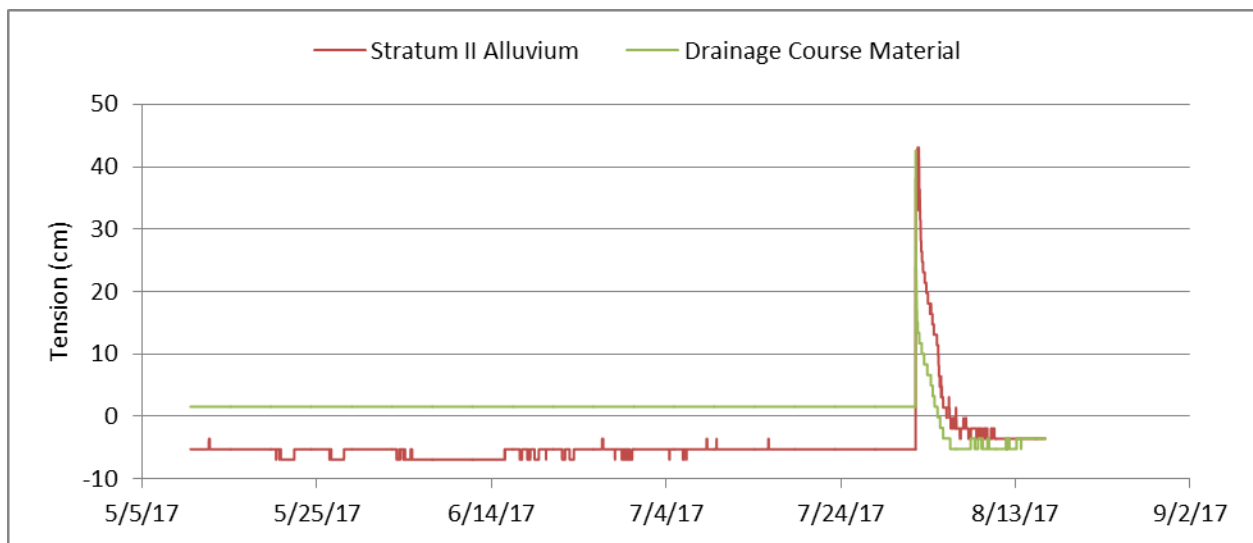

Figure A-11. Water tension in the 55-ton instrumented tube at 26 and 29-ft depths.
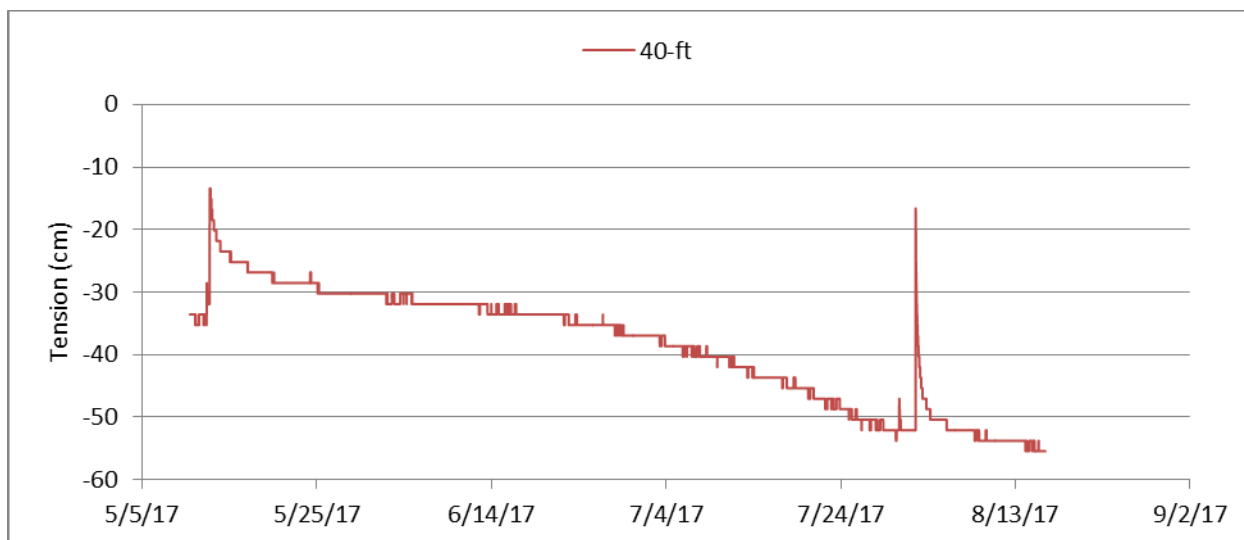
Figure A-12. Water tension in the 55-ton 45-ft drilled borehole.
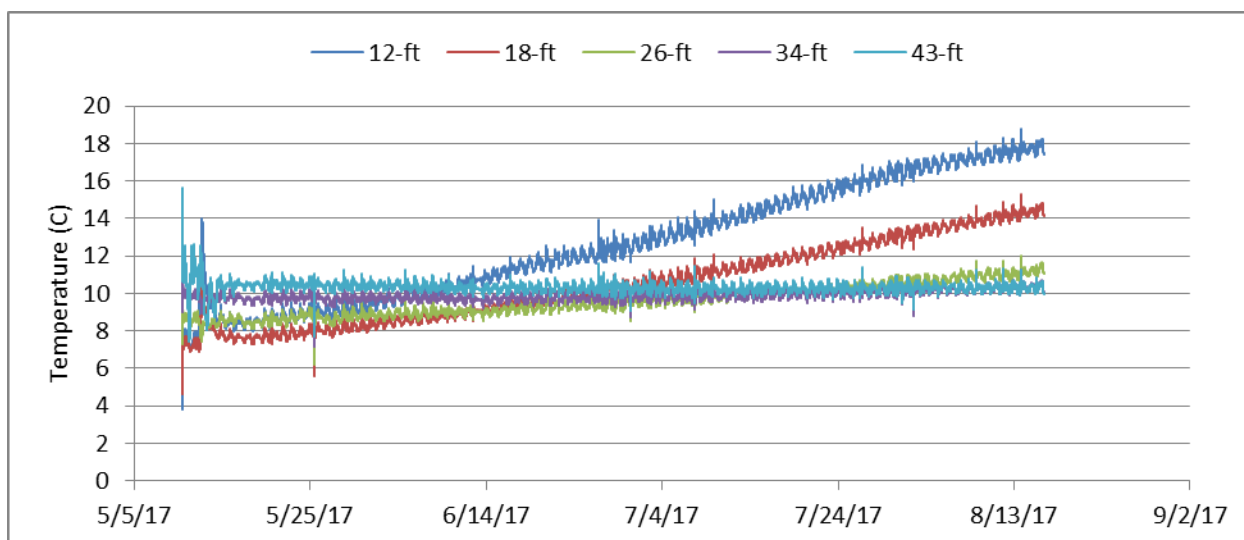
Figure A-13. Temperature in the 55-ton 45-ft drilled borehole.

A-2.1.4 Apparent Influence of the NuPac-West and NuPac-East Characterization Tests at the 55-Ton and Performance Assessment Vault Locations

In addition to containing the typical bi-modal response to the characterization test conducted in May at the 55-ton vault test location, Figure A-10 also contains a second bi-modal water arrival about 70 days after the first wetting front. The second bi-modal set of peaks occurs on about July 21, 2017. While the first bi-modal arrival is typical, the second bi-modal arrival was not observed in any of the NuPac data. It is hypothesized that the second flux of water originated at characterization at the NuPac-East characterization test location because of the following installation details:

- The NuPac-East characterization test was conducted on the south side of the Nupac vault array approximately 27.5 m (90 ft) north of the 55-ton characterization test location and about the same distance from the PA Confirmation Vaults.

126

- The 55-ton vaults and PA Confirmation Vaults are 122 cm (48 in.) taller than the NuPac vaults (see Table 2).

- As shown in the excavation plan for the facility (see Figure A-14), the height offset was accommodated by excavating the Stratum II alluvium 122 cm (48 in.) deeper under the 55-ton and PA Confirmation Vaults. The vertical offset started approximately 12 m (40 ft) south of the NuPac vaults and ended the same distance north of the 55-ton vaults as shown in Figure A-15.

- The drainage course material was then placed over the unexcavated Stratum II alluvium with it extending approximately 3 m (10 ft) from the outer edge of the perimeter blocks at the NuPac and 55-ton vault locations.

- Excavation and installation of the drainage course material resulted in the vertical material profile shown in Figure A-16. As shown in Sections 6 and 7, the material contrast between the drainage course material and alluvial fill limits water penetration into the drainage course and focuses water flow into the alluvial fill instead. It is likely there is a compaction contrast interface between the unexcavated Stratum II alluvium and alluvial fill.

During the NuPac-East characterization test, and similar to the PA Confirmation Vault test, water was observed to extend to the south for a distance in excess of 10-ft beyond the edge of the 8-ft x 8-ft test box area at land surface. The extended infiltration area could have allowed the infiltrating water to approach the vertical offset area shown to be close to the edge of the drainage course in Figure A-16. As the water reached the vertical offset plane, it is likely that material properties contrast between the alluvial fill and Stratum II alluvium would enhance flow along that interface, allowing the infiltrating water to reach the 55-ton sensor location. The increased flow path length could account for delay in water arrival at the 55-ton sensor location compared to the earlier arrival in May from the actual test conducted at the 55-ton test site.

Figures A-17, A-18, and A-19 contain the θ recorded during the July 2016 to August 2017 time period at the PA-South instrumented tube, PA-North instrumented tube, and PA-45 ft drilled borehole, respectively. Figure A-17 shows migration of the melting snow water as it infiltrates past the WCR sensors in the PA-South location during February and March 2017. During this year, Idaho had above normal snow fall, which, as it melted, resulted in an approximate 2% increase in moisture content at the 12 and 18-ft depths in the perimeter drainage material and in the 29-ft Stratum II alluvium. Just after May 5th, there was a slight increase in moisture content. This increase occurred prior to the May 12th NuPac-West characterization test; therefore, it is unrelated to the test.

Figure A-18 shows the snow melt resulted in a more temporally dispersed moisture migration at the PA-North location. The increased dispersion was likely caused by the alluvial fill material that has drainage behavior more typical of soil than the gravelly perimeter drainage material. Similar to the PA-South location, there is a slight increase in moisture content that occurs prior to the May 12th NuPac-West characterization test.

Figure A-19 shows the migration of moisture at the 45-ft depth that originates with snowmelt. The behavior in this figure suggests that moisture is arriving from two distinct events at the surface, which could be indicative of increased water from the shallower excavations under the NuPac vaults.

Figure A-14. Excavation plan for the RH-LLW Disposal Facility vault system (INL Drawing 788786).

Figure A-15. Photograph of vault system (looking northwest) during installation, showing the extent of deeper excavation between the NuPac (upper left –northwest) vault array and 55-ton (lower left – southwest) vault array. The two PA Confirmation Vaults are west of the 55-ton vault array.
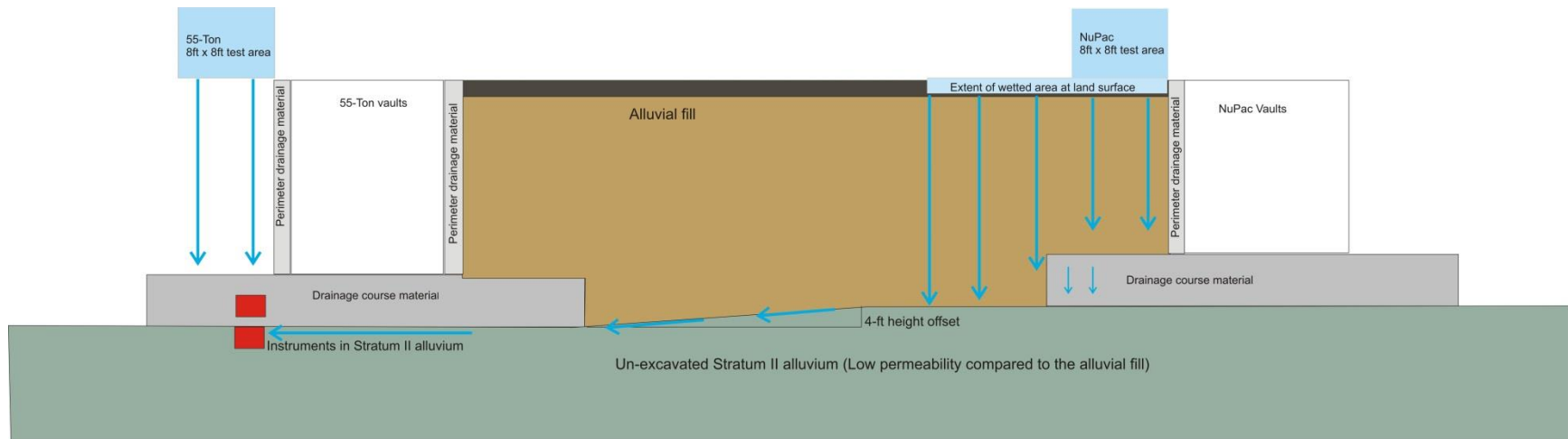
Figure A-16. Vertical profile of materials between the NuPac-East test location and the 55-ton monitoring and characterization instrumentation. The drainage course thickness is 18 in. and is exaggerated in this figure.

Figure A-17. θ calculated using measured permittivity and the second-order calibration curve for the perimeter drainage material, drainage course material, and the Topp equation for the Stratum II alluvium in the PA-south instrumented tube.
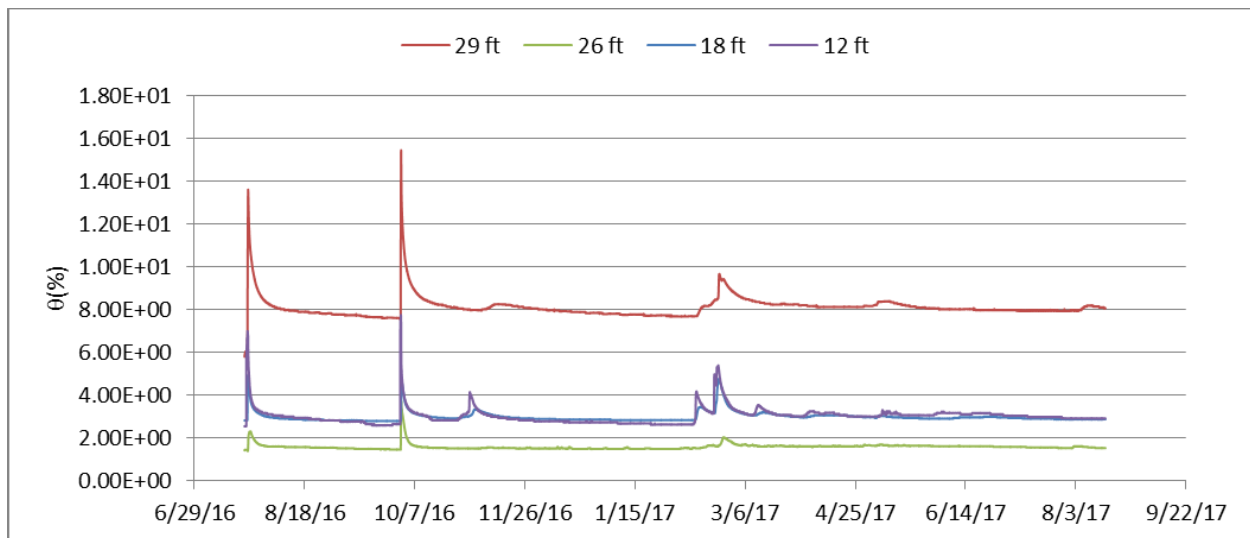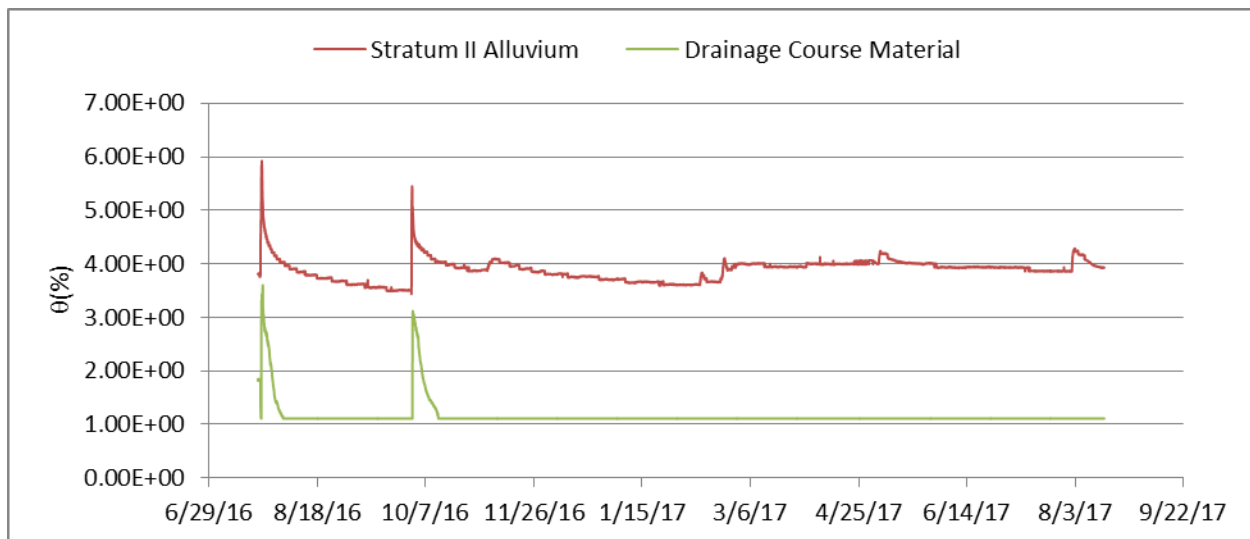

Figure A-18. θ calculated using measured permittivity and the second-order calibration curve for the drainage material and the Topp equation for the Stratum II alluvium in the PA-North instrumented tube.
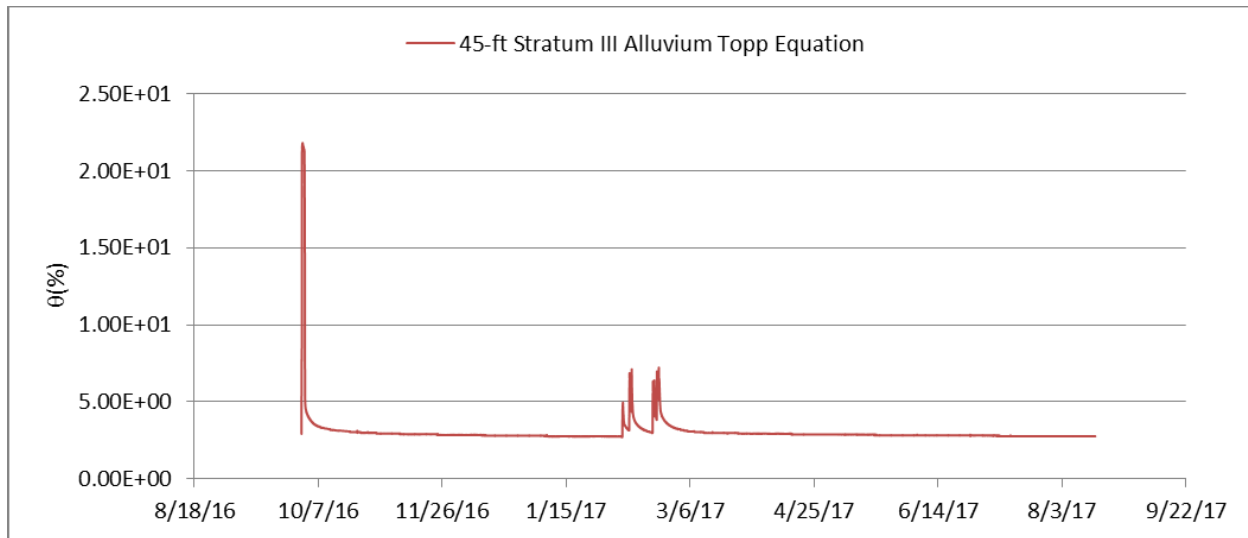
Figure A-19. θ calculated using measured permittivity and the Topp equation in the PA 45-ft drilled borehole.

A-3. SUMMARY OF WEST-SIDE FIELD CHARACTERIZATION TEST DATA

The purpose of conducting the west-side field characterization test was to assess the net performance of the perimeter drainage material and drainage course material following high rate infiltration for relatively high water application times. The overall hydraulic drainage system performance was evaluated using the field characterization tests conducted at the PA vault array. The PA vaults and all vaults on the west-side arrays were installed using the same materials and installation methods. The data from the west-side field characterization tests are shown in Table A-3. The maximum θ reached during and after these tests is shown in Column 3 and the elapsed time to return to θ_r is given in Column 4. These values are somewhat lower than observed during the PA vault array field characterization tests because of the shorter water application times and smaller total water volumes applied. The results support the conclusions of the PA vault array field characterization tests that were conducted at higher rates and for longer application times. The maximum θ would not be expected to ever exceed the values shown in Table A-3 under normal precipitation infiltration rates and durations.

Table A-3. Summary of east-side vault array field characterization test results.

Location	Material	Maximum θ	Elapsed time to return to θ_r
NuPac-West	Drainage Course	3.5%	1-3 days for the peak, ~10 days to reduce to within 90% of θ_r
	Stratum II Alluvium	28%	1-3 days for the peak, ~2 months to reach θ_r
	45-ft Stratum II/III	<2%	
NuPac-East	Drainage Course	4.5%	1-3 days for the peak, ~10 days to reduce to within 90% of θ_r
	Stratum II Alluvium	19%	1-3 days for the peak, ~2 months to reach θ_r
	45-ft Stratum II/III	AT not WCR	> 3 months
55-Ton	Drainage Course	1.7%	1 day
	Stratum II Alluvium	20%	~10 days then the NuPac West peak arrives
	45-ft Stratum II/III	AT not WCR	> 3 months

132

Appendix B

Characterization Test Data for the East-Side Vault Arrays

Appendix B

Characterization Test Data for the East-Side Vault Arrays

B-1. INTRODUCTION

This appendix contains characterization test data obtained for the LCC and MFTC vault arrays located on the east-side of the RH-LLW Disposal Facility vault system. The test procedure followed the procedure outlined in Section 6.4 and used the test apparatus discussed in Section 6.3. Differences in the characterization tests compared to the test conducted at the PA Confirmation Vaults (see Section 6) are as follows:

- **Test Location.** Three test apparatuses were assembled for use adjacent to the LCC-West, MFTC-West, and MFTC-East monitoring system locations (see Figure B-1). The three test apparatuses are similar to the apparatus discussed in Section 6.3.
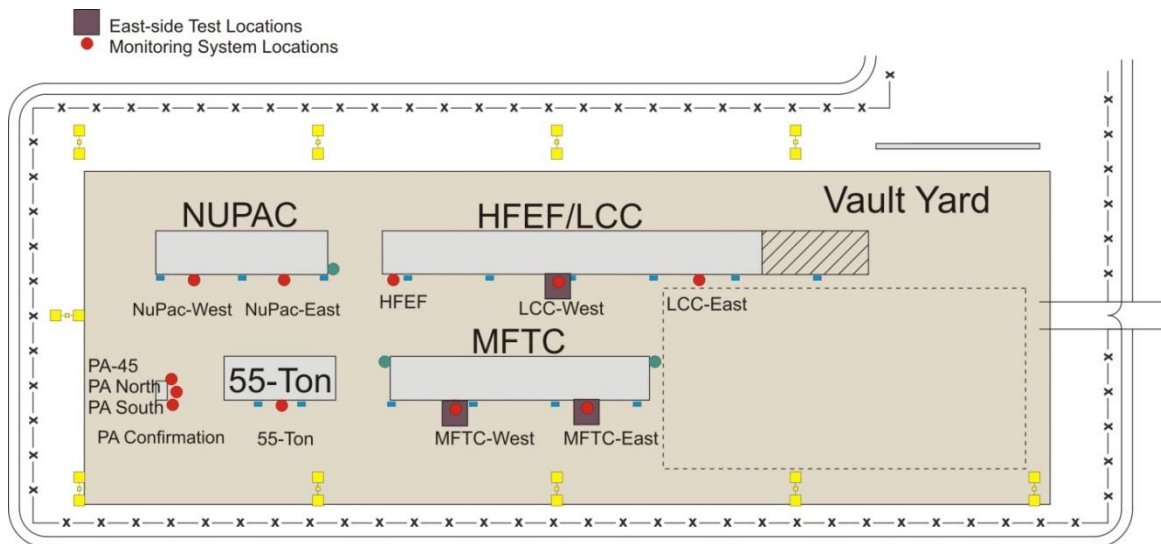

Figure B-1. Locations for the east-side vault array characterization tests.

- **Test Design.** The test was conducted to obtain moisture content history on the drainage course material and Stratum II alluvium at the test locations for comparison to test data collected at the PA vaults.

- **Test Procedure.** The test procedure outlined in Section 6.4 was used at all three of the west-side vault test locations.

- **Monitoring System.** The monitoring and characterization system at the test locations is presented in INL/EXT-17-43081 (INL 2017).

- **Calibration Data.** WCR calibration data are discussed in Section 6.6.2. Calibration used for the drainage course material and perimeter drainage course materials is provided in Figure 16 and for the shallow alluvium in Figure 21. The Topp calibration relationship was used for the Stratum III alluvium. AT calibration data are provided in Table B-1.

Table B-1. AT calibration data for the east-side vault array characterization tests.

Location	Stratum II Alluvium (deep) (U1 Data Logger Connection)			Perimeter Drainage Material (shallow) (U2 Data Logger Connection)		
	Depth (ft)	Slope	Offset	Depth (ft)	Slope	Offset
HFEF-West	26	1.6883	-2092	22	1.6702	-2089
LCC-West	26	1.6780	-2083	22	1.6479	-2047
LCC-East	26	1.7150	-2115	22	1.6921	-2094
MFTC-West	26	1.6608	-2061	22	1.6920	-2095
MFC-East	26	1.7784	-2184	22	1.6857	-2079

Location	Stratum III Alluvium (45-ft depth) (U1 Data Logger Connection)	
	Depth (ft)	
HFEF-45-East	42	No AT at this location
LCC-45-West	41.75	1.6908 -2084
LCC-45-East	43.75	No AT at this location
MFTC-45-West	43.8	No AT at this location
MFC-45-East	41.75	1.6869 -2091

B-2. CHARACTERIZATION TEST DATA AND INTERPRETATION

The east-side vault array characterization tests were conducted on August 4, 2017. The infiltration tests were conducted over a period of approximately 10.5 hours, keeping the infiltration rates roughly constant as shown in Table B-2. Data were collected using the monitoring instruments in the instrumented tubes and 45-ft drilled boreholes at each of the three locations. The raw data were calibrated as indicated in the following subsections.

Table B-2. Volumetric rates applied during the east-side vault array characterization tests.

Characterization Test Conducted 8/4/2017 at the LCC-West Location				
Water Depth in Tank				
Time	Elapsed Time (minutes)	Water Level (inches)	Water Used (inches)	Flow Rate (in./hour)
7:00 a.m.				
8:36		24		
9:06	0:30	18	6	12
10:31		23.5		
11:01	0:30	19.125	4.375	8.75
11:21		16.875		
11:51	0:30	11.125	5.75	11.5
12:19		22.875		
12:49	0:30	20.75	2.125	4.25
1:08		17.75		
1:38	0:30	11	6.75	13.5
2:10		23.5		
2:40	0:30	16.75	6.75	13.5
4:22		16.5		
5:22	1:00	4	12.5	12.5
17:35	Test end			
Test duration	10.58 (hours)			
Tank diameter (in)		50		
Total volume of water		225,615 (in³)		
Total volume of water		977 (gallons)		

Time	Elapsed Time (minutes)	Water Level (inches)	Water Used (inches)	Flow Rate (in./hour)
		Characterization Test Conducted 8/4/2017 at the MFTC-West Location		
		Water Depth in Tank		
7:06 a.m.				
8:18		23.5		
8:48	0:30	15.5	8	16
10:22		23.375		
10:52	0:30	15.25	8.125	16.25
12:09		22.375		
12:39	0:30	14.375	8	16
1:58		23.75		
2:28	0:30	15.25	8.5	17
4:28		22.5		
5:28	1:00	6.25	16.25	16.25
17:29	Test end			
Test duration	10.38 (hours)			
Tank diameter (in)		44.5		
Total volume of water		263,229 (in^3)		
Total volume of water		1,140 (gallons)		

Time	Elapsed Time (minutes)	Water Level (inches)	Water Used (inches)	Flow Rate (in./hour)
		Characterization Test Conducted 8/4/2017 at the MFTC-East Location		
		Water Depth in Tank		
7:10 a.m.				
8:40		23		
9:10	0:30	15.5625	7.4375	14.875
10:37		24		
11:07	0:30	16.375	7.625	15.25
12:29		23		
12:59	0:30	15.25	7.75	15.5
2:15		24		
2:45	0:30	16.25	7.75	15.5
4:15		22.75		
5:15	1:00	7.5	15.25	15.25
17:45	Test end			
Test duration	10.58 (hours)			
Tank diameter (in)		44.5		
Total volume of water		251,428 (in^3)		
Total volume of water		1,088 gallons		
Average rate		1.4 gpm		

B-1.1   Calibrated Characterization Test Data

B-1.1.1   LCC-West Instrumented Tube and 45-ft Drilled Borehole

The calibrated θ data for the LCC-West instrumented tube are given in Figure B-2. These data collected in the drainage course material show that very little water arrived in the drainage course material. They also show that the maximum θ in the Stratum II alluvium was at 8%, which is lower than previous characterization test data obtained at the west-side vault array test locations. The return to θ_r in

the Stratum II alluvium occurs within the 3 weeks shown, reflecting very fast drainout of the alluvial fill material compared to previous test data at other locations.

Water tension shown in Figure B-3 in the drainage course material shows that it remains very dry and drier than the Stratum III alluvium. Tension in the Stratum III alluvium shows an initial higher peak with a lower magnitude peak later, which is typical of behavior observed in the WCR data collected following each of the west-side vault array characterization tests.

Water tension data for the LCC-West 45-ft drilled borehole are shown in Figure B-4. This instrument shows an initial response to the AT being charged and to the August 4th test. Water tension is relatively constant after the initial flux of water, which is indicative of the Stratum II material retaining the water at this depth instead of the water infiltrating downward over this time period.

Figure B-5 contains the temperature obtained for sensors installed at depths of 12, 18, 26, 34, and 43-ft. These data do not require calibration and represent the "raw" signal. Unlike the longer record data for the MFTC-West, MFTC-East, and 55-ton thermocouples in Appendix A, this record is too short to show the transition from colder April to hotter August day-time temperatures. However it is sufficient to show the initial passage of the infiltration front and equilibration to steady-state temperatures.
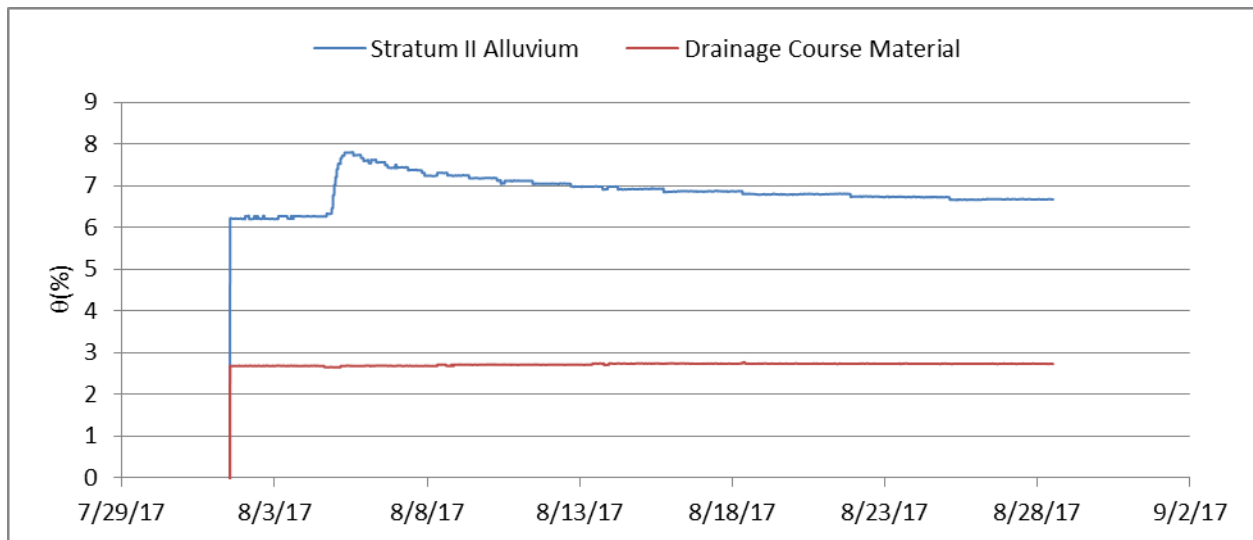

Figure B-2. θ calculated using measured permittivity, first order calibration curve for data at 22-ft depth and second order calibration curve for data at 26 ft in the LCC-West instrumented tube.
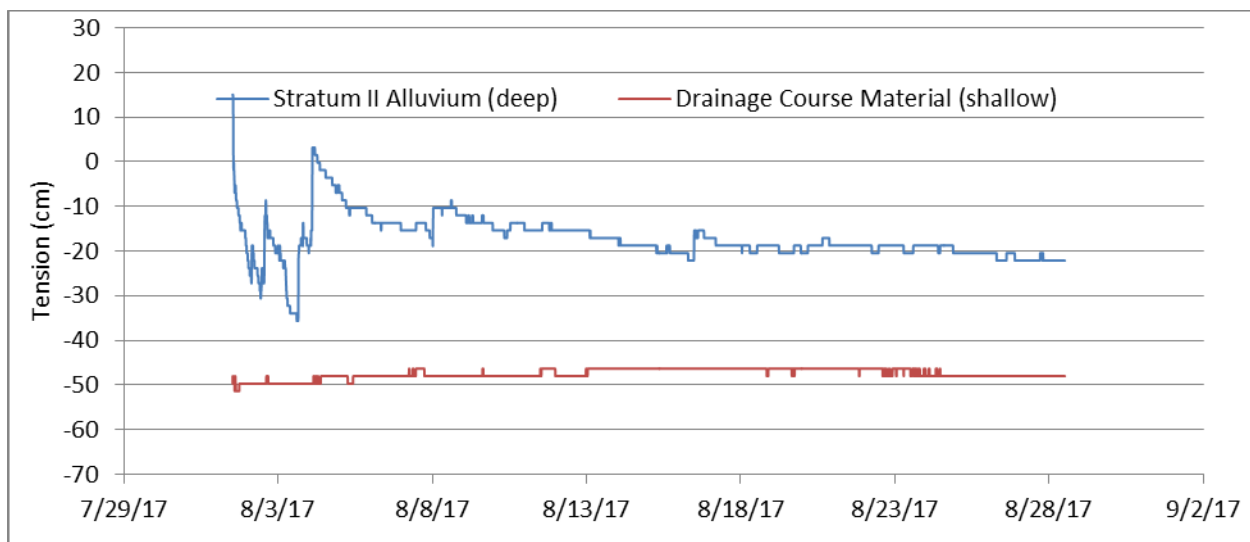
Figure B-3. Water tension in the LCC-West instrumented tube at depths of 22 and 26 ft.
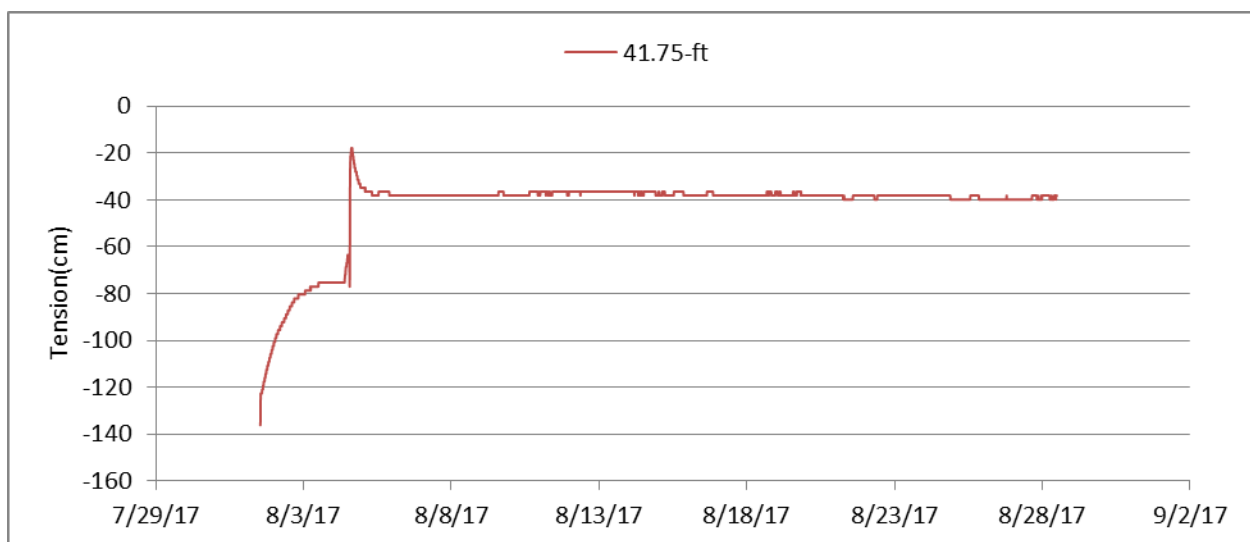

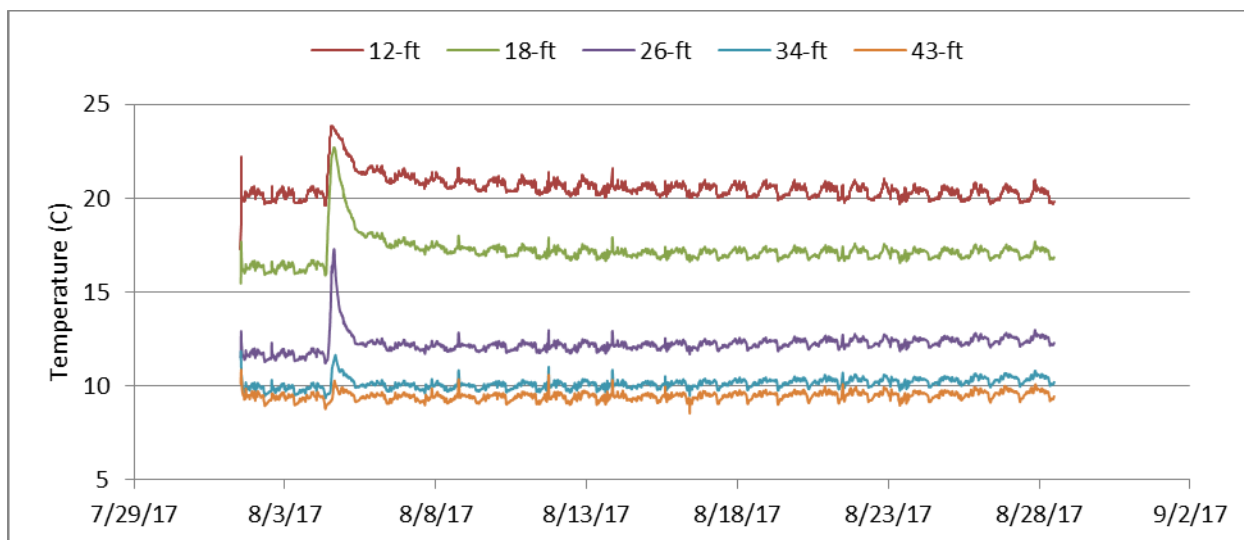Figure B-4. Water tension in the LCC-West 45-ft drilled borehole.

Figure B-5. Temperature in the LCC-West 45-ft drilled borehole.

B-1.1.2   MFTC-West Instrumented Tube and 45-ft Drilled Borehole

The calibrated θ data for the MFTC-West instrumented tube are given in Figure B-6. Data collected in the drainage course material and in the Stratum II alluvium show a single peak value in contrast to data collected during the west-side tests provided in Appendix A. During the MFTC-West test, there was very little lateral migration of water at land surface, indicating that crushed gravel base course material at land surface was able to accommodate the test infiltration rates. These data show the maximum θ in the drainage course material was 2% and was 22% in the Stratum II alluvium. The drainage course material and Stratum II alluvium both remained drier than observed during the west-side tests, which could be a result of slightly lower total water being applied to the test area. As with the data shown in Section 6 and Appendix A, the return to θ_r occurs within days in the drainage course material. However, in contrast to previous tests, the return to θ_r in the Stratum II alluvium occurred much faster, indicating faster drainout through the alluvial fill material.

The water tension shown in Figure B-7 in both the drainage course material and Stratum II alluvium is negative with increasing negative tension over time. Behavior of the AT data is excellent in this installation.

The θ data computed from permittivity for the MFTC-West 45-ft drilled borehole are shown in Figure B-8. These data show an initial decrease in tension as WCR equilibrates to the native material. However, the computed θ is negative, indicating that the θ is less than 2%, which is a characteristic of the Topp equation applied to very low permittivities as indicated in Figures 16 and 21. Although the calibrated θ is negative, the permittivity used to calculate θ is clearly decreasing, showing the instrument is connected correctly and the data logger is recording the permittivity.

Figure B-9 contains the temperature obtained for sensors installed at depths of 12, 18, 26, 34, and 43-ft. These data are very similar to those obtained in the LCC-West 45-ft drilled borehole. The difference in temperature is a function of the geothermal gradient and temperature at land surface. After responding to the influx of characterization test water, the temperature does not remain completely constant. Instead of being constant, there appears to be a daily fluctuation in the temperature, which is unlikely at a depth of 45-ft. It is more likely the data logger is not completely removing the daily temperature fluctuation (i.e., signal differencing is not complete).
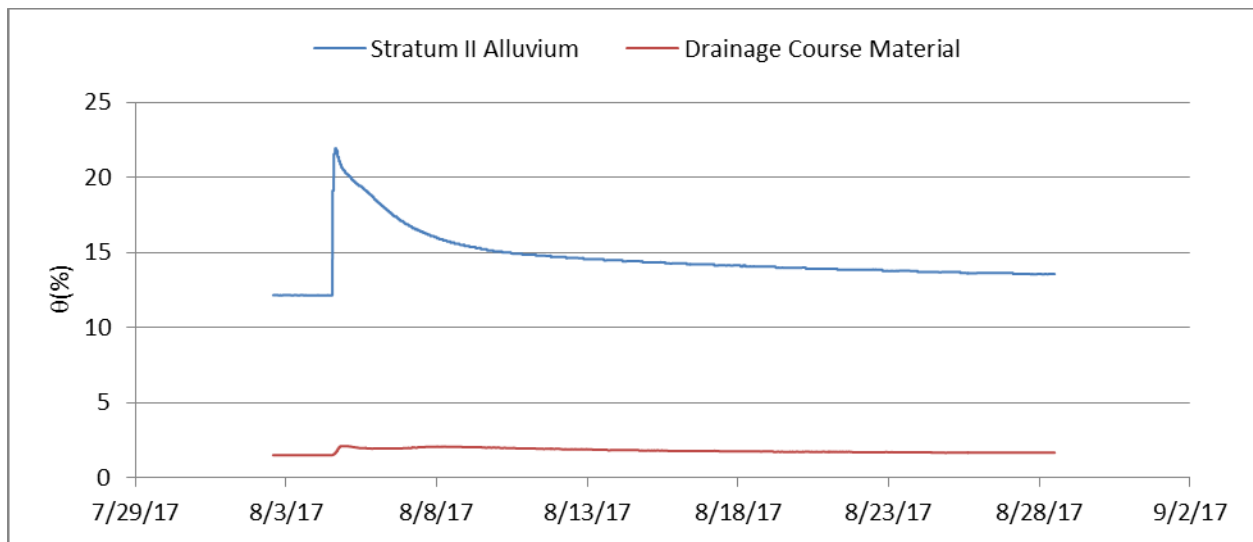
139

Figure B-6. θ calculated using measured permittivity, a first order calibration curve for data at the 22-ft depth, and a second order calibration curve for data at 26 ft in the MFTC-West instrumented tube.
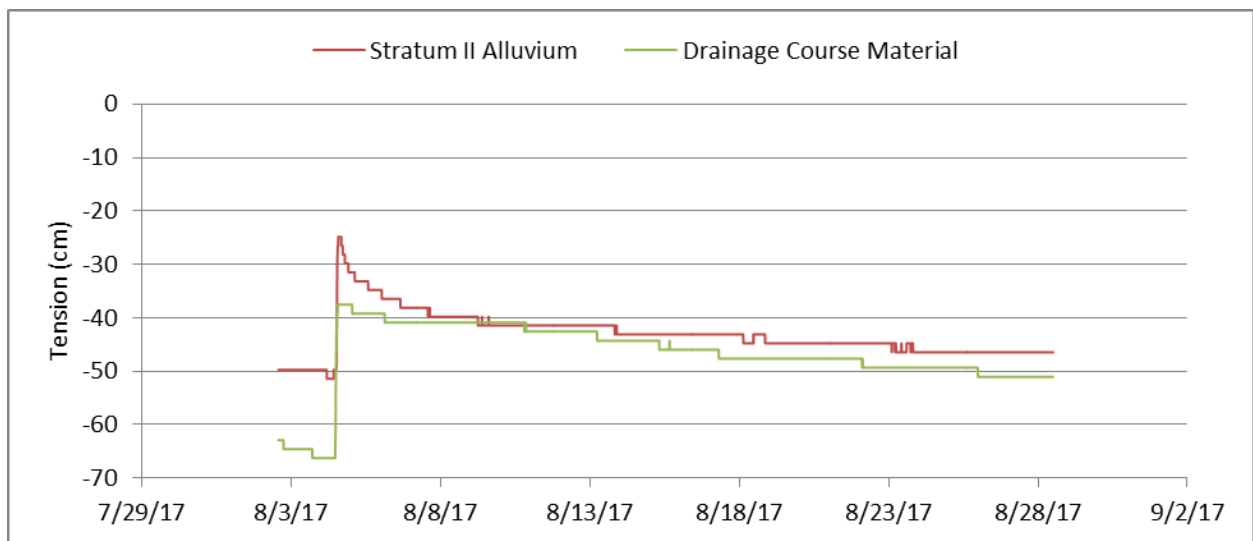

Figure B-7. Water tension in the MFTC-West instrumented tube.
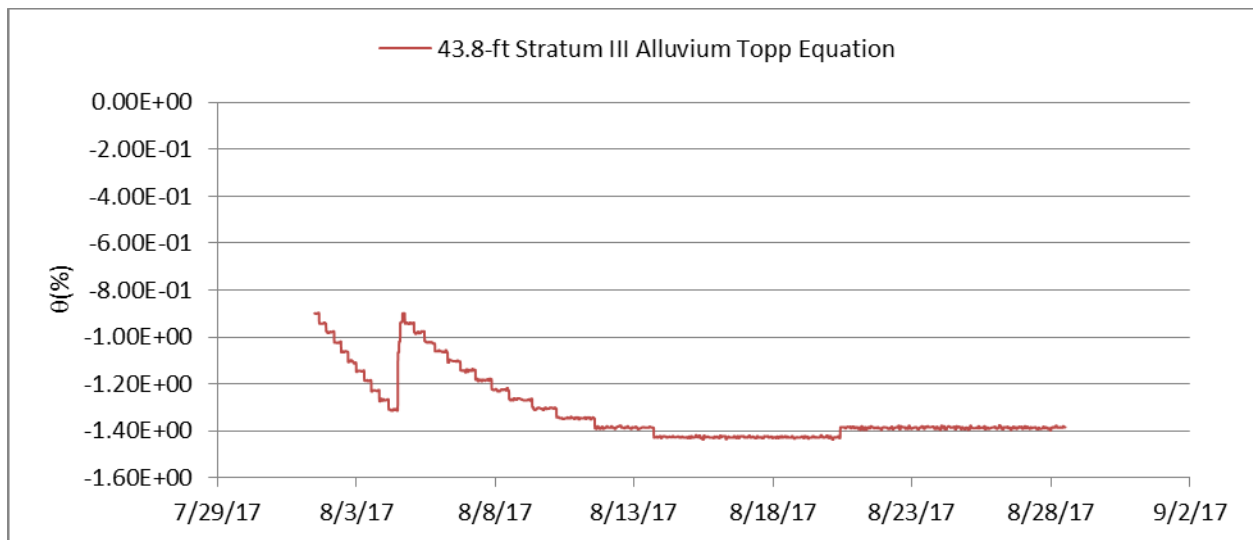
Figure B-8. θ calculated using measured permittivity and the Topp equation in the MFTC-West 45-ft drilled borehole.
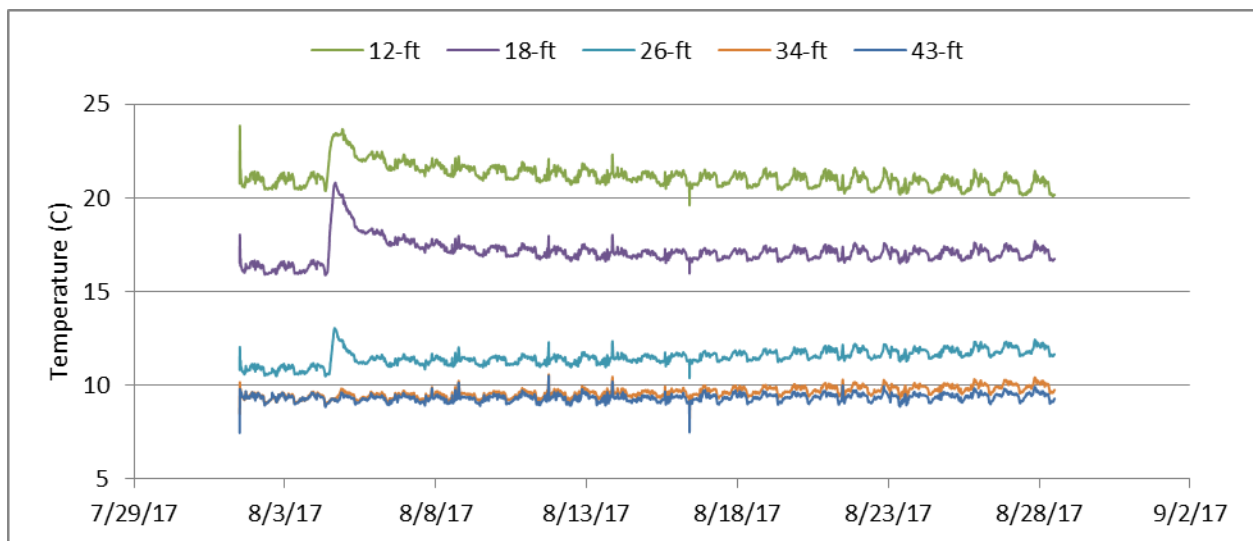

Figure B-9. Temperature in the MFTC-West 45-ft drilled borehole.

B-1.1.3 MFTC-East Instrumented Tube and 45-ft Drilled Borehole

The calibrated θ data for the MFTC-East instrumented tube are given in Figure B-10. Data collected in the drainage course material and Stratum II alluvium do not show the typical characteristic peak within 12 hours of the pumps being turned off. Instead, these data show a very slow response with a maximum θ increase of about 0.25%. The MFTC-East test location is on the south side of the MFTC vault array. At the time of this infiltration event, the surface grade had been prepared for installation of the surface road base. This resulted in a 2% slope to the south from the vault arrays with the crushed gravel base course being packed to specifications. During the test, water was observed to flow southward and to accumulate in the electrical trench on the south side of the road apron. These data show the effectiveness of the crushed gravel base course in diverting infiltrating water away from the perimeter drainage material and the resultant very low moisture content that will be expected during operations of the vault system.

Water tension is given in Figure B-11. Tension parallels the slight increase in θ for the drainage course material; however, a similar response in the Stratum II alluvium is not apparent. With the very small increase in θ, in order to see a tension response, the data logger would have to record voltages at higher resolution than the mVolts allowable.

Water tensions in the MFTC-East 45-ft drilled borehole are shown in Figure B-12. These data show an initial decrease in tension as WCR equilibrates to the AT being recharged followed by the response to the characterization test. The subsequent increase in tension shows the Stratum III alluvium at this location has equilibrated at this data collection time, and shows that the instrument is connected correctly and the data logger is recording the permittivity.

Figure B-13 contains the temperature obtained for sensors installed at depths of 12, 18, 26, 34, and 43-ft. These data re very similar to those obtained in the other east-side 45-ft drilled boreholes. After responding to the influx of the characterization test water, the temperature does not remain completely constant. Instead of being constant, there appears to be a daily fluctuation in temperature, which is unlikely at a depth of 45 ft. It is more likely that data logger is not completely removing the daily temperature fluctuation (i.e., signal differencing is not complete).
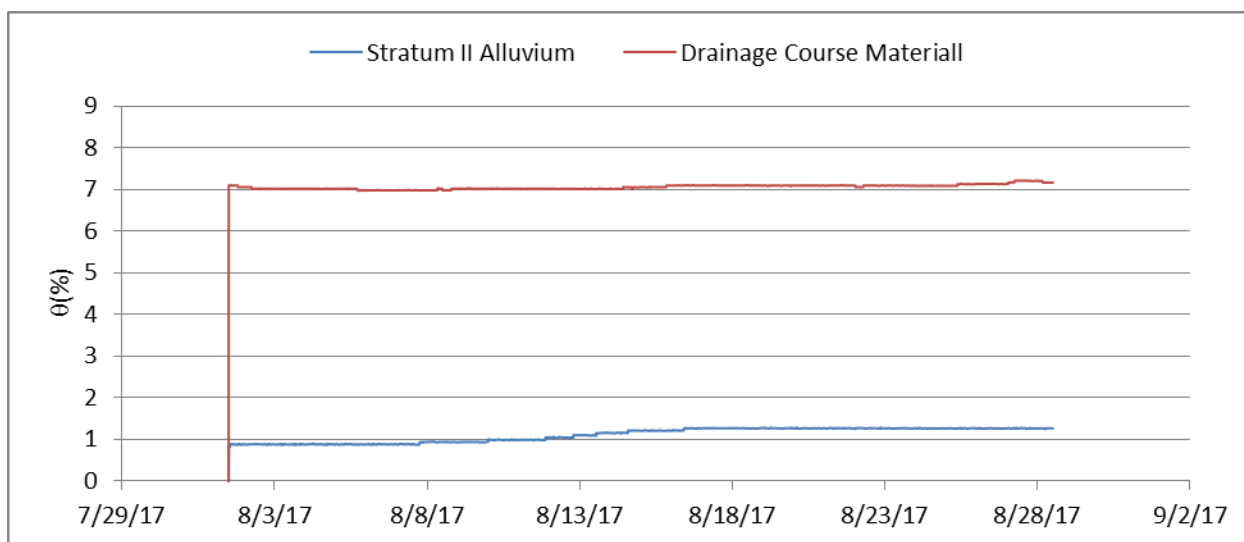

Figure B-10. θ calculated using measured permittivity, the first order calibration curve for data at a 22-ft depth, and the second order calibration curve for data at 26 ft in the MFTC-East instrumented tube.
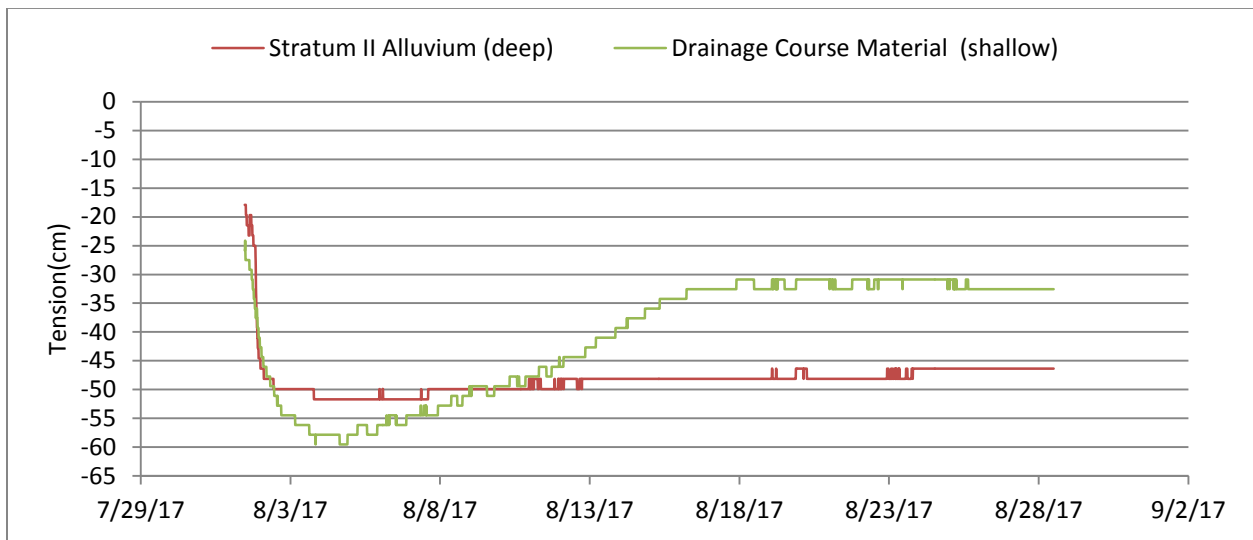
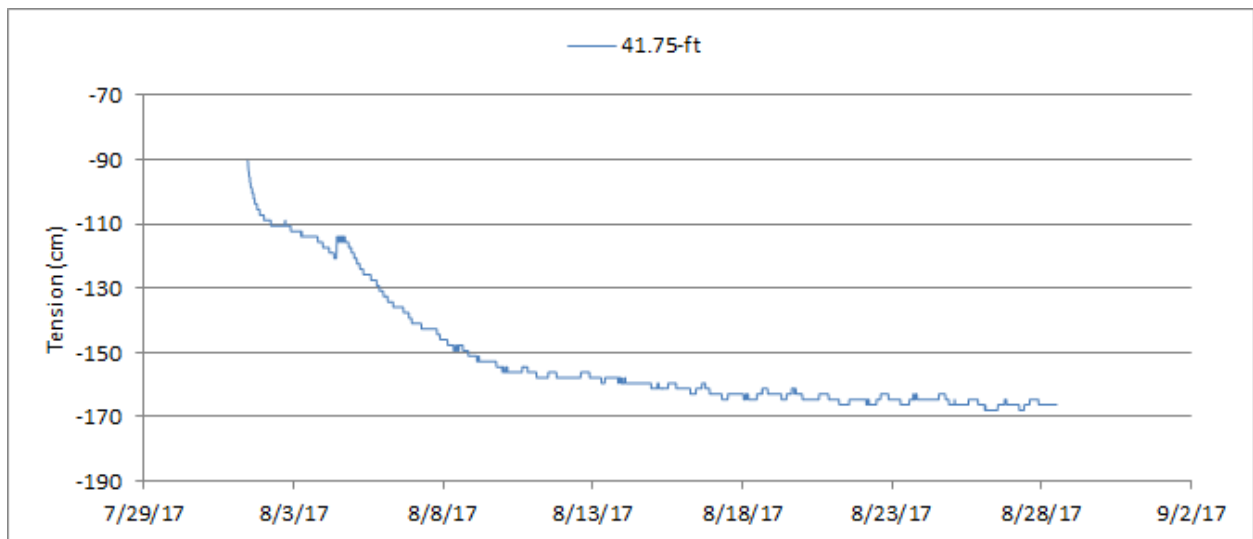Figure B-11. Water tension in the MFTC-East instrumented tube.

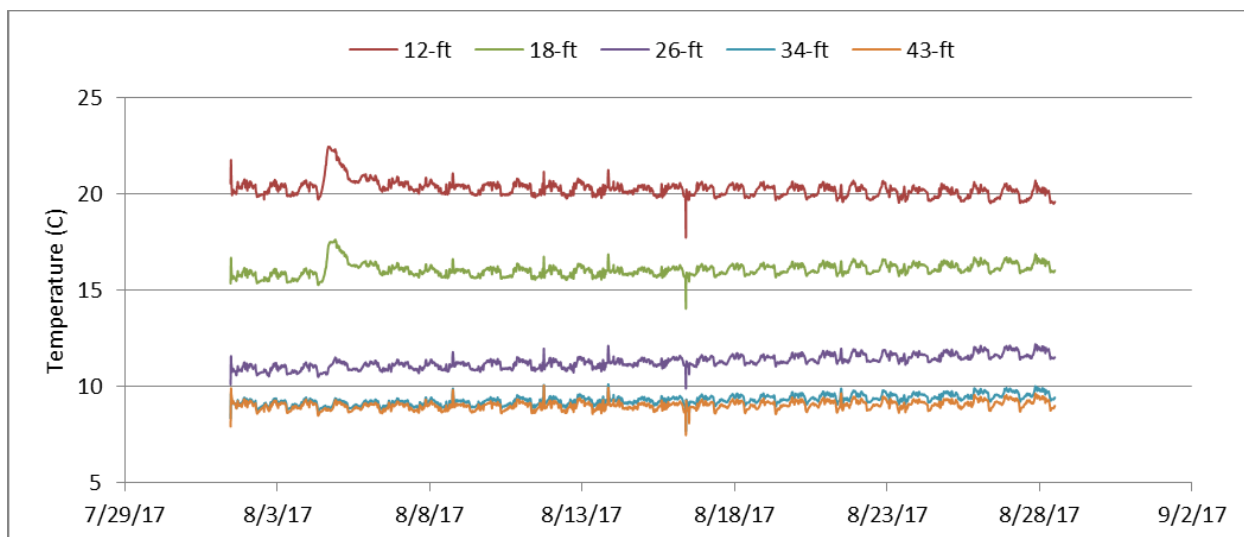Figure B-12. Water tension in the MFTC-East 45-ft drilled borehole.

143

Figure B-13. Temperature in the MFTC-East 45-ft drilled borehole.

B-1.1.4   HFEF-East Instrumented Tube and 45-ft Drilled Borehole

Calibrated θ data for the HFEF-East instrumented tube are given in Figure B-14. The HFEF-East instrumented tube is west of the LCC-West instrumented tube. The infiltration test was conducted using the test apparatus at the LCC-West, MFTC-West, and MFTC-East locations. No water was introduced at the HFEF-East location. The distance between the HFEF-East instrumented tube from the test locations is large enough that no moisture from the test locations was expected or detected.

Water tension at the HFEF-East instrumented tube location is given in Figure B-15. Tension in the Stratum II alluvium initially equilibrates to recharging the AT and subsequently reaches a steady-state background value. Tension in the drainage course is highly erratic, and is probably being influenced by the surface road vibratory compactors as the surface road base is being installed.

Water tensions in the HFEF-East 45-ft drilled borehole are shown in Figure B-16. These data show no indication that water from the active test locations are being detected at the HFEF-45-East location. Figure B-17 contains temperature obtained for sensors installed at depths of 12, 18, 26, 34, and 43. There is no indication of moisture arrival in any of these sensors from the east array infiltration tests.
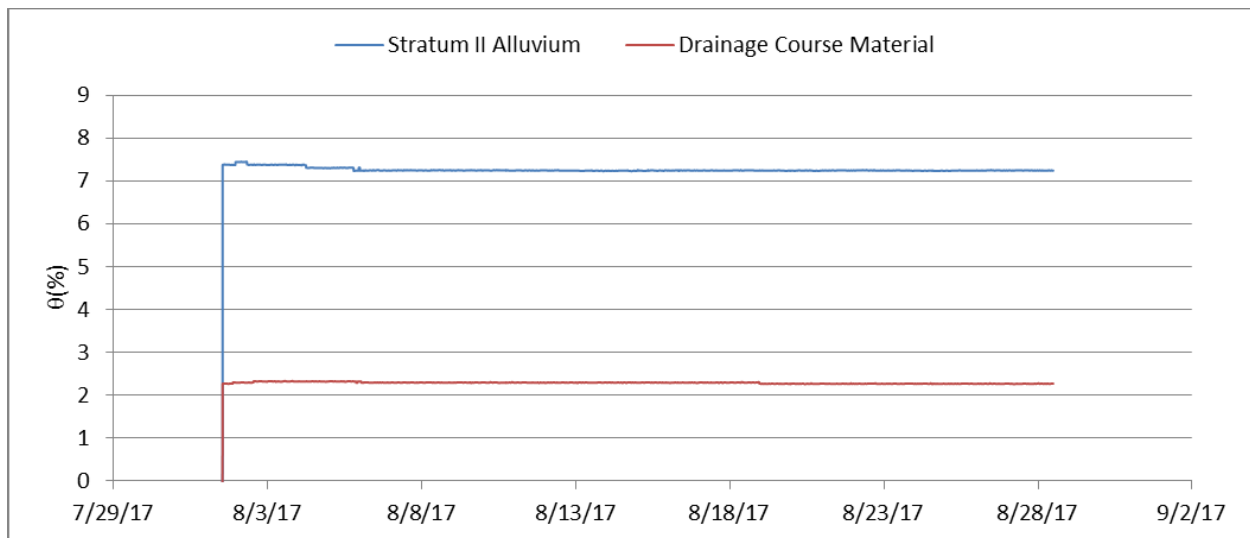
144

Figure B-14. θ calculated using measured permittivity, first order calibration curve for data at the 22-ft depth, and second order calibration curve for data at 26 ft in the HFEF-East instrumented tube.
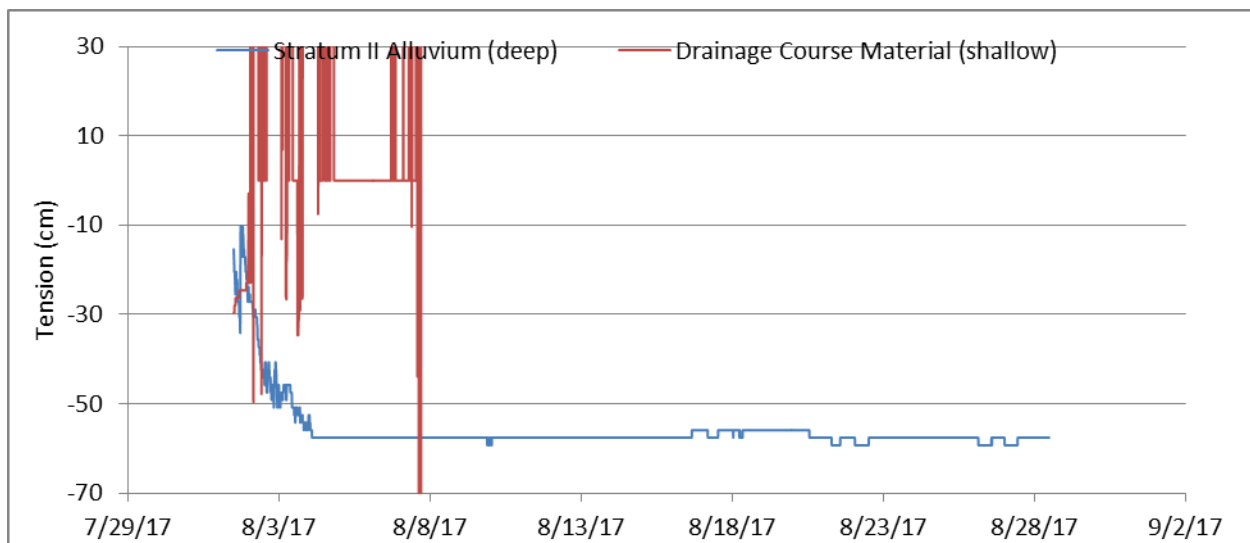

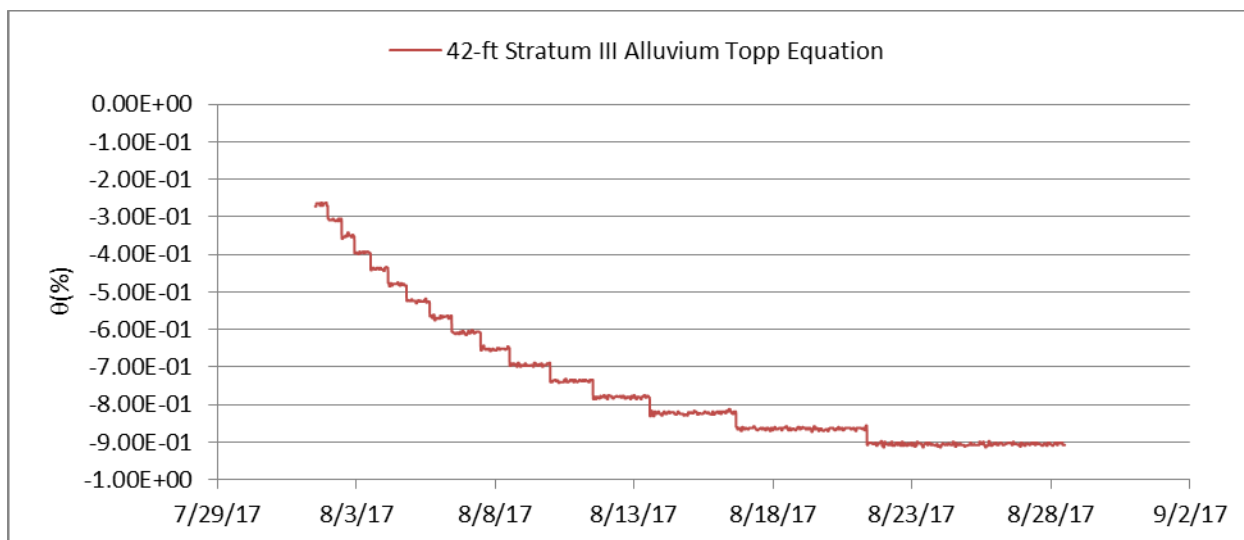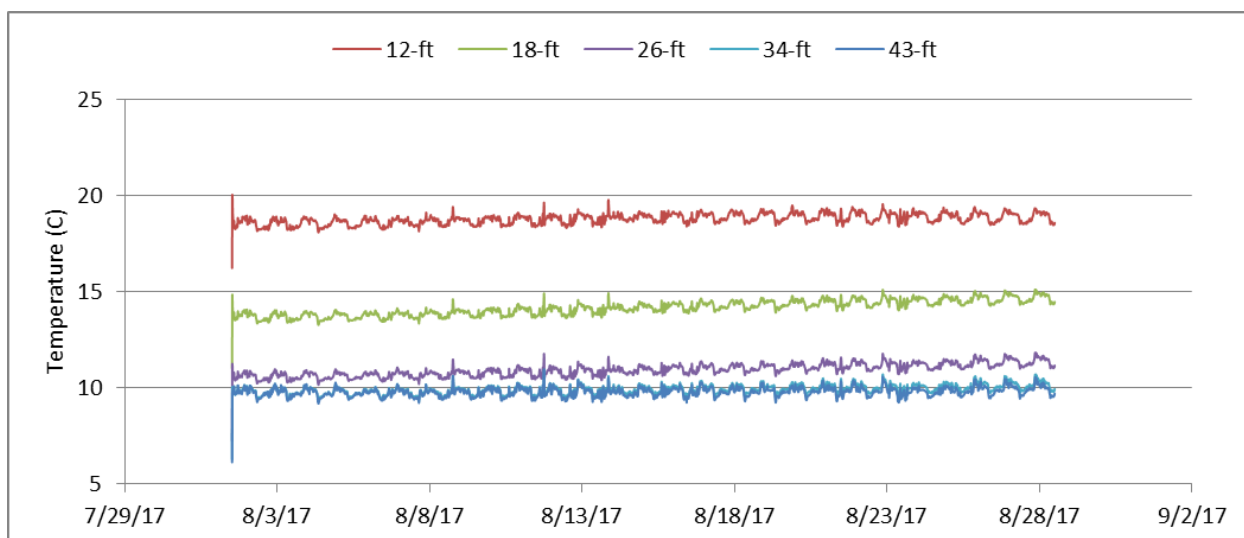Figure B-15. Water tension in the HFEF-East instrumented tube.

Figure B-16. θ calculated using measured permittivity and the Topp equation in the HFEF-East 45-ft drilled borehole.

B-17. Temperature in the HFEF-East 45-ft drilled borehole.

B-3. SUMMARY OF EAST-SIDE FIELD CHARACTERIZATION TEST DATA

The purpose of conducting the east-side field characterization test was to assess the net performance of the perimeter drainage material and drainage course material following high rate infiltration for relatively high water application times. The overall hydraulic drainage system performance was evaluated using the field characterization tests conducted at the PA vault array. The PA vaults and all vaults on the east-side arrays were installed using the same materials and installation methods. The data from the east-side field characterization tests are shown in Table B-3. The maximum θ reached during and after these tests is shown in Column 3 and the elapsed time to return to θ_r is given in Column 4. These values are somewhat lower than observed during the PA vault array field characterization tests because of the

146

shorter water application times and smaller total water volumes applied. The results support the conclusions of the PA vault array field characterization tests that were conducted at higher rates and for longer application times. The maximum θ would not be expected to ever exceed the values shown in Table B-3 under normal precipitation infiltration rates and durations.

Table B-3. Summary of east-side vault array field characterization test results.

Location	Material	Maximum θ	Elapsed time to return to θ_r
LCC-West	Drainage Course	<1%	Unobservable increase
	Stratum II Alluvium	8%	<1 month
	45-ft Stratum II/III	AT not WCR	> 1 months
MFTC-West	Drainage Course	2%	1 day
	Stratum II Alluvium	22%	~1 month
	45-ft Stratum II/III	<2%	10-15 days
MFTC-East	Drainage Course	7%	Unobservable increase
	Stratum II Alluvium	1.5%	~15 days
	45-ft Stratum II/III	AT not WCR	~10 days